

In the name of God

**ARTICULATIONS IN FLOATING ARRAYS**

**By**

**ABBAS NOBAKHTI**

**A thesis Submitted for the Degree of Doctor of Philosophy  
In the Faculty of Engineering, University of London**

**Department of Mechanical Engineering  
University College London**

March 2001

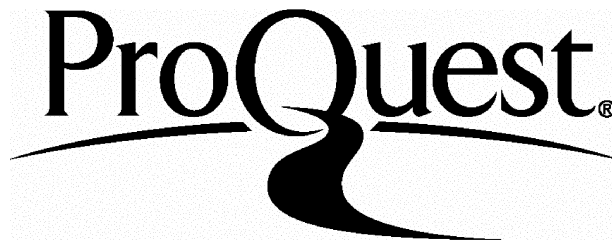
ProQuest Number: U642068

All rights reserved

INFORMATION TO ALL USERS

The quality of this reproduction is dependent upon the quality of the copy submitted.

In the unlikely event that the author did not send a complete manuscript and there are missing pages, these will be noted. Also, if material had to be removed, a note will indicate the deletion.



ProQuest U642068

Published by ProQuest LLC(2015). Copyright of the Dissertation is held by the Author.

All rights reserved.

This work is protected against unauthorized copying under Title 17, United States Code.  
Microform Edition © ProQuest LLC.

ProQuest LLC  
789 East Eisenhower Parkway  
P.O. Box 1346  
Ann Arbor, MI 48106-1346

## ABSTRACT

This thesis describes an investigation principally to explore the displacements due to static loading of floating structures, which consist of several similar modules connected together. The study includes theoretical development and experimental work of both in-line and mat arrays of modules.

To establish module displacements it is necessary to find the stiffness matrix. For the in-line array two methods have been employed. First, by the use of constraint equations which are inserted in the global stiffness matrix. In this case each module is considered as a rigid body and the displacements result from hydrostatic stiffness represented by elastic foundation. The second method is by the use of the finite element method, and potential energy, in which the structural stiffness matrix is due to the elasticity of the structure, and the hydrostatic stiffness matrix represented as an elastic foundation. The effects of connections play an important role and these are considered in the study. For the mat array constraint equations are employed. Different connections, such as hinged, elastic, rigid, and hinged-rigid are evaluated. The main emphasis is concentrated on hinged-rigid connections. For these the system behaves as a hinged connection between consecutive modules up to threshold value and after that the system will act rigidly.

The experimental work for in-line arrays is reported for hinged-rigid connections with different arrangements, different locking angles between consecutive modules, and also for several loading conditions. The hinged and hinged-rigid connections were used in experimental work for the mat array with several loading conditions.

Based on the developed theory computer code has been generated to model the stiffness matrices for different types of connections to calculate the displacements. The theoretical and experimental results for displacements in in-line arrays are shown to be very similar. However the mat array exhibits some differences.

*To*

*My wife*

## **ACKNOWLEDGEMENT**

I would first like to thank the Ministry of Culture and Higher Education of the Islamic Republic of Iran for providing an opportunity and finance for my Ph.D. research work.

I would like to express my sincere gratitude to my supervisors, Dr G J Lyons and Dr D T Brown for their valuable guidance, advice, help and especially their support throughout this work.

I wish to thank Professor D R Broome and Dr K R Drake for their valuable advice and suggestions.

My thanks also go to Mr O Pearson and Mr M Dixon at the Santa Fe Laboratory for Offshore Engineering for their friendly help.

I also would like to thank Mr F Arthur and his colleagues in the UCL Department of Mechanical Engineering workshop for their assistance with the experimental aspects.

## CONTENTS

<b>ABSTRACT.....</b>	<b>2</b>
<b>ACKNOWLEDGEMENT .....</b>	<b>4</b>
<b>CONTENTS .....</b>	<b>5</b>
<b>GLOSSARY OF KEY SYMBOLS AND ABBREVIATIONS .....</b>	<b>10</b>
<b>CHAPTER 1 INTRODUCTION.....</b>	<b>12</b>
1.0 Principal aims.....	12
1.1 Overview .....	12
1.1.1 Connection types .....	13
1.2 Applications of multipli-connected floating structures.....	14
1.2.1 Wave energy devices.....	14
1.2.2 Wave breakers .....	14
1.2.3 Floating marine terminals.....	15
1.2.4 Other uses .....	15
1.3 Objectives of present work.....	16
1.3.1 Connection type.....	16
1.3.2 Structural arrangement .....	16
1.3.3 Hinged-rigid connection as the focus of this study .....	17
<b>CHAPTER 2 LITERATURE REVIEW.....</b>	<b>19</b>
2.1 General .....	19
2.2 Review of closely related literature.....	19
2.2.1 Theoretical studies.....	19
2.2.2 Experimental work .....	27
2.3 Relevant issues from "International Workshop on VLFS".....	28
2.3.1 Design philosophy of VLFS .....	28

2.3.2 Example of conceptual design.....	30
2.3.3 Strength and reliability .....	32
2.3.4 At-sea construction and maintenance technologies.....	33
2.3.5 External loads and response analysis .....	34
2.3.6 Mooring technology.....	40
2.4 Standard package.....	40
2.5 Review Summary .....	41

## **CHAPTER 3 DEVELOPMENT OF HYDROSTATIC STIFFNESS FORMULATION ..... 42**

3.1 Introduction .....	42
3.2 Constraint equations.....	42
3.3 In-line array .....	43
3.3.1 Basic hydrostatics .....	43
3.3.2 Extension of the models for an in-line array .....	44
3.3.3 Constraint relationship.....	45
3.3.4 Connections .....	47
3.3.4.1 Hinged.....	47
3.3.4.2 Rigid.....	51
3.3.4.3 Hinged-rigid.....	52
3.3.5 Results for in-line array .....	53
3.4 Mat array .....	55
3.4.1 Basic hydrostatics .....	55
3.4.2 Extension of the models for mat array configurations .....	57
3.4.3 Constraint equations for hinged connection .....	57
3.4.4 Alternative method of using constraint equation for mat array.....	59
3.4.5 Results for mat array.....	60
3.5 Discussion .....	61

## **CHAPTER 4 GENERAL SOLUTION USING AN ENERGY APPROACH 62**

4.1 In-line array .....	62
-------------------------	----

4.1.1 Introduction .....	62
4.1.2 Definition of the problem .....	63
4.1.3 Potential energy .....	63
4.1.4 Interpolation function for an element in the context of the primary assumptions .....	64
4.1.4.1 Interpolation function for element with both ends pinned.....	64
4.1.4.2 Interpolation function for element with both ends built-in.....	66
4.1.4.3 Interpolation function for element with one end pinned, other end built-in.....	69
4.1.4.4 Interpolation function for element with one end built-in other end pinned.....	71
4.1.5 Potential energy for an element.....	71
4.1.5.1 Potential energy for element with both ends pinned.....	72
4.1.5.2 Potential energy for element with both ends built-in.....	74
4.1.5.3 Potential energy for element with one end pinned and one end built-in.....	76
4.1.5.4 Potential energy for element with one end built-in and the other end pinned.....	78
4.1.6 Potential energy for complete structure.....	81
4.1.7 Finding reaction and stress of both ends of elements.....	84
4.1.8 Discussion.....	85
4.1.9 Explanation of the software.....	87
4.1.10 Worked Examples .....	88
4.1.10.1 Example for experimental dimensions .....	88
4.1.10.2 Example for full size dimensions .....	91
4.2 Mat array .....	92
<b>CHAPTER 5 EXPERIMENTS .....</b>	<b>93</b>
5.1 Experimental apparatus .....	93
5.1.1 Pontoon model.....	93
5.1.2 Potentiometers – data logger .....	95
5.2 Experimental procedure .....	95
5.2.1 Test series for in-line array.....	96

5.2.1.1 Test series 1 .....	96
5.2.1.2 Test series 2 .....	97
5.2.1.3 Test series 3 .....	98
5.2.2 Mat array.....	98
5.2.2.1 Test series 1 .....	98
5.2.2.2 Test series 2 .....	99
<b>CHAPTER 6 DISCUSSION .....</b>	<b>100</b>
6.1 Theoretical work by use of constraint equations.....	100
6.2 Use of finite element method and potential energy.....	101
6.3 Use of a standard FEA package .....	103
<b>CHAPTER 7 CONCLUSIONS .....</b>	<b>105</b>
7.1 Existing design Software.....	105
7.2 Theoretical work .....	106
7.2.1 Theoretical work by use of constraint equations .....	106
7.2.2 Use of finite element method and potential energy.....	106
7.3 Unlocking solved.....	107
7.4 Extension to full scale .....	108
7.5 Physical models.....	108
7.6 Mat array .....	109
7.6.1 Mat array.....	109
7.6.2 Dynamic loading .....	110
7.6.3 Advantage of hinged- rigid connections.....	111
7.7 Future work .....	111

<b>REFERENCES .....</b>	<b>112</b>
<b>BIBLIOGRAPHY.....</b>	<b>120</b>
<b>FIGURES.....</b>	<b>121</b>
<b>APPENDICES .....</b>	<b>185</b>
APPENDIX A .....	185
APPENDIX B .....	191
APPENDIX C .....	197
APPENDIX D .....	203
APPENDIX E.....	213
APPENDIX F.....	223
APPENDIX G .....	227
APPENDIX H .....	242

## GLOSSARY OF KEY SYMBOLS AND ABBREVIATIONS

A	Coefficient for the interpolation function
$b$	Breadth of the pontoon
B	Coefficient for the interpolation function
BEM	Boundary Element Method
C	Coefficient for the interpolation function
$d$	Draft of pontoon in still water
D	Coefficient for the interpolation function
E	Young's modulus
EI	Bending rigidity
FEM	Finite Element Method
$F_i$	Force acting at centre of gravity of $i^{\text{th}}$ pontoon
$F_{ij}$	Force acting at centre of gravity of $i^{\text{th}}$ pontoon in the $j^{\text{th}}$ row
$g$	Acceleration due to gravity
[G]	The coefficients of the constraint equation
$GM_l$	Longitudinal metacentric height
$GM_t$	Transversal metacentric height
I	2 <sup>nd</sup> moment of area
K	Stiffness due to gravity
$L$	Length of pontoon
$M_i$	Hydrostatic moment acting on centre of gravity of $i^{\text{th}}$ pontoon
$M_{ij}$	Moment acting at centre of gravity of $i^{\text{th}}$ pontoon in the $j^{\text{th}}$ row about the y-axis
$M_{2ij}$	Moment acting at centre of gravity of $i^{\text{th}}$ pontoon in the $j^{\text{th}}$ row about the x-axis
$P_i$	Pontoon number $i$
$P_{ij}$	$i^{\text{th}}$ pontoon in the $j^{\text{th}}$ row
$P_r$	Resultant force
P(x)	Distributed load applied on beam
r	Typical row of the matrix K
{S}	Vector of known constraint

VLFS	Very Large Floating Structure
$z$	Vertical displacement
$z_{ij}$	Vertical displacement of $i^{\text{th}}$ pontoon in the $j^{\text{th}}$ row

### Symbols

$\alpha$	Coefficient for constraint equations
$\alpha_1$	Coefficient for constraint equations
$\beta$	Coefficient for constraint equations
$\beta_1$	Coefficient for constraint equations
$\gamma$	Coefficient for constraint equations
$\gamma_1$	Coefficient for constraint equations
$\varepsilon$	Locking angle between two pontoon
$\{\Delta_e\}$	Transformation matrix contains $r$ degrees of freedom
$\{\Delta_c\}$	Transformation matrix contains $(n-r)$ degrees of freedom
$\theta_i$	Pitch angle of $i^{\text{th}}$ pontoon
$\theta_{ij}$	Pitch angle of $i^{\text{th}}$ pontoon in the $j^{\text{th}}$ row
$\rho$	Density of water
$\varphi_i$	Roll angle of $i^{\text{th}}$ pontoon
$\varphi_{ij}$	Roll angle of $i^{\text{th}}$ pontoon in the $j^{\text{th}}$ row
$\psi$	Coefficient for constraint equations
$\psi_1$	Coefficient for constraint equations

## **CHAPTER 1 INTRODUCTION**

### **1.0 Principal aims**

The aims of this work are to consider the behaviour of multipli-connected floating structures, with hinged-rigid connections, due to static and quasi-static loading. The floating structures considered are in the shape of an in-line or a mat array configuration.

There are two main differences between this work and those previously carried out by others in this area. Firstly the type of connection is different from those used in previous studies. In this work the hinged-rigid connection will be considered, whereas in previous works only hinged, elastic or rigid connections have been studied. The second main difference is in the arrangement of the structure, which may consist of multipli-connected floating units in a mat array. In previous works multipli-connected floating structures have been generally considered only in an in-line array.

### **1.1 Overview**

From early times floating platforms such as pontoon bridges have been used for crossing rivers. In their most primitive form these platforms mainly consisted of several sections of wood joined by a piece of rope. The use of these systems has developed, and nowadays primarily due to land shortage, a number of countries have plans to make VLFS for different purposes. For example the inherent interest in ocean space, especially space above the sea surface, has historically been keen in Japan. Therefore, ocean space utilisation has been considered as one of the most important subjects in the governmental policies concerning ocean development. Although reclamation has been so far used in most cases of practice, creation of space above the sea surface by use of very large floating structure is being considered as another alternative method.

The advent of the next millennium will trigger a wide variety of visionary projects throughout the world. One or more of these could well involve applications of very large floating structures. While research must and will continue to develop better materials, more efficient systems, and economically attractive end products, there are strong reasons to believe that funds can be brought together for major investments in the open ocean. In the past, military interests had the potential to develop such platforms. The end of the Cold War has largely removed this option. Development of VLFS have wide range of motivations such as, national pride, profit, environmental benefits, scientific merit, public works (floating airport, industrial plants and off shore waste disposal) and floating cities.

Other uses of such structures include construction of wave breakers, piers, liquid storage tanks, as well as floating bridges. Although construction of these systems require much more elaborate and sophisticated engineering work, the ideas are similar to those used in building early floating platforms such as bridges, namely, connecting several similar modules in an array consisting of one or several rows.

### **1.1.1 Connection types**

The connection between the constituent units plays a significant role in determining the behaviour of multi-connected system. The simple connection which had been used in early days has been replaced by more advanced links, which are summarised below:

a) Hinged connections. They are also known as revolute joints for 1-D and a ball joint for 2-D arrays, each model is being joined to the adjacent model. The translational displacement of two consecutive modules at the point of connection is identical, but the angle of rotation (pitch angle) can be different, fig 1.1.

b) Rotationally elastic connections. The translational displacements of two adjacent modules at the point of connection are the same but the angle of rotation may be different, dependent on the elasticity of joints, fig 1.2.

c) Rigid connections. Both the translational displacements at the point of connection and angle of rotation of two adjacent components are the same, fig 1.3.

c) Hinged-rigid connections. The system behaves as a hinged connection, until the angle between two consecutive modules reaches a design threshold value, at which point the system acts rigidly, fig 1.4.

## **1.2 Applications of multi-connected floating structures**

### **1.2.1 Wave energy devices**

As a result of oil price rises in the mid 1970s, together with environmental concern over the use of fossil fuels serious consideration has been given to the exploitation of alternative energy resources. Wave energy, which is both relatively abundant and benign, has received much attention in industrial countries with appropriate coastlines. The extent, to which this resource is exploited, is currently dependent on the provision of future government and commercial funding. Over the period 1974-79 numerous studies were carried out concerning the utilisation of wave energy. These studies have centred on a number of prototype devices, many of which use some kind of multi-connected floating structure [1-3]. Some examples are shown in figures 1.5 to 1.7.

### **1.2.2 Wave breakers**

World-wide there are many large areas of protected water with abundant recreational boating opportunities. These areas also support commercial fishing operations. As a result, there is a large demand for sheltered moorage for these vessels. Traditionally, rubble-mound breakwaters for marina protection have accommodated this demand. At present in most of the sites where rubble-mound breakwater construction is economically feasible, they have been used. Conditions at many of the remaining areas for marina development are unsuitable for traditional construction techniques. In general, the cost is excessive because

the water is too deep, change of the elevation of the water is too great, or the environmental degradation resulting from marina development is unacceptable. To satisfy the demand for moorage, while at the same time overcoming other restrictions, floating breakwaters have been employed at many new marina facilities.

In the 1970s keen interest was shown in the development of floating breakwaters. Several new concepts were studied and more traditional approaches to floating breakwater construction found interesting applications. In many areas of the Pacific Northwest, there were many applications for the floating breakwater and a large number have been installed [4-7]. Some examples are shown in fig 1.8 to 1.15.

### **1.2.3 Floating marine terminals**

Major improvements in port engineering have occurred in the past three decades. Achievement in the fields of port planning, design, construction and operation have been extensively discussed in many technical papers (see for example [8]). During this time there has been a need to resolve port construction and operation problems by using floating wharves. Experiences gained in constructing floating wharves in Peru, Brazil, USA, Saudi Arabia and USSR, clearly shows that under specific conditions (e.g. deep water, strong current, short periods suitable for construction, high change in water level, and construction in remote areas), floating marine terminals can be a competitive solution compared to the fixed waterfront concept. Some floating terminals are shown in figures 1.16 to 1.19.

### **1.2.4 Other uses**

It is anticipated that there will be further growth in the size of large industrial complexes, civil constructions and research facilities in the oceans due to increasing demand for space resource utilisation. Some of these developments may require very large floating structure (VLFS) as compared with existing

offshore structures. Floating industrial complexes consisting of, for example, manganese processing plants, airports, and runways each of which is likely to be very large. Description of some of these structures can be seen in [11], for example, runways (Takarada, 1982), entire floating cities (Takarada, 1989), and oil storage (Uki, 1988).

The Times newspaper, October 29, 1995, described a runway, which is planned to be built in the US for future use.

### **1.3 Objectives of present work**

In the work presented herein, the behaviour of multipli-connected floating structures is considered. In particular, the response of the loading is examined. The work advances research in two areas associated with connected floating structures, namely the connection type and the structural arrangement.

#### **1.3.1 Connection type**

Previous studies have concentrated either on hinged connections between structures [4-7], [11], elastic, or rigid connections [11]. The present work investigates the hinged-rigid connection. The system behaves as a hinged connection until the angle between two consecutive modules, reaches a design threshold limit, at which point the system acts as a rigid body figure 1.4. This has the advantages of lower displacement in comparison with hinged connections and less moment in the connections in comparison with rigid connections. Further reasons for the selection of this type of connection is given in detail later.

#### **1.3.2 Structural arrangement**

Other works on multipli-connected floating structures have concentrated on studies of a single row [4-11] of several modules through hinged, rigid, or elastic

connections. The present work has intended to extend the study to the behaviour of systems consisting of arrays of components in single and several rows (i.e. mats).

### **1.3.3 Hinged-rigid connection as the focus of this study**

There were mainly two reasons why this study was focused on the hinged-rigid type connection.

Of the main two types of connections, namely the hinged and the rigid, the rigid connection is widely preferred to the hinged for the basic reason that a structure with such connections has much higher load capacity than the same structure with hinged connection. However to obtain a perfect rigid connection between pontoons is very difficult. This is because of many factors such as manufacturing tolerances and the allowances that are in the connections such that they can be easily assembled on the site in very little time. This gives rise to hinged-rigid connections, which when manufactured were intended as rigid connection, but due to the factors mentioned, slack is introduced in the joint which allows for some hinge action. The fact that this happens more often than not and that previously this effect had not been studied in detail, was the first reason why this type of connection was concentrated on in this study. The objective was that one could predict the effect of the hinged action has on the structure before it is made and thus not only could predict its performance more accurately, but if necessary make modifications to the design in the very early stages of the design process. This is of course preferred to having to make the structure and then experimentally observe the effect of the hinged action on the whole structure. This work from this perspective has a lot of time and money saving potential.

However the second and the main reason for this choice is of a more practical and performance related nature. A hinged-rigid connection allows the designer to make use of the benefits that are offered by the two standard types of connections, the hinged and the rigid. The designer, by increasing or decreasing the amount of locking angle can make the hinged-rigid connection behave more like a hinged or

rigid connection respectively. This aims to solve the problem with the two types of connections that are used frequently. A structure with hinged connections is very responsive to loads and reacts by large amounts of displacements in an effort to reduce the moment on the connections. On the other hand the structure with the rigid connection is not so responsive because the load is distributed to the whole structure via the joints. Thus while the displacement of the structure is much less, the moment on the joints can reach the critical limit and damage the structure. In a rigidly connected structure, if one could reduce the amount of the load that the joints had to transfer to the rest of the structure, the moment on the joints would be reduced, thus increasing the structure's load capacity. A hinged-rigid connection aim to do just that. In such a structure, a portion of the load works against the force of buoyancy to drive the connections into a locking position, by which time the structure acts as a rigid one. However now, a lesser part of the load is left for the joints to distribute to the rest of the structure. The amount of locking angle will ultimately determine how much of the load is shed and how much is transferred. This ability makes this type of joint very practical and beneficial.

## **CHAPTER 2 LITERATURE REVIEW**

### **2.1 General**

In recent years, multipli-connected structures have gained a noticeable interest among researchers and a lot of work has been carried out in this area. However those dealing with connection types and specially the ones discussed in this work are rare. Given below is a review of the literature from both closely related works and the works that have a more remote relation to this work.

### **2.2 Review of closely related literature**

The work that comes under this heading can itself be further sub-divided into two areas, theoretical studies and experimental work.

#### **2.2.1 Theoretical studies**

Adee [4-7] in early work on floating breakwater design considered the wave following impact effect. These studies concentrated on measuring the transmission coefficient of the incident wave, which was found by dividing the transmitted wave height by the incident wave height. In the work it was assumed that both incident wave and the body motions were small.

The work separated the computation of the performance of a floating breakwater into three parts as follows:

1. Formulate equation of motion
  - Calculate hydrostatic forces and moments.
  - Evaluate hydrodynamic coefficients in equations of motion.
  - Compute exciting forces on breakwater.

- Solve for the motions and motion-generated waves.
  - Compute static mooring-line response and calculate forces in the mooring lines.
2. Solve for the waves diffracted by a rigidly restrained breakwater.
  3. Sum component to obtain total reflected and total transmitted waves.

In his work, Adee, was less concerned with the actual forms of the floating structures and the method of connecting them and his main objective, as mentioned, was to formulate the transmission coefficient of the wave energy through the structure.

Tsinker [8] described the specifics of multipli-connected floating structures including the following:

1. Chain of pontoons with individual deck sections (Fig 2.1).
2. Linked pontoon system (Fig 2.2), which the forces are shown in connections (Fig 2.3).
3. Redundant pair system (Fig 2.4).

In addition, he also performed some analysis for different models of multipli-connected structures such as a double-cantilever system with suspended intermediate span and continuous beam over pontoons.

He investigated two different methods of connecting the structure together. In one method, the pontoons were connected to each other via hinged connections, and in the second method, a deck was installed on the pontoons, such that the pontoons were connected to each other via the deck, which consisted of sheets connected to each other by a hinged connection.

The chain of pontoons with individual deck sections (Fig 2.1) and redundant pair system (Fig 2.4) are not related to this work. The linked pontoon system is a set of pontoons with hinged connections (Fig 2.2) is relevant.

Piskorski [9] considered a floating pontoon bridge with limited free rotation between the pontoons in one direction. The work divided the pontoon bridge into two separated zones. The contact zone, characterised by the lack of voids between the pontoons (which was considered as a rigid body) and open zones on both sides of the contact zone. The work treated the open zone region as a super element with linear elastic characteristics and considered the vibration in the open zone excited by the concentrated force at its edge. The work utilised Lagrange's formula but did not consider damping forces.

In his work, Piskorski was more interested in the open zone, whereas the subject of this thesis however is primarily interested in the contact zone and its analysis. He does however suggest some modifications to his formulations if they were to be used to analyse the contact zone.

Although there are some similarities, the formulation that he carried out for the open zone can not be extended for hinged-rigid connections which is the main aim of this work.

Che et al. [10] presented a method for predicting the loading and response of a very large floating structure (VLFS) in regular waves. The motion of a system of integrated modules acted upon by waves was solved. Two-dimensional hydro-elastic theory was applied to a VLFS with multiple modules and extended in the longitudinal direction. A modified strip theory was employed to analyse the hydrodynamic coefficients. The mooring system was not considered with the structure, but assumed to remain stationary on location. The system was modelled in two ways. In the first model, the longitudinal sequence of modules was considered to form a single beam having varying shear and flexural rigidities. In the second model, the module was considered to be rigid, that is undeformable as a result of the wave loading. The boundary-element method and Greens function methods were used to obtain a connected system of semi-submersibles.

Their conclusion is that one can reduce an array of VLFS modules to a simple model of rigid bodies with hinged connections and the numerical results will be still valid and accurate. They state that the simplified method employed in the case

of the rigid modules with hinged connections also appears to be useful for the engineering design of VLFSs.

Their work is good enough for hinged and elastic connections however one can not apply this formulation for hinged-rigid connections.

Takaki and Tango [11] studied both theoretically and experimentally wave drift forces acting on a very large floating structure consisting of multiple barge type modules. The wave drift forces were estimated on the multiple floating structure, linked with rotationally rigid connectors. The effects of wave drift forces on the connector condition and the numbers of bodies were discussed. Three dimensional panel methods were used to determine the hydrodynamic forces with hydrodynamic interaction effects included, and the coupled equations of motion were solved directly. The number of modules was shown to effect the amplitude of motion in head sea conditions. Furthermore the effect of the connecting condition was discussed on the wave drifting forces.

They show that the way the modules are connected together in VLFS (i.e. rigid or hinged) can greatly affect its performance in terms of wave drifting forces. It was shown that for long wavelengths (i.e. when the wavelength to VLFS length ratio,  $\lambda/L$  exceeds 4) the hinged structure is considerably more resistant to drifting forces. For smaller wavelengths ( $\lambda/L < 1$ ) both types of structures showed similar behaviours, however for mid-range wavelengths ( $1 < \lambda/L < 3$ ) the hinged connection was considerably more effected by the drifting forces than the rigid structure.

Huang [12] presents the motion characteristics of a pair of coupled International Organisation for Standardisation (ISO)-configured pontoons as observed in a hydraulic model test, and addresses the significance of these tests to the design of rigid connections. This work is part of a program run by the US navy to develop the connecting technology required for assembling floating platforms under conditions of elevated sea states, using ISO-configured pontoons suitable for rapid transport aboard commercial containerships.

He concluded that it is feasible to assemble large floating platform on the open sea using prefabricated modules configured for rapid ocean transport abroad commercial ships. Further it was pointed out the greatest difficulty in doing this was the relative wave induced motions of the two to-be-connected modules, and that effective control of relative motion and especially relative surge is very important to the entire assembly procedure. To safely and easily assemble the structure, he stated that there needs to be a large separation force maintained within the pontoon array to offset surge forces generated by wave action.

Hatch, Huang and Barthelemy [13] conducted and surveyed the results of a series of sea trials to assess the credibility of a new connection system for joining multiple pontoon barges in elevated seaways. These new connectors and supporting methods of rigging and joining were designed to reduce and relieve the dynamic loads that occur as a result of relative motion and tug-induced forces.

After pointing out that currently the only commercially used flexible connecting systems are limited almost exclusively to inland waters, they conclude that there is great potential for the new NFESC (Naval Facilities Engineering Service Centre) developed connector system for both commercial and military uses.

Takaki, Lin and Higo [14] studied the motion of a very large floating structure consisting of multiple barge type modules. They used a three-dimensional panel method to determine the hydrodynamic forces taking into account accurately the effect of hydrodynamic interactions among the modules. They also estimated the wave drifting forces on the multiple floating structure with several kinds of connectors (hinged, rigid and elastic).

The results of this work are very similar to those of Takaki and Tango [11], namely that the connecting condition makes a contribution to the wave drifting forces, especially in long wave length range. The wave drifting forces on the structure with hinge connectors and elastic connectors (the elastic connector was not analysed in [11]) become smaller than those of the structure with rigid connectors. On the other hand, there is little effect of connecting conditions in the short wave length range. Further, the structure with rigid connectors doesn't have a

peak value of the wave drifting forces around the natural period of the first mode, whereas in the structure with hinged and elastic connectors, the wave drifting force coefficient exceeds the value of 2 around the natural period.

Ohmatsu [15] uses the principle of linear superposition to perform time domain analysis on the hydroelastic response of VLFS in irregular waves. For this he uses the response amplitude operator from the numerical analysis code developed for pontoon-type VLFS with the capability to analyse hydroelastic responses in regular waves of relatively short wavelength. By the same manner he estimates the response to the impact due to dropping objects or landing of aircraft on the VLFS.

He continues to validate the linear superposition theory by use of experimental and theoretical results, and he shows that the theory can also be applied for an elastic response to the short wavelength to a  $\lambda/L=0.06$ , at least. It is also stated that for structures of size less than 5000m, the computation time of this method is smaller than the direct solving method of the equation of the motion in the time domain.

Haeda et al. [16] developed the estimating method of the hydroelastic response of a very large pontoon type floating structure. In this method, the pressure distribution method with shallow draft assumption was used to obtain the hydrodynamic forces considering the elastic motion of a floating body. The elastic responses of very large floating structure were estimated by using 1-D beam modelling. On the other hand, to observe the elastic response of a large pontoon type structure they carried out experiments in head sea and head-beam sea conditions. The experimental model was an elastic model of pontoon type large floating body.

It is a conclusion of their work that the responses of the vertical displacement and the bending moment show fairly significant differences because the frequency characteristic of the vertical displacement is relatively simple, but the characteristic of the bending moment is rather complicated. Namely that in the wave frequency range of  $\lambda/L>0.067$ , the vertical displacement is small, hence

the effect of the bending stiffness can be neglected. In the wave frequency range of  $\lambda/L > 0.067$ , considering the difference of the vertical displacement related to the bending stiffness, it may be concluded, they state, that smaller bending stiffness is rather advantageous.

Sannasiraj et al. [17] used finite-element techniques to study the diffraction/radiation boundary value problem arising from the interaction of oblique waves with a freely floating structure. Further, the hydrodynamic behaviour of two-dimensional horizontal floating structures under the action of multi-directional waves has been studied. They use the linear transfer function to determine the wave exciting forces and motion responses of a structure of finite length in short-crested seas.

Lee and Newman [18] present a computational analysis for the effect of waves on very large hinged vessels consisting of several modules, connected by simple hinges. They consider two generic types of modules, rectangular barges and semi-submersible. The results presented include computation of the vertical motions, structural deflections, and hinge shear forces in head and oblique waves, for a configuration with 5 modules each of length 300 metres. To permit a quantitative assessment of the importance of hydroelasticity, a range of structural stiffness parameters were considered.

The results demonstrate that it is feasible to analyse linearized wave interactions for several interacting semi-subs. They also characterised the hydroelastic effect with the non-dimensional stiffness parameter  $S$ . Based on Length  $L=300\text{m}$  for each module, they find that hydroelastic effects are important in the range  $10^{-4} < S < 10^{-3}$  however for larger values of  $S$  the structure is effectively rigid. For smaller values of  $S$  the structure behaves like a completely flexible monohull.

Their results also indicate that relatively small draft of the barges can be significant in this context. It is thus dangerous to idealise a large floating structure by a mat, unless the stiffness is sufficiently large to diminish the importance of the higher modes where the body inertia is significant.

Wang et al. [19] describe a simplified analysis procedure based on 3-D hydroelasticity, which can be used to determine the motions and intermodule forces of a multi-module VLFS. Their method is applicable to an arbitrary geometric layout of the modules, but to simplify the work, the modules considered were all rigid and thus meaning that all deformations occur in the module connectors. The procedure was used to analyse the response of a 5-module VLFS in both regular and irregular waves.

Their results indicate that for VLFS, the fluid coupling of the modules is relatively weak. However, the mechanical coupling through connectors can have a significant impact on the motions. If the connectors provide substantial resistance to the relative rotations of adjacent modules, then the vertical and rotational (pitch) motions are substantially reduced compared to the motions for a single module. However, if the connectors do not provide sufficient rotational stiffness, the module pitching can be dramatically increased compared to the motions of a single module.

Concerning practical issues the Murdoch and Bretz [20] paper is a report on the task given to the Naval Facilities Engineering Services Centre (NFESC) to develop a conceptual design package for an expeditionary port facility capable of rapid installation. Simultaneous offloads of two deep draft cargo ships are intended during operation, and located up to 3km offshore. The so called Rapidly Developed Pier (RDP) would include a floating multi-deck pierhead moored by a single point mooring at the bow and a compliant mooring system aft, allowing the pierhead to be rotated about the SPM pivot point.

### 2.2.2 Experimental work

Endo et al. [21] carried out analysis on experimental models to estimate the modal properties such as natural frequencies, damping ratios, and mode shapes for a unit-linked large floating structure model. Fluid-structure coupled vibration tests were carried out. The experiment was performed by hitting the force transducers arranged on each unit with an impact hammer made of soft rubber. A number of models, namely one, two, and eight unit linked models, were used in the study. Each unit consisted of a rectangular prism connected to each other by steel plates. A floating model was anchored by two spring-wires on the base edges of each unit, Fig 2.5.

The vertical acceleration responses were measured on the upper surfaces of the model by arranging acceleration sensors on each unit. The transfer functions defined by normalised input and output data were established. The modal properties such as natural frequencies, damping ratios, and mode shapes were estimated by carrying out curve fitting of the transfer function obtained in the vibration tests

Furthermore, the two-dimensional formulation of fluid-coupled free vibration analysis with the aid of the BEM (Boundary element method) was used to take into account fluid-structure interaction. The coupled natural frequencies and the corresponding mode shapes were obtained and compared to the experimental data.

Their results show that the natural frequencies and mode shapes obtained by experimental modal analysis and two-dimensional theoretical calculations almost agree on every mode. Thus to obtain the modal parameter of the structure with lower stiffness, the experimental modal analysis is an effective tool.

## **2.3 Relevant issues from "International Workshop on VLFS"**

These papers discuss issues, which are more distantly related to this work, and only the most relevant are considered here.

### **2.3.1 Design philosophy of VLFS**

Suzuki and Yoshida [22] write about how a large floating structure is characterised by its significant elastic response. They present discussion on the elastic response and design of the structure. General dynamic response characteristics are shown, and according to the understanding of the elastic behaviour a new type of the structure whose perimeter structure is modified to suppress excessive response is proposed. Secondly the authors propose a structural type whose redundancy and safety are augmented. They introduced mechanical connectors to the structure and the whole structure was constructed from independent element floating structures, which were connected, to each other by the mechanical connectors. They also state that the safety of the structure in the construction stage can also be improved by this method.

Takarada [23] discusses the fact that much progress has been made over the last 20 years on construction technologies for very large floating structures, and that we have reached the stage where we are now able to safely and economically build such structures. Here, in the interests of making the structures even better, the author presents a few very short comments relating to the control of environmental conditions and to the combination of structural types and human factors.

Gustavsen et al. [24] briefly outlines current design philosophies for floating bridges, with an eye on aspects that are deemed to be of interest in the context of Very Large Floating Structures (VLFS). Since design of submerged floating tunnels (SFT) rests with people in the same milieu and is dealing with many of the same problems as in the design of floating bridges, while being in some respect more critical, some of the design philosophy on that subject has also been included

by the authors. The authors also point out that the design philosophy and methodology for floating and submerged tunnel bridges draws heavily on Norwegian experiences in two large fields. Namely: (1) offshore structures, and (2) conventional bridges.

He concludes very briefly that the long life of most VLFS will depend on no more than 7 factors, namely, careful attention to areas such as

- Met-ocean data
- Loads
- Materials
- Proper application of well formulated design rules
- Design analysis and verification
- Careful construction and quality assurance
- Planned maintenance and instrumented verification of behaviour.

Arita [25] discusses the maintenance philosophy of VLFS from viewpoint of its total safety. Purposes of maintenance, consideration at each stage of lifetime, maintenance strategies, new technologies and databases to be developed in order to realise VLFS were studied. The author reasons that VLFS are quite different from floating structures constructed up to now in scale and service period. VLFS maintenance should start at its initial stage of preliminary plan of a project and precisely discussed at every stage its project. VLFS maintenance proposed is based on an estimation of structural deterioration over the whole life period of the VLFS. They state that if the structure reaches its given life time or the gap between estimated and measured deterioration exceeds a given criterion, it is the end of its service period. VLFS maintenance from the author's point of view is a system consisted of maintenance strategy, estimation technologies, databases and evaluation committee. The author deduces that new technology necessary to be developed includes an estimation method of structural deterioration, modification method of a gap between estimated and measured values and the definition of end of service period. Databases necessary to be developed includes those of deterioration of materials used for the structure and its protection, accident data of

offshore structures and other databases necessary to support the maintenance system.

He draws his work to a close by categorising the VLFS maintenance into three purposes of structural, social, and functional. To satisfy the three purposes mentioned he states the maintenance system is to be consisted of three parts, which are the main part, databases and evaluation committee. The function of an evaluating committee would be to evaluate all the maintenance activities, initial deterioration estimation, modification method of gap between evaluated and observed deterioration and decision on the end of service period based on the condition of the end of service defined in advance.

Yutaka [26] discusses two main proposals that were given in the two phases of the completion of the Kansai International Airport (KIA). The first proposal was for a semi-submergible type of floating structure, however this was later overshadowed by a proposal for box-shaped pontoon with breakwaters around it to compete economically with land reclamation. He also conducts surveys from expected future users of these structures.

### **2.3.2 Example of conceptual design**

Maeda et al. [27] aim to tackle the problem of adopting a VLFS for use as a base for power generation. Two main structures are put forward, the semi-submergible and the pontoon boxes. The idea will be mainly developed for renewable energies such as solar heat and light, wave, wind and OTEC (Ocean Thermal Energy Conversion). The authors further go on to make suggestions as to how make these plants more economically competitive with non-renewable power sources.

Murdoch and Bretz [28] discuss and analyse a conceptual design of a moored floating system. The structure conceived consists of a pierhead that is a custom designed and fabricated barge structure with an overall length of 950 feet, 106 foot width, and 71 foot depth. The pierhead mooring system consists of a single point mooring (SPM) located at the bow (shoreward end) of the pierhead and four

anchor legs at the stern. This mooring configuration ensures minimal movement of the pierhead at the bow where it must interface with the fixed approachway, but allows the pierhead to be rotated over an arc of ninety degrees, forty-five degrees to either side of the initial orientation, with the SPM defining the rotation point. The final link in the system is the approachway system, built of individual pile supported spans each nominally 60 feet long, 24 feet wide and 7 feet deep, which provides a fixed, elevated roadway connecting the pierhead to the shore.

Young Chung and Hoon Chung [29] develop key technologies for the design and fabrication of floating barge systems for various kinds of plants such as desalination plants, waste-treatment plants, etc. The work also includes research on the floating breakwater systems for mitigation of wave and current loads on floating plants.

Blood [30] puts together a report on the modelling and testing of a Pneumatically Stabilised Platform. A 1:22.85 scale model of a proposed 100 x 300 foot prototype Pneumatically Stabilised Platform (PSP) was constructed and tested to gather data to confirm the accuracy of the hydrodynamic and structural design tools under development. Because it was impractical to scale atmospheric pressure, the tests were limited to confirmation of the "air pocket factor," a parameter relating hydrostatic stiffness to the compressibility of air, and the gathering of rudimentary data on air movement, stability, and wave attenuation. After conducting a series of tests he concludes that the modelling was successful.

After showing the many benefits of the PSP, he points out that there are many uses for such a system in commercial areas such as, airports, shipping port, conversion plants, and other on-sea applications. Also the PSP has some advantages that makes it attractive for defence purposes. One such advantage is that unlike a barge platform, which must respond directly to different heave forces, a PSP absorbs these forces in compressed air, which can be distributed throughout the platform. Further, unlike the semi-sub platform, the PSP provides relatively calm water on its down wave sides due to its natural wave attenuation which enables it to be used to create harbour-like conditions in an open seaway.

Ohmatsu [31] in his work deals with a brief outline of the Ship Research Institute

(SRI) type VLFS that is composed by pontoon type main body and semi-sub type wave breaking structure around that main body. He proposes a wave breaking structure, which can reduce wave effect and elastic deformation of the main body. The SRI VLFS has the claimed advantage of less construction and maintenance cost of pontoon type structures and also the advantage of better wave damping capability, associated with semi-submersible structures.

### **2.3.3 Strength and reliability**

Okada et al. [32] provide a structured reliability assessment method for fatigue strength of large-scale marine space structures under non-linear and irregular wave induced loads by using a varying load simulation technique. The applicability of the method is investigated through numerical examples successively applied to hybrid type structures with floating bodies and supporting foundations under some irregular sea state conditions. After conducting some tests they deduced that the effect of the number of supporting foundations on the reliability level is remarkable for large significant wave height.

Endo and Yago [33] in their work, perform a case study in order to try and determine the statistical maximum wave-induced load that a given pontoon will be subjected to. They produce their results based on short-term and long-term predictions and their method takes into account the modelling error and the uncertainty of the load. They come to the conclusion that the given pontoon (300×60m) has no problem when subjected to a 100-year-return wave load.

Yao and Fujikubo [34] in their work show that incorporating a simple modification in the standard method for structural analysis of VLFS can be of benefit. In this modification, on top of considering the 2D-grillage model, stiffness evaluation for grillage-beam elements and load applications, the torsional stiffness of grillage-beam elements is also employed. Later on they also compare and contrast three methods of converting fluid pressure to nodal forces, which are LAM-1, LAM-2 and LAM-3. The three different methods differ in the location and the node that the fluid pressure is modelled to apply to.

The main conclusions of this work were that, the influence of a Poisson's effect of deck and bottom plating on the calculated results is small and that the coarser mesh model gives the smaller deformation.

#### **2.3.4 At-sea construction and maintenance technologies**

Nakano, Kinoshita and Kozai [35] produce a report on the modelling of an ultra large floating structure. The model was constructed by joining 9 massive floating module blocks in open-sea conditions. During the completion of the 300 Maniar 60×2m model, several experimental procedures were attempted. These included water sealing, the application of a work vessel to access the bottom of the model in water and welding of the bottom plates on one side and both sides. At the end the authors consider these new procedures to be effective and useful in the fabrication of real ultra large floating structures.

Okubo et al. [36] describe a method of estimating the forces acting on joints between floating units when they are connected at sea. An important process in the construction of pontoon-type floating units now being proposed for use in off-shore floating airports. Since the height-to-length ratio of prefabricated floating units is smaller than that of conventional small-scale floating structures, the enhanced effect that elastic deformation has on these forces is a matter of concern. They investigated this issue through experiments on a model subjected to wave motion in a water tank. The forces acting on inter-unit joints, the vertical displacement of the units, and the strains in the units were measured. The response characteristics of the forces were studied while the units were subjected to wave motion and the relationship between the forces and elastic deformation in higher-order modes was clarified from these measurements.

Messier and Thompson [37] compiled a non-linear, three dimensional finite element modelling technique, developed for computing the dynamic response of a large floating structure to wave and current excitation. Airy wave theory was used

to characterise the ocean model. After the credibility of the program (computational) was confirmed by comparison of some results with experimental data, a series of computational studies were conducted to examine the effects of varying inter module connector location and structural stiffness on the predicted forces of constraint between floating structural modules. Several sea states were considered. Relative displacements and forces of constraint were computed.

### **2.3.5 External loads and response analysis**

Faltinsen [38] in this work has derived an estimate of local stresses due to bottom slamming on a floating airport. This is related to wet deck slamming on multihull vessels and theoretical and experimental results from drop tests of horizontal elastic plates of steel and aluminium on regular waves. He remarks that the results from the experiments agree well with the numerical computations and that this study reveals, both numerically and experimentally, that the slamming induced local stresses are highly influenced by dynamic hydroelastic effects. The maximum bending stresses are not sensitive to where the waves hit, or to maximum pressures. He further adds that measured maximum pressures are very sensitive to external conditions and cannot be used as a measure of maximum local bending stresses.

The work concludes that the maximum stress is proportional to the impact velocity and is not sensitive to where the waves hit the plate. It is also shown that the maximum stresses decrease with increasing the values of  $L/R$ , where  $L$  is the plate length and  $R$  is the curvature radius of the wave crest. Also the linear dependence between the maximum stresses and the impact velocity makes it possible to use the statistical properties of the impact velocity in a sea state to express the extreme values for the maximum local slamming induced stresses in the wetdeck of a multihull vessel.

Yoshimoto et al. [39] in this work investigated the occurrence and the prediction of impact pressure due to the slamming, which acts on a very large floating structure (VLFS). The main conclusions were as follows:

- The occurrence of slamming of the VLFS depends on the extent of the bottom emergence and the rising speed of the relative wave height at the bow. The peak values of the impact pressure components depend on the rising speed of the relative wave height at the bow.
- In the case of the model with low rigidity, its extent of the bottom emergence is smaller than the high rigidity. However, the rising speed of relative wave height at the bow of the model with low rigidity becomes larger due to its large elastic response, so that the large impact pressure occurs.

Takagi [40] in this work, theoretically and experimentally, discusses elastic deformations and the mooring force of 8 very large floating bodies with tsunami waves. The theory was based on a shallow water wave theory and the matched asymptotic expansion method and the modified Boussinesq equations were employed for the representation of long waves beneath a floating elastic plate which was a simplified model of the very large floating body in tsunami waves. Measurements of the elastic deformation and the mooring force of floating elastic plate with the solitary wave were also carried out.

It was concluded that the experimental results of the elastic deformation and the mooring force are in very good agreement with those of the theoretical simulation. Hence it was confirmed that the theoretical simulation is accurate enough as a design tool of the very large floating body against the excitation due to tsunami waves.

Newman, Maniar and Lee [41] here present computations based on three-dimensional radiation/diffraction theory for several examples of VLFS configurations, to show the feasibility of using existing panel methods for the analysis of wave effects. They focus their attention on structures, which are very large relative to the wavelength. The examples considered include large rectangular arrays of vertical cylinders, a floating ship with a long cylindrical hull,

a long submerged body, a rectangular barge, and a floating mat.

Ohkusu and Nanba [42] in this work present a new method to analyse the response of a thin elastic plate of large horizontal size floating in waves. Huge horizontal size and small thickness are typical of the recent designs of floating airport. A benefit of this new method is that one does not need the modal analysis of the body motion. Furthermore, the solution of a hydrodynamic boundary value problem and the solution for the body motion including the elastic deflection are simultaneously obtained.

They present an efficient method to predict the elastic deflection of a very large platform of thin plate configuration in waves. A thin elastic plate floating on the free surface is interpreted as a part of the free surface and this free surface motion is itself the deflection of the plate. The problem is considered as a boundary value problem in hydrodynamics rather than the determination of the elastic response of the body to hydrodynamic action. It was demonstrated that correct understanding of the hydroelasticity of the platform is attainable with this approach. Simpler numerical implementation of the phenomena will be a benefit of this approach. This has applications such as predicting the complicated hydroelastic behaviour of very large platforms like floating airports in waves.

Kashiwagi [43] work revolves around two new ideas. First a new calculation scheme is described for the pressure distribution method, giving directly the pressure on the bottom of a VLFS with shallow draft. This method also utilises bi-cubic B-spline functions for representing the unknown pressure and a Galerkin method for converting the integral equation into algebraic simultaneous equations. Secondly he proposes a mode-expansion method for solving the vertical vibration equation of a rectangular plate. He backs up his methods with confirmation of the results matching known experimental cases

Takaki and Gu [44] in this work deal with three-dimensional responses of huge floating structure in head and quartering seas. A huge mat-like floating structure is considered as an elastic plate. First the authors estimate dry-eigenmodes of the completely free plate by employing the finite element method. Then,

hydrodynamic pressures exerted on it are evaluated by combining the pressure distribution method and the dry-eigenmodes. Wave-induced motions of the plate are expressed as a superposition of the dry-eigenmodes, and the principal coordinates are finally determined by solving a set of equations of motion. They verify the modal analysis through comparisons of calculated amplitudes of vertical motions and instantaneous shapes of a plate model in head seas with available measured data. They show reasonable agreements. Then they applied this method to a large floating module of 300m×60m, and investigated its motions and disturbance waves around it in head and quartering seas. Finally, response amplitude operators of its first 10 modes in all heading waves with various wavelengths are shown in their work.

Kagemoto et al. [45] in this work propose a method whereby one can predict hydroelastic behaviours of a very large floating structure. By dividing the structure into a number of small structures and the continuous deformation of the structure is represented by the succession of the discrete displacement of each small structure. Each structure is treated as if it were an independent floating body while the structural constraints are taken into account as additional restoring forces on its motions. The hydrodynamic interactions among the divided structures are accounted for in the evaluation of hydrodynamic forces once their complex motion amplitudes are known. The motion amplitudes are, in turn, determined from the equation of motions, which are excited by the hydrodynamic forces. Therefore by solving the equations of hydrodynamic interactions and those of motions simultaneously, the hydroelastic interactions are properly accounted for and the motions of each small structure, which represent the local behaviours of the total VLFS, are determined in one computation.

In this work a new method that enables us to carry out the hydroelastic analysis of a VLFS is presented. The present method does not restrict the type of structures and can be applied to a box-shaped VLFS, to a leg-supported VLFS, both of which are now being studied in Japan, as well as a semi-submersible type VLFS(MOB), which is being studied in the US.

Price, Salas Inzunza, and Temarel [46] apply hydroelasticity theory to investigate the dynamic behaviour of stationary and neutrally buoyant barge type (i.e. rectangular box) structures in waves. Beam and plate finite element (FE) models are used to describe the dynamic characteristic of the barge in vacuo. A potential flow model, whereby the wet surface of the barge is discretised by rectangular panels containing a source at their centre, is used for the wet analysis. The effects of barge size and flexibility on the use of different FE idealisations and the wave-induced loads are discussed

Inoue, Zhang and Tabeta [47] put forward a linearized analysis of the hydrodynamic forces on the very large floating structure in waves. The hydrodynamic interactions of the elastic deformations and the hydrodynamic external forces are also discussed. The motion responses and wave drift forces of a floating airport is investigated. They also carry out numerical simulations by means of a multilevel model to discuss the interaction of ocean currents and a large floating structure in a bay.

Quanming et al. [48] present the time simulation of motion responses of a moored VLFS in waves. The equations based on Cummins' concept of impulse responses are employed, and solved in the time domain by using Adams prediction-correction method. They obtain hydrodynamic coefficients and first order wave-exciting forces involved in the equations from a three-dimensional potential theory in the frequency domain. The second order wave drift forces and the non-linear mooring forces are also taken into account. The numerical results of a multi-module large floating structure consisting of five identical semi-submersibles responding to waves with three incident wave angles and two sea states are illustrated

Yasuzawa et al. [49] in this work point out that when we estimate dynamic responses of VLFS structures, fluid-structure interaction cannot be ignored because elastic defamations as well as rigid motion of the structure produces hydrodynamic forces. In the present study, the authors have developed a numerical code for dynamic response analysis of a flexible floating structure of mat-type in regular waves and examined dynamic characteristics of the flexible

floating structure. The floating structure is treated as a rectangular flat plate by use of finite elements, and boundary elements are used in the formulation of the sea region.

Riggs [50] in this work derives the hydrostatic stiffness coefficients for flexible floating structures. The formulation includes the hydrostatic pressure term as well as the effect of the structural (i.e., gravity) loads. Riggs finds that the hydrostatic term agrees with a formulation presented previously by Newman. The advantage of the present formulation is that it also includes the structural loads, as well as providing an alternative equivalent expression for the hydrostatic terms. The results are useful both in hydroelastic analyses as well in finding the deformations in the static equilibrium position. Riggs presents several examples to investigate the magnitude of errors that result from certain simplifications, which are sometimes used, in the determination of the hydrostatic stiffness, such as ignoring the gravity loads.

The result of this work was the derivation of formulation for the hydrostatic stiffness coefficients of flexible structures, which includes the effect of both the hydrostatic pressure as well as the structural gravity loads. The formulation was used to investigate the impact on the stiffness coefficients of common simplifications often used in hydroelastic analyses. In particular, it was found that ignoring the volumetric strain could result in significant errors in the stiffness coefficients. The errors, introduced by ignoring Poisson's ratio are directly proportional to the ratio. Depending on the value of an effective Poisson's ratio for practical, built-up structures, it was shown that the errors may be of the same order as the correct coefficients.

Watanabe and Utsunomiya [51] show a numerical method for analysing transient response of a Very Large Floating Structure as an aircraft lands. The method employed is the Finite Element Method (F.E.M.) for both structure and fluid domain. The effect of the dynamic coupling between the fluid and structure has been considered together with the effect of free surface of the fluid. The authors model the structure as an elastic floating plate having circular shape, and the impulsive loading has been applied at the centre of the circular plate. The

numerical examples show that the effect of the added-mass of the fluid is very large; the dynamic responses with the effect of the added-mass are reduced compared with those without considering the effect of the added-mass.

Ueda et al. [52] in their work establish a computational analysis method to calculate motions, mooring forces, deformations and working stresses of floating bridges subjected to wind and waves.

Shiraishi et al. [53] in their work evaluate the effect of the incident wave direction, wave height, wave period and rigidity of the floating body on the characteristics of the motion and the deformation of long flexible floating structures. Hydraulic model tests were also carried out and the results were analysed.

### **2.3.6 Mooring technology**

Sekita et al. [54] deal with the motion response analyses of fluctuating winds and seismicity including the deformability of mooring dolphin structures required for rare intense loads. This work also discusses the functions required of shock absorbing mechanisms indispensable to mooring facilities such as mooring dolphin.

## **2.4 Standard package**

There are a number of commercial software packages for structure analysis purposes. Many of these were considered with their relevance to this work in mind. Of those, SAP, ANSYS, NASTRAN and ABAQUS are the most widely used and powerful ones. In particular ABAQUS was considered to be the one most suited to this work. Having said that, due to difficulties that will be discussed in section 6.3, ABAQUS was found to be of limited use. It was not suitable for the hinged-rigid type of connector.

## 2.5 Review Summary

As has been shown in this chapter, many associated studies have been conducted in this field previously. While all of these were considered on multi-connected structures and VLFS, only one paper [9] was related to work on hinged-rigid type connections. However even in this work, Piskorski [9] considered the floating pontoon bridge with limited free rotation between the pontoons in only one direction. He divided the pontoon bridge into two separated zones. The contact zone, characterised by the lack of voids between the pontoons (which was considered as a rigid body) and open zones on both sides of the contact zone. The work presented in this thesis differs from his in that here it is primarily interested in the contact zone and its analysis, while Piskorski was more interested in the open zone. Hence as can be seen there is a real absence of work and studies done in this particular field which highlights the need for such studies.

Related to the last point, one also had difficulty in finding suitable codes that could be used for this study. The most powerful ones such as ABAQUS had their strengths in areas not used by this work and were otherwise weak so far as meeting the demands of this study were concerned (see section 6.3). This issue made it necessary for customised codes to be written which are detailed later.

## **CHAPTER 3 DEVELOPMENT OF HYDROSTATIC STIFFNESS FORMULATION**

### **3.1 Introduction**

To determine the displacements of joints, in order to be able to calculate the stresses occurring in the members, the stiffness of the structure must be evaluated. The stiffness of a multi-connected floating structure can be divided in two components, the structural stiffness and the hydrostatic stiffness. This chapter discusses theoretical work carried out to find the hydrostatic stiffness matrix of a multi-connected floating structure based on the hydrostatic stiffness matrices of individual pontoons.

### **3.2 Constraint equations**

Constraint equations provide relationships between degrees of freedom that are supplemental to the relationship represented by the basic stiffness equations. Constraints arise in many cases, including the multi-connected floating structure, in particular analysis methods of incompressible materials, treatment of special boundary conditions and in attempts to impose specified patterns of displacement over certain portions of the structure. A number of these situations will be discussed later in this text.

Each constraint equation represents an opportunity to eliminate one of the degrees of freedom in favour of the remaining ones. To take advantage of this point it is possible to form a transformation matrix that can be used to condense as many degrees of freedom as there are constraint equations from the stiffness equation. The matrix enables one to find the various displacement values, using much less algebra.

### 3.3 In-line array

#### 3.3.1 Basic hydrostatics

In order to be able to find the displacement of the joints, one first has to evaluate the modified stiffness matrix. To do this, the constraint equations are inserted into the basic equations of equilibrium. The following is the mathematical representation of the above statement.

The equilibrium equation for the quasi-static response of a multipli-connected structure with several pontoons connected in an in-line configuration can be written as:

$$[K(x)].\{x\} = \{F(x)\} \quad (3.1)$$

The static equation for any individual pontoon (considered as wall sided and with symmetry in the y, z plane Fig 3.1) can be written as:

$$\begin{bmatrix} A & 0 \\ 0 & B \end{bmatrix} \begin{Bmatrix} z \\ \theta \end{Bmatrix} = \begin{Bmatrix} F \\ M \end{Bmatrix} \quad (3.2)$$

$$A = \rho g L b \quad (3.3)$$

$$B = \rho g L b d G M_{\ell} \quad (3.4)$$

$$G M_{\ell} = \frac{d}{2} + \frac{L^2}{12d} - \frac{D}{2} \quad (3.5)$$

Where,

- $\rho$  is density of water
- $g$  is acceleration due to gravity
- $L$  is length of pontoon
- $b$  is breadth of the pontoon
- $D$  is height of the pontoon

- $d$  is draft of pontoon in still water  
 $z$  is vertical displacement  
 $\theta$  is pitch angle  
 $GM_t$  is longitudinal metacentric height  
 $F$  is force acting at centre of gravity of each pontoon  
 $M$  is hydrostatic moment acting on centre of gravity of each pontoon

The static equation for two identical pontoons besides each other without any connection may be written as:

$$\begin{bmatrix} A & 0 & 0 & 0 \\ 0 & B & 0 & 0 \\ 0 & 0 & A & 0 \\ 0 & 0 & 0 & B \end{bmatrix} \begin{Bmatrix} z_1 \\ \theta_1 \\ z_2 \\ \theta_2 \end{Bmatrix} = \begin{Bmatrix} F_1 \\ M_1 \\ F_2 \\ M_2 \end{Bmatrix} \quad (3.6)$$

### 3.3.2 Extension of the models for an in-line array

The expanded equation for  $n$  pontoons without any connection becomes as follows:

$$\begin{bmatrix} A & 0 & 0 & 0 & \dots & \dots & \dots & 0 & 0 & 0 & 0 \\ 0 & B & 0 & 0 & \dots & \dots & \dots & 0 & 0 & 0 & 0 \\ 0 & 0 & A & 0 & \dots & \dots & \dots & 0 & 0 & 0 & 0 \\ 0 & 0 & 0 & B & \dots & \dots & \dots & 0 & 0 & 0 & 0 \\ \dots & \dots \\ \dots & \dots \\ \dots & \dots \\ 0 & 0 & 0 & 0 & \dots & \dots & \dots & A & 0 & 0 & 0 \\ 0 & 0 & 0 & 0 & \dots & \dots & \dots & 0 & B & 0 & 0 \\ 0 & 0 & 0 & 0 & \dots & \dots & \dots & 0 & 0 & A & 0 \\ 0 & 0 & 0 & 0 & \dots & \dots & \dots & 0 & 0 & 0 & B \end{bmatrix} \begin{Bmatrix} z_1 \\ \theta_1 \\ z_2 \\ \theta_2 \\ \dots \\ \dots \\ \dots \\ z_{n-1} \\ \theta_{n-1} \\ z_n \\ \theta_n \end{Bmatrix} = \begin{Bmatrix} F_1 \\ M_1 \\ F_2 \\ M_2 \\ \dots \\ \dots \\ \dots \\ F_{n-1} \\ M_{n-1} \\ F_n \\ M_n \end{Bmatrix} \quad (3.7)$$

### 3.3.3 Constraint relationship

In general and in rather complicated form the constraints equation can be written as follows:

$$x_i = \alpha + \beta x_j + \gamma x_k + \psi x_\ell \quad (3.8)$$

Where,  $j = i + 1$ ,  $k = j + 1$ ,  $\ell = k + 1$

The constraint equation (3.8) is inserted into equation (3.7). For simplification equation (3.7) may be rewritten as [55]:

$$\sum_{s \neq i, j, k, \ell} K_{rs} x_s + K_{ri} x_i + K_{rj} x_j + K_{rk} x_k + K_{r\ell} x_\ell = p_r \quad (3.9)$$

Where,  $r$  is any row of the matrix  $K$

$p_r$  is the resultant force

Substituting equation (3.8) for  $x_i$  in equation (3.9) gives:

$$K_{rs} x_s + K_{ri} (\alpha + \beta x_{i+1} + \gamma x_{i+2} + \psi x_{i+3}) + K_{ri+1} x_{i+1} + K_{ri+2} x_{i+2} + K_{ri+3} x_{i+3} = p_r \quad (3.10)$$

Factorising (eqn. 3.10) we have:

$$K_{rs} x_s + (\beta K_{ri} + K_{ri+1}) x_{i+1} + (\gamma K_{ri} + K_{ri+2}) x_{i+2} + (\psi K_{ri} + K_{ri+3}) x_{i+3} = p_r - \alpha K_{ri} = q_r \quad (3.11)$$

Due to its nature the above operation has removed the symmetry in the coefficient matrix  $K$ . This can be reinstated by:

- multiplying the  $i^{\text{th}}$  row (3.12) by  $\beta$  and adding to the  $j^{\text{th}}$  row,
- multiplying the  $i^{\text{th}}$  row (3.12) by  $\gamma$  and adding to the  $k^{\text{th}}$  row,
- multiplying the  $i^{\text{th}}$  row (3.12) by  $\psi$  and adding to the  $l^{\text{th}}$  row,

Eventually we obtain:

$j^{\text{th}}$  row

$$\begin{aligned} &(\beta K_{is} + K_{js})x_s + (\beta^2 K_{ii} + \beta K_{ij} + \beta K_{ji} + K_{jj})x_j + (\beta\gamma K_{ii} + \beta K_{ik} + \gamma K_{ji} + K_{jk})x_k \\ &+ (\beta\psi K_{ii} + \beta K_{il} + \psi K_{ji} + K_{jl})x_\ell = \beta q_i + q_j \end{aligned} \quad (3.12)$$

$k^{\text{th}}$  row

$$\begin{aligned} &(\gamma K_{is} + K_{ks})x_s + (\gamma\beta K_{ii} + \gamma K_{ij} + \beta K_{ki} + K_{kj})x_j + (\gamma^2 K_{ii} + \gamma K_{ik} + \gamma K_{ki} + K_{kk})x_k \\ &+ (\gamma\psi K_{ii} + \gamma K_{il} + \psi K_{ki} + K_{kl})x_\ell = \gamma q_i + q_k \end{aligned} \quad (3.13)$$

$l^{\text{th}}$  row

$$\begin{aligned} &(\psi K_{is} + K_{ls})x_s + (\psi\beta K_{ii} + \psi K_{ij} + \beta K_{li} + K_{lj})x_j + (\psi\gamma K_{ii} + \psi K_{ik} + \gamma K_{li} + K_{lk})x_k \\ &+ (\psi^2 K_{ii} + \psi K_{il} + \psi K_{li} + K_{ll})x_\ell = \psi q_i + q_\ell \end{aligned} \quad (3.14)$$

Thus the matrix regains its symmetry.

In the above matrix there is no  $i^{\text{th}}$  column. It is possible then to insert the constraint equation (3.8) in place of the  $i^{\text{th}}$  row. After multiplication by  $K_{ii}$  we have:

$$-K_{ii}x_i + \beta K_{ii}x_j + \gamma K_{ii}x_k + \psi K_{ii}x_\ell = -\alpha K_{ii} \quad (3.15)$$

Recalling that the stiffness matrix  $K$  is symmetric, the  $i^{\text{th}}$  column must be completed with  $\beta K_{ii}x_i$  in the  $j^{\text{th}}$  row:

$$\begin{aligned} 0 &= \beta K_{ii}x_i - \beta K_{ii}x_i \\ 0 &= \beta K_{ii}x_i - \beta K_{ii}(\alpha + \beta x_j + \gamma x_k + \psi x_\ell) \\ 0 &= \beta K_{ii}x_i - \beta^2 K_{ii}x_j - \beta\gamma K_{ii}x_k - \beta\psi K_{ii}x_\ell - \alpha\beta K_{ii} \end{aligned} \quad (3.16)$$

Finally the corrected rows have the following form:

$j^{\text{th}}$  row

$$(\beta K_{is} + K_{js})x_s + \beta K_{ii}x_i + (\beta K_{ij} + \beta K_{ji} + K_{jj})x_j + (\beta K_{ik} + \gamma K_{ji} + K_{jk})x_k + (\beta K_{il} + \psi K_{ji} + K_{jl})x_l = \beta q_i + q_j + \alpha \beta K_{ii} \quad (3.17)$$

$k^{\text{th}}$  row

$$(\gamma K_{is} + K_{ks})x_s + \lambda K_{ii}x_i + (\gamma K_{ij} + \beta K_{ki} + K_{kj})x_j + (\gamma K_{ik} + \gamma K_{ki} + K_{kk})x_k + (\gamma K_{il} + \psi K_{ki} + K_{kl})x_l = \gamma q_i + q_k + \alpha \gamma K_{ii} \quad (3.18)$$

$l^{\text{th}}$  row

$$(\psi K_{is} + K_{ls})x_s + \psi K_{ii}x_i + (\psi K_{ij} + \beta K_{li} + K_{lj})x_j + (\psi K_{ik} + \gamma K_{li} + K_{lk})x_k + (\psi K_{il} + \psi K_{li} + K_{ll})x_l = \psi q_i + q_l + \alpha \psi K_{ii} \quad (3.19)$$

Now we have obtained an expression for the modified stiffness matrix. This is the theoretical model for n pontoons. In the following section the above method is employed in the different cases.

### 3.3.4 Connections

#### 3.3.4.1 Hinged

Using Fig 3.2, small angle identity and basic geometric relationships, the constraint equation for hinged-connections for the above system becomes:

$$z_i + \left(\frac{L+L_1}{2}\right)\theta_i + \left(\frac{L+L_1}{2}\right)\theta_{i+1} = z_{i+1} \quad (3.20)$$

Rearranging (3.20) gives:

$$z_i = -\left(\frac{L+L_1}{2}\right)\theta_i + z_{i+1} - \left(\frac{L+L_1}{2}\right)\theta_{i+1} \quad (3.21)$$

This can be written as:

$$z_i = \alpha + \beta\theta_i + \gamma z_{i+1} + \psi\theta_{i+1} \quad (3.22)$$

Where:

$$\alpha = 0$$

$$\beta = \frac{L+L_1}{2}$$

$$\gamma = 1$$

$$\psi = -\frac{L+L_1}{2}$$

$L_1$  is distance between two pontoons

$L$  is length of pontoon

Combining equations (3.15), (3.17), (3.18) and (3.19) with equation (3.6) will result in the modified matrix for the two pontoons:

Please note the following substitutions;

$$\begin{array}{cccc} x_i = z_1 & x_j = \theta_1 & x_k = z_2 & x_\ell = \theta_2 \\ i = 1 & j = 2 & k = 3 & \ell = 4 \end{array}$$

From equation (3.15) the  $i^{\text{th}}$  row becomes

$$-Az_1 + \beta A\theta_1 + \gamma Az_2 + \psi A\theta_2 = -\alpha A \quad (3.23)$$

From equation (3.17) the  $j^{\text{th}}$  row becomes

$$\beta Az_1 + B\theta_1 + 0 + 0 = M_1 + \beta F_1 + \alpha \beta A \quad (3.24)$$

From equation (3.18) the  $k^{\text{th}}$  row becomes

$$\gamma Az_1 + 0 + Az_2 + 0 = F_2 + \gamma F_1 + \alpha \gamma A \quad (3.25)$$

From equation (3.19) the  $l^{\text{th}}$  row becomes

$$\psi Az_1 + 0 + 0 + \beta \theta_2 = M_2 + \psi F_1 + \alpha \psi A \quad (3.26)$$

Equations (3.23 to 3.26) can be written as (3.27). This is the modified matrix for a system comprising two pontoons.

$$\begin{bmatrix} -A & \beta A & \gamma A & \psi A \\ \beta A & B & 0 & 0 \\ \gamma A & 0 & A & 0 \\ \psi A & 0 & 0 & B \end{bmatrix} \begin{bmatrix} z_1 \\ \theta_1 \\ z_2 \\ \theta_2 \end{bmatrix} = \begin{bmatrix} -\alpha A \\ M_1 + \beta F_1 + \alpha \beta A \\ F_2 + \gamma F_1 + \alpha \gamma A \\ M_2 + \psi F_1 + \alpha \psi A \end{bmatrix} \quad (3.27)$$

Adding a third pontoon to the two pontoons configuration will result in (3.28).

$$\begin{bmatrix} -A & \beta A & \gamma A & \psi A & 0 & 0 \\ \beta A & B & 0 & 0 & 0 & 0 \\ \gamma A & 0 & A & 0 & 0 & 0 \\ \psi A & 0 & 0 & B & 0 & 0 \\ 0 & 0 & 0 & 0 & A & 0 \\ 0 & 0 & 0 & 0 & 0 & B \end{bmatrix} \begin{bmatrix} z_1 \\ \theta_1 \\ z_2 \\ \theta_2 \\ z_3 \\ \theta_3 \end{bmatrix} = \begin{bmatrix} -\alpha A \\ M_1 + \beta F_1 + \alpha \beta A \\ F_2 + \gamma F_1 + \alpha \gamma A \\ M_2 + \psi F_1 + \alpha \psi A \\ F_3 \\ M_3 \end{bmatrix} \quad (3.28)$$

Please note the following substitutions;

$$\begin{array}{ccccc} x_s = z_1, \theta_1 & x_i = z_1 & x_j = \theta_1 & x_k = z_2 & x_\ell = \theta_2 \\ s = 1, 2 & i = 3 & j = 4 & k = 5 & \ell = 6 \end{array}$$

From equation (3.15) the  $i^{\text{th}}$  row becomes

$$-Az_2 + \beta A \theta_2 + \gamma Az_3 + \psi A \theta_3 = -\alpha A \quad (3.29)$$

From equation (3.17) the  $j^{\text{th}}$  row becomes

$$(\gamma\beta A + \psi A)z_1 + 0 + \beta Az_2 + B\theta_2 + 0 + 0 = (M_2 + \psi F_1 + \alpha\psi A) + \beta(F_2 + \gamma F_1 + \alpha\gamma A) \quad (3.30)$$

From equation (3.18) the  $k^{\text{th}}$  row becomes

$$\gamma^2 Az_1 + 0 + \gamma Az_2 + 0 + Az_3 + 0 = F_3 + \gamma(F_2 + \gamma F_1 + \alpha\gamma A) \quad (3.31)$$

From equation (3.19) the  $l^{\text{th}}$  row becomes

$$\gamma\psi Az_1 + 0 + \psi Az_2 + 0 + 0 + B\theta_3 = M_3 + \psi(F_2 + \gamma F_1 + \alpha\gamma A) \quad (3.32)$$

Bearing in mind equations (3.29) to (3.32), and matrix symmetry, the equation for a system with three pontoons can be written as follows:

$$\begin{bmatrix} -A & \beta A & 0 & \gamma\beta A + \psi A & \gamma^2 A & \gamma\psi A \\ \beta A & B & 0 & 0 & 0 & 0 \\ 0 & 0 & -A & \beta A & \gamma A & \psi A \\ \gamma\beta A + \psi A & 0 & \beta A & B & 0 & 0 \\ \gamma^2 A & 0 & \gamma A & 0 & A & 0 \\ \gamma\psi A & 0 & \psi A & 0 & 0 & B \end{bmatrix} \begin{Bmatrix} z_1 \\ \theta_1 \\ z_2 \\ \theta_2 \\ z_3 \\ \theta_3 \end{Bmatrix} = \quad (3.33)$$

$$\left\{ \begin{array}{c} -\alpha A \\ M_1 + \beta F_1 + \alpha\beta A \\ -\alpha A \\ (M_2 + \psi F_1 + \alpha\psi A) + \beta(F_2 + \gamma F_1 + \alpha\gamma A) \\ F_3 + \gamma(F_2 + \gamma F_1 + \alpha\gamma A) \\ M_3 + \psi(F_2 + \gamma F_1 + \alpha\gamma A) \end{array} \right\}$$

The operation is also applicable for  $n$  pontoons with hinged connections, however the algebra gets tedious for more than 3 pontoons. Hence subroutine COND in programme HINGE was written to calculate this.

If there are additional different constraints the above operation must be repeated for each new constraint with appropriate coefficients.

### 3.3.4.2 Rigid

For rigid connections, the additional constraint equation is:

$$\theta_i = \theta_{i+1} \quad (3.34)$$

or

$$\theta_i = \alpha_1 + \beta_1 z_{i+1} + \gamma_1 \theta_{i+1} \quad (3.35)$$

where,  $\alpha_1=0$  ,  $\beta_1=0$  and  $\gamma_1=1$

Combining equations (3.15), (3.17), (3.18) and (3.19) with equation (3.27) will result in the modified matrix for the two pontoons:

Please note the following substitutions;

$$\begin{array}{cccc} x_s = z_1 & x_i = \theta_1 & x_j = z_2 & x_k = \theta_2 \\ s = 1 & i = 2 & j = 3 & k = 4 \end{array}$$

From equation (3.15) the  $i^{\text{th}}$  row becomes

$$-\beta A \theta_1 + 0 + \beta A \theta_2 = -\alpha_1 \beta A \quad (3.36)$$

From equation (3.17) the  $j^{\text{th}}$  row becomes

$$\gamma A z_1 + 0 + A z_2 = F_2 + \gamma F_1 + \alpha \gamma A \quad (3.37)$$

From equation (3.18) the  $k^{\text{th}}$  row becomes

$$(\beta A + \psi A) z_1 + B \theta_1 + 0 + B \theta_2 = (M_1 + \beta F_1 + \alpha \beta A) + (M_2 + \psi F_1 + \alpha \psi A) \quad (3.38)$$

Equations (3.36 to 3.38) can be written as (3.39). This is the modified matrix for a system comprising two pontoons with rigid connection.

$$\begin{bmatrix} -A & 0 & \gamma A & \beta A + \psi A \\ 0 & B & 0 & B \\ \gamma A & 0 & A & 0 \\ \beta A + \psi A & B & 0 & B \end{bmatrix} \begin{Bmatrix} z_1 \\ \theta_1 \\ z_2 \\ \theta_2 \end{Bmatrix} = \begin{Bmatrix} -\alpha A \\ -\alpha_1 B \\ F_2 + \gamma F_1 + \alpha \gamma A \\ (M_1 + \beta F_1 + \alpha \beta A) + (M_2 + \psi F_1 + \alpha \psi A) \end{Bmatrix} \quad (3.39)$$

The operation is also applicable for n pontoon with rigid connections, however the algebra gets tedious for more than 2 pontoons. Hence subroutine COND in programme RIGID was written to calculate this.

### 3.3.4.3 Hinged-rigid

In the case of the hinged-rigid configuration the constraint equation is:

$$-\varepsilon \geq \theta_{i+1} - \theta_i \geq \varepsilon \quad (3.35)$$

The above constraint inequality can be separated into two;

$$|\theta_{i+1} - \theta_i| < \varepsilon \quad (3.36)$$

$$|\theta_{i+1} - \theta_i| \geq \varepsilon \quad (3.37)$$

When (3.36) holds true, the system is in a hinged connection mode in which case we follow the formulation outlined in 3.3.4.1. However when (3.37) holds true, the system is in a rigid connection mode and we follow the formulation outlined in 3.3.4.2. The subroutine DEF in programmes Hinge-Rigid1 and Hinge-Rigid2, identifies which inequality holds true.

### 3.3.5 Results for in-line array

The calculations for an in-line array (section 3.3) were coded in software and are included in the following appendices:

Appendix A, Program Hinged, for hinge connection

Appendix B, Program Elastic, for elastic connection

Appendix C, Program Rigid, for rigid connection

Appendix D, Program Hinge-Rigid1, for hinged-rigid connection in one direction

Appendix E, Program Hinge-Rigid2, for hinged-rigid connection in two directions

The following table gives the values of the individual pontoon parameters used in the experimental studies. The same parameter values were also used in the above programmes so that a comparison could be made between the theoretical and experimental results. The details of the experiments are given in Chapter 5.

<i>Parameter</i>	<i>value</i>
Length	0.6 m
Width	0.28 m
Height	0.2 m
Draft	0.03 m
Mass	5.04 kg
Hinged-Rigid angle	0.011765 rads 0.674 degrees

Table 1

The results of the program "Hinge-Rigid1" are shown in Fig 3.4. Fig 3.4a shows the general displacement of pontoons with different loads applied to the central module. The displacement and pitch angle of any individual pontoon against load

increment can be seen in Fig 3.4b and Fig 3.4c respectively. Fig 3.4d contains the difference between any two adjacent pitch angles, in which it is clearly shown that when this difference reaches the design threshold the angle remains constant (in one direction).

The results of program "Hinged-Rigid2" are shown in Fig 3.5. The description of figure 3.5 is the same as Fig 3.4 but in this case when the difference between two adjacent pitch angles reaches the design threshold angle, it stays there constant in both directions, as is shown in Fig 3.5d.

Based upon this theory the simulation works very well for hinged, elastic, and rigid connections but there is some difficulty with the hinged-rigid connection. Programs "Hinged-Rigid1" and "Hinged-Rigid2" indicate that when the difference of pitch angles of two adjacent pontoons reaches the design threshold angle, the program will transform this joint from hinged to a rigid connection, but it is unable to transform the rigid connections to hinge connections when necessary. For example in Fig 3.5 when joints 2 and 9 become locked (that is in opposite direction of joints 4, 5, 6 and 7) joints 3 and 8 must change from being rigid to hinged. However in the simulation these joints (3 and 8) remain locked. As a result pontoons 1 and 9 displace upwards. Since the load and buoyancy must be in equilibrium at all times, the resultant effect is that there will be more displacement in pontoons 3, 4, 5, 6, and 7 the effect is clearly shown in Fig 3.5a and 3.5b.

The more successful energy approach method was subsequently developed in Chapter 4, before this, attempts to use the method presented so far are extended to the mat array in the next section.

### 3.4 Mat array

#### 3.4.1 Basic hydrostatics

The equilibrium equation for the quasi-static response of a multipli-connected structure with several pontoons connected in a mat array can be written as:

$$[K(x)].\{x\} = \{F(x)\} \quad (3.38)$$

The quasi-static equation for any individual pontoon, considered as wall sided and with symmetry in the y, z plane can be written as:

$$\begin{bmatrix} A & 0 & 0 \\ 0 & B & 0 \\ 0 & 0 & C \end{bmatrix} \begin{Bmatrix} z_{ij} \\ \theta_{ij} \\ \phi_{ij} \end{Bmatrix} = \begin{Bmatrix} F_{ij} \\ M_{1ij} \\ M_{2ij} \end{Bmatrix} \quad (3.39)$$

$$A = \rho g L b \quad (3.40)$$

$$B = \rho g L b d G M_t \quad (3.41)$$

$$C = \rho g L b d G M_t \quad (3.42)$$

$$G M_t = \frac{d}{2} + \frac{L^2}{12d} - \frac{D}{2} \quad (3.43)$$

$$G M_t = \frac{d}{2} + \frac{b^2}{12d} - \frac{D}{2} \quad (3.44)$$

Where,  $\rho$  is density of water.

- $g$  is acceleration due to gravity
- $L$  is length of pontoon
- $L$  is distance between two pontoons
- $b$  is breadth of the pontoon
- $d$  is draft of pontoon in still water
- $D$  is height of the pontoon

$z_{ij}$  is vertical displacement of  $i^{\text{th}}$  pontoon in the  $j^{\text{th}}$  row

$\theta_{ij}$  is pitch angle of  $i^{\text{th}}$  pontoon in the  $j^{\text{th}}$  row

$\varphi_{ij}$  is roll angle of  $i^{\text{th}}$  pontoon in the  $j^{\text{th}}$  row

$GM_l$  is longitudinal metacentric height

$GM_t$  is transverse metacentric height

$F_{ij}$  is force acting at centre of gravity of  $i^{\text{th}}$  pontoon in the  $j^{\text{th}}$  row

$M_{1ij}$  is moment acting at centre of gravity of  $i^{\text{th}}$  pontoon in the  $j^{\text{th}}$  row  
about the y-axes

$M_{2ij}$  is moment acting at centre of gravity of  $i^{\text{th}}$  pontoon in the  $j^{\text{th}}$  row  
about the x-axes

The quasi-static equation for four individual pontoons (two columns  $i=2$ , and two row  $j=2$ ) without any connection may be written as:

$$\begin{bmatrix}
 A & 0 & 0 & 0 & 0 & 0 & 0 & 0 & 0 & 0 & 0 & 0 \\
 0 & B & 0 & 0 & 0 & 0 & 0 & 0 & 0 & 0 & 0 & 0 \\
 0 & 0 & C & 0 & 0 & 0 & 0 & 0 & 0 & 0 & 0 & 0 \\
 0 & 0 & 0 & A & 0 & 0 & 0 & 0 & 0 & 0 & 0 & 0 \\
 0 & 0 & 0 & 0 & B & 0 & 0 & 0 & 0 & 0 & 0 & 0 \\
 0 & 0 & 0 & 0 & 0 & C & 0 & 0 & 0 & 0 & 0 & 0 \\
 0 & 0 & 0 & 0 & 0 & 0 & A & 0 & 0 & 0 & 0 & 0 \\
 0 & 0 & 0 & 0 & 0 & 0 & 0 & B & 0 & 0 & 0 & 0 \\
 0 & 0 & 0 & 0 & 0 & 0 & 0 & 0 & C & 0 & 0 & 0 \\
 0 & 0 & 0 & 0 & 0 & 0 & 0 & 0 & 0 & A & 0 & 0 \\
 0 & 0 & 0 & 0 & 0 & 0 & 0 & 0 & 0 & 0 & B & 0 \\
 0 & 0 & 0 & 0 & 0 & 0 & 0 & 0 & 0 & 0 & 0 & C
 \end{bmatrix}
 \begin{Bmatrix}
 z_{ij} \\
 \theta_{ij} \\
 \varphi_{ij} \\
 z_{i+1j} \\
 \theta_{i+1j} \\
 \varphi_{i+1j} \\
 z_{ij+1} \\
 \theta_{ij+1} \\
 \varphi_{ij+1} \\
 z_{i+1j+1} \\
 \theta_{i+1j+1} \\
 \varphi_{i+1j+1}
 \end{Bmatrix}
 =
 \begin{Bmatrix}
 F_{ij} \\
 M_{1ij} \\
 M_{2ij} \\
 F_{i+1j} \\
 M_{1i+1j} \\
 M_{2i+1j} \\
 F_{ij+1} \\
 M_{1ij+1} \\
 M_{2ij+1} \\
 F_{i+1j+1} \\
 M_{1i+1j+1} \\
 M_{2i+1j+1}
 \end{Bmatrix}
 \quad (3.45)$$

### 3.4.2 Extension of the models for mat array configurations

The expanded equation for  $n \times m$  pontoons without any connection becomes as follows:

$$\begin{bmatrix} A & 0 & 0 & \cdots & \cdots & \cdots & 0 & 0 & 0 \\ 0 & B & 0 & \cdots & \cdots & \cdots & 0 & 0 & 0 \\ 0 & 0 & C & \cdots & \cdots & \cdots & 0 & 0 & 0 \\ \cdots & \cdots \\ \cdots & \cdots \\ \cdots & \cdots \\ 0 & 0 & 0 & \cdots & \cdots & \cdots & A & 0 & 0 \\ 0 & 0 & 0 & \cdots & \cdots & \cdots & 0 & B & 0 \\ 0 & 0 & 0 & \cdots & \cdots & \cdots & 0 & 0 & C \end{bmatrix} \begin{bmatrix} z_{11} \\ \theta_{11} \\ \varphi_{11} \\ \cdots \\ \cdots \\ \cdots \\ z_{nm} \\ \theta_{nm} \\ \varphi_{nm} \end{bmatrix} = \begin{bmatrix} F_{11} \\ M_{111} \\ M_{211} \\ \cdots \\ \cdots \\ \cdots \\ F_{nm} \\ M_{1nm} \\ M_{2nm} \end{bmatrix} \quad (3.46)$$

### 3.4.3 Constraint equations for hinged connection

Using Fig 3.2 we can deduce the constraint relationship for hinged-connections to be:

$$z_{ij} + \left(\frac{L+L_1}{2}\right)\theta_{ij} + \left(\frac{L+L_1}{2}\right)\theta_{i+1j} = z_{i+1j} \quad (3.47)$$

$$z_{ij} + \left(\frac{B+L_1}{2}\right)\varphi_{ij} + \left(\frac{B+L_1}{2}\right)\varphi_{ij+1} = z_{ij+1} \quad (3.48)$$

which can be rewritten as:

$$z_{ij} = 0 - \left(\frac{L+L_1}{2}\right)\theta_{ij} + z_{i+1j} - \left(\frac{L+L_1}{2}\right)\theta_{i+1j} \quad (3.49)$$

$$z_{ij} = 0 - \left(\frac{B+L_1}{2}\right)\varphi_{ij} + z_{ij+1} - \left(\frac{B+L_1}{2}\right)\varphi_{ij+1} \quad (3.50)$$

$$z_{ij} = \alpha + \beta\theta_{ij} + \gamma z_{i+1j} + \psi\theta_{i+1j} \quad (3.51)$$

$$z_{ij} = \alpha_1 + \beta_1 \phi_{ij} + \gamma_1 z_{ij+1} + \psi_1 \phi_{ij+1} \quad (3.52)$$

where:

$$\begin{array}{ll} i = 1 \rightarrow n & j = 1 \rightarrow m \\ \alpha = 0 & \alpha_1 = 0 \\ \beta = \frac{L + L_1}{2} & \beta_1 = \frac{B + L_1}{2} \\ \gamma = 1 & \gamma_1 = 1 \\ \psi = -\frac{L + L_1}{2} & \psi_1 = -\frac{B + L_1}{2} \end{array}$$

The constraint equations (3.51 and 3.52) must be inserted into the system equation (3.46). There are several methods at our disposal for inserting constraint equations into the system equation, which are briefly described below. However it is important to realise, as we shall see later these methods will provide us with different results when applied to the same system.

- a) One method is to insert the constraint equation (3.51) into the system equation (3.46) for all rows first ( $i=1 \rightarrow n, j = \text{constant}$ ), and then insert the constraint equation (3.52) between different rows.
- b) This method is similar to the previous one, with the difference being that here the constraint equation (3.52) for all columns are calculated first ( $i = \text{constant } j = 1 \rightarrow m$ ), then the constraint equation is inserted (3.51) between different columns.
- c) It is possible to insert constraints (3.51) and (3.52) for all pontoons module at once ( $i=1 \rightarrow n, j = 1 \rightarrow m$ ).

The operation for inserting constraint equation in the system equation is rather long and therefore it is not included here.

### 3.4.4 Alternative method of using constraint equation for mat array

Consider the case where  $r$  constraint equations are present in a system composed on  $n$  degrees of freedom. A general representation of linear constraint equations for this case would be of the form [57].

$$[G]_{r \times n} \{\Delta\}_{n \times 1} = \{S\}_{r \times 1} \quad (3.53)$$

Where the terms of  $[G]$  are the coefficients of the constraint equation and  $\{S\}$  is a vector of known constraint and  $\Delta$  is a transformation matrix. To avoid tedious algebra only the case with  $\{S\}=0$  will be dealt with here.

In order to develop the transformation matrix the  $n$  degrees of freedom will be divided into two groups,  $\{\Delta_e\}$  and  $\{\Delta_c\}$ , where  $\{\Delta_e\}$  contains  $r$  degrees of freedom and  $\{\Delta_c\}$  contains  $(n-r)$  degrees of freedom. So,

$$[G_{e_{r \times r}} \quad G_{c_{r \times n-r}}] \begin{Bmatrix} \Delta_e \\ \Delta_c \end{Bmatrix} = 0 \quad (3.54)$$

Thus, the degrees of freedom have been segregated so that  $\{\Delta_e\}$  degrees of freedom are selected corresponding to  $r$  number of constraint equations. The intent as explained previously is to remove these degrees of freedom from the potential energy functional by use of a condensation scheme. Although the choice of which degrees of freedom are to be removed is arbitrary, occasions do arise when great care must be exercised in their selection, otherwise, while the result will be the same, the mathematical operations would run into pages.

Solving equation (3.54) for  $\{\Delta_e\}$  gives,

$$\{\Delta_e\} = -[G_e]^{-1} [G_c] \{\Delta_c\} = [G_{ec}] \{\Delta_c\} \quad (3.55)$$

In accordance with the procedures developed, this can be used to form the transformation of degrees of freedom.

$$\begin{Bmatrix} \Delta_e \\ \Delta_c \end{Bmatrix} = \begin{bmatrix} G_{ec} \\ I \end{bmatrix} \{\Delta_c\} = [\Gamma_c] \{\Delta_c\} \quad (3.56)$$

Applying this now to the global equations via  $[\Gamma_c]^T [k] [\Gamma_c]$  gives a reduced stiffness matrix referred to  $\{\Delta_c\}$  alone and also a reduced load vector

$$\begin{Bmatrix} \hat{p}_e \\ p_c \end{Bmatrix} = [\Gamma_c]^T \begin{Bmatrix} p_e \\ p_c \end{Bmatrix} \quad (3.57)$$

$$[\Delta_c] = [k_c]^{-1} [p_c] \quad (3.58)$$

$$[\Delta_e] = [G_{ec}] [\Delta_c] \quad (3.59)$$

Solution of the reduced stiffness equation yields  $\{\Delta_c\}$ , which may then be substituted into equation (3.55) for calculation of  $\{\Delta_e\}$ .

### 3.4.5 Results for mat array

The reasons the methods mentioned in 3.4.3 fail to produce satisfactory results for individual methods a, b and c are given below.

- a) The constraint equation is applied to all the pontoons for all individual rows and then between different rows. The result is that the symmetry of displacement in x-axes (rows) is lost, although the symmetry in displacement in y-axes remains. This is unacceptable since we require to have symmetry in displacement when a symmetrical load is applied.
- b) The results produced here are replicas of the previous case with the main difference being that whereas before the symmetry in the x-axes was lost,

here it is the y-axes that loses symmetry. This is a direct result of the way the operation is carried out.

- c) The last and final case does not produce encouraging results either. Here the symmetry of the displacement is lost in both the y and the x-axis, which is totally undesirable.

### **3.5 Discussion**

Having studied the results of the methods mentioned in this chapter, it must be said that in some cases they have failed. For example while in the in-line array it managed to produce acceptable outputs in the cases of the hinged, elastic and rigid connections, it failed in the hinged-rigid connection set-up. Also in the mat array none of the results were acceptable. Two options were open, firstly to continue developing these in the hope of achieving the required results or secondly to develop a new theory. It was decided that even should the effort be made to develop the current theories, it will be very unlikely that it will produce the desired results. Hence from now, the effort was subsequently focused on developing a new theory, which as we shall see later does work extremely well.

In the new theory an energy approach to the situation is adopted, in which the equations for the beams on elastic foundation are found using the minimisation of the potential energy method.

Chapter 4 contains the development and formulation of this new theory.

## **CHAPTER 4 GENERAL SOLUTION USING AN ENERGY APPROACH**

### **4.1 In-line array**

#### **4.1.1 Introduction**

Minimisation of potential energy is used here to develop the necessary equations for a beam on an elastic foundation by successive application of incremental loading. The total length of the structure is divided into numerous elements in which any element represents a pontoon module. At first a deformation function for each element is defined. Based on this function the stiffness matrix and nodal forces can then be defined. By use of the connection matrix the global stiffness matrix for the complete structure is obtained. Then solving the resultant equations the displacements and rotations of the joints can be calculated. Hence using element equilibrium, all the pontoon element end stresses can be calculated in successive loading passes. The element end stresses are the internal stresses of the structure.

In any incremental loading step the stiffness matrix will generally vary and must be defined for each step. In this method for the first loading pass the connections of all elements are pinned, and hence the global stiffness matrix comprises only of the stiffness matrices of beam elements with both ends pinned on an elastic foundation with elasticity  $K$ . In the first pass the load which is sufficient to cause a connection to become locked can be determined and the stresses caused by this load may be calculated and stored. In the next pass only the stiffness matrix of those elements either side of a locked joint will be changed. In this case the difference between the stiffness matrix of a single end built-in element may be added to that of an element with both ends pinned. The next step is to solve the problem with the new stiffness matrix. Once again the load which causes change from one form of connection to the other (either pinned to rigid, or rigid to pin) can be calculated and again the element end stresses also may be found and stored.

This operation is repeated until the total stored load becomes equal to the external loading. The sum of stored internal stress in different loading steps is the internal stress of the system.

The method is developed here for an in-line array of pontoons.

#### 4.1.2 Definition of the problem

Consider a beam on an elastic foundation of elasticity  $K$ / unit length, with length  $L$  (length of one module) and rigidity  $EI$  (which is constant along one pontoon). Such a beam is illustrated in Fig 4.1. Point loads  $F_1, F_2, \dots, F_n$  and moments  $M_1, M_2, \dots, M_n$  are applied on the joints, and also distributed load  $P(x)$  is applied to the beam. The connection between elements can be hinged or rigid. The aim is to find the displacement and rotation of each joint together with the internal stress.

#### 4.1.3 Potential energy

The deformations, which satisfy boundary conditions and minimisation of the potential energy, enable a solution. The potential energy is equal to the stored elastic energy minus the work of external forces. The total potential energy is:

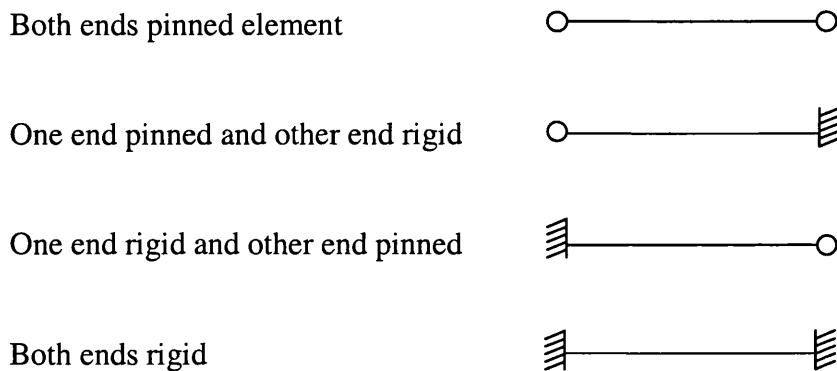
$$W = \frac{1}{2} \int_0^L EI(x) [y''(x)]^2 dx + \frac{1}{2} \int_0^L K(x) [y(x)]^2 dx - \sum F_i y_i - \sum M_i y_i' - \int_0^L P(x) y(x) dx \quad (4.1)$$

where the first term is potential energy due to the elasticity of the beam. The second term represents the potential energy due to the elastic foundation. The third and fourth terms are work done by external forces and moments, and the last term represents distributed external forces.

#### 4.1.4 Interpolation function for an element in the context of the primary assumptions

For each element  $EI$ ,  $K$  and  $P(x)$  are constant along its length. If there are any point loads along the element, these point loads will be transferred to the end of element.

The continuity of displacement and rotation of both element ends must be considered. The element connections are either pinned or rigid. Therefore to define the interpolation function of an element four combinations have to be considered:



##### 4.1.4.1 Interpolation function for element with both ends pinned

In this case there is continuity of displacement on both ends of the element, therefore there are two degrees of freedom for each element. It is possible to choose a first order interpolation function as follows:

$$y = A\mu + B \quad (4.2)$$

Consideration of the boundary conditions allows the constants  $A$  and  $B$  to be found.

$$\mu = 0 \quad \rightarrow y = y_i \quad \rightarrow y_i = B \quad (4.3)$$

$$\mu = L \quad \rightarrow y = y_j \quad \rightarrow y_j = AL + y_i \quad \rightarrow A = \frac{y_j - y_i}{L} \quad (4.4)$$

$$\begin{cases} \mu = 0 \\ \mu = L \end{cases} \rightarrow y' = y_i' = y_j' = A = \frac{y_j - y_i}{L} \quad (4.5)$$

By substitution of equation (4.3), (4.4), (4.5) in equation (4.2) and rearranging of  $y$  based on displacement and rotations this may be written as [56]:

$$y = \left[ 1 - \frac{\mu}{L} \quad 0 \quad \frac{\mu}{L} \quad 0 \right] \begin{Bmatrix} y_i \\ y_i' \\ y_j \\ y_j' \end{Bmatrix} \quad (4.6)$$

Or in simpler form

$$y = [y_1 \quad y_2 \quad y_3 \quad y_4] \{\delta_i\} = [Y] \{\delta_i\} \quad (4.7)$$

Where:

$$y_1 = 1 - \frac{\mu}{L}; \quad y_2 = 0; \quad y_3 = \frac{\mu}{L}; \quad y_4 = 0 \quad (4.8)$$

$$[\delta_i] = [y_i \quad y_i' \quad y_j \quad y_j'] \quad (4.9)$$

$$[\delta_i] = \{\delta_i\}^T \quad (4.10)$$

Differentiating  $y$  with respect to the  $x$  and substituting  $x = x_i + \mu$  gives:

$$y' = \frac{dy}{dx} = \frac{dy}{d\mu} \quad (4.11)$$

$$y' = \begin{bmatrix} -1/L & 0 & 1/L & 0 \end{bmatrix} \begin{Bmatrix} y_i \\ y_i' \\ y_j \\ y_j' \end{Bmatrix} \quad (4.12)$$

We can further simplify eqn 4.12 to get:

$$y' = [y_1' \quad y_2' \quad y_3' \quad y_4'] \{\delta_i\} = [Y'] \{\delta_i\} \quad (4.13)$$

$$y'' = 0$$

Hence we have found the interpolation function for the beam pinned at both ends.

#### 4.1.4.2 Interpolation function for element with both ends built-in

In this case each element has four degrees of freedom,  $(y_i, y_i', y_j, y_j')$ . Therefore a third order polynomial can be chosen for the interpolation function:

$$y = A\mu^3 + B\mu^2 + C\mu + D \quad (4.14)$$

Considering boundary conditions, the constants A, B, C and D in terms of degrees of freedom for both ends of the beam can be found.

$$\begin{array}{ll} \mu = 0 & \begin{cases} y = y_i \\ y' = y_i' \end{cases} & \mu = L & \begin{cases} y = y_j \\ y' = y_j' \end{cases} \\ \mu = 0 & y = y_i & y_i = D & \end{array} \quad (4.15)$$

$$\mu = 0 \quad y' = y_i' \quad y_i' = C \quad (4.16)$$

$$\mu = L \quad y = y_j \quad y_j = AL^3 + BL^2 + CL + D \quad (4.17)$$

$$\mu = L \quad y' = y_j' \quad y_j' = 3AL^2 + 2BL + C \quad (4.18)$$

Solving the linear equations (4.15) to (4.18) the constants A, B, C, D are found to be:

$$A = \frac{-2}{L^3}(y_j - y_i) + \frac{1}{L^2}(y_i' + y_j')$$

$$B = \frac{-2}{L^2}(y_j - y_i) - \frac{1}{L}(2y_i' + y_j')$$

$$C = y_i'$$

$$D = y_i \quad (4.19)$$

Substitution of equation (4.19) in equation (4.14) and rearranging y based on displacement and rotations yields:

$$y = \left[ \frac{1}{L^3}(2\mu^3 - 3L\mu^2 + L^3) \quad \frac{1}{L^2}(\mu^3 - 2L\mu^2 + L^2\mu) \quad \frac{1}{L^3}(-2\mu^3 + 3L\mu^2) \right. \\ \left. \frac{1}{L^2}(\mu^3 - L\mu^2) \right] \begin{Bmatrix} y_i' \\ y_i \\ y_j' \\ y_j \end{Bmatrix} \quad (4.20)$$

Which can be simplified to,

$$y = [y_1 \ y_2 \ y_3 \ y_4] \{\delta_i\} \quad y = [Y] \{\delta_i\} \quad (4.21)$$

Where:

$$\begin{aligned}
 y_1 &= \frac{1}{L^3}(2\mu^3 - 3L\mu^2 + L^3) \\
 y_2 &= \frac{1}{L^2}(\mu^3 - 2L\mu^2 + L^2\mu) \\
 y_3 &= \frac{1}{L^3}(-2\mu^3 + 3L\mu^2) \\
 y_4 &= \frac{1}{L^2}(\mu^3 - L\mu^2)
 \end{aligned} \tag{4.22}$$

$$[\delta_i] = [y_i \quad y_i' \quad y_j \quad y_j'] \tag{4.23}$$

$$[\delta_i] = \{\delta_i\}^T \tag{4.24}$$

Again differentiating  $y$  with respect to the  $x$  and substituting  $x = x_i + \mu$ :

$$y' = \frac{dy}{dx} = \frac{dy}{d\mu} \tag{4.25}$$

$$\begin{aligned}
 y' &= \left[ \frac{1}{L^3}(6\mu^2 - 6L\mu) \quad \frac{1}{L^2}(3\mu^2 - 4L\mu + L^2) \quad \frac{1}{L^3}(-6\mu^2 + 6L\mu) \right. \\
 &\quad \left. \frac{1}{L^2}(3\mu^2 - 2L\mu) \right] \begin{Bmatrix} y_i \\ y_i' \\ y_j \\ y_j' \end{Bmatrix}
 \end{aligned} \tag{4.26}$$

Or in simpler form

$$y' = [y_1' \quad y_2' \quad y_3' \quad y_4'] \{\delta_i\} = [Y'] \{\delta_i\} \tag{4.27}$$

And we obtain a similar expression as before,

$$y'' = \left[ \frac{1}{L^3}(12\mu - 6L) \quad \frac{1}{L^2}(6\mu - 4L) \quad \frac{1}{L^3}(-12\mu + 6L) \right. \\ \left. \frac{1}{L^2}(6\mu - 2L) \right] \begin{Bmatrix} y_i \\ y_i' \\ y_j \\ y_j' \end{Bmatrix} \quad (4.28)$$

$$y'' = [y_1'' \quad y_2'' \quad y_3'' \quad y_4''] \{\delta_i\} = [Y''] \{\delta_i\} \quad (4.29)$$

#### 4.1.4.3 Interpolation function for element with one end pinned, other end built-in

In this case there is continuity of displacement at both ends of the element and also continuity of rotation at the built-in end. Therefore each element has three degrees of freedom  $(y_i, y_j, y_j')$ . The interpolation function can be shown to be as follows:

$$y = A\mu^3 + B\mu + C \quad (4.30)$$

Again the boundary conditions enable the constants A, B, C, to be found, as:

$$\mu = 0 \quad y = y_i \quad y_i = C \quad (4.31)$$

$$\mu = L \quad y = y_j \quad y_j = AL^3 + BL + C \quad (4.32)$$

$$\mu = L \quad y' = y_j' \quad y_j' = 3AL^2 + B \quad (4.33)$$

yielding:

$$A = \frac{1}{2L^3}(y_i - y_j) + \frac{1}{2L^2}y_j'$$

$$B = \frac{-3}{2L}(y_i - y_j) - \frac{1}{2}y_j'$$

$$C = y_i \quad (4.34)$$

Substituting equation (4.34) in equation (4.30) and rearranging of  $y$  based on displacement and rotation give:

$$y = \left[ \frac{1}{2L^3}\mu^3 - \frac{3}{2L}\mu + 1 \quad 0 \quad \frac{-1}{2L^3}\mu^3 + \frac{3}{3L}\mu \right] \begin{Bmatrix} y_i \\ y_i' \\ y_j \\ y_j' \end{Bmatrix} \quad (4.35)$$

Or in simpler form

$$y = [y_1 \quad y_2 \quad y_3 \quad y_4] \{\delta_i\} \quad y = [Y] \{\delta_i\} \quad (4.36)$$

Once again differentiation of  $y$  with respect to the  $x$  and substituting  $x = x_i + \mu$  gives:

$$y' = \frac{dy}{dx} = \frac{dy}{d\mu}$$

$$y' = \left[ \frac{3}{2L^3}\mu^2 - \frac{3}{2L} \quad 0 \quad \frac{-3}{2L^3}\mu^2 + \frac{3}{2L} \quad \frac{3}{2L^2}\mu^2 \right] \begin{Bmatrix} y_i \\ y_i' \\ y_j \\ y_j' \end{Bmatrix} \quad (4.37)$$

Or in simpler form

$$y' = [y_1' \quad y_2' \quad y_3' \quad y_4'] \{\delta_i\} = [Y'] \{\delta_i\} \quad (4.38)$$

Again we obtain a similar expression,

$$y'' = \left[ \frac{3}{L^3} \mu \quad 0 \quad \frac{-3}{L^3} \mu \quad \frac{3}{L^2} \mu \right] \begin{Bmatrix} y_{i1} \\ y_i' \\ y_j \\ y_j' \end{Bmatrix} \quad (4.39)$$

Or in simpler form

$$y'' = [y_1'' \quad y_2'' \quad y_3'' \quad y_4''] \{\delta_i\} = [Y''] \{\delta_i\} \quad (4.40)$$

#### 4.1.4.4 Interpolation function for element with one end built-in other end pinned

In this case the interpolation function is the same as the previous case (4.1.4.3) but the location of joint  $j$  and  $i$  will be reversed.

#### 4.1.5 Potential energy for an element

The total potential energy is calculated by integrating the potential energy of each element of the structure, i.e.

$$W_I = \frac{1}{2} \int_0^L EI y''^2 d\mu + \frac{1}{2} \int_0^L Ky^2 d\mu - \int_0^L Py d\mu \quad (4.41)$$

The first term takes account of the potential energy, which arises due to the beam's elasticity. The second term represent the potential energy created because of the elastic foundation while the last term is the potential energy resulting from external forces.

The first component of potential energy of an element may be written as  $(W_I)_1$ , and:

$$\begin{aligned}
(W_I)_1 &= \frac{1}{2} EI \int_0^L y''^2 d\mu = \frac{1}{2} EI \int_0^L y''^T y'' d\mu = \frac{1}{2} EI \int_0^L [\delta_I] \{y''\} \{y''\}^T [\delta_I]^T d\mu \\
&= \frac{1}{2} [\delta_I] (EI \int_0^L \{y''\} \{y''\}^T d\mu) \{\delta_I\}
\end{aligned} \tag{4.42}$$

The element rigidity stiffness matrix, is given by:

$$[A_I] = EI \int_0^L \{y''\} \{y''\}^T d\mu \tag{4.43}$$

Expanding the second component of equation (4.41).

$$(W_I)_2 = \frac{1}{2} \int_0^L Ky^2 d\mu = \frac{1}{2} K \int_0^L y^T y d\mu = \frac{1}{2} [\delta_I] (K \int_0^L y^T y d\mu) \{\delta_I\} \tag{4.44}$$

So the elastic foundation stiffness matrix is  $B_I$ , which is mathematically defined as:

$$[B_I] = K \int_0^L y^T y d\mu \tag{4.45}$$

Finally the third component of equation (4.41) may be written:

$$(W_I)_3 = \int_0^L Py d\mu = P \int_0^L y d\mu = (P \int_0^L [y] d\mu) \{\delta_I\} \tag{4.46}$$

The force matrix will be:

$$[P_I] = P \int_0^L [y] d\mu \tag{4.47}$$

#### 4.1.5.1 Potential energy for element with both ends pinned

In this case the element rigidity stiffness matrix is equal to zero.

$$y'' = 0 \quad \rightarrow \quad [A_r] = 0$$

The elastic foundation stiffness matrix of the element will be:

$$[B_r] = K \int_0^l y^T y d\mu$$

Substituting definition of  $y_i$  from equation (4.8) into equation (4.45) yields:

$$B_{11} = K \int_0^l y_1 y_1 d\mu = K \int_0^l \left(1 - \frac{\mu}{L}\right) d\mu = \frac{KL}{3}$$

$$B_{12} = B_{21} = B_{14} = B_{41} = B_{22} = B_{23} = B_{32} = B_{24} = B_{42} = B_{34} = B_{43} = B_{44} = 0$$

$$B_{13} = B_{31} = K \int_0^l y_1 y_3 d\mu = K \int_0^l \frac{\mu}{L} \left(1 - \frac{\mu}{L}\right) d\mu = \frac{KL}{6}$$

$$y_1 = \frac{1}{L^3} (2\mu^3 - 3L\mu^2 + L^3)$$

$$y_2 = \frac{1}{L^2} (\mu^3 - 2L\mu^2 + L^2\mu)$$

$$y_3 = \frac{1}{L^3} (-2\mu^3 + 3L\mu^2)$$

$$y_4 = \frac{1}{L^2} (\mu^3 - L\mu^2)$$

Hence the elastic foundation stiffness matrix for elements pinned on both ends, is given by:

$$[B_r] = \frac{KL}{6} \begin{bmatrix} 2 & 0 & 1 & 0 \\ 0 & 0 & 0 & 0 \\ 1 & 0 & 2 & 0 \\ 0 & 0 & 0 & 0 \end{bmatrix} \quad (4.48)$$

we have the forces matrix:

$$[P_1] = P \int_0^L [y] d\mu$$

$$P_1 = P \int_0^L y_1 d\mu = P \int_0^L \left(1 - \frac{\mu}{L}\right) d\mu = \frac{PL}{2}$$

$$P_2 = 0$$

$$P_3 = P \int_0^L y_3 d\mu = P \int_0^L \left(1 - \frac{\mu}{L}\right) d\mu = \frac{PL}{2}$$

$$P_4 = 0$$

Hence the forces matrix is:

$$[P_1] = \begin{bmatrix} \frac{PL}{2} & 0 & \frac{PL}{2} & 0 \end{bmatrix} \quad (4.49)$$

#### 4.1.5.2 Potential energy for element with both ends built-in

In this case element rigidity stiffness matrix is as follows:

$$[A_1] = EI \int_0^L \{y''\} [y''] d\mu.$$

Substitution  $\langle y'' \rangle$  from equation (4.28) into above equation yields:

$$A_{11} = EI \int_0^L y_1'' y_1'' d\mu = \frac{12EI}{L^3}$$

$$A_{12} = A_{21} = EI \int_0^L y_1'' y_2'' d\mu = \frac{6EI}{L^2}$$

$$A_{13} = A_{31} = EI \int_0^L y_1'' y_3'' d\mu = -\frac{12EI}{L^3}$$

$$A_{14} = A_{41} = EI \int_0^L y_1'' y_4'' d\mu = \frac{6EI}{L^2}$$

$$A_{22} = EI \int_0^L y_2'' y_2'' d\mu = \frac{4EI}{L}$$

$$A_{ij} = A_{ji} = EI \int_0^L y_i'' y_j'' d\mu \quad i, j = 1, 2, 3, 4$$

Finally the bending stiffness matrix  $[A_i]$  the bending stiffness matrix will be:

$$[A_i] = EI \begin{bmatrix} \frac{12}{L^3} & \frac{6}{L^2} & -\frac{12}{L^3} & \frac{6}{L^2} \\ & \frac{4}{L^2} & -\frac{6}{L^3} & \frac{2}{L^2} \\ & & \frac{12}{L^3} & -\frac{6}{L^3} \\ & & & \frac{4}{L^2} \end{bmatrix} \quad (4.50)$$

*Symmetric*

Performing the same operation and by using equation (4.22) the stiffness matrix due to elastic foundation will be:

$$[B_i] = K \int_0^L y^T y d\mu$$

$$B_{ij} = B_{ji} = K \int_0^L y_i y_j d\mu \quad i, j = 1, 2, 3, 4$$

$$[B_i] = \frac{K}{420} \begin{bmatrix} 156L & 22L^2 & 54L & -13L^2 \\ & 4L^3 & 13L^2 & -3L^3 \\ & & 156L & -22L^2 \\ & & & 4L^3 \end{bmatrix} \quad (4.51)$$

*Symmetric*

The force vector is given by:

$$[P_i] = P \int_0^L [y] d\mu$$

$$P_1 = P \int_0^L y_1 d\mu = \frac{PL}{2}$$

$$P_i = P \int_0^L y_i d\mu$$

$$[P_i] = \left[ \frac{PL}{2} \quad \frac{PL^2}{12} \quad \frac{PL}{2} \quad -\frac{PL^2}{12} \right] \quad (4.52)$$

#### 4.1.5.3 Potential energy for element with one end pinned and one end built-in

The element rigidity stiffness matrix is:

$$[A_i] = EI \int_0^L \{y''\} [y''] d\mu.$$

Using equation (4.39) into above equation yields:

$$A_{11} = EI \int_0^L y_1'' y_1'' d\mu = EI \int_0^L \left(\frac{3}{L^3}\right)^2 d\mu = \frac{3EI}{L^3}$$

$$A_{12} = A_{21} = 0$$

$$A_{13} = A_{31} = EI \int_0^L y_1'' y_3'' d\mu = EI \int_0^L \left(\frac{3}{L^3}\mu\right) \left(\frac{-3}{L^3}\right) d\mu = \frac{-3EI}{L^3}$$

The complete bending stiffness matrix is given by:

$$[A_r] = \begin{bmatrix} \frac{3EI}{L^3} & 0 & -\frac{3EI}{L^3} & \frac{3EI}{L^2} \\ 0 & 0 & 0 & 0 \\ \text{Symmetric} & & \frac{3EI}{L^3} & -\frac{3EI}{L^2} \\ & & & \frac{3EI}{L} \end{bmatrix} \quad (4.53)$$

For the elastic foundation stiffness matrix

$$[B_r] = K \int_0^L y^T y d\mu$$

Which by using equation (4.35) can be written as:

$$B_{11} = K \int_0^L y_1 y_1 d\mu = K \int_0^L \left( \frac{1}{2L^3} \mu^3 + \frac{3}{2L} \mu + 1 \right) d\mu = \frac{33KL}{140}$$

$$B_{12} = B_{21} = 0$$

$$B_{13} = B_{31} = K \int_0^L y_1 y_3 d\mu = \frac{39KL}{280}$$

$$B_{14} = B_{41} = K \int_0^L y_1 y_4 d\mu = \frac{-11KL^2}{280}$$

The complete element rigidity stiffness matrix will be as follows:

$$[B_i] = \begin{bmatrix} \frac{33KL}{140} & 0 & \frac{39KL}{280} & \frac{-11KL^2}{280} \\ & 0 & 0 & 0 \\ & & \frac{17KL}{35} & \frac{-3KL^2}{35} \\ \text{symmetric} & & & \frac{2KL^3}{35} \end{bmatrix} \quad (4.54)$$

The forces vector in this case will be as follows:

$$[P_i] = P \int_0^L [y] d\mu$$

$$P_1 = P \int_0^L y_1 d\mu = \frac{3PL}{8}$$

$$P_i = P \int_0^L y_i d\mu$$

$$[P_i] = \begin{bmatrix} \frac{3PL}{8} & 0 & \frac{5PL}{8} & \frac{-PL^2}{8} \end{bmatrix} \quad (4.55)$$

#### 4.1.5.4 Potential energy for element with one end built-in and the other end pinned

This case is similar to the previous one (4.1.5.3), the only difference is that the position of the nodes at both ends will be interchanged ( $j$  and  $i$  will interchange).

The element rigidity stiffness matrix

$$[A_i] = \begin{bmatrix} \frac{3EI}{L^3} & \frac{3EI}{L^2} & \frac{-3EI}{L^3} & 0 \\ & \frac{3EI}{L} & \frac{-3EI}{L^2} & 0 \\ & & \frac{3EI}{L^3} & 0 \\ \text{Sym} & & & 0 \end{bmatrix} \quad (4.56)$$

The elastic foundation stiffness matrix is:

$$[B_i] = \begin{bmatrix} \frac{17KL}{35} & \frac{3KL^2}{35} & \frac{39KL}{280} & 0 \\ & \frac{2KL^3}{105} & \frac{11KL^2}{280} & 0 \\ & & \frac{33KL}{140} & 0 \\ \text{Sym} & & & 0 \end{bmatrix} \quad (4.57)$$

The forces vector is:

$$[P_i] = \left[ \frac{5PL}{8} \quad \frac{PL^2}{8} \quad \frac{3PL}{8} \quad 0 \right] \quad (4.58)$$

Therefore the potential energy of an element can be written as:

$$W_i = \frac{1}{2} [\delta_i] [A_i] \{\delta_i\} + \frac{1}{2} [\delta_i] [B_i] \{\delta_i\} - [P_i] \{\delta_i\} \quad (4.59)$$

Hence the displacement matrix is:

$$\{\delta_i\} = \begin{Bmatrix} y_i \\ y_i' \\ y_j \\ y_j' \end{Bmatrix} = \begin{bmatrix} 0 & 0 & \dots & 0 & 1 & 0 & \dots & 0 & 0 & \dots & 0 \\ 0 & 0 & \dots & 0 & 0 & 1 & \dots & 0 & 0 & \dots & 0 \\ 0 & 0 & \dots & 0 & 0 & 0 & \dots & 1 & 0 & \dots & 0 \\ 0 & 0 & \dots & 0 & 0 & 0 & \dots & 0 & 1 & \dots & 0 \end{bmatrix} \begin{Bmatrix} y_1 \\ y_1' \\ y_2 \\ y_2' \\ \cdot \\ \cdot \\ \cdot \\ y_i \\ y_i' \\ \cdot \\ \cdot \\ y_j \\ y_j' \\ \cdot \\ \cdot \\ \cdot \\ y_n \\ y_n' \end{Bmatrix} \quad (4.60)$$

where the right hand side vector contains the displacements and rotations of all the nodes in the beam which is denoted as  $\{u\}$  given  $n$  is the total number of nodes of the beam.

Hence we have:

$$\{\delta_i\} = [C_i]\{u\} \quad (4.61)$$

The matrix  $[C_i]$  in which all components are 0 or 1 as shown in equation (4.60) is called the connection matrix. By using equation (4.61) it is possible rewrite equation (4.59) as follows:

$$W_i = \frac{1}{2}[u][C_i]^T ([A_i] + [B_i])[C_i]\{u\} - [P_i][C_i]\{u\} \quad (4.62)$$

$$[R_i] = [C_i]^T ([A_i] + [B_i])[C_i] \quad (4.63)$$

where matrix  $[R_i]$  is the stiffness matrix of one element which equates to:

$$[R_i] = \begin{bmatrix} 0 & \dots & 0 & 0 & \dots & 0 & 0 & \dots & 0 \\ & \vdots \\ & & A_{11} + B_{11} & A_{12} + B_{12} & \dots & A_{13} + B_{13} & A_{14} + B_{14} & \dots & 0 \\ & & & A_{22} + B_{22} & \dots & A_{23} + B_{23} & A_{24} + B_{24} & \dots & 0 \\ & & & & \vdots & \vdots & \vdots & \vdots & \vdots \\ & & & & & A_{33} + B_{33} & A_{34} + B_{34} & \dots & 0 \\ & & \text{Sym} & & & & A_{44} + B_{44} & \dots & 0 \\ & & & & & & & \vdots & \vdots \\ & & & & & & & & 0 \end{bmatrix} \quad (4.64)$$

Matrix  $[R_i]$  is a  $2n \times 2n$  symmetric matrix where again  $n$  is the number of nodes in the structure.

The vector of external forces is:

$$[S_i] = [P_i][C_i]$$

$$[S_i] = [0 \quad \dots \quad P_1 \quad P_2 \quad \dots \quad P_3 \quad P_4 \quad \dots \quad 0] \quad (4.65)$$

Therefore it is possible to simplify the potential energy of an element as:

$$W_i = \frac{1}{2} [u][R_i]\{u\} - [\delta_i]\{u\} \quad (4.66)$$

#### 4.1.6 Potential energy for complete structure

By using equation (4.1) the total energy of the complete structure can be written as:

$$W = \sum_{l=1}^{n-1} W_l - \sum_{l=1}^n F_l Y_l - \sum_{l=1}^n M_l Y_l' \quad (4.67)$$

By substituting (4.66) into (4.67) we have:

$$W = \frac{1}{2}[u] \left( \sum_{l=1}^{n-1} [R_l] \right) \{u\} - \left( \sum_{l=1}^{n-1} [S_l] \right) \{u\} - [F_1 M_1 F_2 \cdots M_n] \{u\} \quad (4.68)$$

Since

$$[R] = \sum_{l=1}^{n-1} [[R_l]] \quad (4.69)$$

And

$$[T] = \sum_{l=1}^{n-1} [S_l] + [F_1 \quad M_1 \quad F_2 \quad M_2 \quad \cdots \quad M_n] \quad (4.70)$$

Hence equation (4.68) becomes:

$$W = \frac{1}{2}[u][R]\{u\} - [T]\{u\} \quad (4.71)$$

Now it is necessary to minimise  $W$  by considering the boundary conditions. If  $i$  is a node which is simply supported ( $y_i = 0$ ) and  $j$  is a node with zero rotation then minimisation of  $W$  with respect to  $\{u\}$  results in  $(y_i), (2i-1)^{\text{th}}$ , and  $(y_j), (2j)^{\text{th}}$  components of  $\{u\}$  to be zero. Therefore the Lagrange function for this problem will be:

$$W^* = W + \frac{1}{2}[u][A_{2i-1}]\{u\} + \frac{1}{2}[u][A_{2j}]\{u\} \quad (4.72)$$

In equation (4.72) all components of the matrix  $[A_{2i-1}]$  are zero with the exception of  $a_{2i-1,2i-1}$ , which is large, while in matrix  $[A_{2j}]$  all values, except the  $a_{2j,2j}$  component (which has a large value) are zero.

Considering equation (4.71), equation (4.72) becomes:

$$W^* = \frac{1}{2}[u]([R] + [A_{2i-1}] + [A_{2j}])\{u\} - [T]\{u\} \quad (4.73)$$

Where:

$$[R^*] = [R] + [A_{2i-1}] + [A_{2j}]$$

Matrix  $[R^*]$  is matrix  $[R]$  to which a large number is added to the diagonal terms  $(2_{i-1}, 2_{i-1})$  and  $(2_j, 2_j)$ . Matrix  $[R^*]$  is the corrected global stiffness matrix.

$$W^* = \frac{1}{2}[u][R^*]\{u\} - [T]\{u\} \quad (4.74)$$

Equation (4.74) must be minimised; therefore for this reason the derivative in terms of  $u$  for all components is set to zero.

$$\text{grad } W^* = [R^*]\{u\} - \{T\} = 0 \quad (4.75)$$

or

$$[R^*]\{u\} = \{T\} \quad (4.76)$$

Therefore the linear equations (4.76) may be solved, and the terms of vector  $u$ , which are the displacements and rotations, may be found.

#### 4.1.7 Finding reaction and stress of both ends of elements

After finding the displacements and rotations of all nodes (Eq. 4.76), an element such as that in (fig 4.3) is studied to find the reactions and stresses of both its ends.

The potential energy for any element will be:

$$W_I = \frac{1}{2} EI \int_0^L y''^2 d\mu + \frac{1}{2} K \int_0^L y^2 d\mu - T_L y_I + T_R y_J - M_L y'_I + M_R y'_J - \int_0^L P y d\mu \quad (4.77)$$

To achieve the objective we must go about minimising equation (4.77).

Considering equations (4.42), (4.44) and (4.46), equation (4.77) may be written as:

$$W_I = \frac{1}{2} [\delta_I] [A_I] \{\delta_I\} + \frac{1}{2} [\delta_I] [B_I] \{\delta_I\} - [P_I] \{\delta_I\} - [T_L \ M_L - T_R - M_R] \{\delta_I\} \quad (4.78)$$

Equation (4.78) may be simplified to:

$$W_I = \frac{1}{2} [\delta_I] ([A_I] + [B_I]) \{\delta_I\} - [P_I] \{\delta_I\} - [T_L \ M_L - T_R - M_R] \{\delta_I\} \quad (4.79)$$

From minimisation of equation (4.79), the stresses of both ends of the element may be found.

$$\frac{\partial W_I}{\partial \delta_I} = ([A_I] + [B_I]) \{\delta_I\} - [P_I] - \begin{Bmatrix} T_L \\ M_L \\ -T_R \\ -M_R \end{Bmatrix} = 0 \quad (4.80)$$

or

$$\begin{Bmatrix} T_L \\ M_L \\ -T_R \\ -M_R \end{Bmatrix} = ([A_I] + [B_I])\{\delta_I\} - \{P_I\} \quad (4.81)$$

which can be expanded into:

$$\begin{Bmatrix} T_L \\ M_L \\ -T_R \\ -M_R \end{Bmatrix} = \begin{bmatrix} A_{11} + B_{11} & A_{12} + B_{12} & A_{13} + B_{13} & A_{14} + B_{14} \\ A_{21} + B_{21} & A_{22} + B_{22} & A_{23} + B_{23} & A_{24} + B_{24} \\ A_{31} + B_{31} & A_{32} + B_{32} & A_{33} + B_{33} & A_{34} + B_{34} \\ A_{41} + B_{41} & A_{42} + B_{42} & A_{43} + B_{43} & A_{44} + B_{44} \end{bmatrix} \begin{Bmatrix} y_I \\ y_I' \\ y_J \\ y_J' \end{Bmatrix} - \begin{Bmatrix} P_1 \\ P_2 \\ P_3 \\ P_4 \end{Bmatrix} \quad (4.82)$$

#### 4.1.8 Discussion

Software has been developed in order to calculate the global stiffness matrix and the vector of forces of beam elements on elastic foundations and solve the resultant equations for various end conditions; both ends built-in, both ends pinned, one end built-in one end pinned and vice versa.

In the developed code the structure consists of several similar modules of the same length and the same locking hinge angle limit. The second moment of area and elasticity of the elastic foundation are assumed identical for each module. The structure can receive different loading. Distributed loads along its length and concentrated loads, which can be applied at the nodes only. The moments are also applied only at the nodes.

In this method for the first loading step all connections are taken to be hinged. The stiffness matrix and forces vector for a both ends pinned element on elastic foundation with elasticity  $K$ , equations (4.48) & (4.49), are used in this case. It is then possible to establish the stiffness matrix for the complete structure. After completing the stiffness matrix and considering the loading applied on the structure and solving the equations, the displacement and rotation of all nodes may be found. Having displacements and rotations and comparing the rotations of nodes with the locking hinged angle limit it is possible to find the load which the

first connection will be changed from hinged to rigid. Consequently the load displacements and rotations, bending moments and shear forces on nodes may be found, and this loading step is complete.

The next loading step is started with modifications to the stiffness matrix. In this step only the stiffness matrix and forces vector of elements either side of the locked joint are changed and the difference in the stiffness of the elements is added to the stiffness matrix of the complete structure. The problem is solved with a new stiffness matrix from which the new load that can cause joint status change, is calculated (i.e. locked to unlocked or vice versa). The internal stresses due to this load are calculated and stored. This procedure must be repeated until the sum of stored loads from each repeat equates to the external load. Then the sums of stored stresses give the final stresses of the system.

In changing the connection form at the nodes it must be considered that if any node becomes locked then this node will be considered as a built-in node. Should the node to the right hand side of the locked node be hinged, then the stiffness matrix of the element (between the locked node and the node on the right hand side of locked node) becomes that of an element with one end built-in and the other end pinned. If the node to the left-hand side of the locked node is hinged, the stiffness matrix of the element (between the node left-hand side of locked node and locked node) becomes that of an element with one end pinned and the other end built-in. In the case any neighbouring node to the locked node becomes locked; then the stiffness matrix of the element (between the two locked nodes) becomes that of an element with both ends built-in.

It is important that in addition to consideration of the locking of joints in the positive and negative directions, the unlocking of the joints must also be remembered. Should a previously locked node become unlocked, then based on the status of the nodes either side of it, different approaches are taken. If a node either side of the unlocked node is hinged or locked, the stiffness matrix of a both ends pinned element, or a one end pinned with the other end built-in element is used respectively.

#### 4.1.9 Explanation of the software

The software provided for analysis of multipli-connected floating structures consists of two parts. The first part is a coded program for preparing the inputs for the main program. The second part is the main program. Both programs are provided in appendices F and G respectively.

The main coded software consists of twenty-two subroutines and is able to analyse the following structures:

- Symmetric multipli-connected floating structures with symmetric loading
- Any multipli-connected floating structure with arbitrary loading
- Continuous beam on elastic foundation

With the first two types of structure the analysis is based on the assumption that there is some freedom in the connections (hinged-rigid). In the first option because of the symmetrical property, only half of structure needs to be analysed, and is therefore faster than the second option. In computing multipli-connected floating structures with limited freedom of joints, first all connections are taken as hinged and on this basis the stiffness matrix and the force vector are determined (subroutine number 5). Only in the first type (symmetric structure) are the axes of symmetry in the position of the last joint, which can carry bending moment but can not carry shear forces (subroutine number 14).

In the third type where there is not any freedom in the connections (rigid), the problem is analysed using a single step (subroutine number 22) procedure.

After determination of the stiffness matrix and forces vector the system of equations is solved using Cholesky's method (subroutine number 2) and according to the conditions of both ends of elements, the displacement and rotations of all joints by use of subroutine numbers 6, 7, 8 and 9 are calculated. The moment and shear force acting on the joints are calculated using subroutine numbers 10, 11, 12, and 13.

Subroutine 2 calculates and stores the minimum load by which the status of a connection is changed, and the stress caused by this load. Then according to the change of condition of this joint the stiffness matrix is modified. If the joint changes from hinged to rigid, by considering the status of the joints at the right-hand and left-hand sides of the changed joint, the stiffness matrix is increased (subroutine 14, 15, 16, and 17). Whereas should the joint change from rigid to hinged the stiffness matrix is decreased (subroutine 18, 19, 20, and 21).

Then after modification of the stiffness matrix and the forces vector again the system of equations is solved with Cholesky's method and the above procedure is repeated. When the sum of loads applied over consecutive steps matches the external loading then the stress is the sum of resultant stresses in the different steps. These steps are summarised in the figure 4.4.

#### **4.1.10 Worked Examples**

Two worked examples will be outlined here. First we use pontoon dimensions as of those used in the practical experiment. This will give a basis for comparison of the theoretical and experimental results. Later we also use pontoon dimensions likely to be used in real life applications. This will give us a picture of the theory's performance and the calculations involved, when used to design and diagnose full-scale structures.

##### **4.1.10.1 Example for experimental dimensions**

For this simulation a multipli-connected structure consisting of nine pontoons in-line is considered. A 15 kg load is applied on the centre of pontoon number five, which is situated at the middle of the system.

The dimensions of each pontoon are as follows;

<i>Parameter</i>	<i>value</i>
Length	0.6 m
Width	0.28 m
Height	0.2 m
Draft	0.03 m
Mass	5.04 kg
Hinged-Rigid angle	0.011765 rads 0.674 degrees

Table 2

Refer to fig 4.5 for schematic of the system where, the upper numbers represent joints and the lower numbers represent elements. In the program, R is defined, as a step dependent scalar coefficient, such that if multiplied by the forces vector, will result in the required load value that causes a change in the status of one or more joints at that particular loading step.

All the following steps are shown in Fig 4.12.

In the first loading step all elements are connected together with hinged joints. In the simulation it is calculated that the first change in joint status will happen when R is 0.0775. Therefore with 1.1625 kg load (which is  $R \times F$  or  $0.0775 \times 15$  kg), joints 4 and 7 become locked in the negative direction (Fig 4.6). This stage completes the first loading step.

The second loading step starts with modifications to the stiffness matrices of elements in both sides of the changed joints. The stiffness matrices of elements 3, 4, 6, and 7 are changed from both ends hinged to hinged-rigid, rigid-hinged, hinged-rigid and rigid-hinged respectively. R in this step is 0.1298, which means that further changes in joint status will happen. With this value of R (1.947-kg load) joints 5 and 6 become locked in the positive direction (Fig 4.7). This completes the second loading step.

The next loading step starts with modifications to the stiffness matrices of elements ending to joints number 5 and 6, which became locked in the previous loading step. Therefore the stiffness matrices of elements 4, 5, and 6 will change respectively from rigid-hinged, both ends hinged and hinged-rigid to both ends rigid. R in this step is found to be 0.1512, and such value corresponds to a load of 2.268 kg that will unlock joints 4 and 7 (Fig 4.8) hence ending the third loading step.

The subsequent loading step starts with modifications to the stiffness matrices of elements ending at joint numbers 4 and 7 that became open in the previous loading step. Therefore the stiffness matrix of elements 3, 4, 6, and 7 change from hinged-rigid, both ends rigid, both ends rigid, and rigid-hinged to both ends hinged, hinged-rigid, rigid-hinged, and both ends hinged respectively. R in this step is found to be 0.3296, and such value corresponds to a load of 4.944 kg that will lock joints 3 and 8 in the negative direction (Fig 4.9), hence ending the fourth loading step.

The fifth loading step similarly modifies stiffness matrices for elements ending at joint numbers 3 and 8 which became locked in the previous loading step. The stiffness matrices of elements 2, 3, 7 and 8 change from both ends hinged to hinged-rigid, rigid-hinged, hinged-rigid, and rigid-hinged respectively. R in this step is found to be 0.6915, and such value corresponds to a load of 10.3725 kg that will lock joints 2 and 9 in the negative direction (Fig 4.10), hence ending the fifth loading step.

The next loading step requires a start with modification of stiffness matrices of elements ending at joint numbers 2 and 9 (locked in the previous loading step). Hence the stiffness matrices of elements 1, 2, 8, and 9 will change from both ends hinged, hinged-rigid, rigid-hinged, and both ends hinged to hinged-rigid, both ends rigid, both ends rigid, and rigid-hinged respectively. R in this step is found to be 1, and such value corresponds to a load of 15 kg that will lock joints 4 and 7 in the positive direction (Fig 4.9), hence ending the sixth loading step.

The next loading step starts with modifications to the stiffness matrix of elements ending at joint numbers 4 and 7 (locked in previous loading step). Therefore the stiffness matrix of elements 3, 4, 6 and 7 will be changed from rigid-hinged, hinged-rigid, rigid-hinged and hinged-rigid to both ends rigid. However since  $R$  has reached unity in the previous loading step no further changes will occur in the form of connections for this load (15 kg) and that will be the final step (Fig 4.11).

#### 4.1.10.2 Example for full size dimensions

For this simulation a multipli-connected structure of total size 180m by 12m is considered, consisting of 60 pontoons, which are arranged in a mat array of 4 rows, 15 columns. The connection between each pontoon in the longitudinal direction is of a hinged-rigid type, and each pontoons is connected rigidly to the transverse direction. Thus the whole structure can be considered as 15 pontoon units in an in-line array, where each pontoon unit is made up of 4 single pontoons rigidly connected together. Hence the dimension of a pontoon unit is 12m by 12m. Two 72000 kg loads (12000 kg/m) typical of an army tank are first applied on the pontoon unit number 1 and then this load is moved to pontoon unit 15.

The dimensions of each single pontoon are as follows;

<i>Parameter</i>	<i>value</i>
Length	12.00 m
Width	3.00 m
Height	2.00 m
Draft	0.50 m
Mass	18000 kg
Hinged-Rigid angle	0.005 rads 0.286 degrees

Table 3

The displacements due to this loading is shown in figure 4.13 to 4.17 respectively. The displacements of all pontoons resulting from successive loading on different

pontoons are shown in figure 4.17. Also the calculation of different load steps when the load is applied on unit pontoon eight is given as an example in appendix H. The result of this calculation is plotted in figure 4.18.

The draft of this structure is 0.5m with own weight and due to this loading the draft will increase up to 0.85m. Therefore the freeboard of the structure will be 1.15m which is enough for this particular structure (floating bridge or floating quay). The maximum displacement, which is under the moving load, is the same for each section along the structure except pontoon units 1 and 15, which are at the end of the structure. In order to decrease the displacement in both ends of the structure it would be practical to increase the hydrostatic stiffness of the structure by increasing the width of the structure. This might take the form of attaching some more pontoons in the beginning and end of structure.

## **4.2 Mat array**

The above operation (section 4.1.10) can be changed such that it could be used for mat array systems as well. To enable this, elements in the mat array should be considered as shell or solid elements (each pontoon will be a shell or solid element on an elastic foundation). The connections between two neighbouring elements are thought of as two beam elements, where one end of each beam element is connected to the shell or solid element, and the other ends are connected together in a hinged or rigid connection. As a result if suitable shape functions are found for a shell or solid element on elastic foundation, it enables us to follow procedures that were outlined in the case of in-line array configuration.

## CHAPTER 5 EXPERIMENTS

### 5.1 Experimental apparatus

#### 5.1.1 Pontoon model

To further improve understanding of the behaviour of the system, and to provide a basis for validation of the theoretical models developed, it was deemed necessary to conduct a series of practical experiments. For this purpose many tests have been carried out which mainly can be divided into two groups, those concerning the in-line array configuration and those of the mat array system. The former series of tests were conducted in a towing tank (with dimensions 15×2×1m) and the later series of tests were carried out in a wave tank (with dimensions 10×2.5×1.5m), both of which are located in the hydrodynamics laboratory of the Department of Mechanical Engineering, UCL.

The pontoon models used in this project were constructed in the workshop of the Department of Mechanical Engineering, UCL. The design was at 1:100 scale. The models were made of plywood, with the following dimensions:

<i>Parameter</i>	<i>value</i>
Length	0.6 m
Width	0.28 m
Height	0.2 m
Draft	0.03 m
Mass	5.04 kg
Hinged-Rigid angle	0.011765 rads 0.674 degrees

Table 4

Different connection designs were adopted in the conduct of the tests. For hinged-rigid connection of the in-line array floating structure, joints were designed to

allow any pontoon module rotations up to a specified value without contact to the adjacent module. Should the specified rotation limit be exceeded between any two pontoons, the joint will lock the two pontoons together, and any further movement in any of the pontoons will be accompanied by the other pontoon, i.e. they act as one body. For hinged connections in the mat array floating structure universal joints were used, which allow any pontoon module to freely rotate about the x and y axes. Finally, for hinged-rigid connections of the mat array, the joints operate on a similar principle to the hinged-rigid connections used in the in-line array, but here the action is in both axes (x and y).

The general arrangements for tests are illustrated in fig 5.1. Single pontoon modules used in different test series are shown in fig 5.2 to 5.4.

The pontoon module with hinged-rigid connections for in-line array is shown in fig 5.2. The pontoon module for hinged connection used in mat array is shown in fig 5.3, and the pontoon module for hinged-rigid connection is shown in fig 5.4.

The assembly of pontoons for hinged-rigid connections as used for the in-line array is shown in fig 5.5. The arrangements of mat array for hinged and hinged-rigid connection are shown in figures 5.6 and 5.7 respectively.

Although many tests with different load condition were carried out for the in-line array, only some of them are show in figures 5.8 to 5.10. Figure 5.11 shows an in-line array in waves.

Fig 5.12 shows load applied on pontoons number two and four located in the middle row of the mat array (3×5) with hinged connections, whilst fig 5.13 shows load applied to the middle pontoon of the mat array with hinged-rigid connections. A mat array system in waves is shown in fig 5.14.

Fig 5.15 to 5.17 show the potentiometers connection to the pontoons and fig 5.18 shows the potentiometers connection to the computer.

### 5.1.2 Potentiometers – data logger

Potentiometers were used to measure the change in pitch angle and heave of each pontoon. The potentiometers were secured on a wooden board in such way that each was attached to one end of the model by a fine nylon line.

The potentiometers were connected to a computer with an Amplicon PC – 126 analogue to digital conversion data acquisition card installed. The proprietary Waveview software supplied with the card was used to view the data stored before exporting for further analysis using the spreadsheet calculator, Excel 7. The output values, taken from the computer, were calibrated to give degrees of pulley rotation and thereby vertical displacement knowing the pulley diameter.

### 5.2 Experimental procedure

The procedure used for each test is briefly described here. The five volts DC coming from the power-unit was connected to each potentiometer (the input and null of potentiometer). Then each potentiometer was connected to the data logger (from output and null of potentiometer). The data logger was subsequently connected to the computer for recording the data. For any load condition the measurement of voltage took place twice, once before loading and once after loading. The difference of the two voltage readings is due to this loading.

During one full rotation, the potentiometer will go from having very little resistance to having an extremely large resistance, hence after one full rotation the voltage across the device is five volts and since the input is set at five volts, the output must be 0 volts. Knowing this, we can formulate a relationship connecting the rotation of the wheel in radians to the voltage offset across the input and output, i.e. in this case a  $\pi$  radians rotation of the potentiometer, will result in 2.5 volts difference between input and output. Since the wheel connected to the potentiometer has a diameter of 43mm, a full rotation of such wheel will correspond to a 135mm vertical displacement of the nylon line, which is

connected to the pontoon module and runs over this wheel. Hence in other words each volt represents 27mm vertical displacement of a pontoon module.

The heave displacement is the sum of displacement at both ends of the pontoon module divided by two. The pitch displacement of any pontoon module is the difference of vertical displacement of both ends of pontoon module divided by the length of that pontoon module.

As mentioned the experiments were divided into two sets. The first was for an in-line array floating structure, which consisted of three test series. The second was for a mat array floating structure, and consisted of two test series. The following is a description of the procedures and tests carried out.

## **5.2.1 Test series for in-line array**

### **5.2.1.1 Test series 1**

The first test consisted of five pontoon modules with specific free rotation between any two adjacent pontoons under different load conditions given below:

- Load applied to pontoon 1, fig (5.19)
- Load applied to pontoon 2, fig (5.20)
- Load applied to pontoons 2 & 4, fig (5.21)
- Load applied to pontoon 3, fig (5.22)

Figures (5.19 to 5.22) constitute of four separate sections (a, b, c, and d). The displacements of joints in different load conditions are shown in (a). The heave and pitch displacements with increasing load of any individual pontoon are illustrated in (b) and (c) and the difference of pitch angle of any two adjacent modules can be seen in (d).

The first case where the load is applied to pontoon 1 is explained here as an example. Figure 5.19a shows the displacement of the joints along the length of the

multipli-connected structure. As it can be observed from figures (5.19a to 5.22a) the displacements of the joint nearest to the loading point always have greater magnitude than the displacement of the other joints. Figure 5.19b and 5.19c show that the heave and pitch displacement of the loaded pontoon and the adjacent pontoons increases with increasing load, however heave and pitch displacement of the other pontoons does not necessarily follow the same pattern. The same conclusions about the heave and the pitch displacement in different loading conditions, can be drawn from figures 5.19b to 5.22b. Figure 5.19d shows the difference in rotations between adjacent pontoons. Due to manufacturing imperfections the expected results could not be observed perfectly, but a clear pattern does exist where the difference in rotations increases with load increments up to a certain threshold value, beyond which there is no further increase in the difference of rotations. This threshold value is the maximum allowable free rotation at any joint. For other cases (load conditions) see corresponding figures.

#### **5.2.1.2 Test series 2**

The second test series consisted of five pontoon modules with specific free rotations between adjacent modules (the free rotation in this test was greater than in the first test series) with the same load condition and load increments as part (iv) of the first test series. The configuration of displacements is similar to part (iv) of that series. The results can be seen in Figs 5.23a 5.23b, 5.23c and 5.23d. The difference of displacement between two tests with similar load conditions and load increments, but different free rotation limits is illustrated in figure 5.24. According to this figure there is greater displacement resulting from a higher locking angle at the joints.

### 5.2.1.3 Test series 3

The third test series consisted of nine pontoon modules with free rotation, which was the same as for the first test series, and various load conditions. The results are illustrated in figures 5.25 to 5.32.

- Load applied to pontoon 2, Figure 5.25
- Load applied to pontoon 3, Figure 5.26
- Load applied to pontoon 4, Figure 5.27
- Load applied to pontoon 5, Figure 5.28
- Load applied to pontoon 3 and 7, Figure 5.29
- Load applied to pontoon 3 (12 kg) and 7 (1 to 12 kg), Figure 5.30
- Load applied to pontoon 4 and 8, Figure 5.31
- Load applied to pontoon 4 (12 kg) and 8 (1 to 12 kg), Figure 5.32

The individual sections within figures 5.25 to 5.32 have the same plots as those described in 5.2.1.1 for figures 5.19 to 5.22.

## 5.2.2 Mat array

The mat array test, which was carried out, consisted of a fifteen-pontoon arrangement in three rows and five columns, this system can be seen in figure 5.33.

### 5.2.2.1 Test series 1

This test series consisted of fifteen pontoons with hinged connection, and also with different load conditions. The results are illustrated in figures 5.34 to 5.41.

- Load applied to pontoon 6, figures 5.34 & 5.35
- Load applied to pontoon 7, figures 5.36 & 5.37

- Load applied to pontoon 8, figures 5.38 & 5.39
- Load applied to pontoon 3, figures 5.40 & 5.41

The result of each loading is illustrated in two separate figures. The first figure is to show the displacement of each pontoon in different rows, while the second figure serves the same purpose but this time the displacement of each pontoon in different columns is plotted.

Here the result of the first case where the load is applied to pontoon 6, will be explained as an example. Figure 5.34 section (1) shows the displacement of the joints along the first row of the multi-connected structure, where it can be seen that the displacement of the joints nearest to the loading point has greater magnitude than the displacement of the other joints. Sections 2 and 3 show respectively the displacement of joints in rows 2 and 3 where the same principle can be observed. Figure 5.35 is also made up of five sections where each section from 1 to 5 shows respectively the joint displacement of columns 1 to 5 in the mat array structure. For other cases see corresponding figures 5.36 to 5.41.

### **5.2.2.2 Test series 2**

The second test series for mat-floating structure consisted of fifteen pontoons with some free rotation, and also with different load conditions. The results are illustrated in figures 5.42 to 5.49.

- Load applied to pontoon 6, figures 5.42 & 5.43
- Load applied to pontoon 7, figures 5.44 & 5.45
- Load applied to pontoon 8, figures 5.46 & 5.47
- Load applied to pontoon 3, figures 5.48 & 5.49

The format of each figure given here, follows the same pattern as that of which was explained in the last section.

## CHAPTER 6 DISCUSSION

Two different theoretical approaches have been assessed in this work. In the first method the constraint equations were inserted in the global stiffness matrix of the system of multipli-connected floating structure (Chapter 3). In the second method finite element and potential energy of beam on elastic foundation (Chapter 4) were used to reach a solution. In both cases after developing the equations, the method was coded into software.

### 6.1 Theoretical work by use of constraint equations

In this method, as explained in Chapter 3 each pontoon is assumed to be a rigid body. Therefore the displacement will be that of a rigid body in water. The formulas deriving in Chapter 3 are very satisfactory for calculation of displacements. Most of the results from this method are a good match to the ones obtained from experimental work. The results for the case where 15-kg load was applied on pontoon number five in an array of nine pontoons is shown in figure 6.1, in which a comparison between the theoretical and experimental results can also be observed.

The coded software developed based on this theoretical work produces satisfactory output for hinged, elastic and rigid connections. However, there are some inconsistencies with its use for hinged-rigid connection.

It has been verified theoretically and experimentally that with increasing the value of the locking angle in connection of multipli-connected floating structure, the displacement will also be increased. This statement is illustrated in fig 5.24.

Although this method was satisfactory, but because of some weaknesses which were mentioned, the second method, which was satisfactory for all cases, especially for hinged-rigid connection types, was developed.

## 6.2 Use of finite element method and potential energy

In this method which is developed in Chapter 4, each pontoon is to be assumed as a beam on elastic foundation. For this software was developed to calculate the global stiffness matrix and the vector of forces of the beam elements on elastic foundations and solve the resultant equations for various end conditions.

In the mentioned software, the structure is described to have been built from several similar modules of the same length and the same locking angle limit. Also the second moment of area and elasticity of the elastic foundation are assumed identical for each module. The length of the modules is subject to distributed loading while the nodes are subject to concentrated loading and the moments.

While the detailed operation of this method was given in the previous chapter, a brief outline is given here again. The objective is to calculate the joints displacement from which bending moments, shear forces and the stresses can be found. The method proceeds to calculate the displacement of the joints via a series of loading steps. The software initially assumes the load to be 0 kg and in each step it is incremented by a certain value until it reaches the value of the actual load. The value of each increment is decided by the smallest additional load which will cause a change in the status of any joint, by which we mean a joint becoming locked or unlocked. The increment of each step is added to the total load, which was already applied to the structure from the previous loading steps. Example 4.1.10 serves to illustrate these points more clearly.

After each loading step according to the angle locking/unlocking that have taken place, the stiffness matrix of the concerned pontoons is altered. The alterations to the matrix are a direct result of the changing of the joint's status. In changing the connection form at the nodes it must be remembered that if any node becomes locked then this node will be considered as a built-in node. Should the node to the right hand side of the locked node be hinged, then the stiffness matrix of the element (between the locked node and the node on the right hand side of locked node) becomes that of an element with one end built-in and the other end pinned. If the node to the left-hand side of the locked node is hinged, the stiffness matrix

of the element (between the node on the left-hand side of the locked node and the locked node) becomes that of an element with one end pinned and the other end built-in. In the case of any neighbouring node to the locked node becomes locked, then the stiffness matrix of the element (between the two locked nodes) becomes that of an element with both ends built-in.

It is important that in addition of considering the locking of joints in the positive and negative directions, the unlocking of the joints must not be forgotten either. Should a previously locked node become unlocked, then based on the status of the nodes either side of it, different approaches are taken. If a node either side of the unlocked node is hinged or locked, the stiffness matrix of a both ends pinned element, or a one end pinned with the other end built-in element is used respectively.

The reader can refer to figure 6.2 in which the theoretical results using this method and the experimental results when 15kg load is exerted on pontoon 5 are compared. To gain a broader picture of the situation, figure 6.3 is more suitable in which the predictions from both theories are compared with the experimental results. Here a comparison between the performance of the theories can be made not only to each other, but also with the experimental results at the same time.

To compare the theoretical results for each different loading conditions with its experimental counterpart would be an unnecessary and not to mention cumbersome operation. While all of the loading conditions were tested both in the theoretical and the experimental aspects, in his work only some of them are given.

Below is a brief outline of the figures containing these results.

Figure No:	load applied to pontoon No:	Value of the load (kg)
6.4	2	12
6.5	3	12
6.6	3 & 7	12 (each)
6.7	3 & 7	12 & 6
6.8	4 & 8	12 (each)
6.9	4 & 8	12 & 6

Table 5

### 6.3 Use of a standard FEA package

As mentioned before, of all the analytical software packages available, ABAQUS was considered as powerful and flexible. However it was still not suitable for the main thrust of this work for the following reasons. ABAQUS offers two facilities that could potentially be used for this work, the use of a non-linear spring as the connection, and the use of constraint equations. Here it will be explained why these two facilities are not very successful for study of hinged-rigid connections.

If one wanted to simulate the hinged-rigid connection by a non-linear spring, the spring would have to have the following form of non-linearity:

$$|\theta_{i+1} - \theta_i| < \varepsilon \quad k = 0$$

$$|\theta_{i+1} - \theta_i| \geq \varepsilon \quad k = \infty$$

where:

$\varepsilon$  = locking angle of the joint

$\theta$  = pitch angle of the pontoon

Unfortunately the non-linear spring as defined in ABAQUS does not cover this range, thus making it unsuitable to simulate the hinged-rigid connection. This leaves us the option of using the constraint equation to model the connection.

In modelling the connection by constraint equations, the constraint itself will be in the form of an inequality (equation 3.35), however ABAQUS can only deal with constraints which are of an equality form, and thus we can not use the constraint equation facility of ABAQUS for the hinged-rigid connection.

However for hinged connections in a mat array where the constraint has an equality form, the connection was modelled in ABAQUS using the constraint equation facility and the result is given in figure 6.10 for an increasing central load. These can be compared with the experimental results which are given in figure 5.38-39, where it can be seen that the modelling is to some extent successful. The subtle

differences between the experimental and the ABAQUS results are due to the boundary conditions especially the low stiffnesses of the mooring lines which were given to ABAQUS. Whilst it was intended that these should be as close as possible to their real values, some of these are evidently inaccurate estimates.

## CHAPTER 7 CONCLUSIONS

This chapter presents the primary conclusion from the thesis and suggests recommendation for further development of the work.

It is shown in this work that any changes in the status of the joints in an articulated floating structure can be occur either by varying the amount of load in a specific point or moving the position of load along the floating structure. The joints could adopt two extreme positional cases, when change is from hinged to rigid (locked) or vice-versa (unlocked). In this work I have investigated this problem by use of new mathematical modelling implemented in software. Some points specifically relating to different sections of the work are given here in sections one to seven.

Section one emphasises the existing design software. Section two discusses new theories, which is used in this work. Section three mentions the unlocking problem and section four explains the extension of the structure to full scale. Section five gives the experiences gained during the experimental work. Section six discusses the mat array, dynamic loading and advantage of hinged-rigid connections. Finally section seven suggests further development in the articulated floating structure.

### 7.1 Existing design Software

As stated in Chapter 2 and discussed in detail in Chapter 6, the existing design software has been shown to predict successfully in some cases for which the constraint equations are an equality, for example hinged connection. However the software has been shown not to work in cases where the constraint equations possess an inequality which is the main subject of this work. In the case of hinged-rigid connections the constraint equation contains an inequality. ABAQUS, a finite element analysis package with non-linear capabilities, was recognised to be the most powerful software for analysis of this type of structure. Having said that, owing to certain difficulties which is discussed in Chapter 6, ABAQUS was not used for the work for hinged rigid connections.

ABAQUS has been shown to be suitable for hinged connections. However experimental tests were not carried out for the in-line array with hinged connections, therefore ABAQUS also was not used for in line array with hinged connection. However ABAQUS used with the constraint equation facility for hinged connections for mat arrays result shows reasonable agreement with experimental data in Chapter 5.

## **7.2 Theoretical work**

### **7.2.1 Theoretical work by use of constraint equations**

The use of constraint equation method, as shown in Chapter 3, has satisfactory results for certain cases, namely ones where the constraint relationship can be written as an equality (e. g. eqn. 3.7). In other cases, such as the hinged-rigid type connection where the constraint relationship takes the form of an inequality, this method fails to produce satisfactory results. Furthermore, to analyse the system using this method, it was assumed that each pontoon is a rigid body and hence its elastic properties were ignored. Bearing in mind the two shortcomings of the method just mentioned, future work based on this method is not advised.

### **7.2.2 Use of finite element method and potential energy**

This method, as shown in Chapter 4, is suitable in that it able to handle all cases including the case of the hinged-rigid connection type where the constraint relationship is an inequality. In analysing a system using this method, a pontoon (or relevant unit of the structure) is assumed to be an elastic beam on an elastic foundation. The rigidity of this beam ( $EI$ ) will, by necessity, have to be large. The performance of the method depends on how close this assumption is to reality. In general so long as the length of the pontoon is comparable to its width, it is appropriate to resemble it as a beam. This assumption is not new to structural

analysis and is in fact widely used in assessment of the structural analysis of ship structures.

In this work the high rigidity and low forces on the beams results in low deflections, which can generally be considered as negligible. However improvements can be made with this method for cases in which significant deflections of the beam will occur. For example rather than assuming each pontoon to be a single beam, we can divide each pontoon into a number of super-elements, namely shell elements which represent the outer skin of the pontoon and beam elements the inner structure of the pontoon. This will increase the number of calculations, however the assumption would be closer to reality, and better results would be obtained.

### **7.3 Unlocking solved**

In the case of rigid bodies for pontoons (Chapter 3) when the angle between two consecutive modules reaches a design threshold limit, at which point the system acts as a rigid body, there is no further increase or decrease in angle between two adjacent pontoons. In other words the difference of pitch angle of two consecutive pontoons remains constant. In the case of elastic beams for pontoons (Chapter 4) after the angle between two consecutive modules reaches a design threshold limit, this angle may vary because of elasticity in the beam. This variation is however quantitatively small. The software generated for arranging and solving the equations in Chapters 3 and 4 from the result of angles between adjacent pontoons will recognise the locking/unlocking status of the joints. For a rigid body after reaching the locking angle, because this angle remains constant further action will not happen. Therefore the problem of unlocking appears. In the case of elastic beams after reaching the locking angle, the body remains elastic. Since this angle is still subject to variations owing to elasticity this angle is subjected to variation, although this variation is very small. If the angle started to increase the status of joint remains locked. However if the angle starts to decrease it is apparent that the phenomenon of unlocking has happened and the software will recognise that. Consequently the major problem of unlocking has been solved.

#### **7.4 Extension to full scale**

A full-scale example has been presented in Chapter 4. Although this example is presented in order to have a real feeling of displacement, some interesting points arise from this example. The maximum displacement, which is under the moving load, is the same for each section along the structure except pontoon units 1 and 15, which are at the end of the structure. In order to decrease the displacement in both ends of the structure it would be practical to increase the hydrostatic stiffness of the structure by increasing the width of the structure. This might take the form of attaching some more pontoons in the beginning and end of structure. The load influences a limited number of pontoons and the rest of the structure remains free of influence of the load. The numbers of pontoons, which are influenced by load, depend on the amount of load and value of locking angle.

#### **7.5 Physical models**

From the comparison of experimental and theoretical results it is concluded that the models built in this work for the purpose of obtaining experimental data were sufficiently accurate. However should even higher accuracy be needed in follow up work, the following modifications are suggested:

- A more refined manufacturing process giving less structure variations from pontoon to pontoon. Chapter 5 indicates that there are slight variations in the locking angle of the pontoons because there were manufacturing inaccuracies.
- Using different materials such as metal alloys, as opposed to plywood to make the pontoons, and hence making the model more similar to the form it would have, should it be employed in real life.
- Reducing the scale (i.e. increasing model size) would give results even closer to real life situations.

- A move to a purely opto-electronic movement detection system would give more accurate results because in such a system very little disturbance would be introduced to the movement of the pontoons. This would also avoid problems such as the nylon line slipping on the wheels. This problem especially effects the pontoons that are at the edges of the array since their change in displacement is greater. In Chapter 6 it can be seen that for pontoons at the end of the array, the difference between the theoretical and experimental results is larger than any other pontoon, and is caused by this.

## **7.6 Mat array**

### **7.6.1 Mat array**

For the mat array configuration with hinged connections two approaches were taken. The methods involved using constraint equations as explained in Chapter 3. As described neither of these methods were entirely satisfactory for mat array configurations. This, coupled with the fact that pursuing the situation using the in-line array analysis would be very cumbersome and time consuming, meant that the development of theory for the mat array configuration with hinged-rigid connections was stopped owing to time constraints.

However experience obtained from the theoretical work in Chapter 4 indicated that with some modifications, the theory from the in-line array analysis could be used for the mat array configuration. As an example, the elements in the mat array could be considered as shell or solid elements. That is each pontoon being represented as a shell or a solid element on an elastic foundation. Also the connections between two neighbouring elements must be thought of as two beam elements, where one end of each beam element is connected to the shell or solid element, and the other end is connected together in a hinged or rigid connection.

Thus if suitable shape functions were to be found for a shell or solid element on elastic foundation, it would enable one to follow the procedures outlined in the case of in-line array configuration for the mat array system. Chapter 5 contains

respectively the results for the hinged connection and the hinged-rigid connection. Further work could use these experimental results if the extension to the in-line analysis method is progressed with mat arrays.

The reasons the methods discussed in Chapter 3 fail to produce satisfactory results for different methods for mat arrays are now discussed. When the constraint equation is applied to all the pontoons for all individual rows and then between different columns, the result is that the symmetry of displacement in x-axis (rows) is lost, although the symmetry in displacement in y-axis remains. This is unacceptable since we require having symmetry in displacement when a symmetrical load is applied. If the constraint equation is applied to all the pontoons for all individual columns and then between different rows, the result is that the symmetry of displacement in y-axis is lost, although the symmetry in displacement in x-axis remains. The remaining case is to insert constraints for all pontoon modules at once. This method also does not produce encouraging results either. Here the symmetry of the displacement is lost in both the y and the x-axis, which is totally undesirable. Because of these inappropriate responses the use of constraint equations is not suitable for mat arrays.

### **7.6.2 Dynamic loading**

Initially it was planned to develop the dynamic loading for in-line and mat arrays as well as considering static and quasi-static loading. However as the project progressed the considerations of dynamic and associated experiments were removed from the work. In respect of the theoretical development this was because the theory for the static and quasi-static aspects proved to be a more difficult than anticipated problem. This was because the unlocking after locking behaviour had not been expected. For the experimental work, although some basic tests were carried out practical difficulties and the lack of suitable equipment meant that the experiments investigating dynamics could not be taken any further. In particular the small width of the tank meant that wall effects influenced the dynamic results for both in-line and mat arrays when subjected to waves.

### **7.6.3 Advantage of hinged- rigid connections**

Previous studies have concentrated either on hinged, elastic, or rigid connections between adjacent structures. The present work investigates the hinged-rigid connection. As it was described before, the system behaves as a hinged connection until the angle between two consecutive modules reaches a design threshold limit, at which point the system acts as a rigid body. This has the advantages of lower pontoon displacement in comparison with hinged connections and less moment in the connections in comparison with rigid connections. In addition a designer can refine the structure by changing the locking angle. It is clear that if the locking angle increases the structure will be a closer representation of hinged connection and these displacements will be increase. This phenomenon is shown in Chapter 5.

### **7.7 Future work**

Success in experimental and theoretical modelling for predicting the unexpected behaviour of an in-line array of pontoons with hinged-rigid connection has been shown in this work. Further work could consider an extension to the theoretical development to consider the dynamic behaviour of in-line arrays. Also the completed work on the quasi-static behaviour of mat arrays provides a suitable database for validation proposes for extension to realistically articulated floating mat arrays.

**REFERENCES**

1. Show R. 1982. 'Wave Energy a Design Challenge'. Ellis Horwood, ISBN0-85312-382-9 (Ellis Horwood Ltd. – library Edn.).
2. Count B. 1980. 'Power From Sea Waves'. Academic Press, ISBN 0-12193550-7.
3. Michael E. 1981. 'Ocean Wave Energy Conversion'. McCormick, ISBN 0-471-085543.
4. Adee B. H. and Martin W. 1974. 'Theoretical Analysis of Floating Breakwater Performance'. Floating Breakwater conference papers, University of Rhode Island, Marine Technical Report Series Number 24, pp 21 – 39.
5. Adee B. H. 3-5 September 1975. 'Analysis of Breakwater Performance'. Proceedings of the symposium on modelling techniques, San Francisco, California.
6. Adee B. H. May 1976. 'A Review of Developments and Problems in Using Floating Breakwater'. Offshore Technology Conference, Houston, Texas.
7. Adee B. H. 1976. 'Floating Breakwater Performance'. Coastal engineering Chapter 159, page 2777.
8. Tsinker Gregory P. 1986. 'Floating Port Design Construction Practices'. Gulf Publishing Company, ISBN 0-87201-723-0.
9. Piskorski R. 1991. 'Dynamics of an Open Zone of Floating Bridge'. Polish Academy of Sciences, Marine Technology Transactions Vol. 2. Gdansk, pp 103-122.

10. Che X. et al. Jan 1992. 'Two Dimensional Hydroelastic Analysis of Very Large Floating Structures'. Marine Technology Vol. 29 No. 1, pp13-24.
11. Takaki Mikio and Tango Yoshihiko. 1994. 'Wave Drifting Forces on Multiple Connected Floating Structures'. Hydroelasticity in Marine Technology Rotterdam, ISBN 9054103876, p 403.
12. Huang Erick T. 1997. 'Motional Dynamics of Coupled pontoons in Seaways'. Naval Facilities Engineering Service Centre Port Hueneme, Proceeding of the Seventh International Offshore and Polar Engineering Conference, Honolulu, USA. ISBN 1-880653-28-1 (Set); ISBN 1-880653-31-1 (Vol. III).
13. Hatch William G., Huang Erick T. and Barthelemy Joseph L. 1997. 'Developing and Testing a Rough-Water Flexible Connector'. Naval Facilities Engineering Service Centre Port Hueneme. Proceeding of the Seventh International Offshore and Polar Engineering Conference, Honolulu, USA. ISBN 1-880653-28-1 (Set); ISBN 1-880653-32-X (Vol. IV).
14. Takaki Mikio, Lin Xin and Higo Yasushi. 1995. 'On the Performance of Large Floating Structures with Different Connectors in Waves'. Hiroshima University. Proceeding of the Fifth International Offshore and Polar Engineering Conference, The Hague, The Netherlands. ISBN 1-880653-16-8 (Set); ISBN 1-880653-17-6 (Vol. I).
15. Ohmatsu Shigeo. 1998.' Numerical calculation of hydroelastic behaviour of VLFS'. Ocean Engineering Division, Ship Research Institute, Ministry of Transport, 6-38-1, Shinkawa, Mitaka, Tokyo 181-0004, Japan.
16. Haeda Hisaaki et al. 1996. 'Hydroelastic Responses of a Pontoon Type Very Large Floating Offshore Structure'. Institute of Industrial Science, University of Tokyo, 7-22-1 Roppongi, Minato-ku, Tokyo, 106 Japan. 1996 OMAE-Volume I –Part A, Offshore Technology ASME 1996.

17. Sannasiraj S. A. et al. 1995. 'The Hydrodynamic Behaviour of Long Floating Structures in Directional Seas'. Ocean Engineering Centre, Indian Institute of Technology, Madras 600036, India.
18. Lee Chang-Ho and Newman Nicholas J. 1998. 'An Assessment of Hydroelasticity for Very Large Hinged Vessels'. Department of Ocean Engineering, Massachusetts Institute of Technology, Cambridge, MA 02139, USA.
19. Wang Dayun et al. 1991. 'Three- Dimensional Hydroelastic Response of a Very Large Floating Structures'. University of Hawaii at Manoa, Honolulu, Hawaii, USA. International Journal of Offshore and Polar Engineering Vol. I, No. 4, December 1991 (ISBN1053-5381).
20. Murdoch Michele A. and Bretz Glenwood. 1997. 'Design of an Expeditionary Port Facility'. Naval Facilities Engineering Service Centre Port Hueneme. Proceeding of the Seventh International Offshore and Polar Engineering Conference, Honolulu, USA. ISBN 1-880653-28-1 (Set); ISBN 1-880653-32-X (Vol. IV).
21. Endo Ryuji et al. June 11/16, 1995. 'Experimental Modal Analysis on Unit-Linked Large Floating Structure Models'. Proceedings of the Fifth International Offshore and Polar Engineering Conference, The Hague, The Netherlands. ISBN 1-880653-16-8 (Set); ISBN 1-880653-17-6 (Vol. I).
22. Suzuki Hideyuki and Yoshida Koichiro. 1996. 'Design Flow and Strategy for Safety of Very Large Floating Structure'. Department of Naval Architecture and Ocean Engineering, Graduate School of Engineering, University of Tokyo. International Workshop on Very Large Floating Structures. Hayama, Japan, paper 3.
23. Takarada Naonosuke. 1996. 'Some Very Short Comments on Further-Considerations for Huge Floating Structures'. Sumitomo Heavy Industries,

- Ltd. International Workshop on Very Large Floating Structures, Hayama, Japan, paper 4.
24. Gustavsen J. et al. 1996. 'Design Philosophy of Floating Bridges with Emphasis on Ways to Ensure Long Life'. International Workshop on Very Large Floating Structures, Hayama, Japan, paper 5.
25. Arita Masayoshi. 1996. 'On the Philosophy of VLFS Maintenance'. Ship Research Institute Ministry of Transport. International Workshop on Very Large Floating Structures, Hayama, Japan, paper 6.
26. Yutaka Ohkawa. 1996. 'Concept and Outline of Mega-float'. Technological Research Association of Mega-float. International Workshop on Very Large Floating Structures, Hayama, Japan, paper 7.
27. Maeda Hisaaki et al. 1996. 'Development of Renewable Energy Park on Oceans'. International Workshop on Very Large Floating Structures, Hayama, Japan, paper 8.
28. Murdoch Michele and Bretz Glenwood. 1996. 'Conceptual Design of a Moored Floating Pier System'. Naval Facilities Engineering Service Centre Port Hueneme, CA, USA. International Workshop on Very Large Floating Structures, Hayama, Japan, paper 9.
29. Young Chung Tae and Hoon Chung Jung. 1996. 'Introduction of Barge-Mounted Plants Project in Korea'. Korea Institute of Machinery and Materials. International Workshop on Very Large Floating Structures, Hayama, Japan, paper 10.
30. Blood H. 1996. 'Model Tests of a Pneumatically Stabilised Platform'. Float Inc. International Workshop on Very Large Floating Structures, Hayama, Japan, paper 12.

31. Ohmatsu Shigeo. 1996. 'Proposal of SRI type VLFS'. Ship Research Institute and Ministry of Transport Japan. International Workshop on Very Large Floating Structures, Hayama, Japan, paper 13.
32. Okada Hiroo et al. 1996. 'A Method for Reliability Analysis of Large Scale Floating Structures Based on Numerical Simulation'. Osaka Prefecture University. International Workshop on Very Large Floating Structures, Hayama, Japan, paper 15.
33. Endo Hisayoshi and Yago Kiyokazu. 1996. 'On the Extreme Load for VLFS'. Ship Research Institute Ministry of Transport Japan. International Workshop on Very Large Floating Structures, Hayama, Japan, paper 16.
34. Yao Tetsuya and Fujikubo Masahiko. 1996. 'On The Structural Analysis of VLFS'. Faculty of Engineering Hiroshima University. International Workshop on Very Large Floating Structures, Hayama, Japan, paper 18.
35. Nakano Shozabura et al. 1996. 'Technological Research on Offshore Construction Towards the Realisation of an Ultra-large Floating Steel Structure using a Very-large-scale Model'. International Workshop on Very Large Floating Structures, Hayama, Japan, paper 20.
36. Okubo Hiroshi et al. 1996. 'An Experimental Investigation Of Required Constructing Forces When Connecting Floating Units During Temporary Fixing, Hiroshi Okubo, Nippon Steel Corporation'. Ship Research Institute, Ministry of Transport Japan. International Workshop on Very Large Floating Structures, Hayama, Japan. paper 21.
37. Messier R. H. and Thomson L. D. 1996. 'Effect of Connector Structural Stiffens on Inter Module Displacements and Forces for Large Modulator Floating Structures'. Department of Mechanical Engineering University of Maine, Orono, ME 04469. International Workshop on Very Large Floating Structures, Hayama, Japan, paper 24.

38. Faltinsen Odd M. 1996. 'Bottom Slamming on a Floating Airport'. Department of Marine Hydrodynamics, Norwegian University of Science and Technology. International Workshop on Very Large Floating Structures, Hayama, Japan, paper 29.
39. Yoshimoto Hirofumi et al. 1996. 'Estimation of Slamming Load Acting on VLFS'. Ship Research Institute Ministry of Transport, Japan. International Workshop on Very Large Floating Structures, Hayama, Japan, paper 30.
40. Takagi Ken. 1996. 'Elastic Deformation and Mooring Force of a Very Large Floating Body on Tsunami Waves'. Department of Naval Architecture and Ocean Engineering Osaka University. International Workshop on Very Large Floating Structures, Hayama, Japan, paper 32.
41. Newman J. N. et al. 1996. 'Analysis of Wave Effects for Very Large Floating Structures'. Department of Ocean Engineering, MIT. International Workshop on Very Large Floating Structures, Hayama, Japan, paper 34.
42. Ohkusu M. and Nanba Y. 1996. 'Analysis of Hydroelastic Behaviour of a Large Floating Platform of Thin Plate Configuration in Waves'. Kyushu University, Fukuoka, Japan. International Workshop on Very Large Floating Structures, Hayama, Japan, paper 35.
43. Kashiwagi Masashi. 1996. 'A B-Spline Galerkin Method for Computing Hydroelastic Behaviours of a Very Large Floating Structure'. Research Institute for Applied Mechanics, Kyushu University. International Workshop on Very Large Floating Structures, Hayama, Japan, paper 36.
44. Takaki Mikio and Gu Xiechong. 1996. 'On Motion Performance of a Huge Floating Structure in Waves'. Hiroshima University. International Workshop on Very Large Floating Structures, Hayama, Japan, paper 37.

45. Kagemoto Hiroshi et al. 1996. 'On Hydrodynamic Forces and Hydroelastic Behaviour of a Very Large Floating Structure in Waves'. University of Tokyo. International Workshop on Very Large Floating Structures, Hayama, Japan, paper 38.
46. Price W.G., Salas Inzunza M. and Tamers P. 1996. 'The Hydroelastic Behaviour of Barge Type Structures in Waves'. Department of Ship Science University of Southampton, UK. International Workshop on Very Large Floating Structures VLFS'96. Hayama, Japan. Paper 39.
47. Inoue Yoshiyuki, Zhang Xuangang and Tabeta Shigeru. 1996. 'On the Hydrodynamic Forces of a Very Large Floating Structure in Oceans'. Yokohama National University. International Workshop on Very Large Floating Structures, Hayama, Japan, paper 40.
48. Quanmig Miao et al. 1996. 'Hydrodynamic Analysis of Moored Very large Floating Structure'. China Ship Scientific Research Centre. International Workshop on Very Large Floating Structures, Hayama, Japan, paper 42.
49. Yasuzawa Yuktaka et al. 1996. 'Wave Response Analysis of a Flexible Large Floating Structure'. Kyushu University and Mitsubishi Heavy industries Ltd. International Workshop on Very Large Floating Structures, Hayama, Japan, paper 45.
50. Riggs H. R. 1996. 'Hydrostatic Stiffness of Flexible Floating Structures'. Department of Civil Engineering, University of Hawaii. International Workshop on Very Large Floating Structures, Hayama, Japan, paper 46.
51. Watanabe Eiichi and Utsunomiya Tomoaki. 1996. 'Transient Response Analysis of a VLFS at Aeroplane Landing'. Department of Civil Engineering, Kyoto University. International Workshop on Very Large Floating Structures, Hayama, Japan, paper 48.

52. Ueda Shigeru et al. 1996. 'Behaviour of Floating Bridge under Wind and Wave Action'. Tottori University, Tottori, Japan and Mitsubishi Heavy industries Japan. International Workshop on Very Large Floating Structures, Hayama, Japan, paper 50.
53. Shiraishi Satoru et al. 1996. 'Experimental Study on Motions of Long Flexible Floating Structures in Waves'. Port and Harbour Research Institute, Ministry of Transport. International Workshop on Very Large Floating Structures, Hayama, Japan, paper 51.
54. Sekita Kinji et al. 1996. 'Design of Mooring Facilities for Large Floating Structures'. School of Marine Science and Technology, Tokai University, and Department of Marine Civil Engineering, Nippon Steel Corp, Tokyo. International Workshop on Very Large Floating Structures, Hayama, Japan, paper 53.
55. Piskorski R. 1992. 'Numerical Methods in Structural Mechanics in Naval Architecture'. Technical University of Gdansk, Gdansk.
56. Cook Robert D. 1994. 'Finite Element Modelling for Stress Analysis'. John Wiley & Sons, ISBN 0-471-10774-3.
57. Gallagher Richard H. 1975. 'Finite Element Analysis Fundamentals'. Pentice Hall, ISBN 0-13-317248-1.

**BIBLIOGRAPHY**

1. Dawe D. J. 1984. 'Matrix and Finite Element Displacement Analysis of Structure' Oxford Engineering Science Series, Clarendon press, Oxford, ISBN 0-19-856213-6.
2. Faltinsen O. M. 1993. 'Sea Loads on Ship and Offshore Structure' Cambridge Ocean Technology Series, Cambridge University press, ISBN 0 521 45870 6.
3. Faltinsen O. et al. 1994. 'Hydroelasticity in Marine Technology'. A. A. Balkema/Rotterdam/Brookfield, ISBN 90 5410 387 6.
4. Glowinski R., Rodin E. Y. and Zinkiewicz O. C. 1979. 'Energy Method in Finite Element Analysis'. John Wiley & sons, ISBN 0-471-99723-9.
5. Lei Aurora Xiaomeng. 1996. 'Dynamic Characteristics of Floating Breakwaters'. Department of Hydraulics, Chalmers University of Technology, Gothenburg, ISBN 91-7179-284-6.
6. Patel Minoo H. 1989. 'Dynamics of Offshore Structure' Butterworths, ISBN 0-408-01074-6.
7. Richards T. H. 1977. 'Energy Method in Stress Analysis'. John Wiley & sons, ISBN 85312-048-X 0-85312-382-9 (Ellis Horwood) Library Edition.
8. Wang S. et al. June 11/16,1995. 'Hydroelastic – Response Analysis of a Box–Link floating Airport of Shallow Draft'. Proceeding of the Fifth International Offshore and Polar engineering Conference. The Hague, The Netherlands.

FIGURES

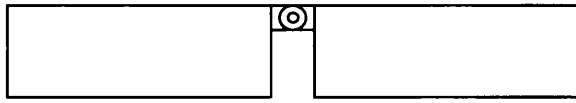


Figure 1.1 Hinged connection (side view)

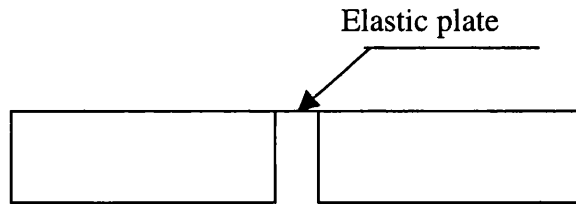


Figure 1.2 Elastic connection (side view)

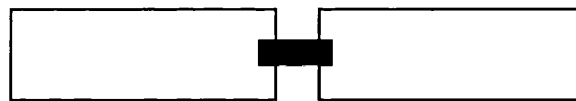


Figure 1.3 Rigid connection (side view)

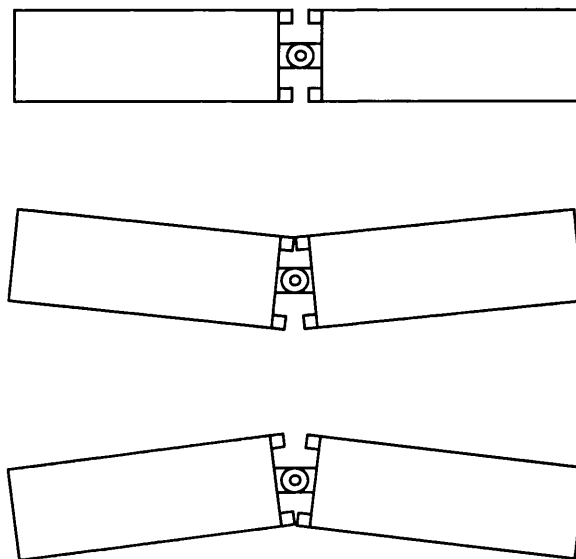


Figure 1.4 Hinged-Rigid connection (side view)

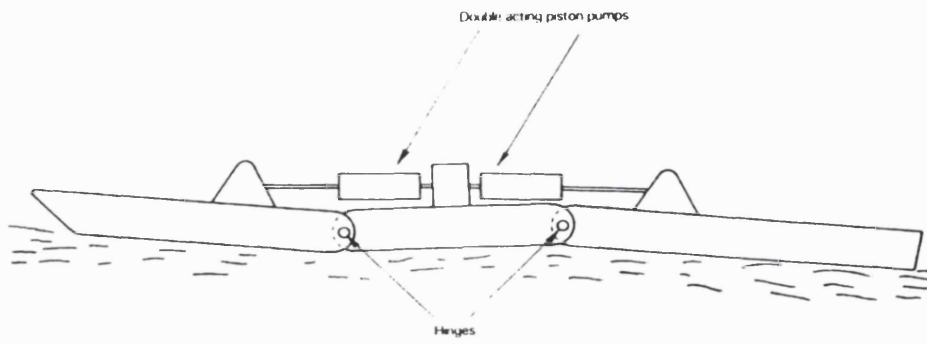


Figure 1.5 the three-raft system of Wavepower [1]

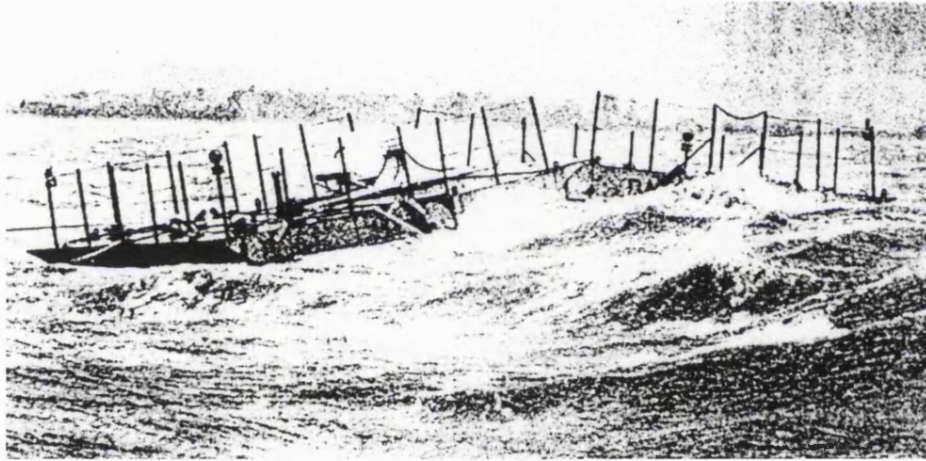


Figure 1.6 One-tenth scale-Cockerel Raft in force 6-7 condition in the Solent, UK.  
Reproduced from a photograph by courtesy of Wavepower Ltd. [1]

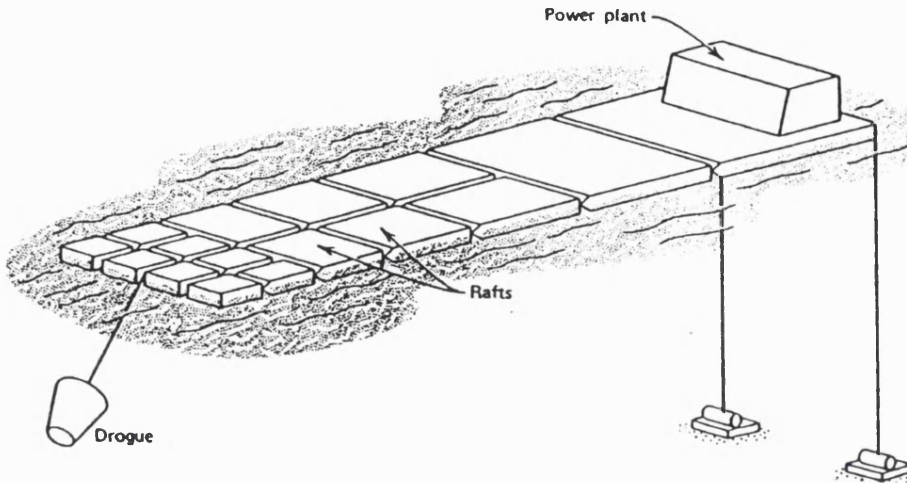


Figure 1.7 Wave (side view) Rafts (Hagen) [3]

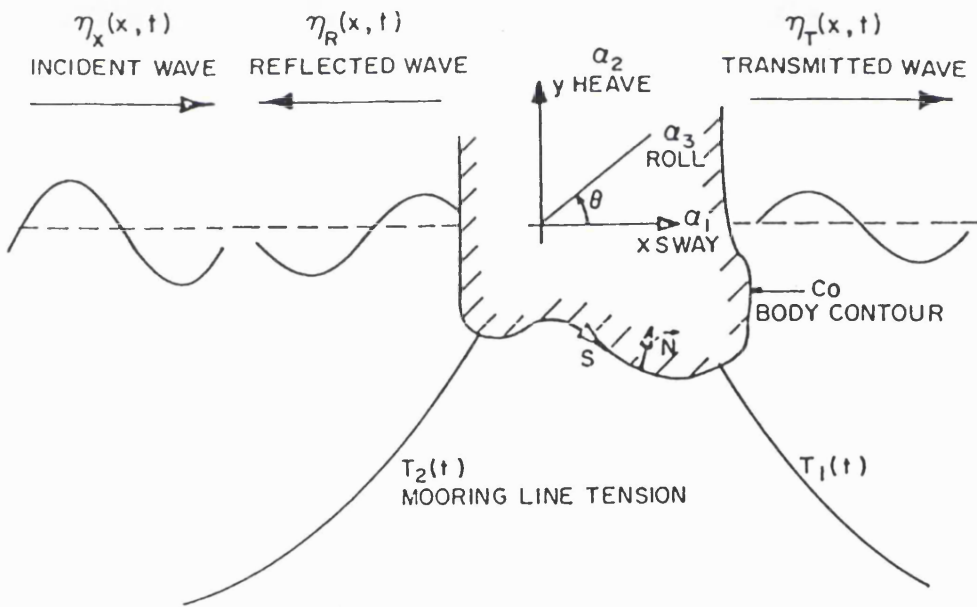


Figure 1.8 A two-dimensional floating breakwater [4]

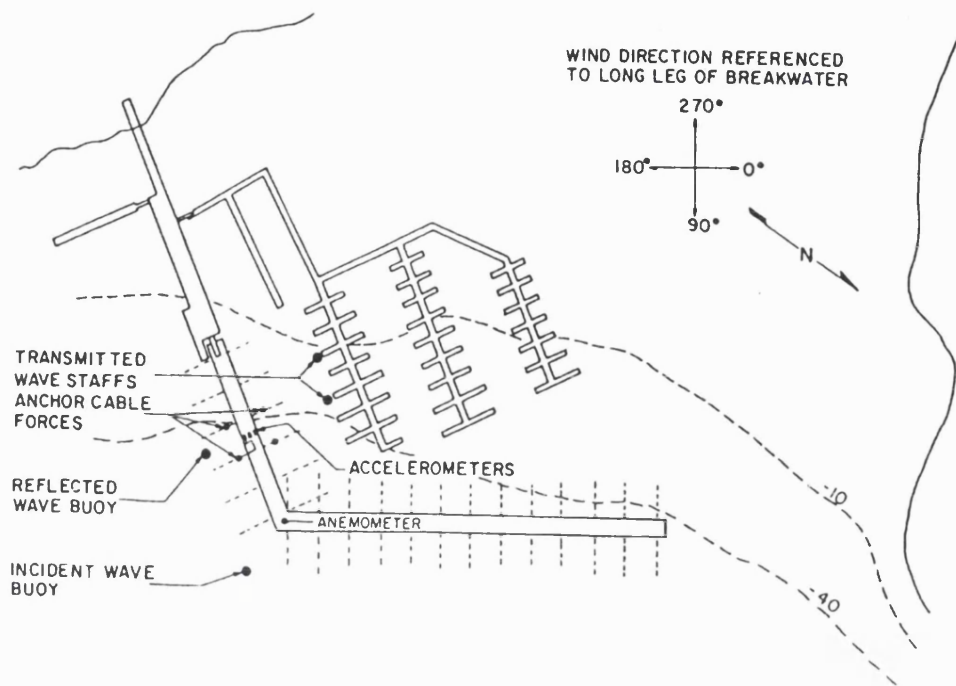


Figure 1.9 Instrumentation location plan, Friday Harbour breakwater [4]

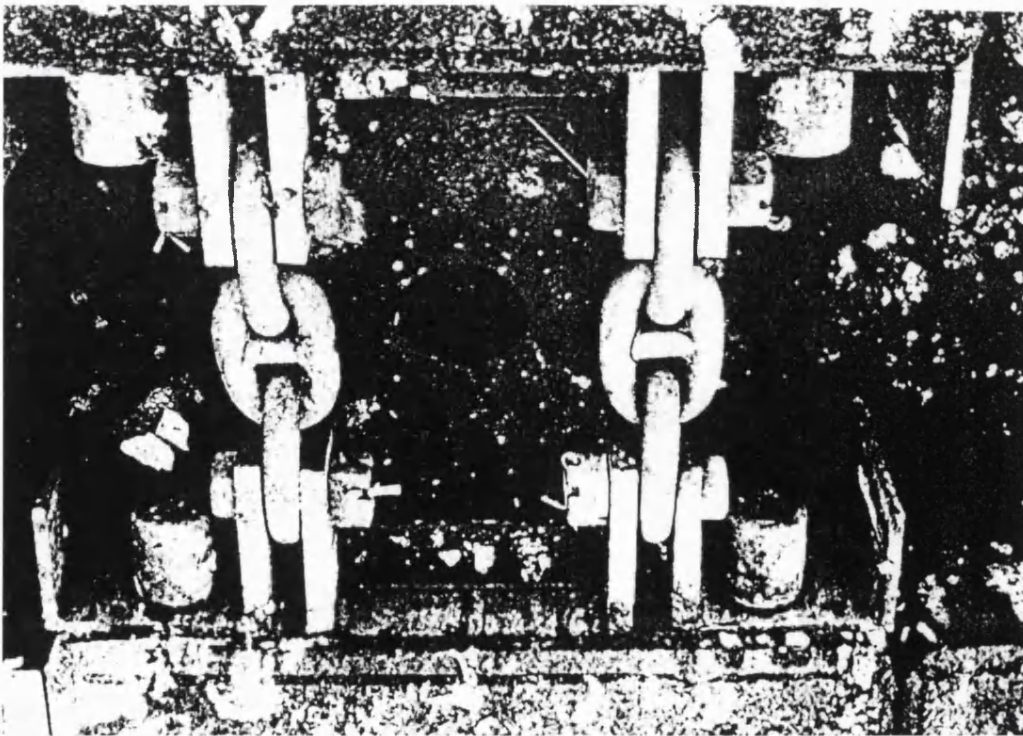


Figure 1.10 Module connection, Sitka, Alaska Floating breakwater [6]

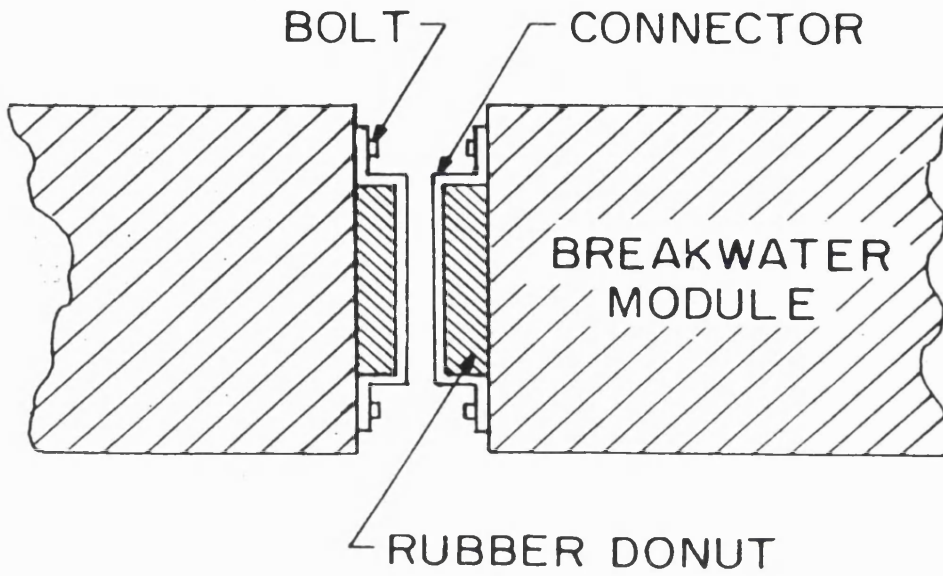


Figure 1.11 Schematic drawing of module connection, Port Urchard, Washington Floating breakwater [6]

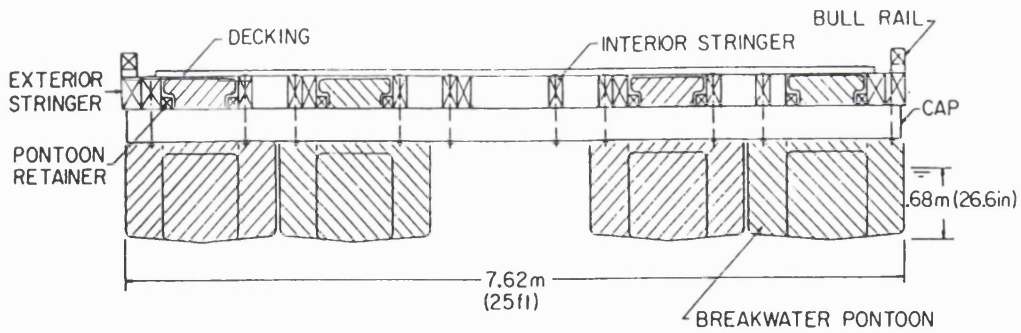


Figure 1.12 Cross section of Friday Harbour breakwater [7]

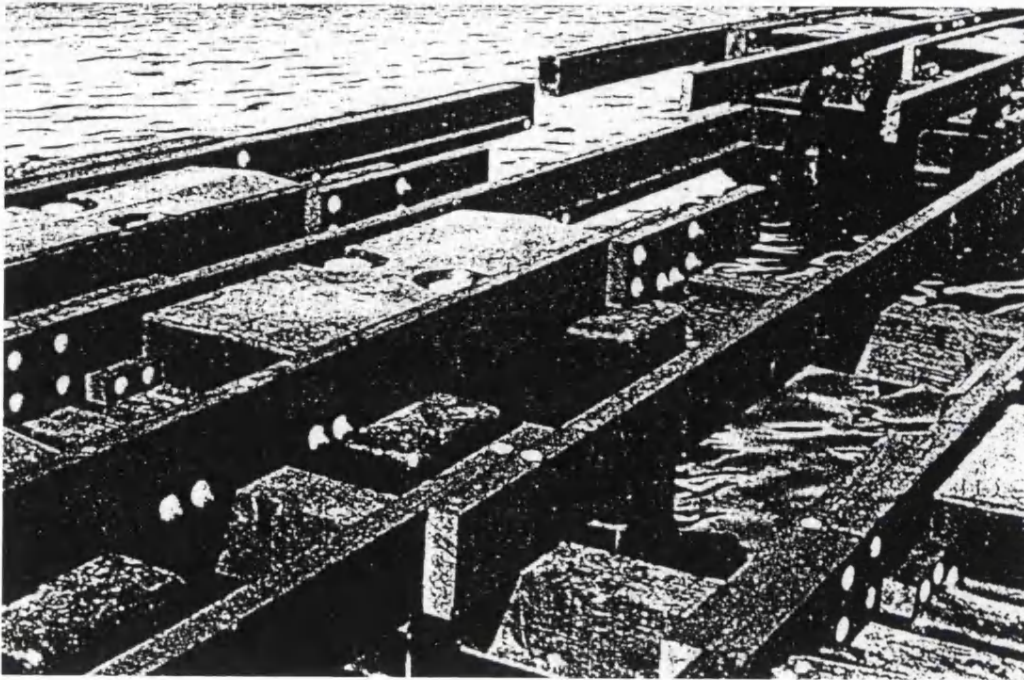


Figure 1.13 Connections of Friday Harbour breakwater [7]

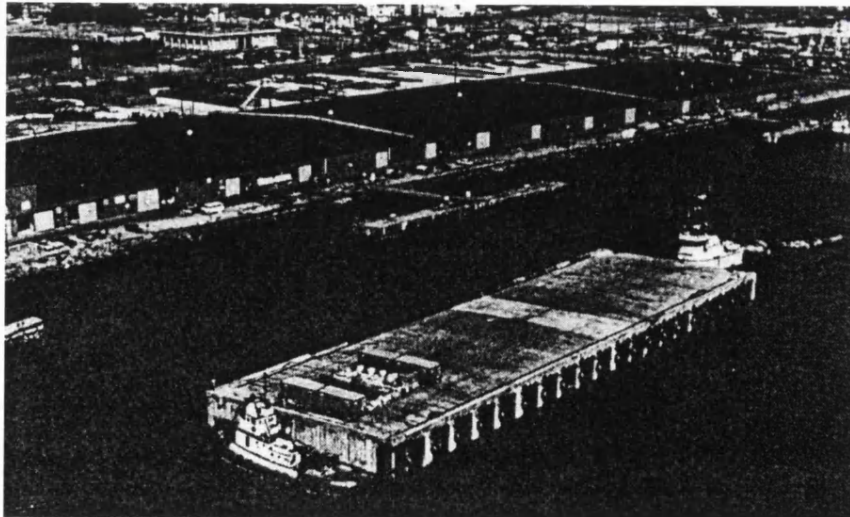


Figure 1.14 Pontoon for Valdez (Alaska) container terminal under tow  
From construction site (Port of Tacoma) to deployment site [8]



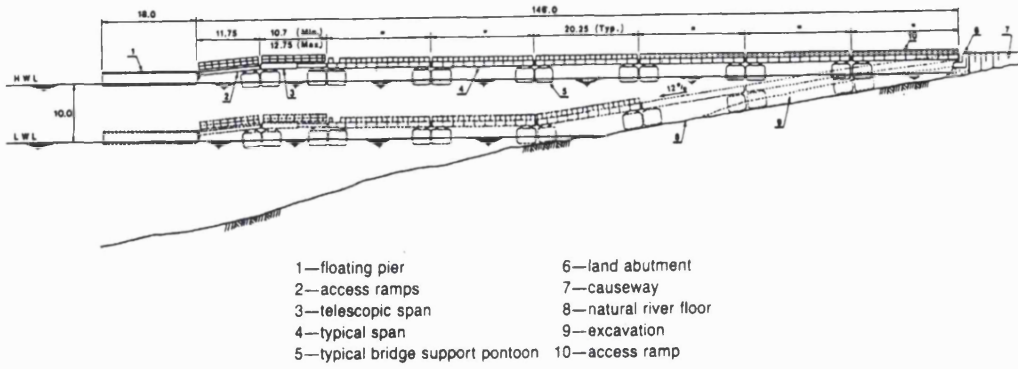


Figure 1.17 Port of Pucallpa, Peru: typical cross section [8]

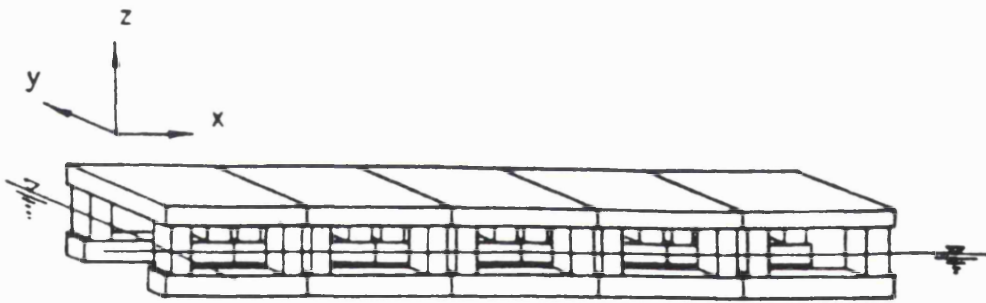


Figure 1.18 Three dimensional view of VLFS [10]

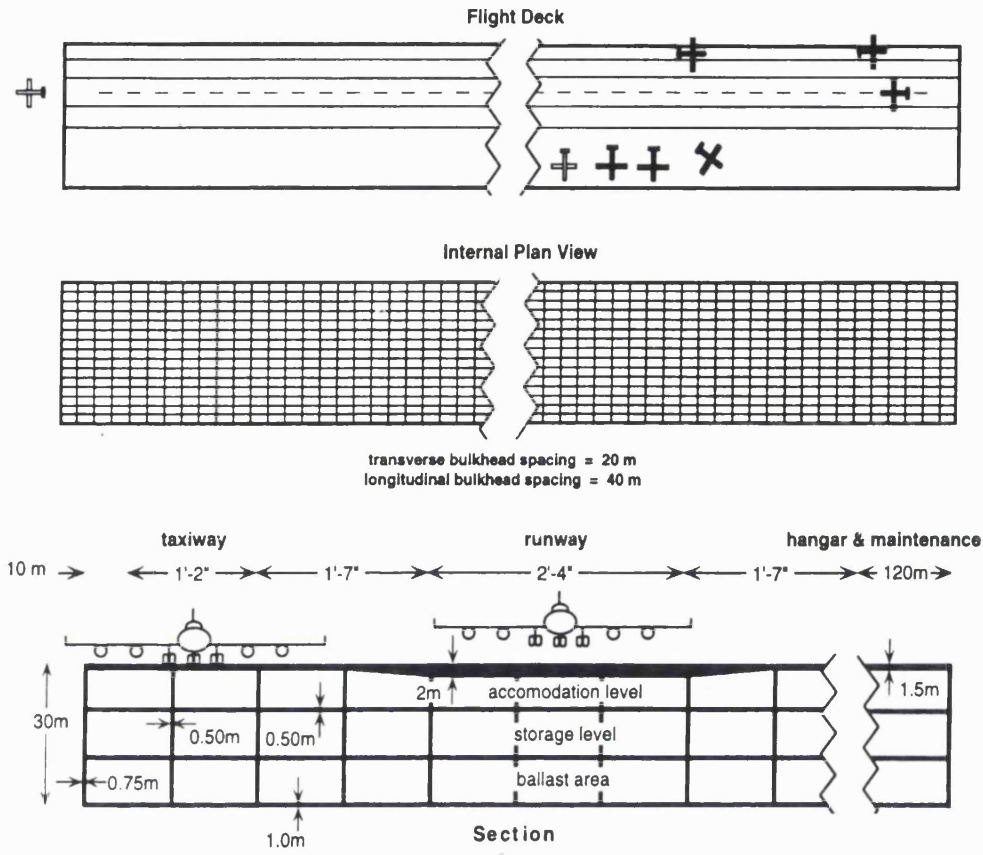


Figure 1.19 Arrangement of potential floating airport [14]

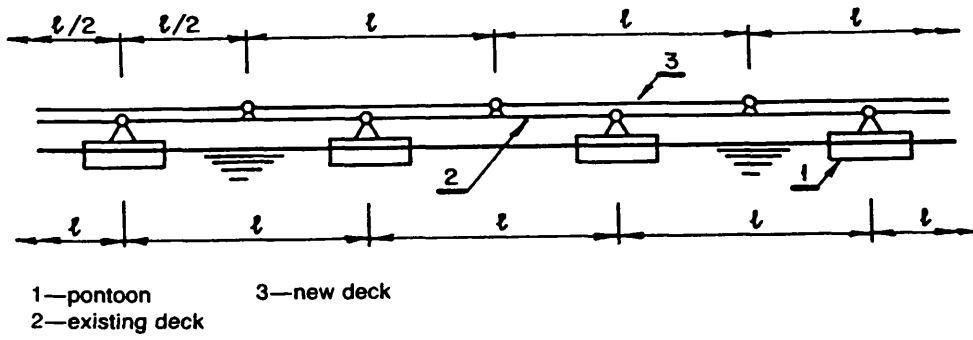


Figure 2.1 Chain of pontoons with individual deck section [8]

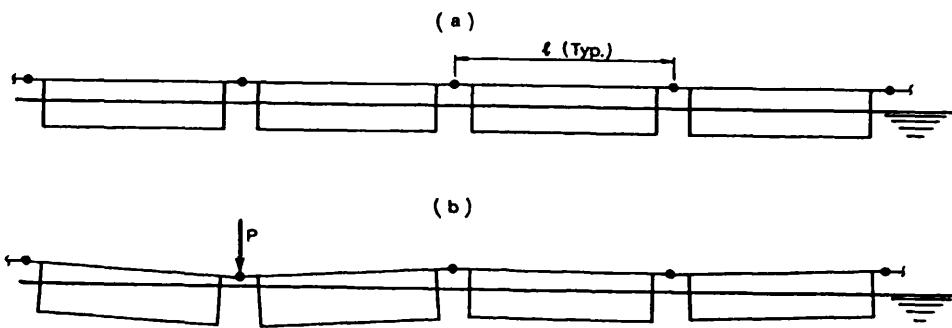


Figure 2.2 Linked pontoons system [8]

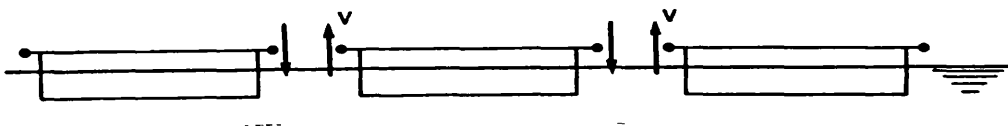


Figure 2.3 Individual pontoon forces [8]

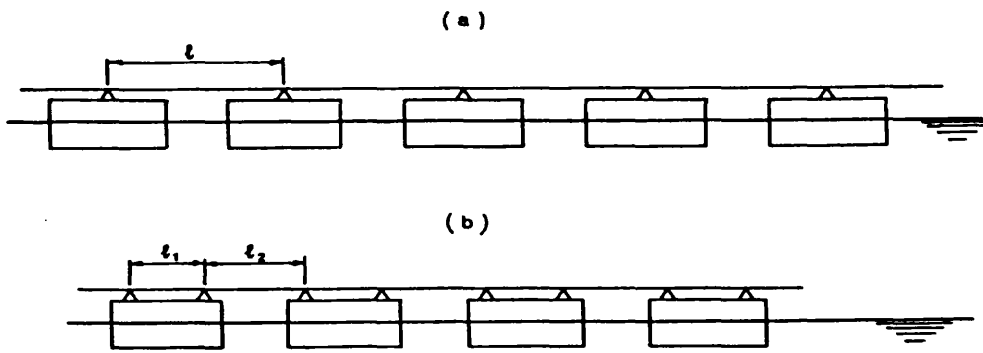
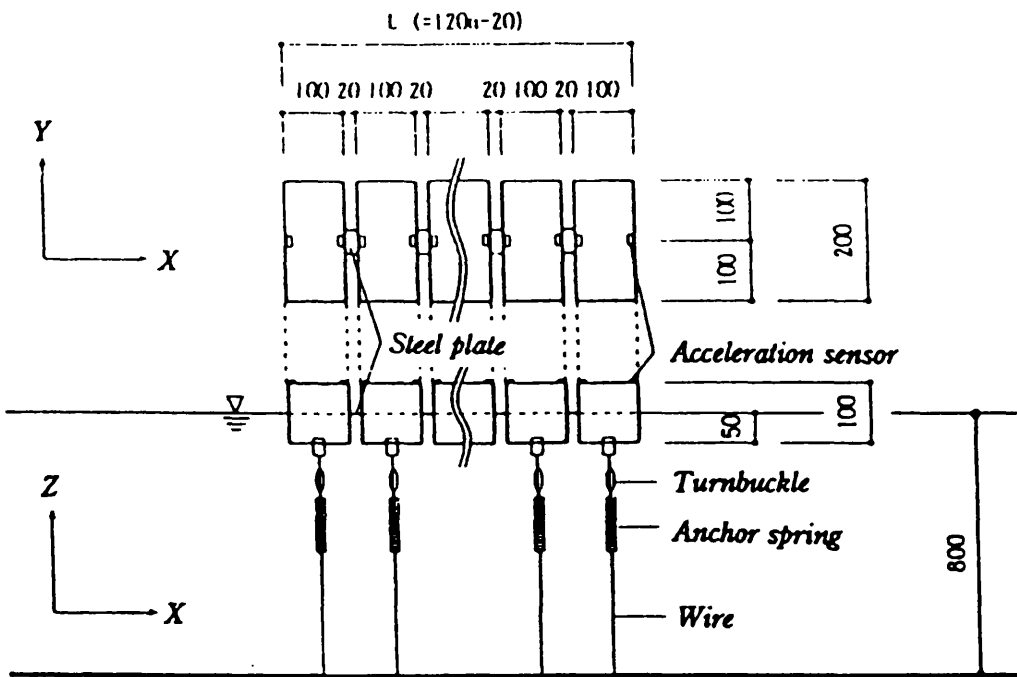


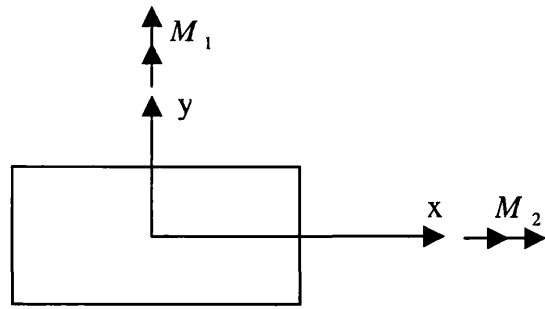
Figure 2.4 Redundant pair system [8]



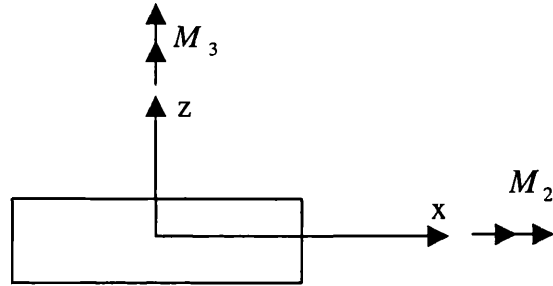
$n$  : Number of unit

Unit : (mm)

Figure 2.5 Set-up condition of experimental floating model [12]

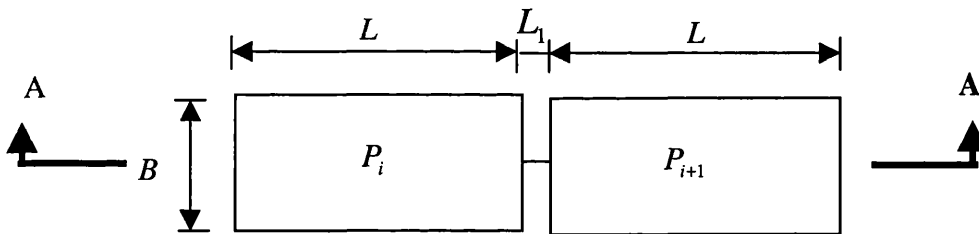


Plan view

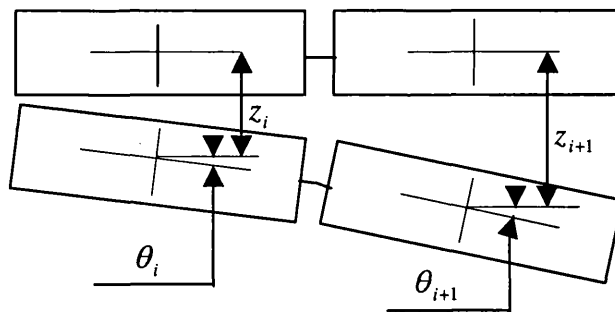


Side view

Fig 3.1 Pontoon module

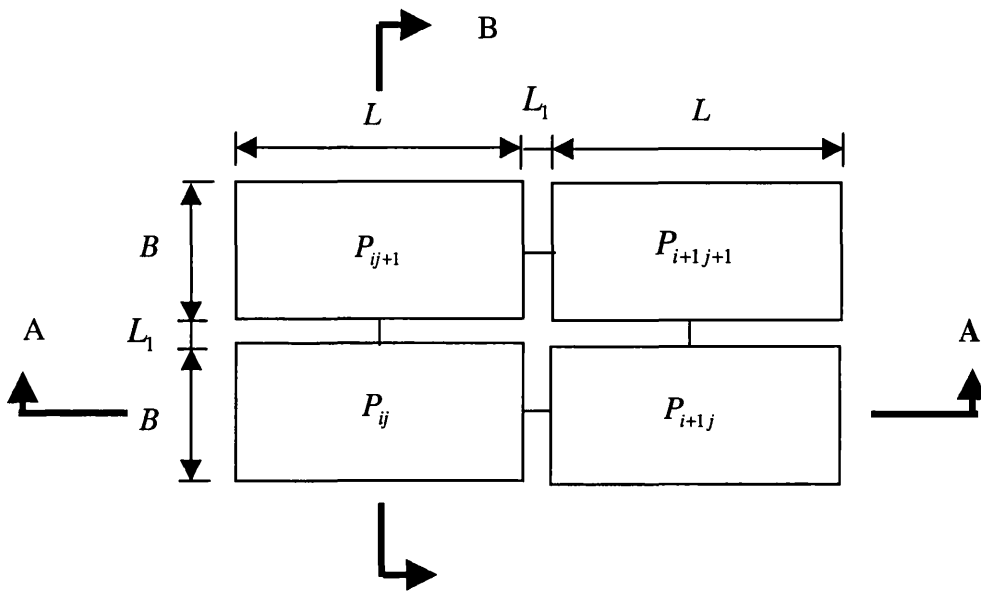


Plan view

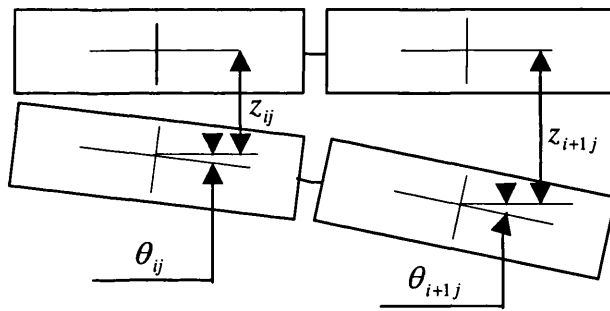


Section A-A

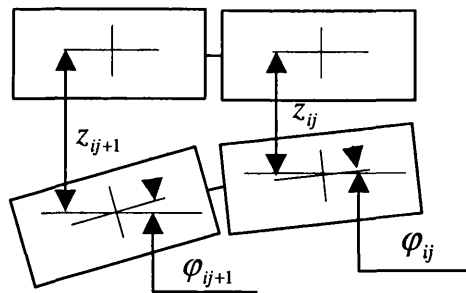
Fig 3.2 Single array connections



Plan view



Section A-A



Section B-B

Fig 3.3 Mat array connections

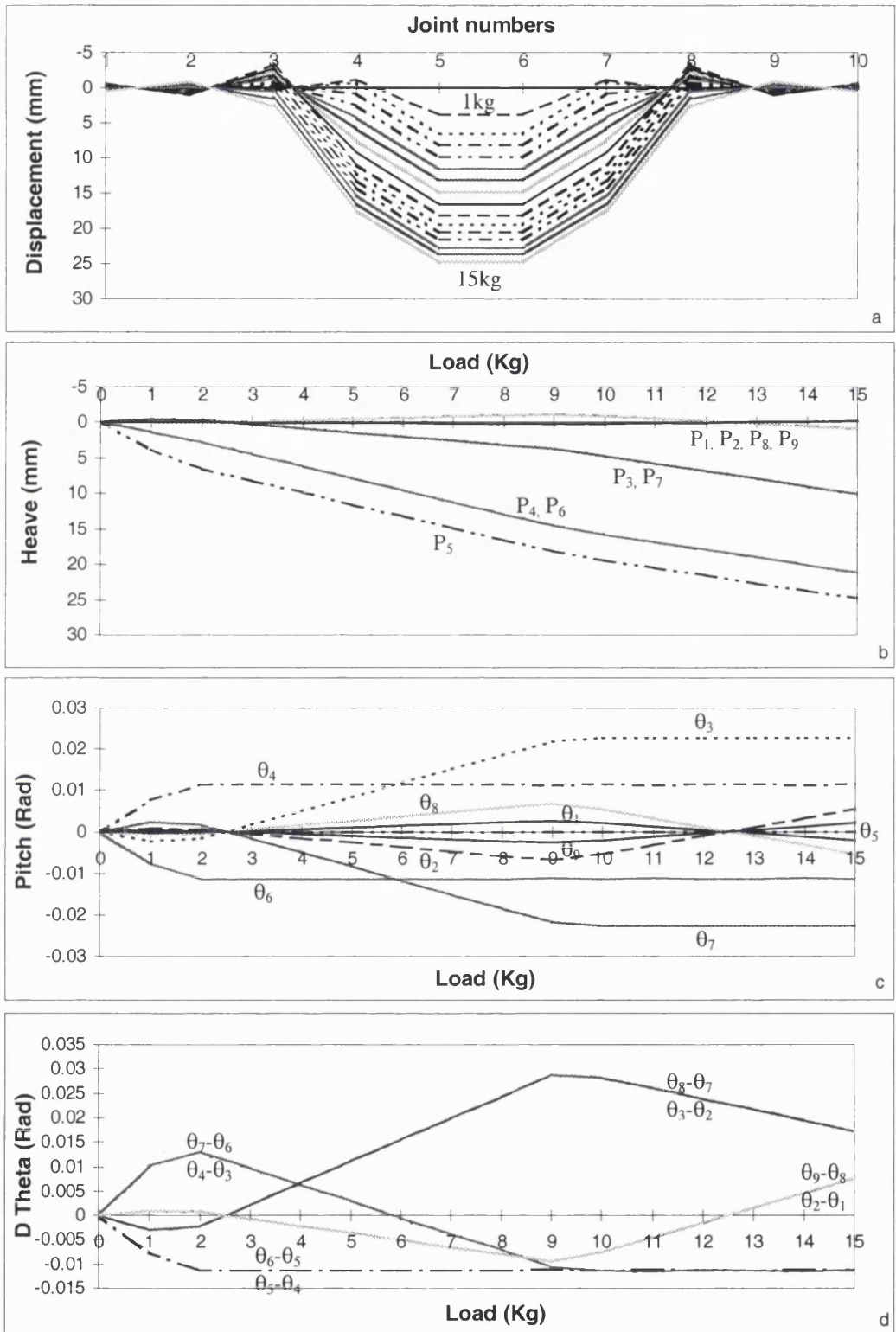


Figure 3.4 Theoretical response when load applied on pontoon 5 with Hinged-rigid connection in one direction.  $P_i$ ,  $\theta_i$  are pontoon number  $i$  and pitch angle of pontoon  $i$  respectively.  $i = 1$  to 9.

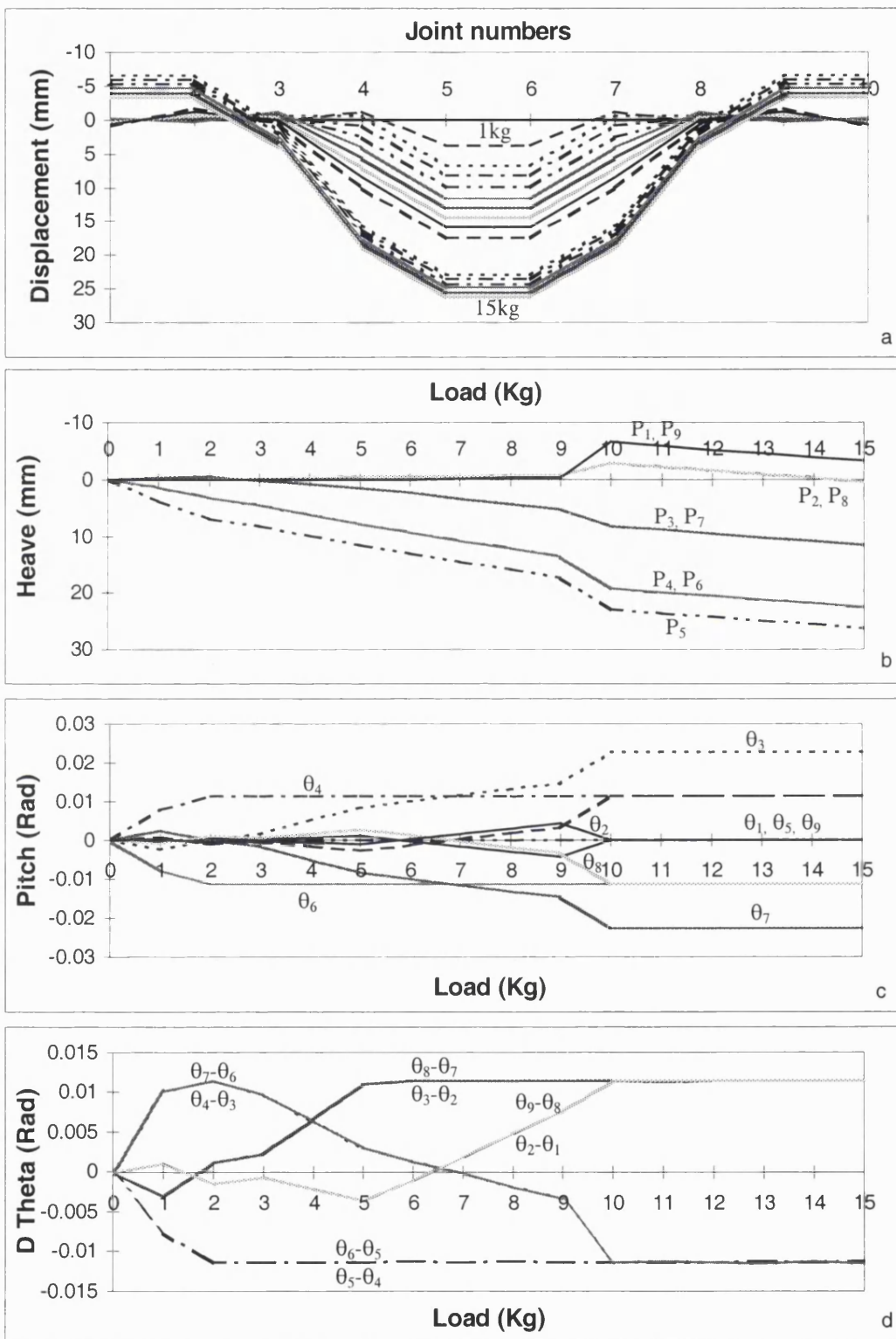


Figure 3.5 Theoretical response when load applied on pontoon 5 in Hinged-rigid connection, in two directions, where  $P_i$  is pontoon number  $i$  and  $\theta_i$  is pitch angle of pontoon  $i$ ,  $i=1$  to 9.

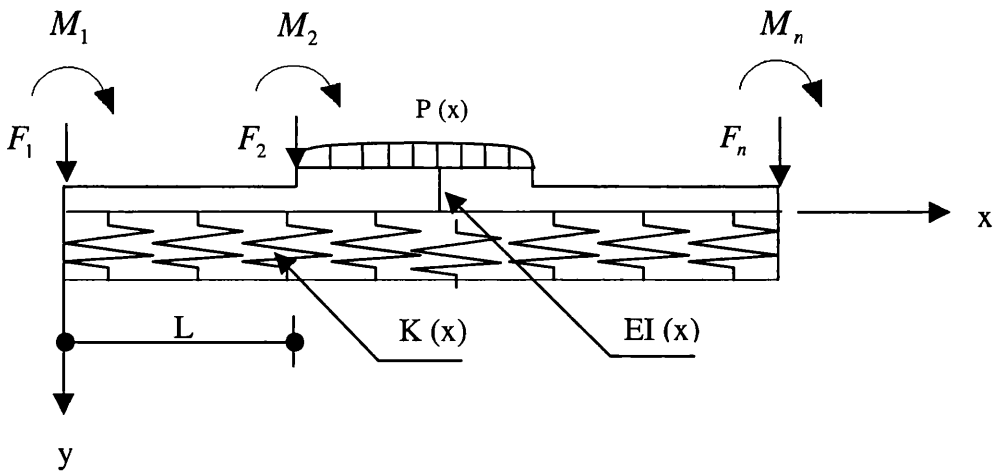


Figure 4.1 Beam on elastic foundation

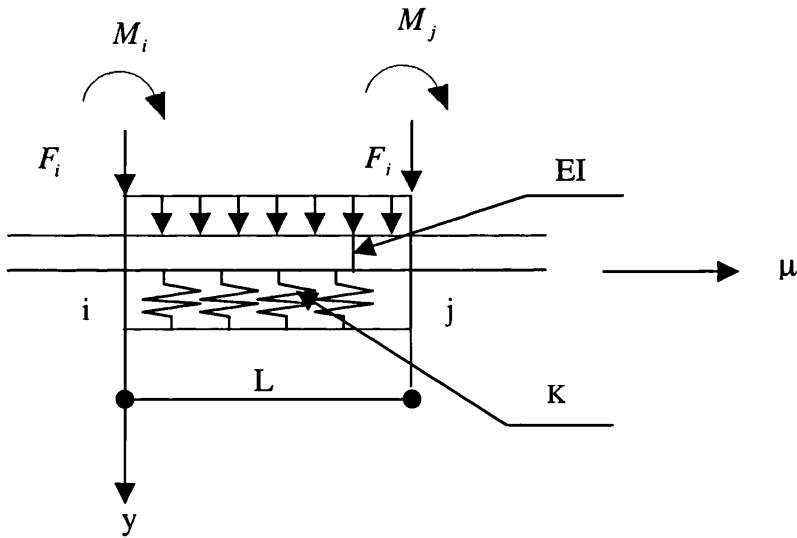


Figure 4.2 An element of beam on elastic foundation

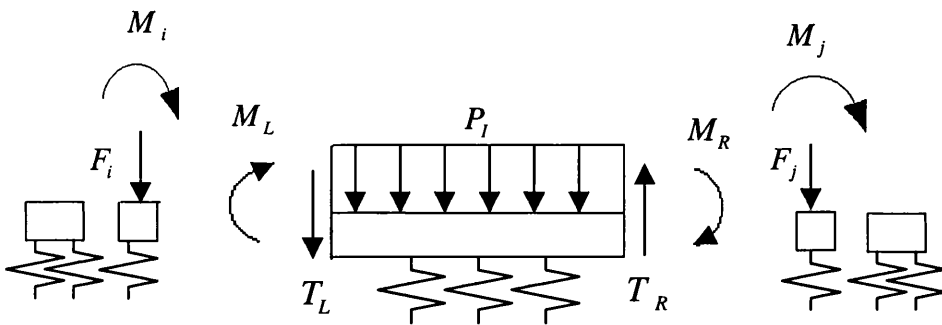


Figure 4.3 Forces and moments of an element on elastic foundation

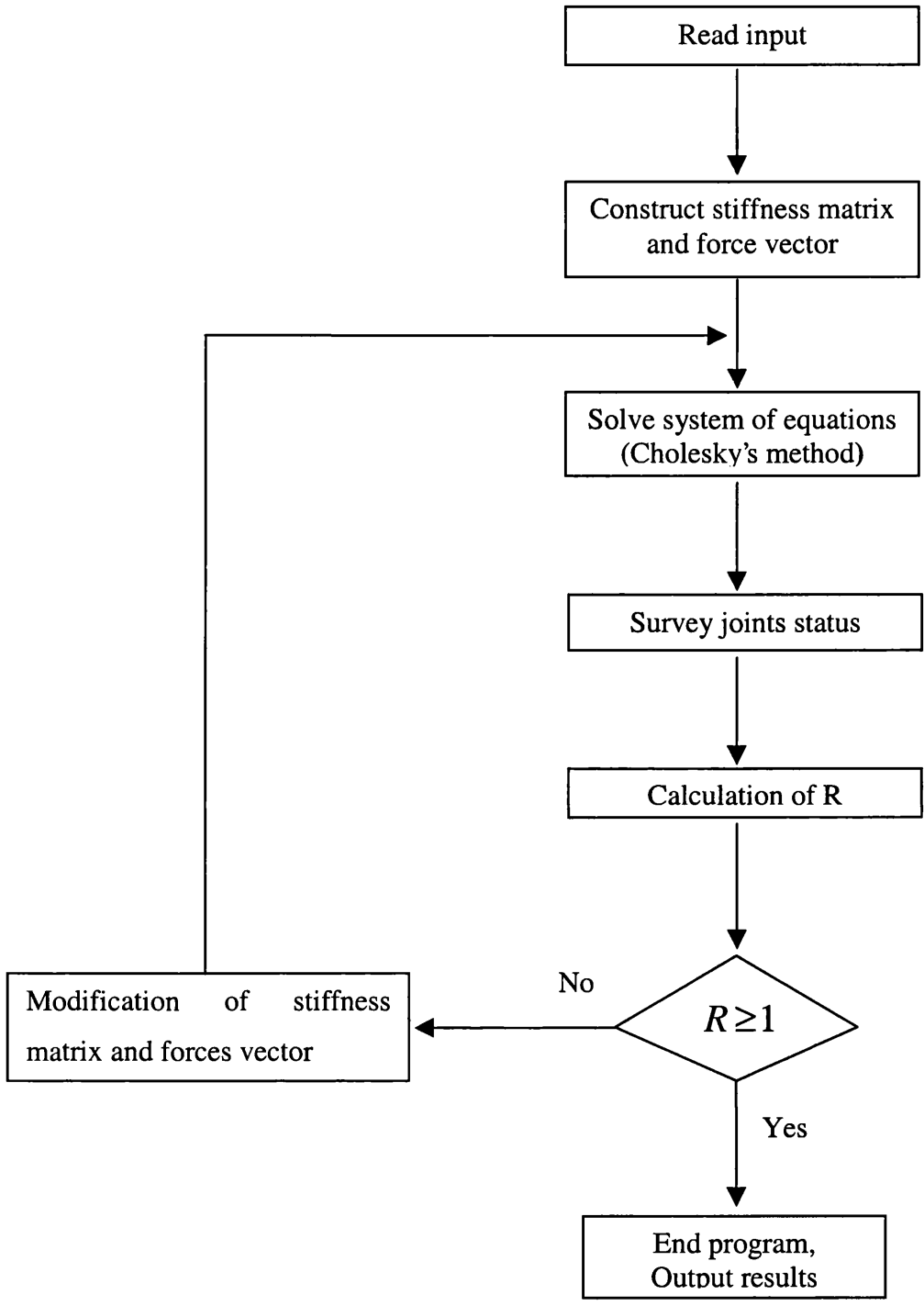


Figure 4.4 Flow chart of steps

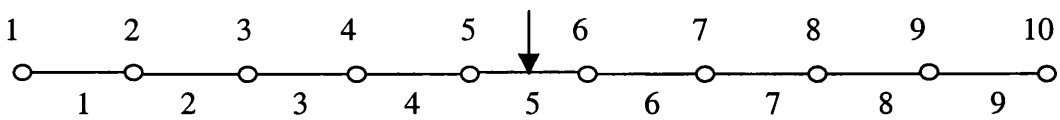


Figure 4.5 Joints and elements of floating structure

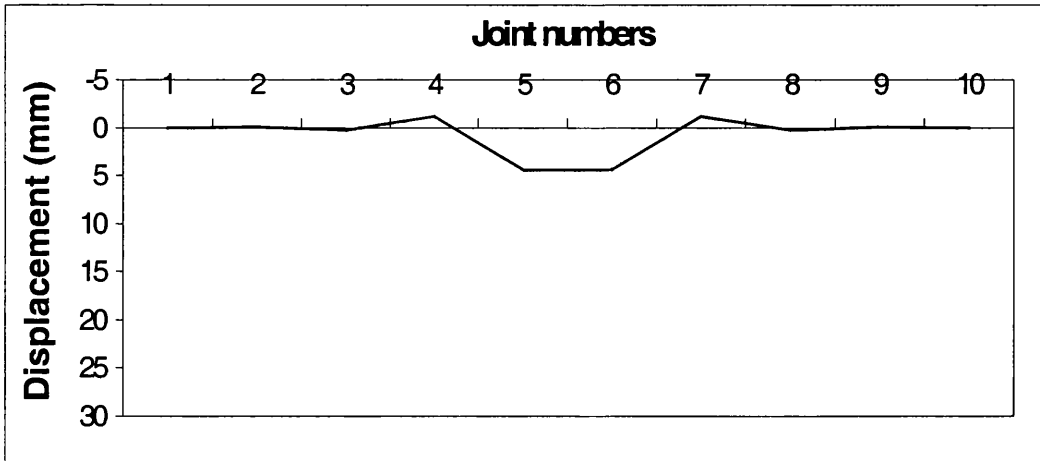


Figure 4.6 Loading step 1, Joints 4,7 (negative direction) are locked.

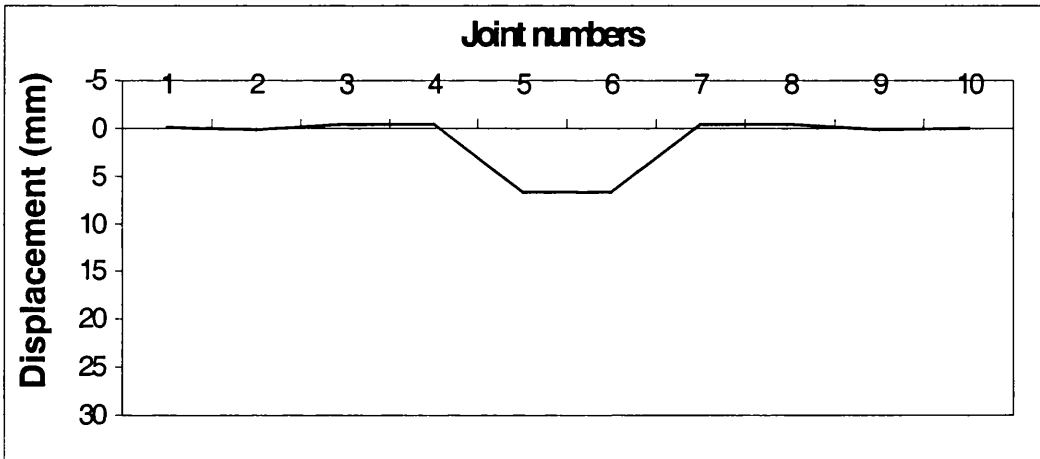


Figure 4.7, Loading step 2, Joints 5, 6 (positive direction) and 4,7 (negative direction) are locked.

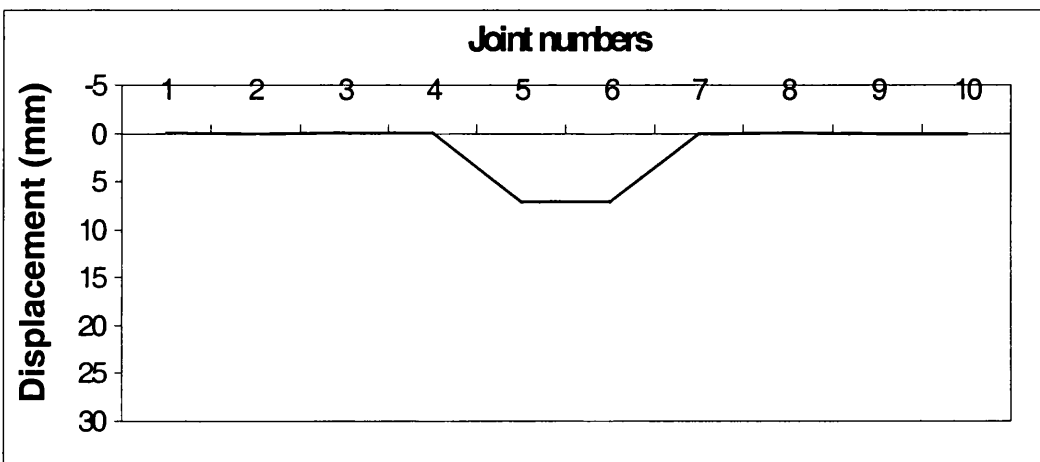


Figure 4.8, Loading step 3, Joints 5, 6 (positive direction) are locked.

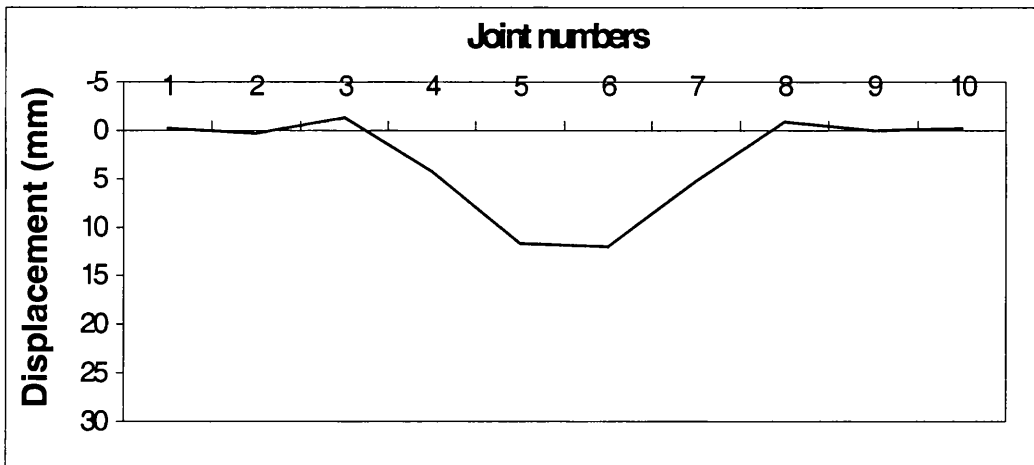


Figure 4.9, Loading step 4, Joints 5,6 (positive direction) and 3,8 (negative direction) are locked.

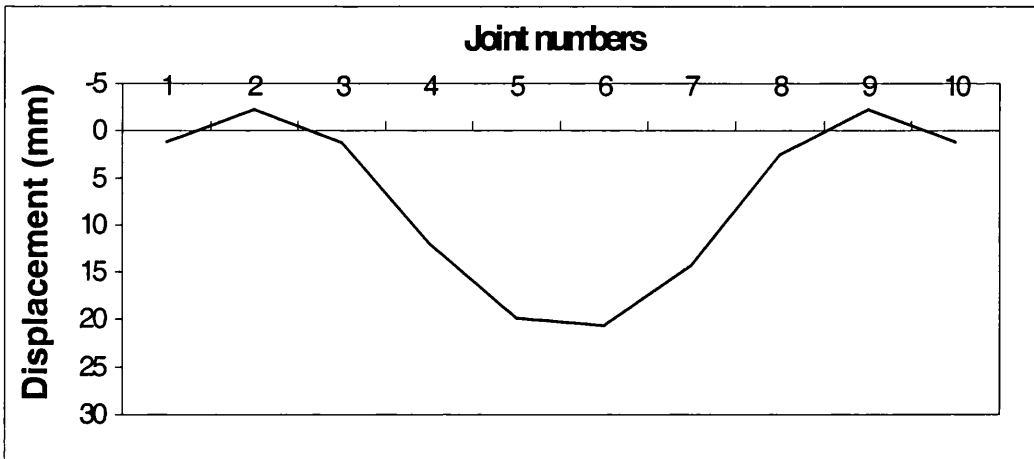


Figure 4.10 Loading step 5, Joints 5,6 are (positive direction), 2,3,8,9 (negative direction) are locked.

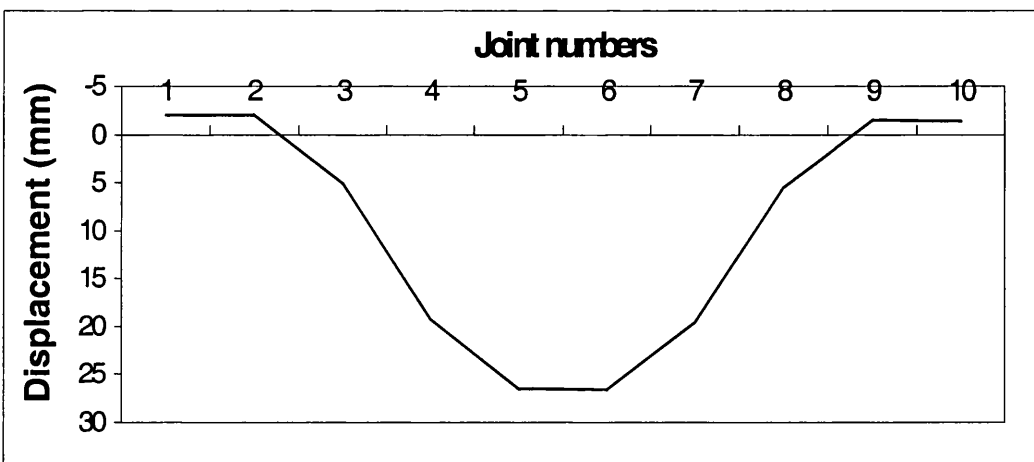


Figure 4.11 Loading step 6 Joints 4,5,6,7 (positive direction), 2,3,8,9 (negative direction) are locked.

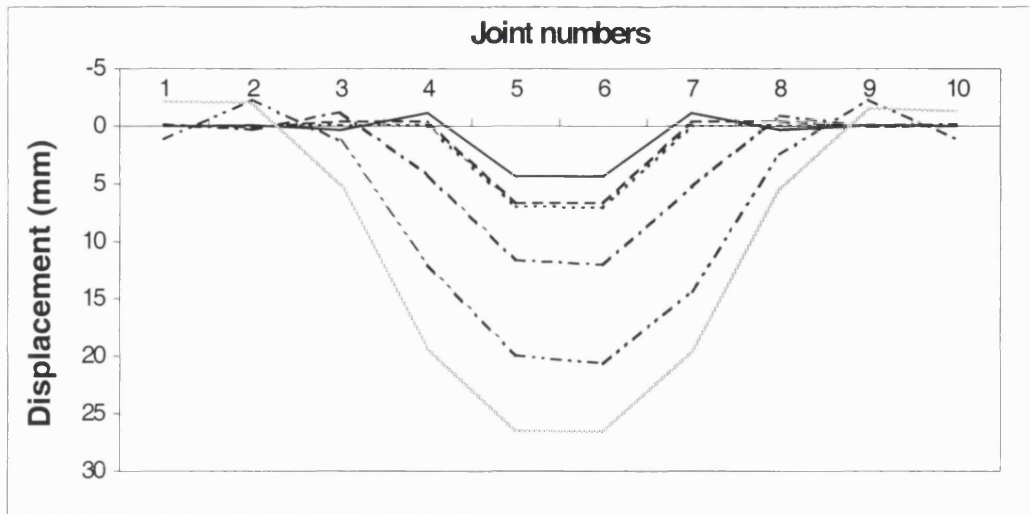


Figure 4.12 All loading steps

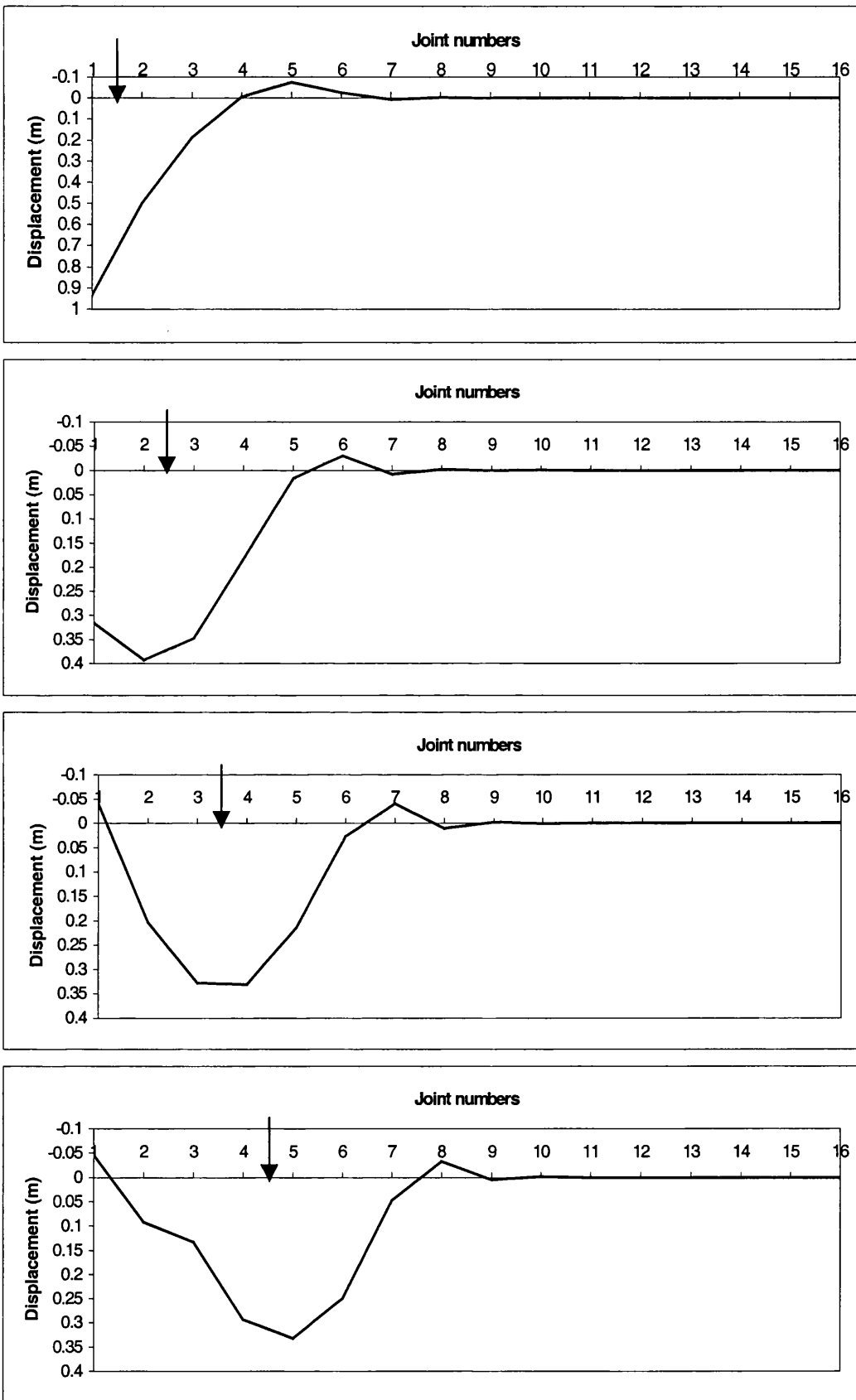


Figure 4.13 Displacement when load moving from unit pontoon 1 to 4

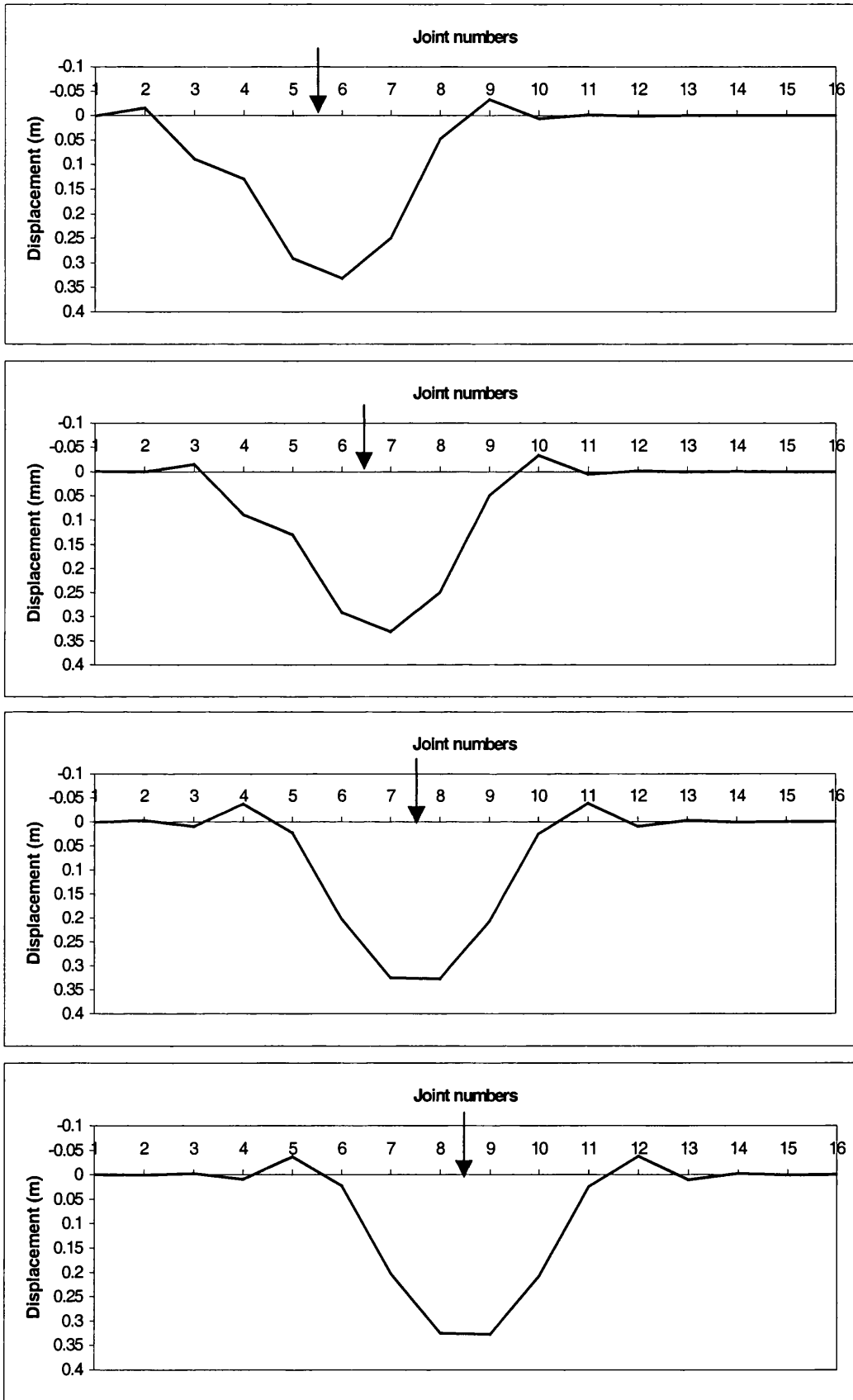


Figure 4.14 Displacement when load moving from unit pontoon 5 to 8

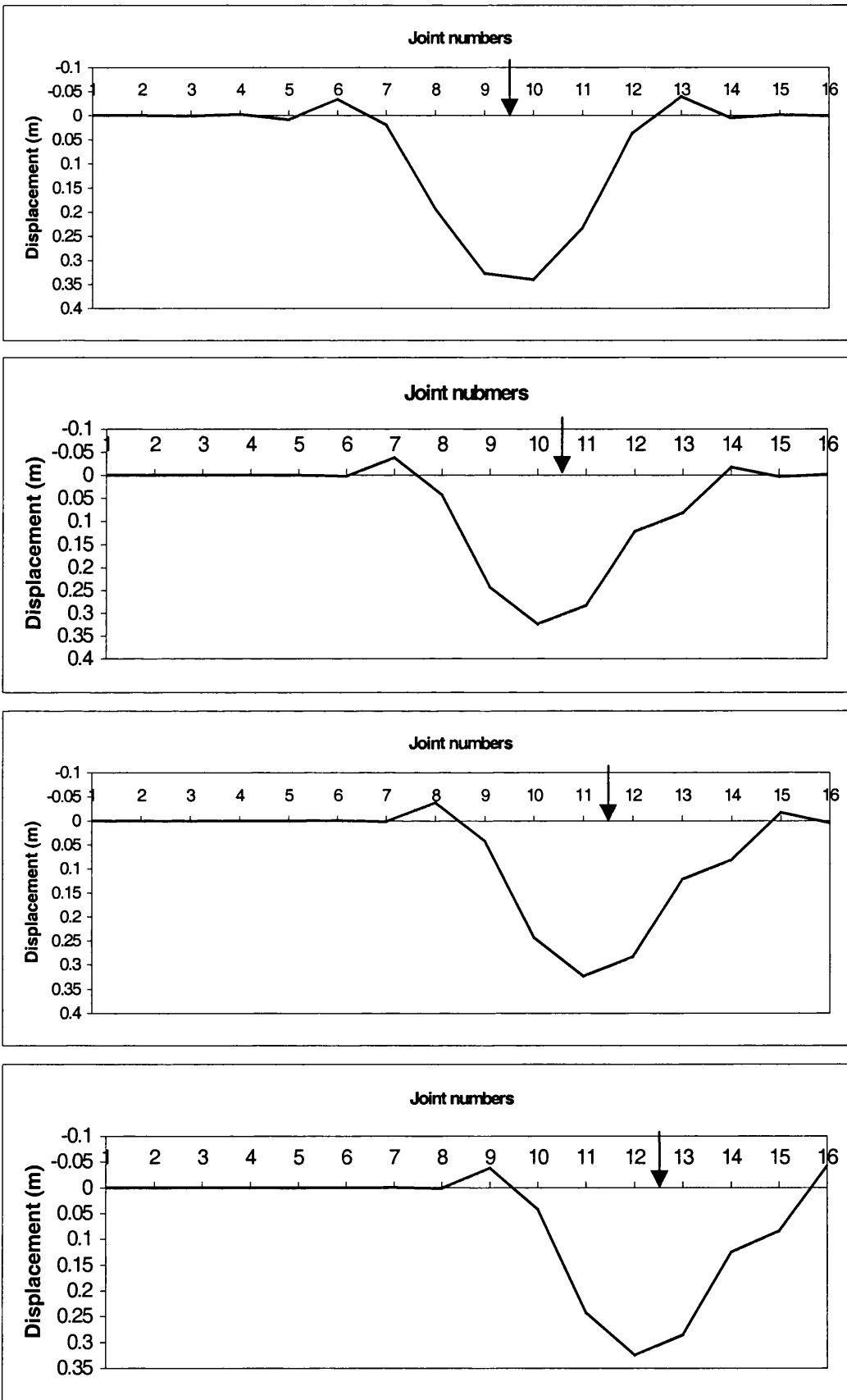


Figure 4.15 Displacement when load moving from unit pontoon 9 to 12

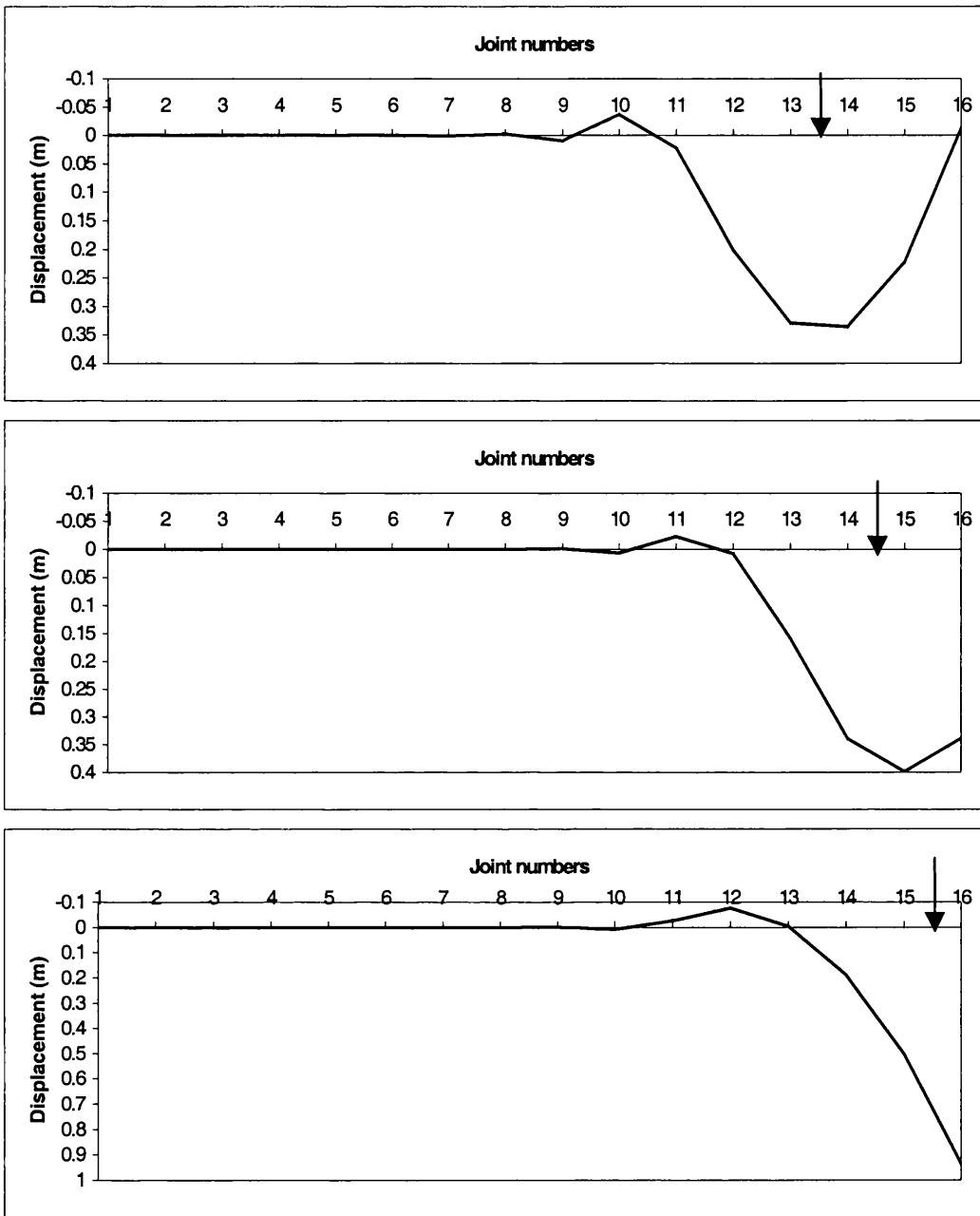


Figure 4.16 Displacement when load moving from unit pontoon 13 to 15

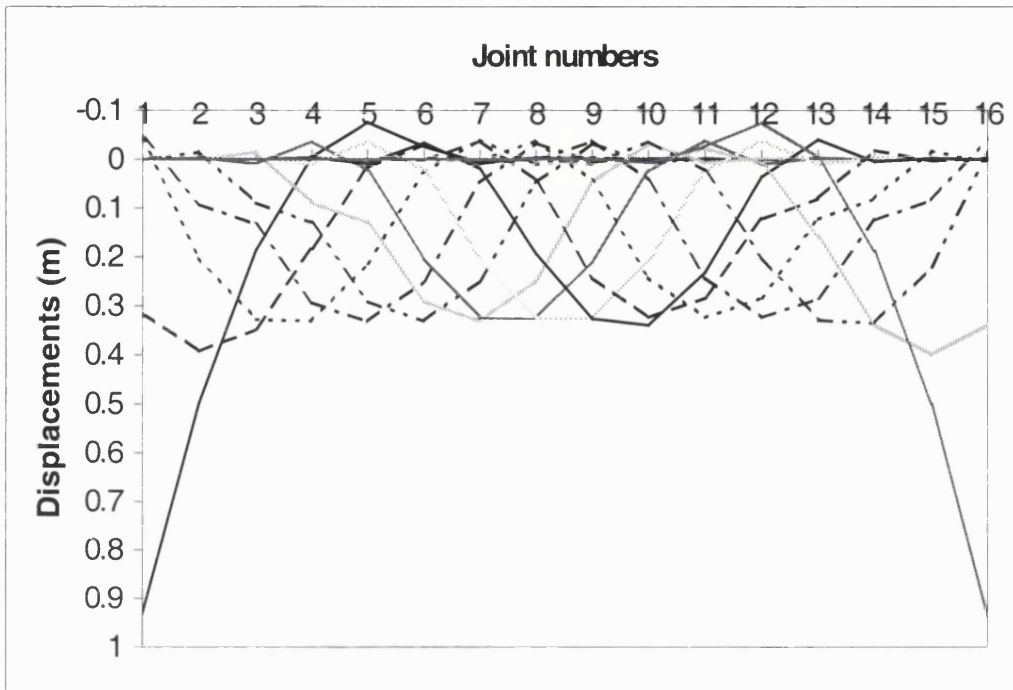


Figure 4.17 Displacement when load moving from unit pontoon 1 to 15

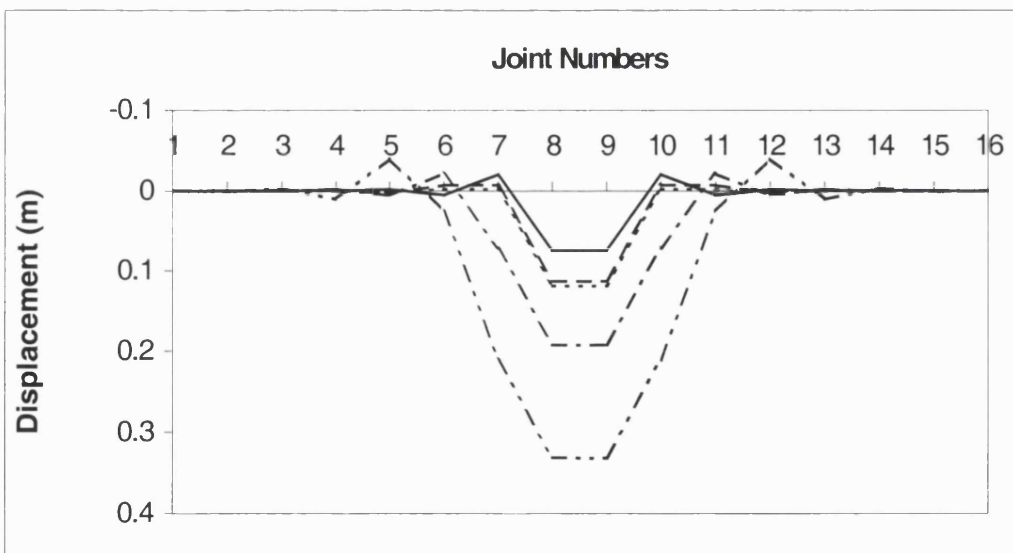


Figure 4.18 Displacement of load steps for example with full size dimension when load applied on unit 8

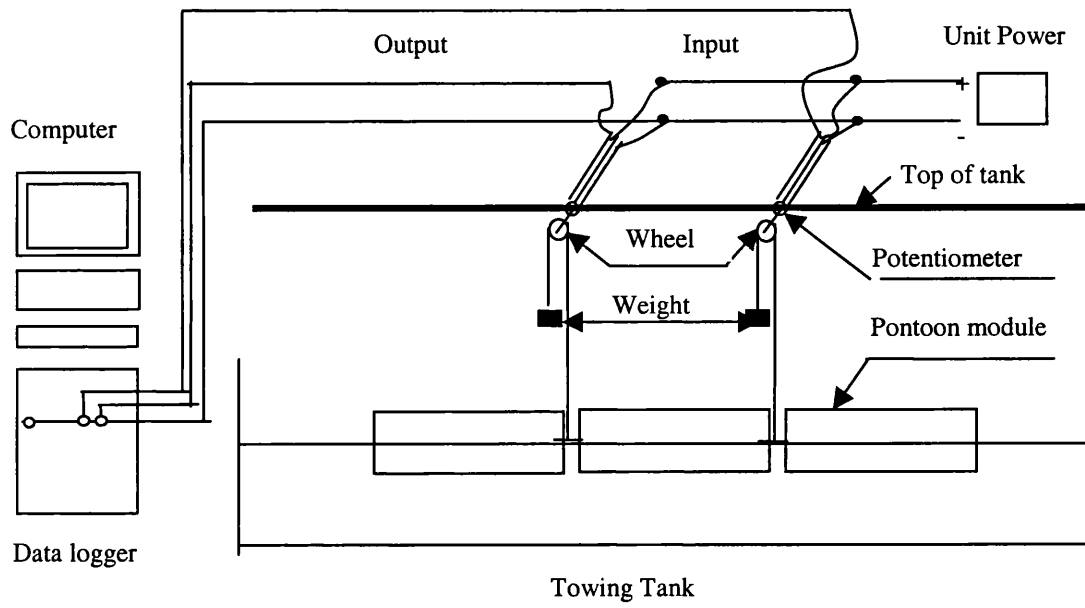


Figure 5.1 Arrangement for tests

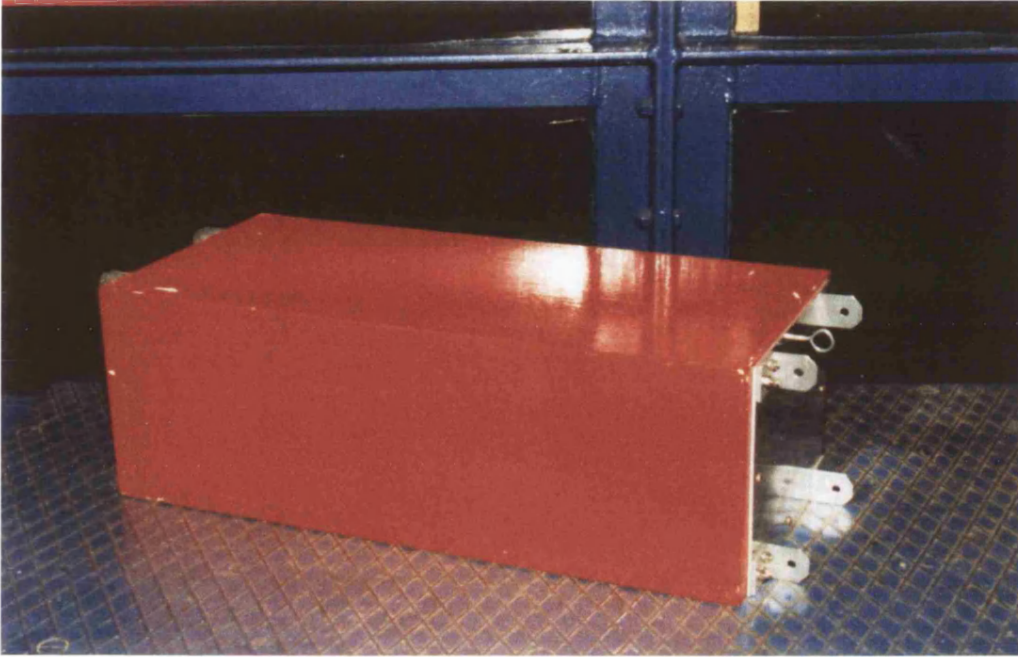


Figure 5.2 Pontoon module for Hinged-Rigid connection for single array

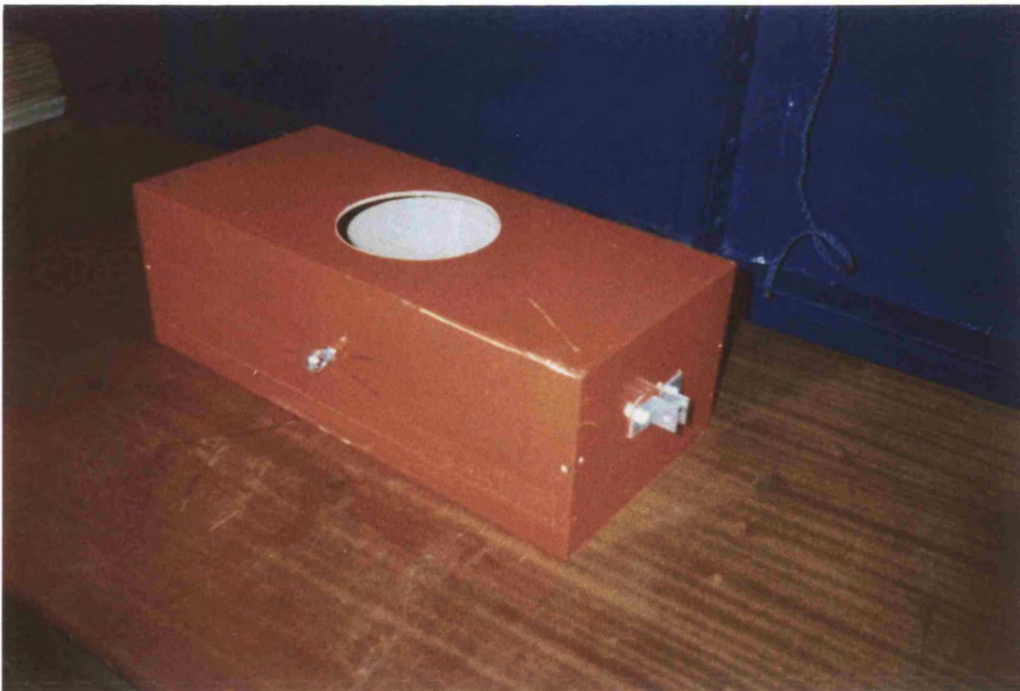


Figure 5.3 Pontoon module for Hinged connection for mat array

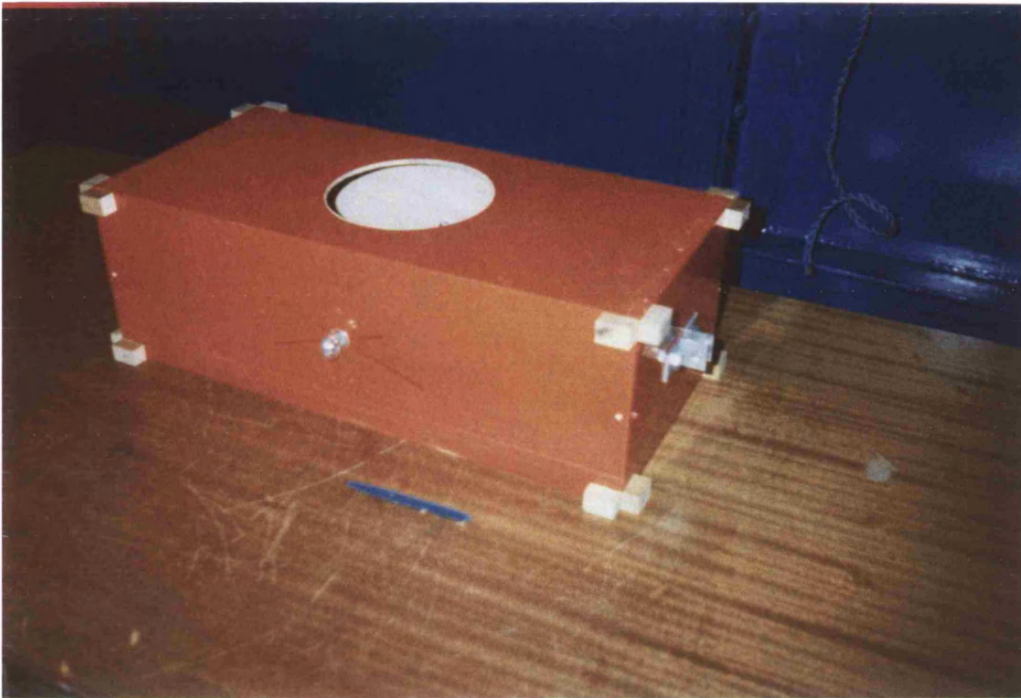


Figure 5.4 Pontoon module for Hinged-Rigid connection for mat array



Figure 5.5 Assembly pontoons for single array



Figure 5.6 Assembly pontoons for hinged connection for mat array

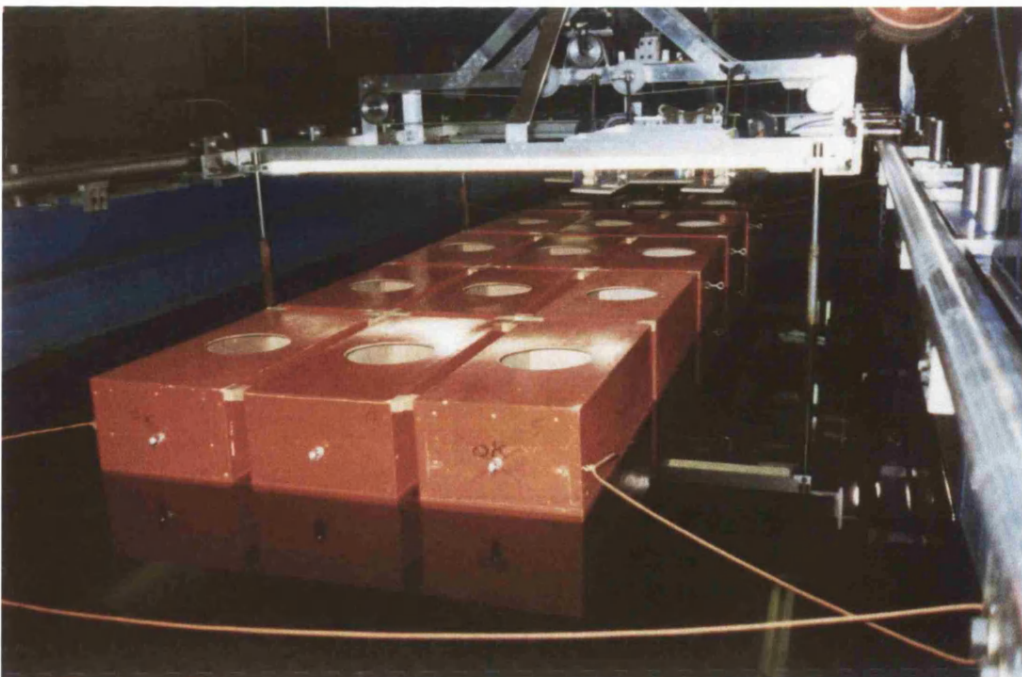


Figure 5.7 Assembly pontoons for Hinged-Rigid connection for mat array



Figure 5.8 Load applied on pontoons module 3 and 7 in single array



Figure 5.9 Load applied on pontoon module 3 in single array with Hinged-Rigid connection

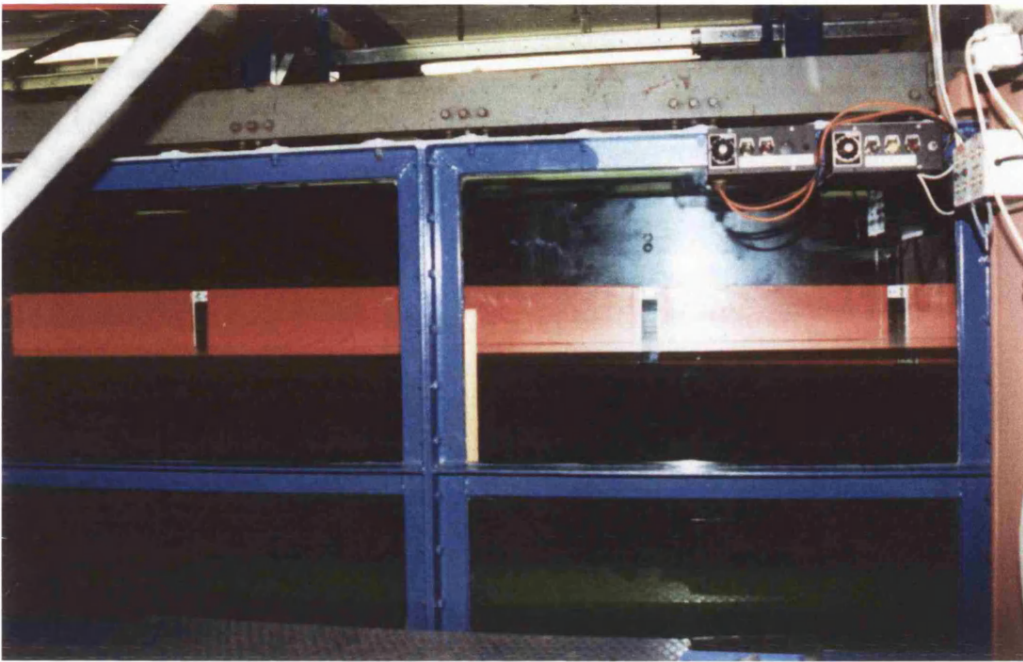


Figure 5.10 Load applied on pontoon module 4 in single array with Hinged-Rigid connection



Figure 5.11 Single array with Hinged-Rigid connection in wave

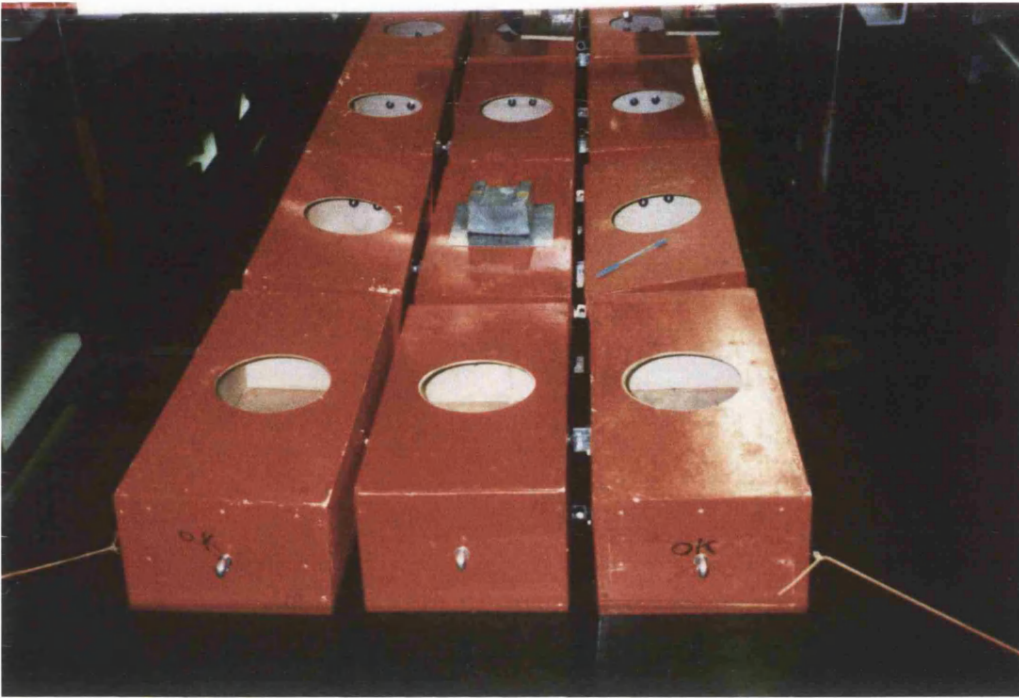


Figure 5.12 Load applied on pontoon module 2 and 4 in the middle row of mat array with Hinged connection

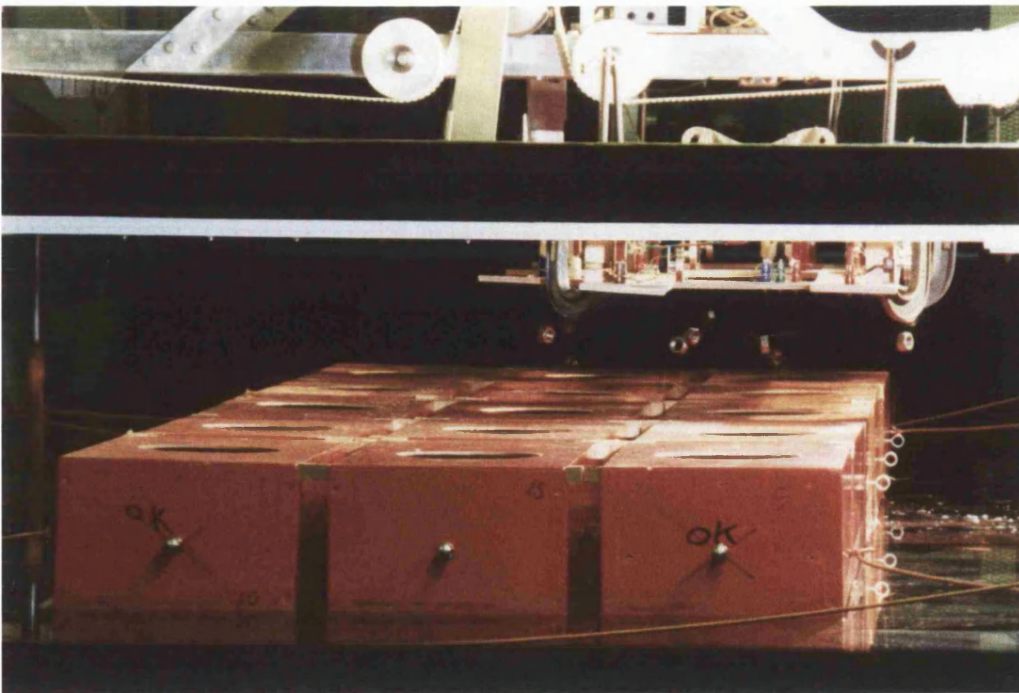


Figure 5.13 Load applied on mat array (3X5) with Hinged-Rigid connection

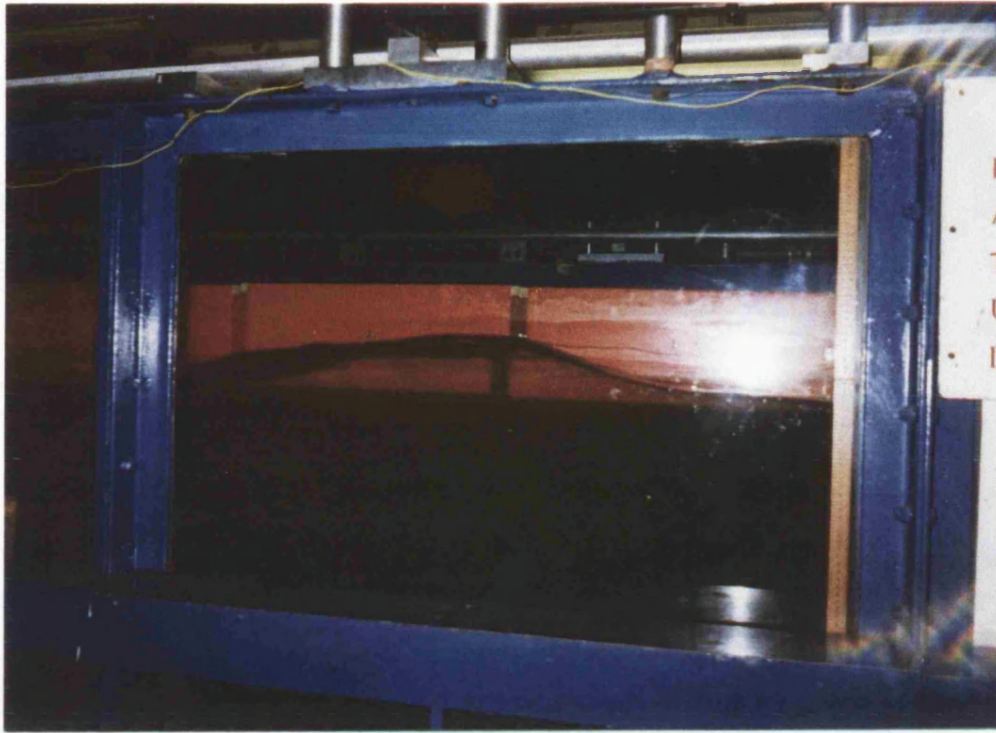


Figure 5.14 Mat array of pontoons with Hinged-Rigid connection in wave

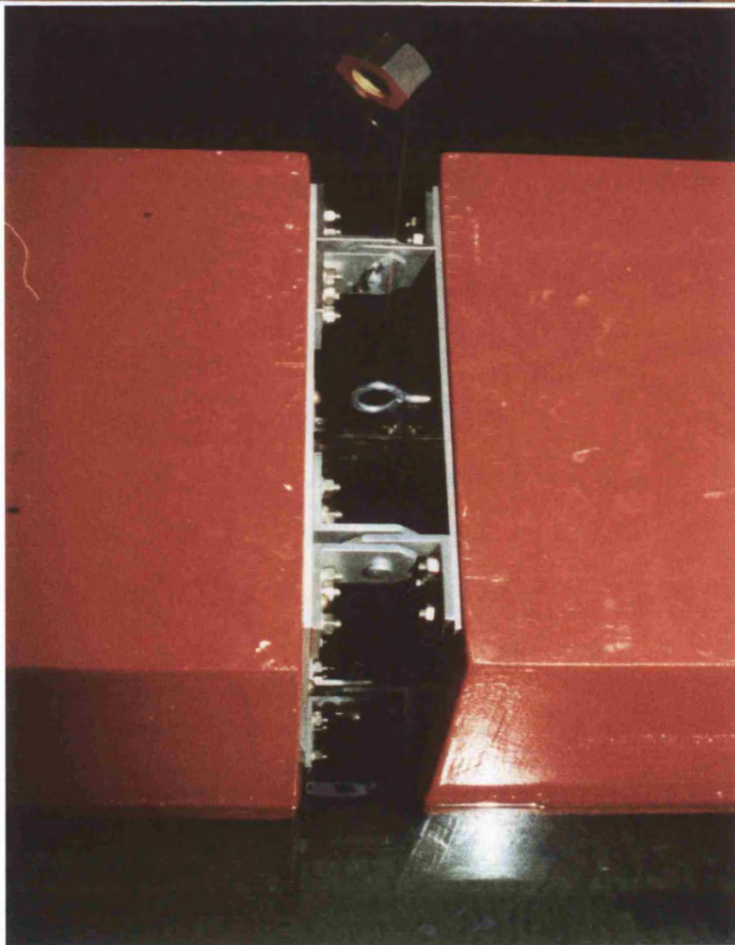
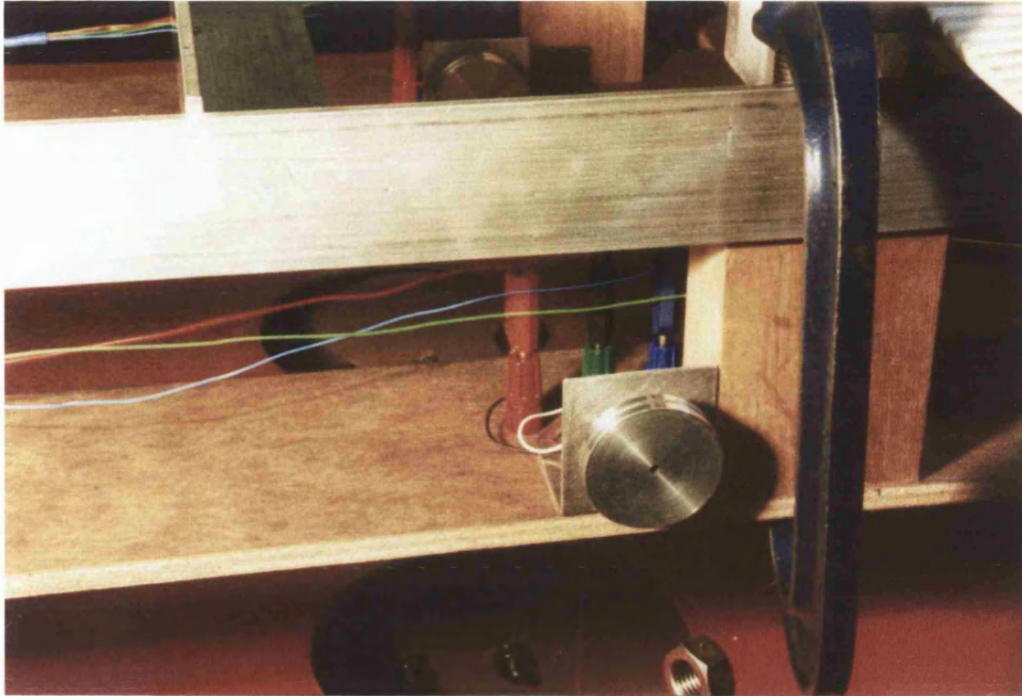


Figure 5.15 Potentiometers connection to the pontoons module

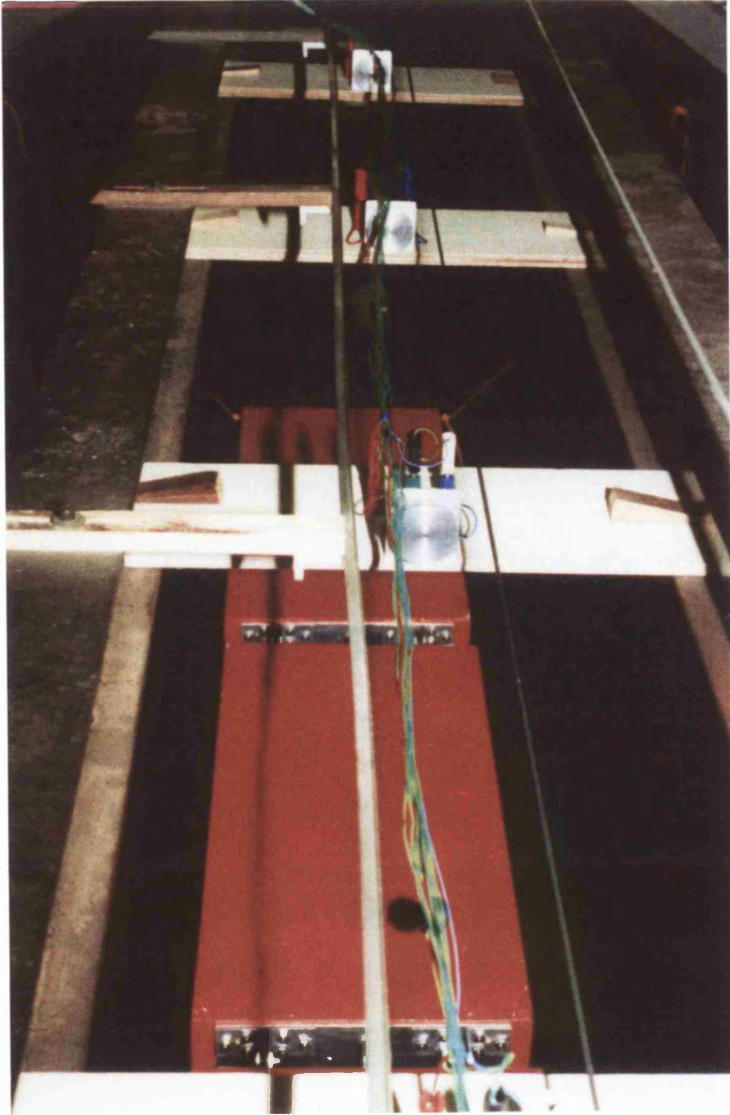


Figure 5.16 Potentiometers arrangement for single array

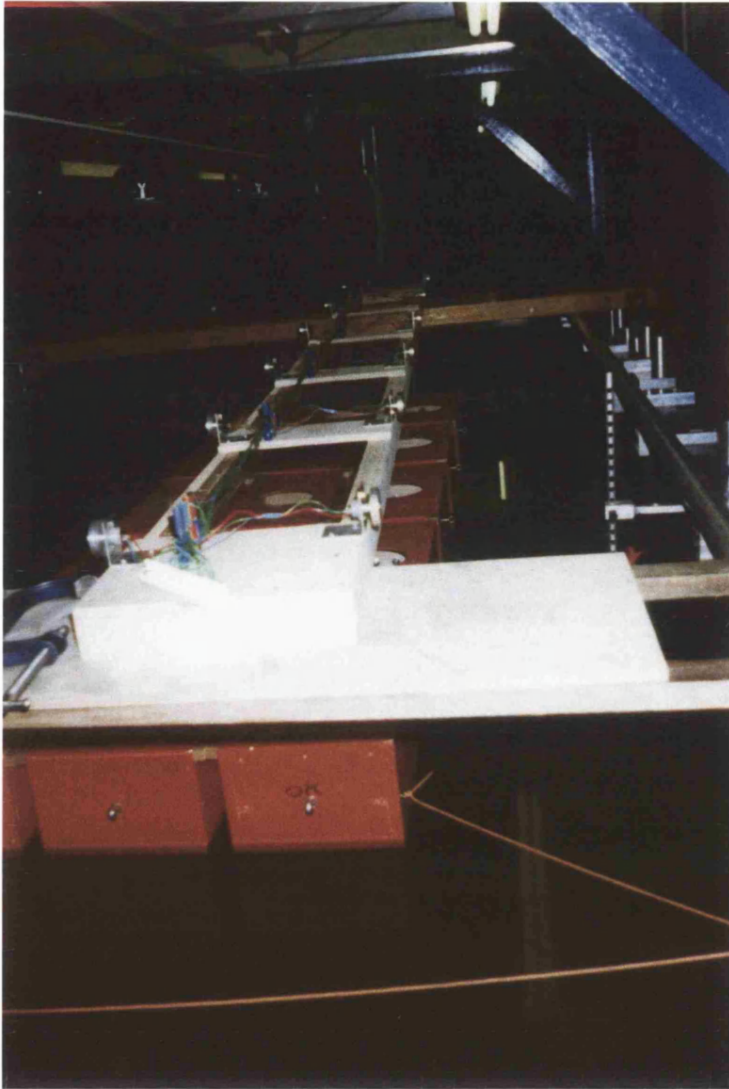


Figure 5.17 Potentiometers arrangement for mats array



Figure 5.18 potentiometer connection to the computer

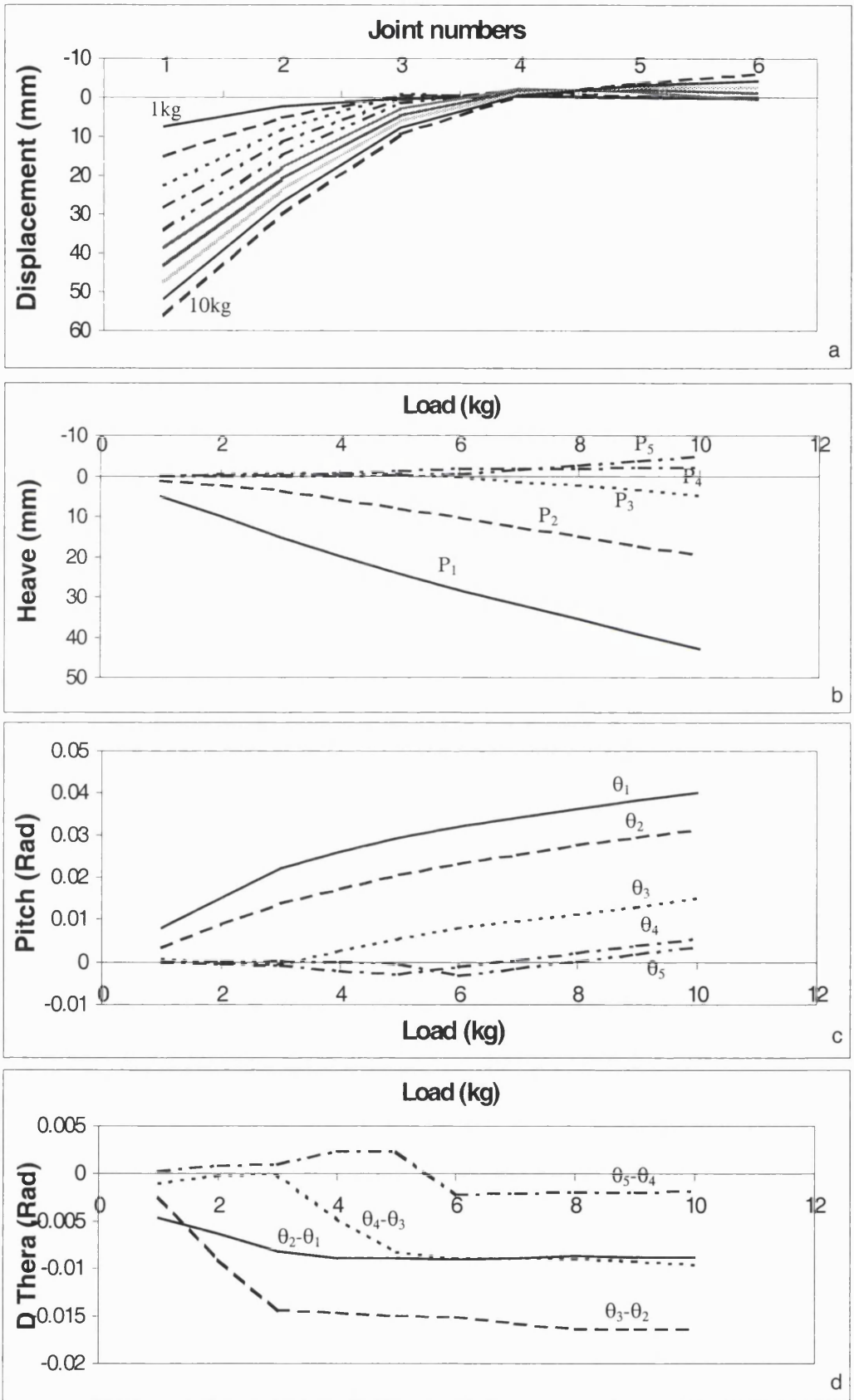


Figure 5.19 Load applied on pontoon 1,  $P_i$  = Pontoon number  $i$  and  $\theta_i$  = Pitch angle of pontoon  $i$ .

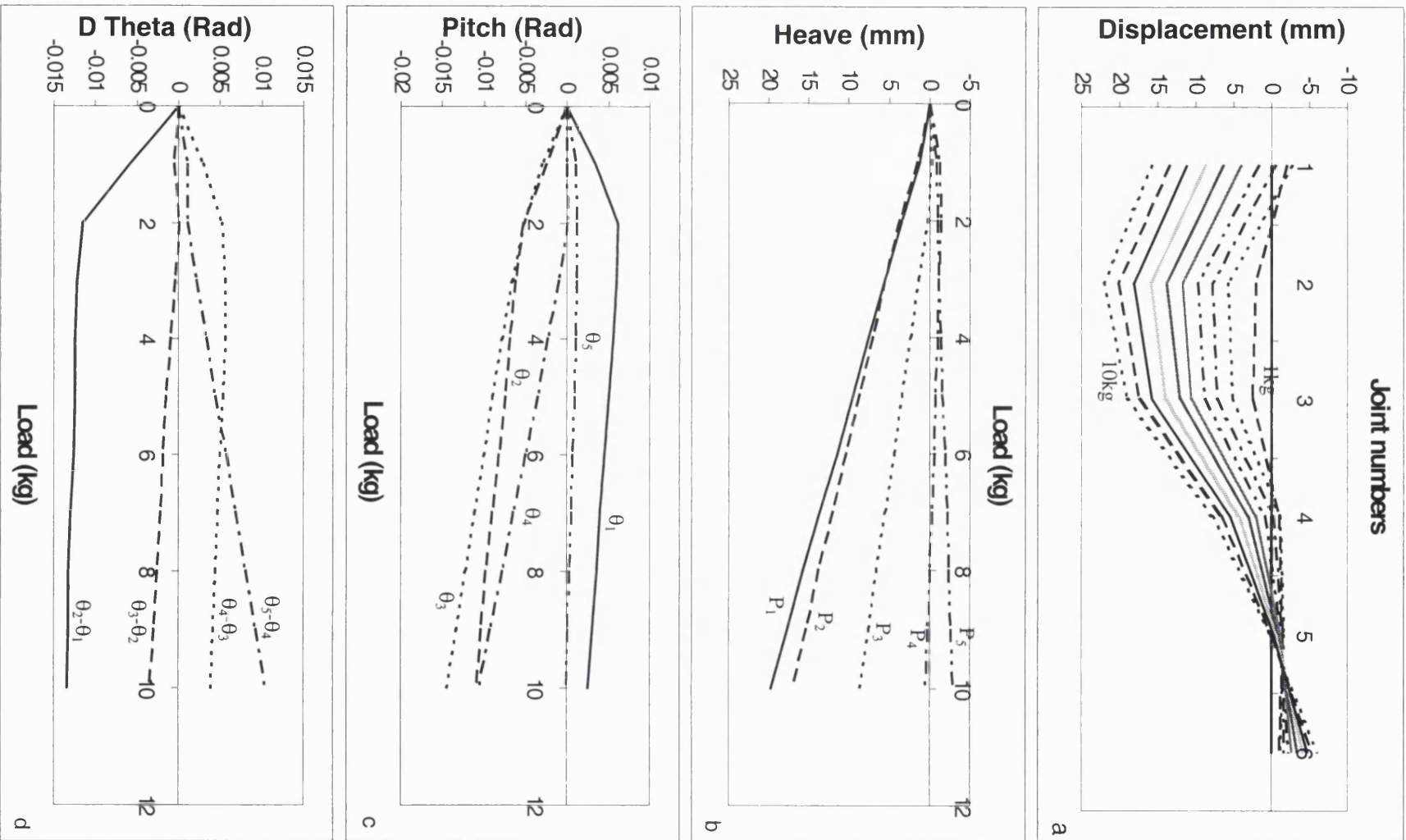


Figure 5.20 Load applied on pontoon 2

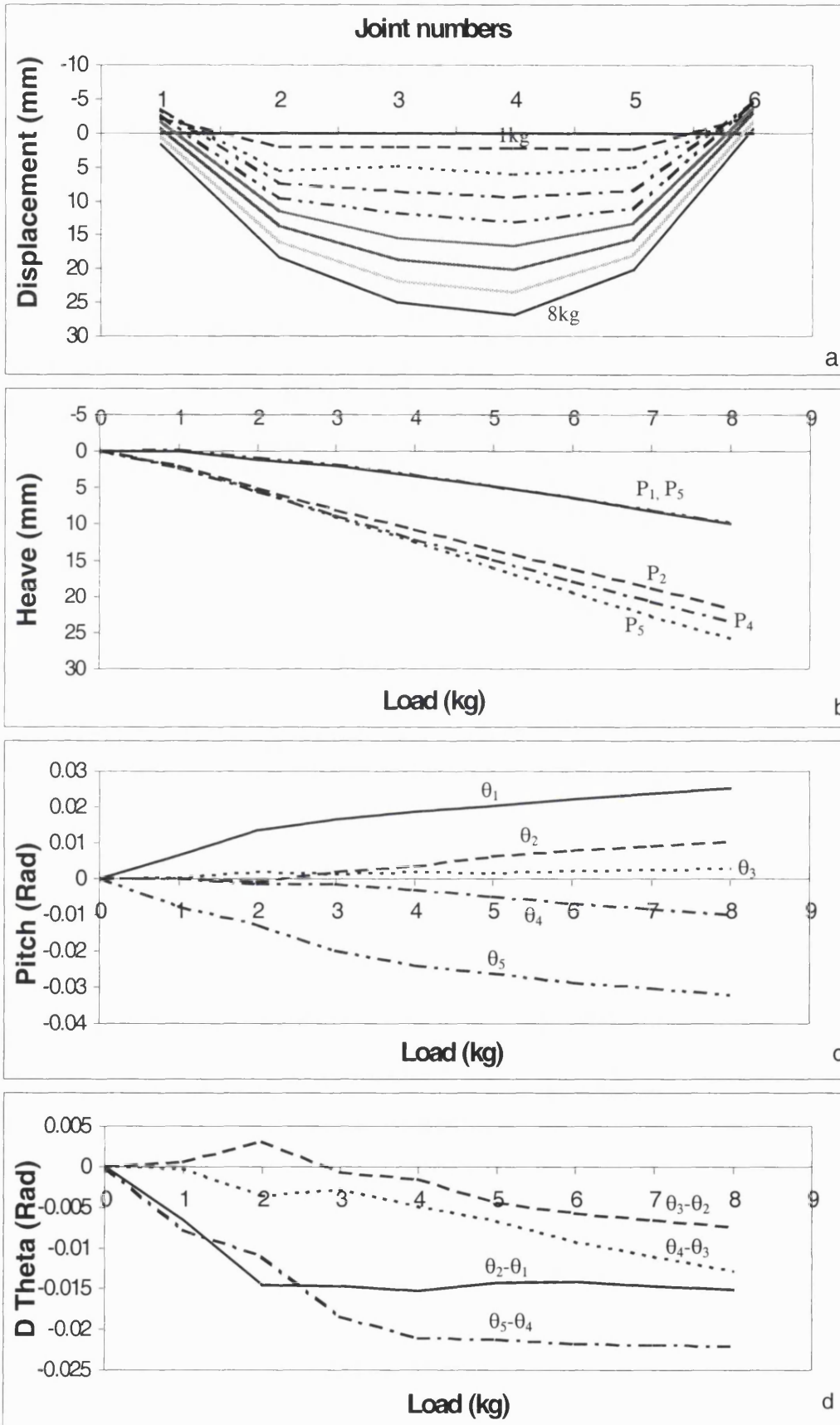


Figure 5.21 Load applied on pontoon 2 and 4

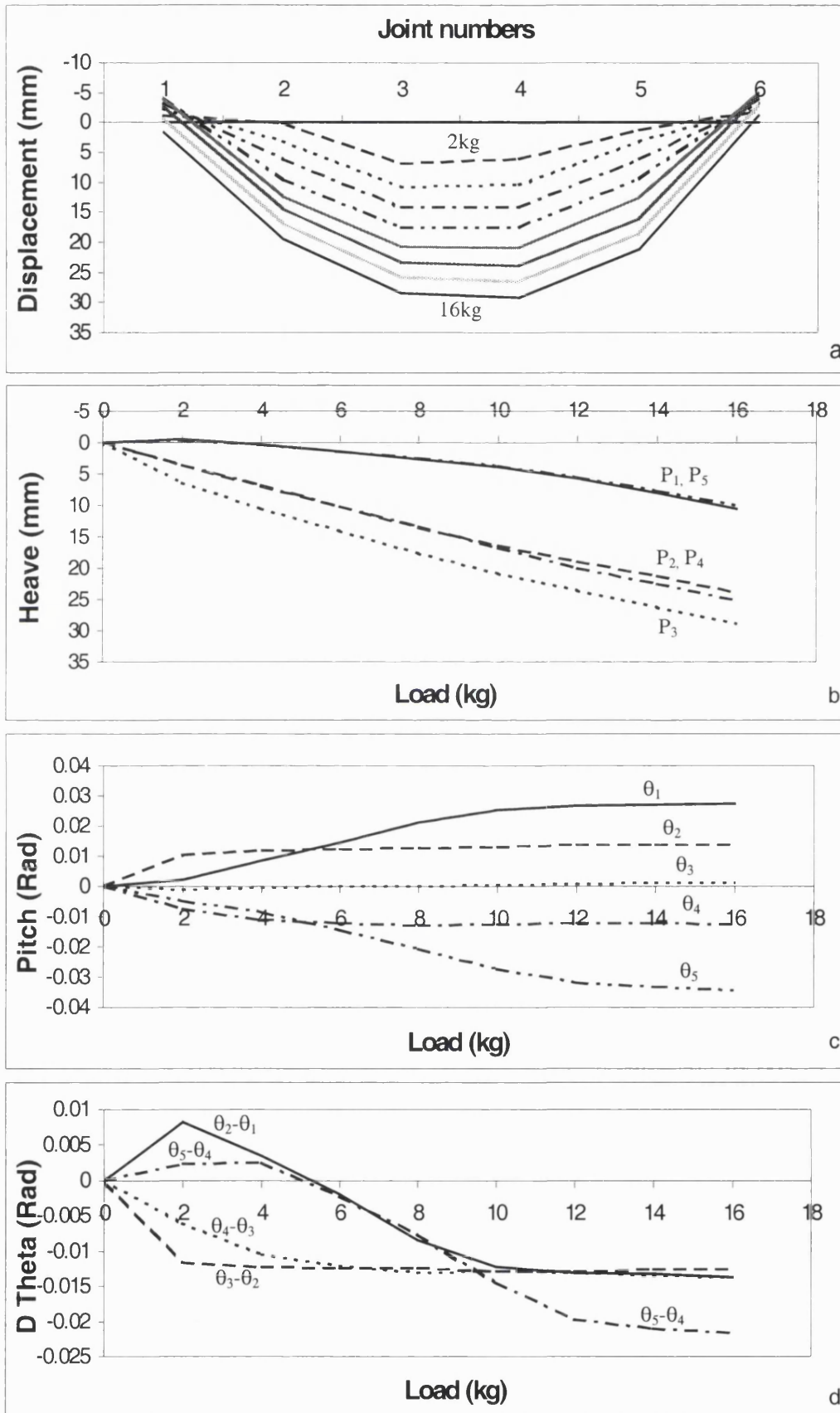


Figure 5.22 Load applied on pontoon 3

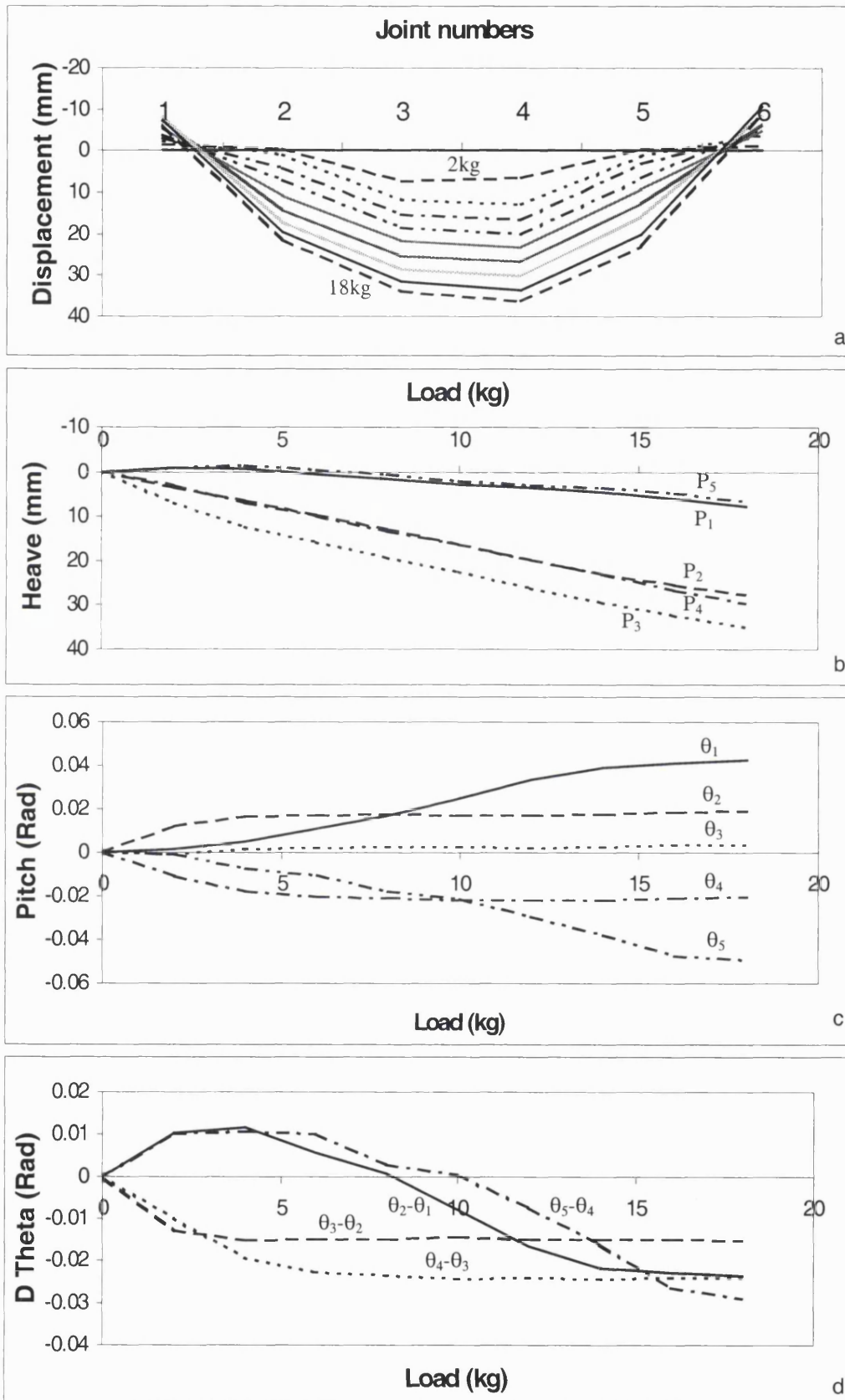


Figure 5.23 Load applied on pontoon 3 (More looseness)

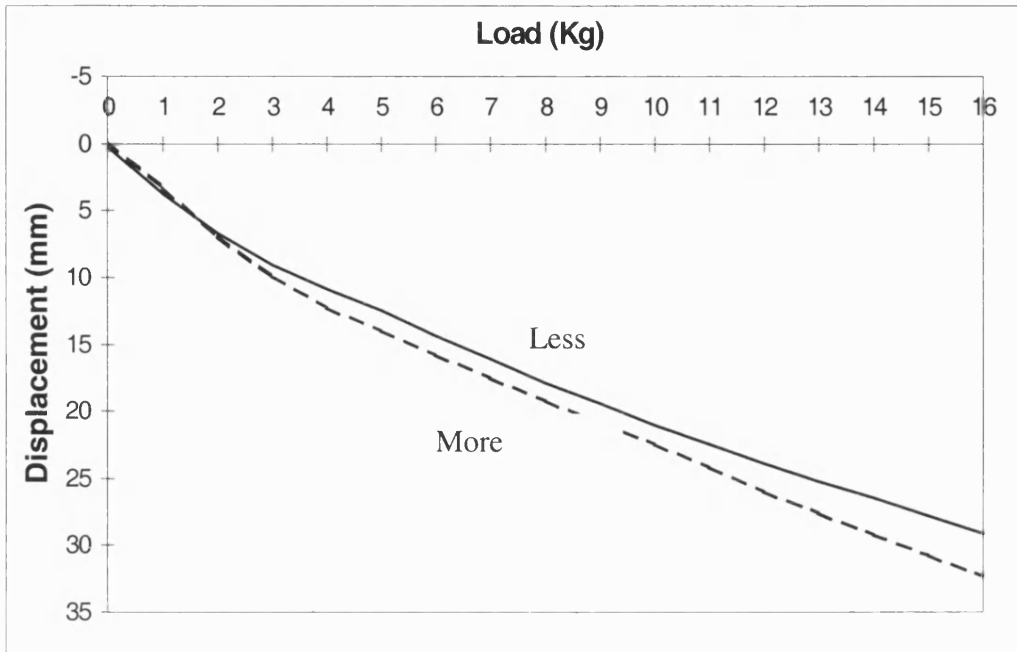


Figure 5.24 Displacement of pontoon 3 with different looseness

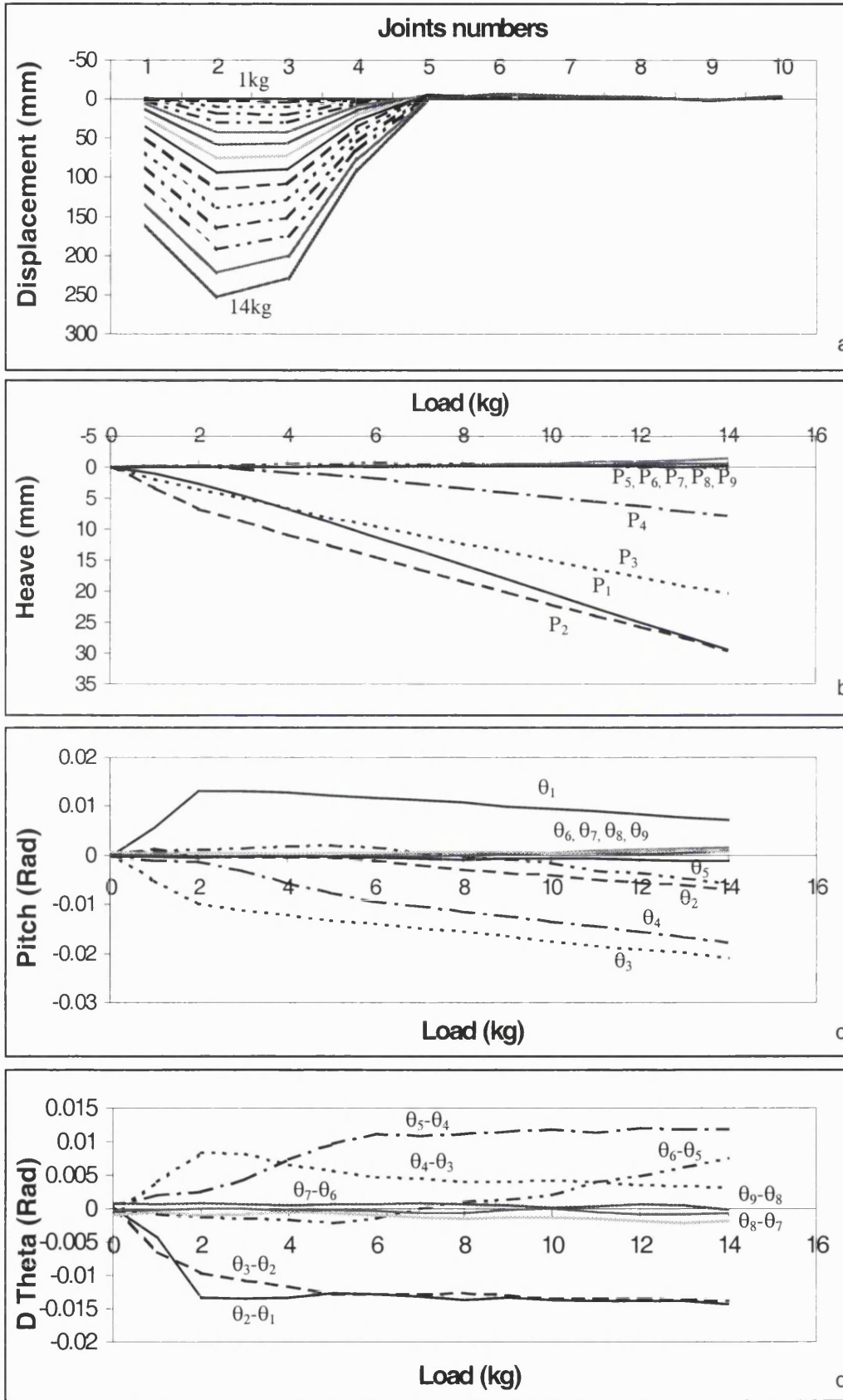


Figure 5.25 Load applied on pontoon 2,  $P_i$  = Pontoon number  $i$ , and  $\theta_i$  = Pitch angle of pontoon  $i$ .

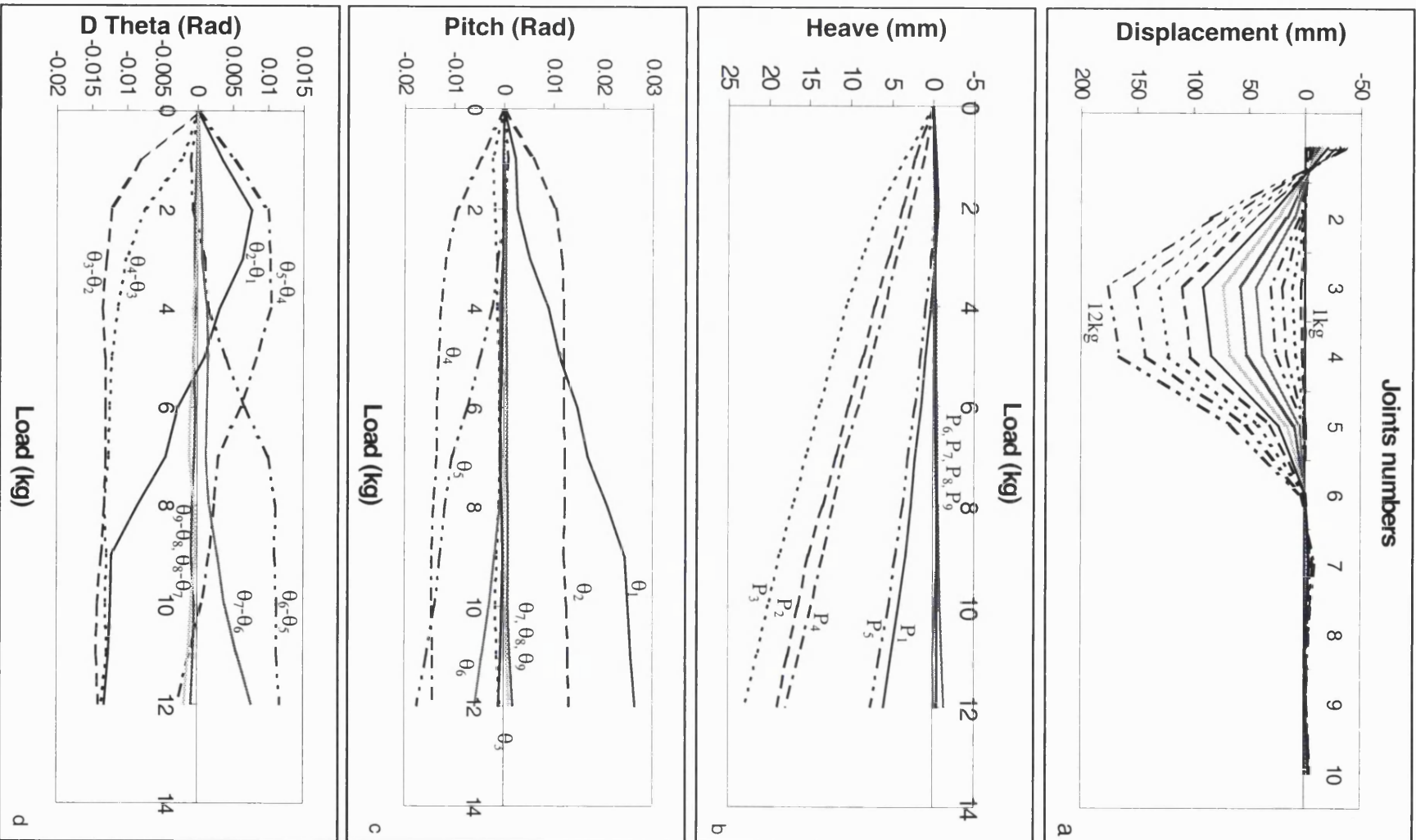


Figure 5.26 Load applied on pontoon 3.

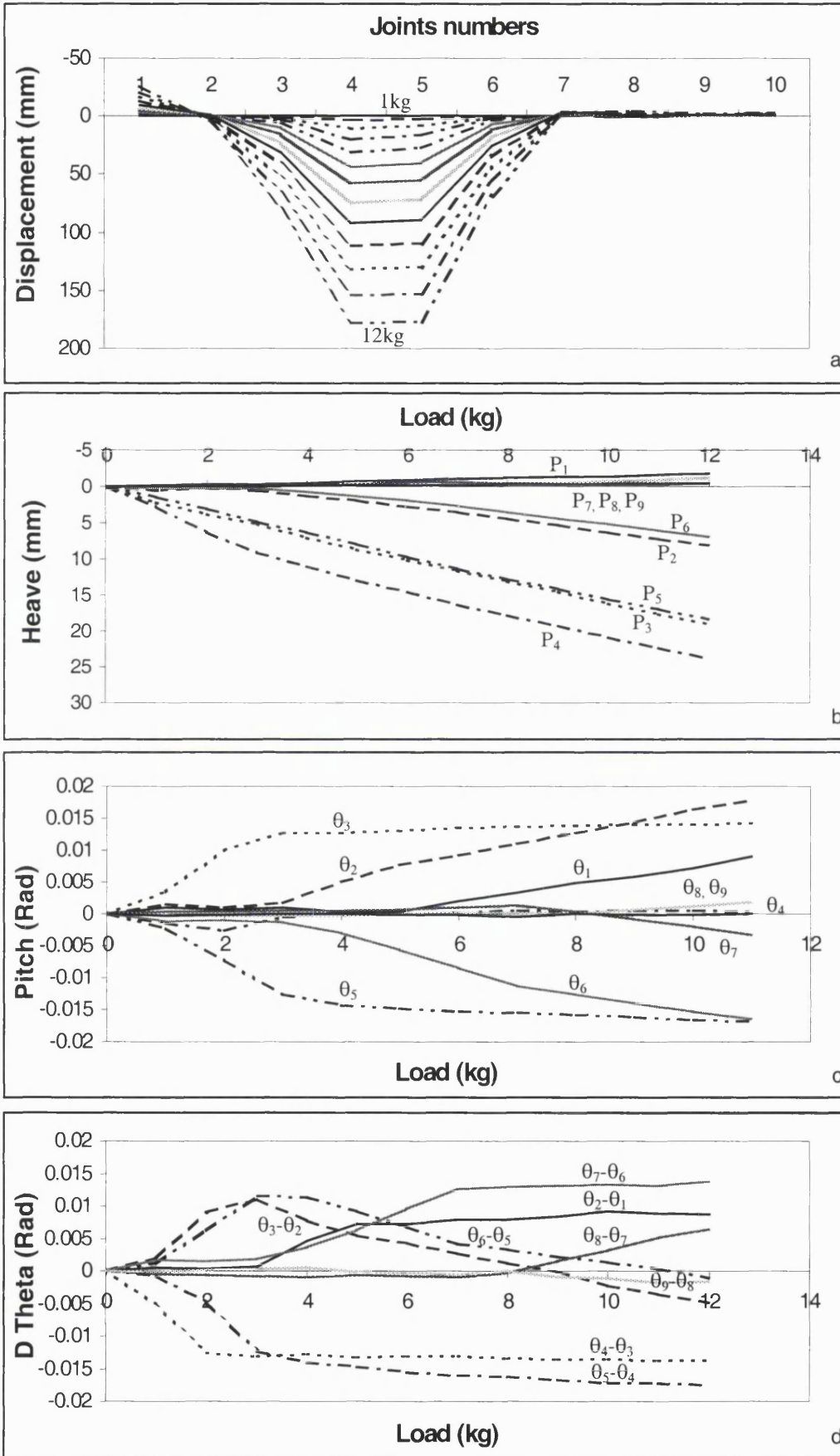


Figure 5.27 Load applied on pontoon 4.

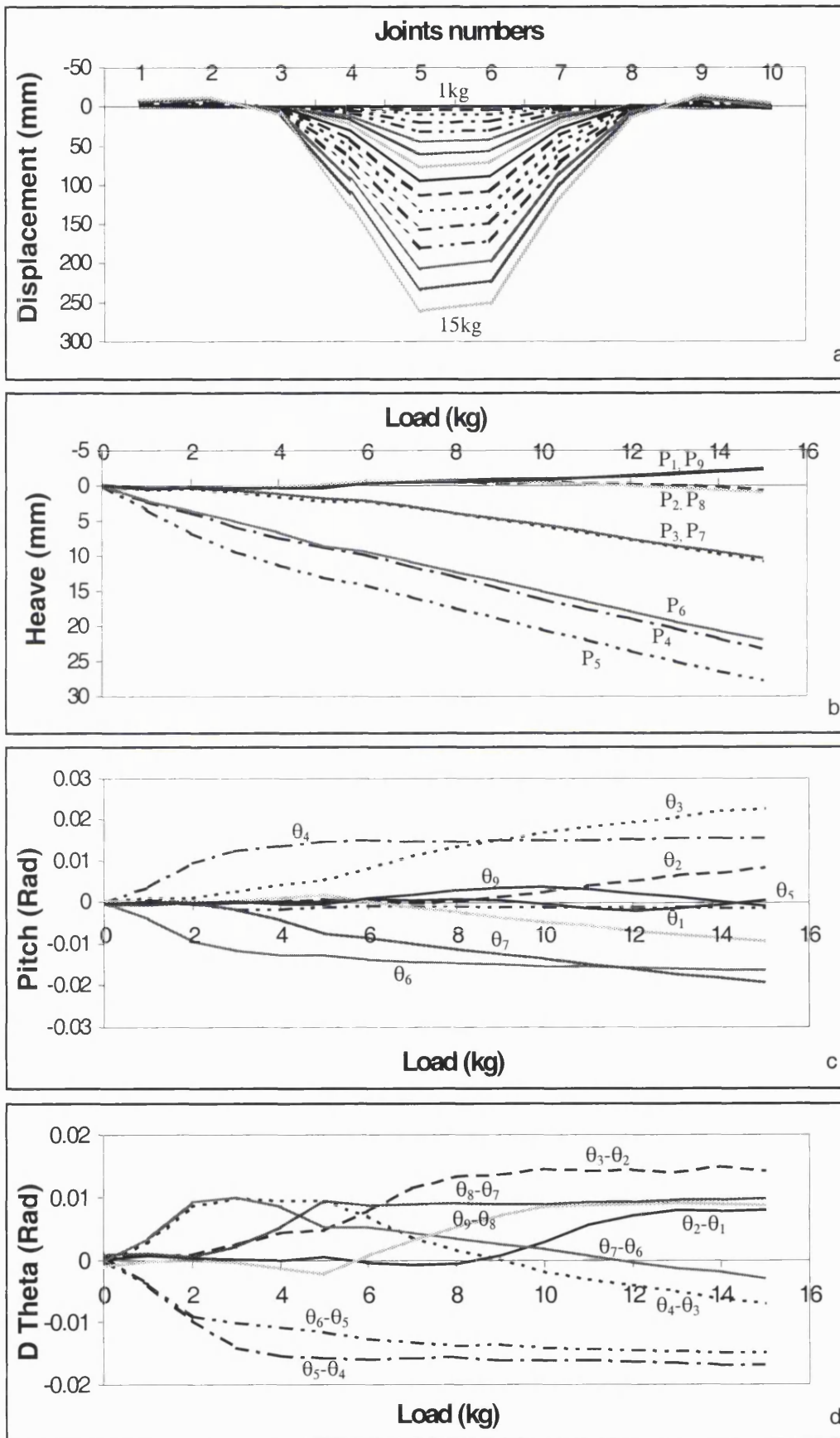


Figure 5.28 Load applied on pontoon 5.

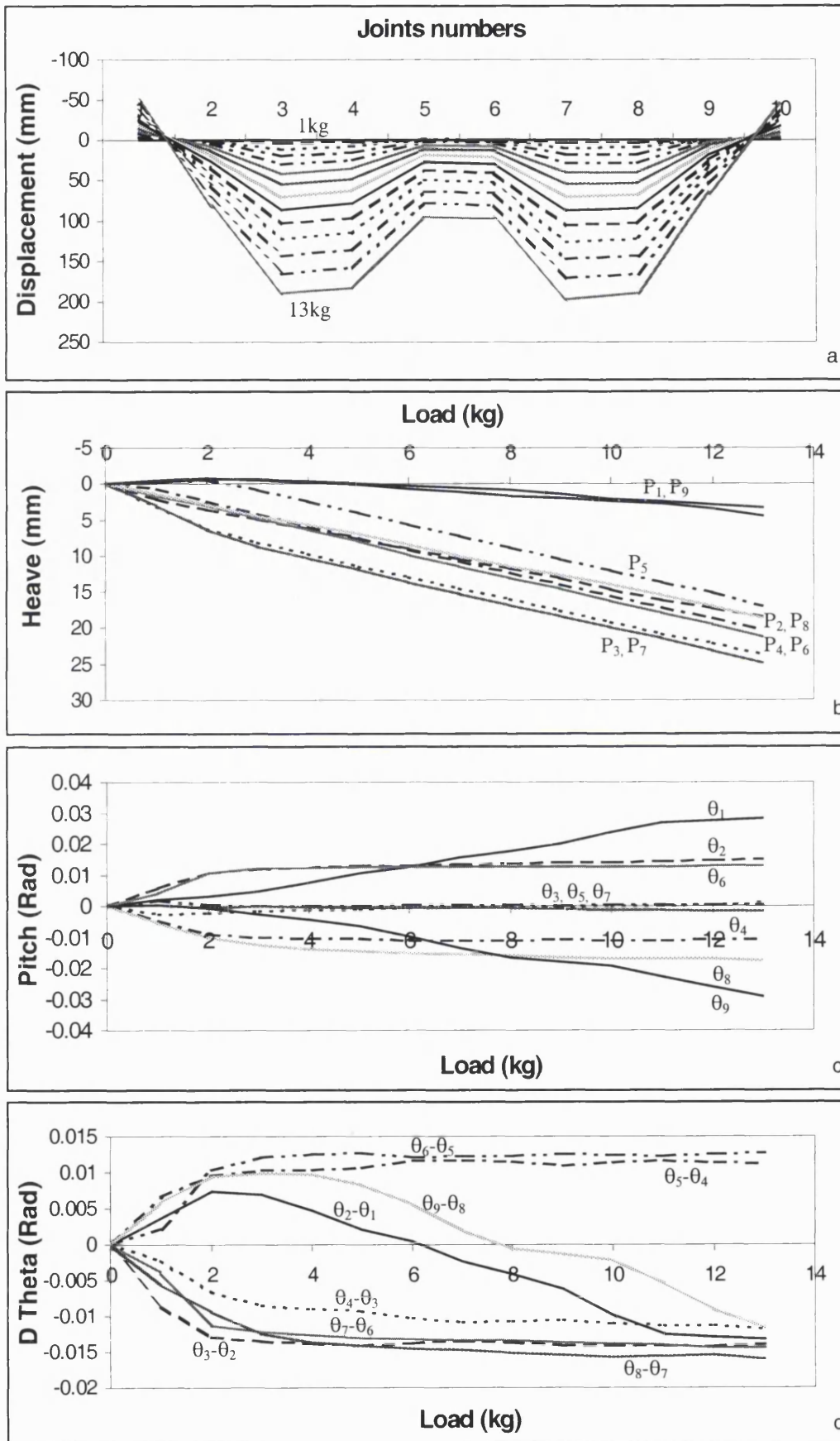


Figure 5.29 Load applied on pontoon 3 and 7.

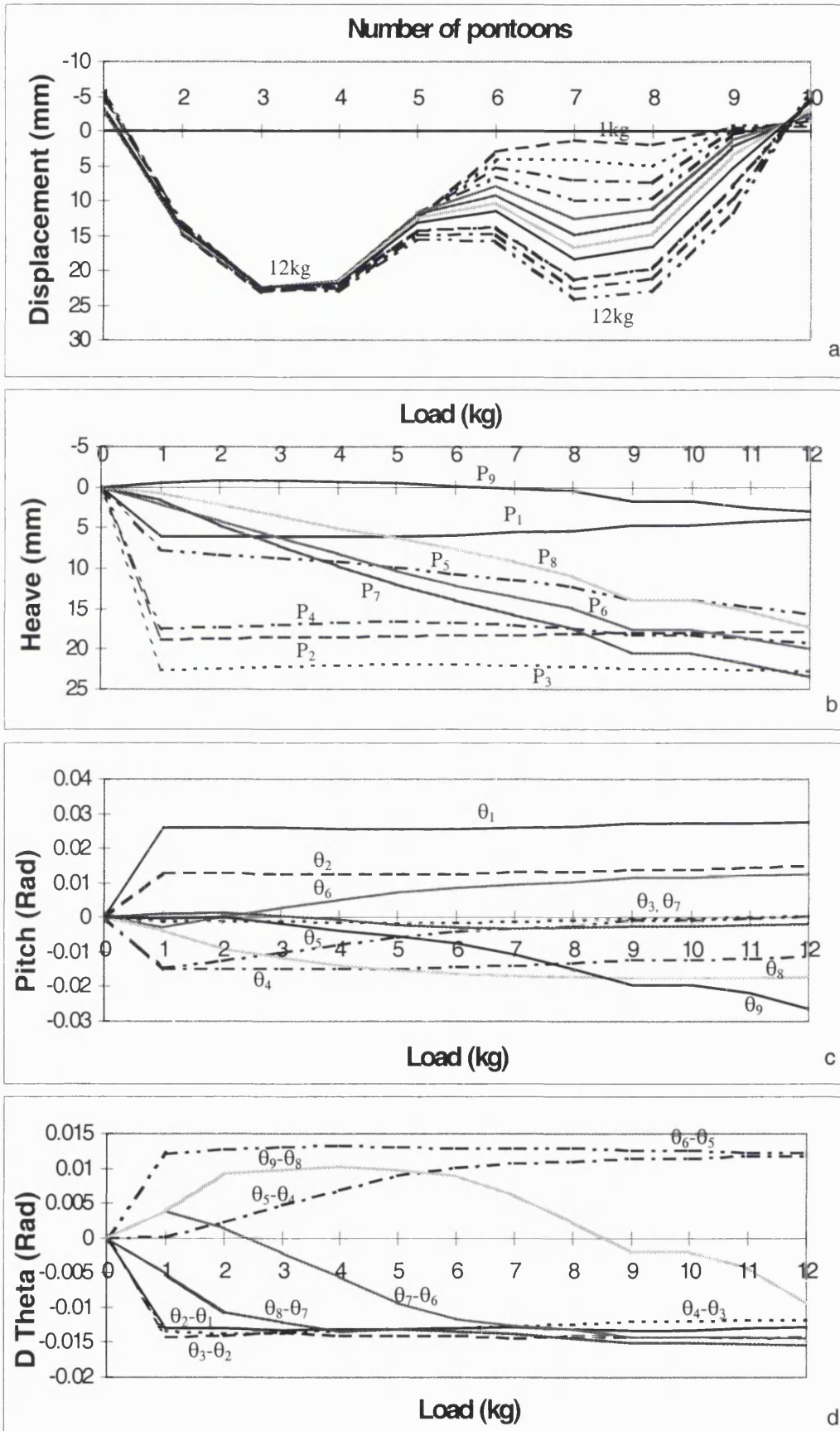


Figure 5.30 Load applied on pontoon 3 (12 kg) and pontoon 7 (1 to 12 kg).

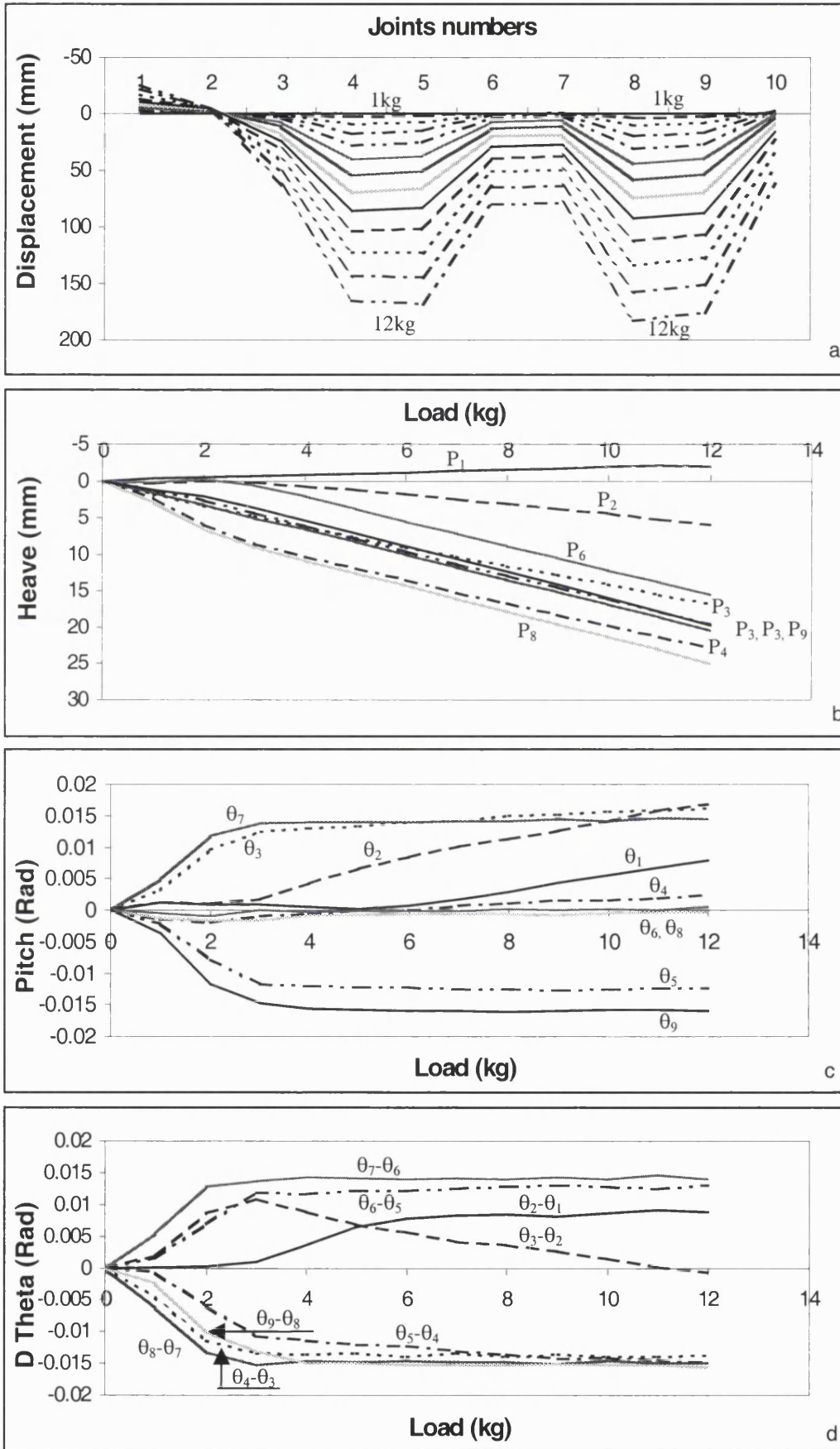


Figure 5.31 Load applied on pontoon 4 and 8.

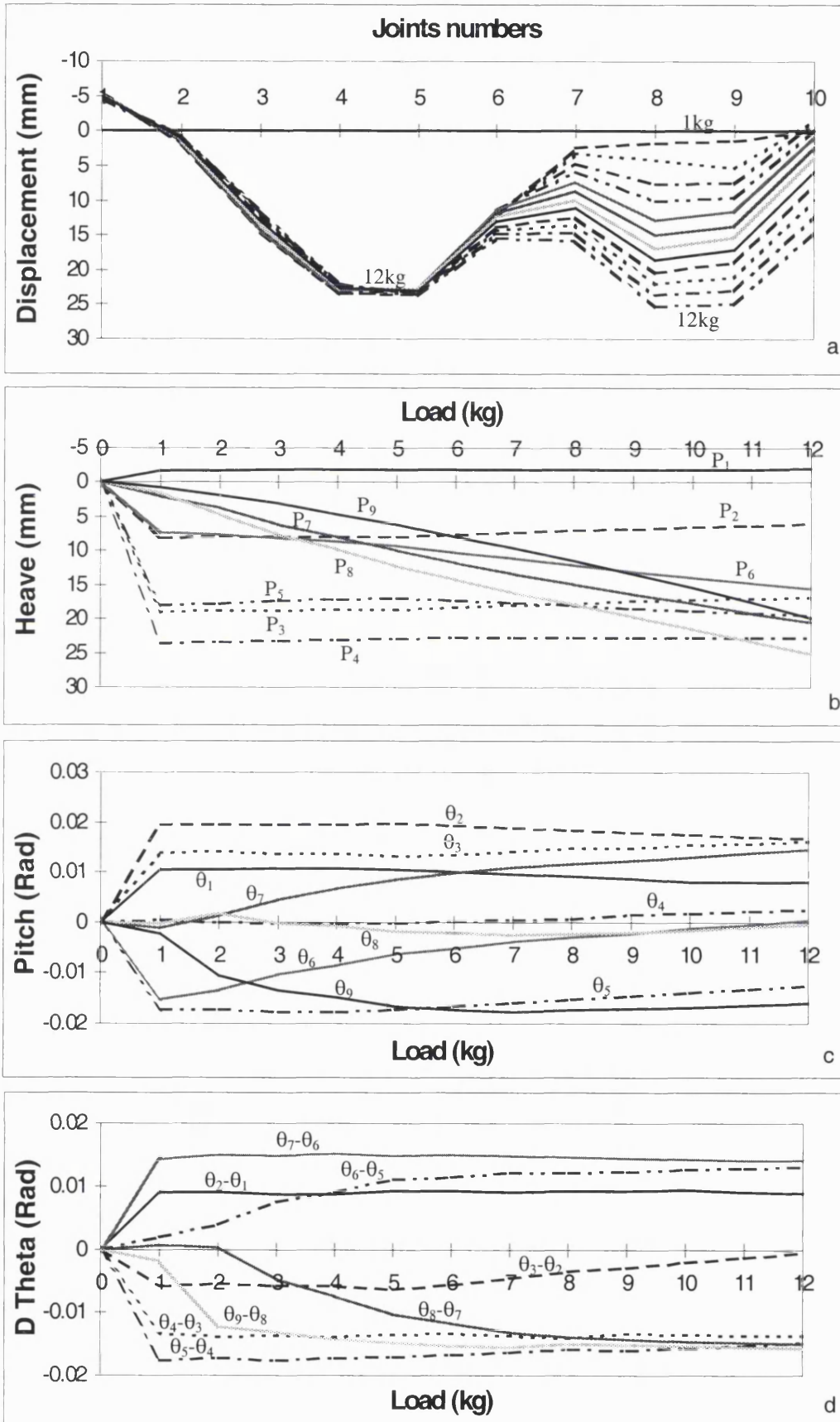


Figure 5.32 Load applied on pontoon 4 (12 kg) and pontoon 8 (1 to 12 kg).



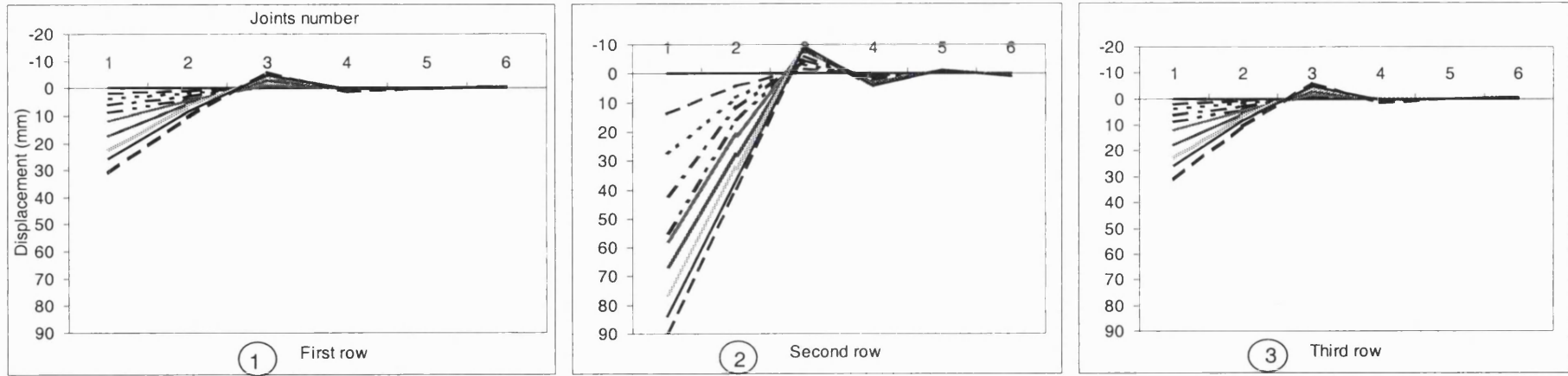


Figure 5.34 Displacement of different rows when load (2 - 18kg) applied on pontoon 6 (hinged connection)

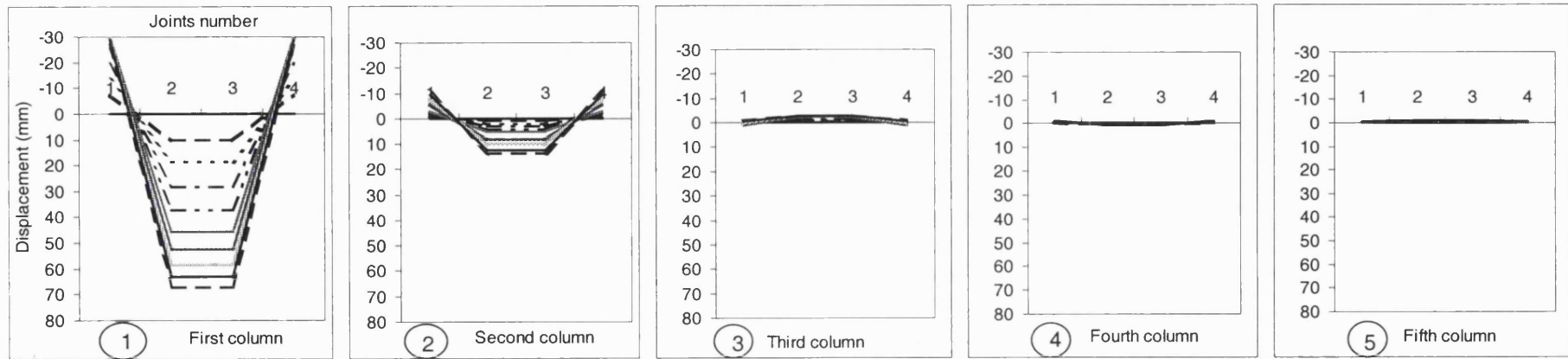


Figure 5.35 Displacement of different columns when load (2 - 18kg) applied on pontoon 6 (hinged connection)

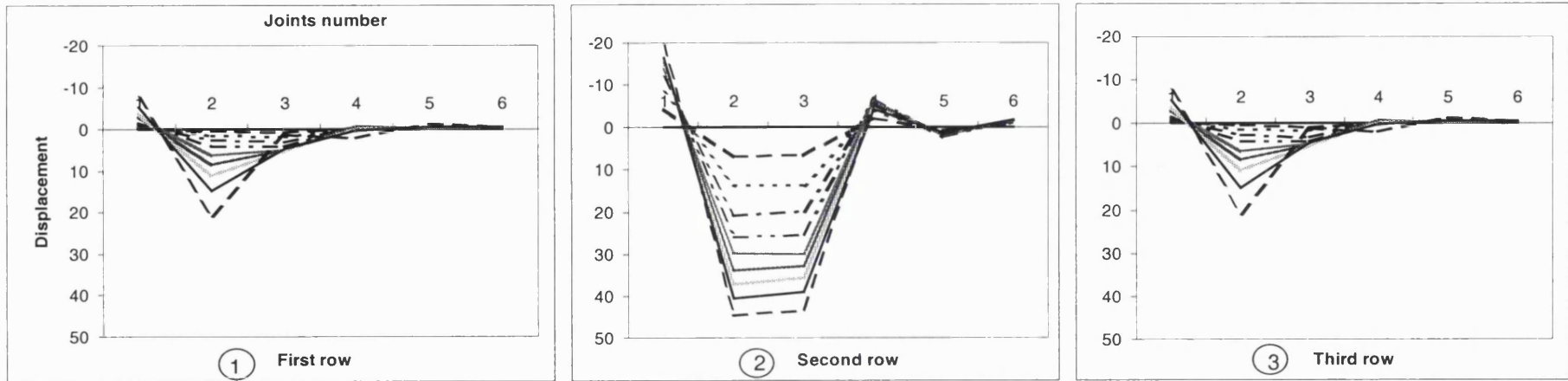


Figure 5.36 Displacement of different rows when load (2 - 18kg) applied on pontoon 7 (hinged connection)

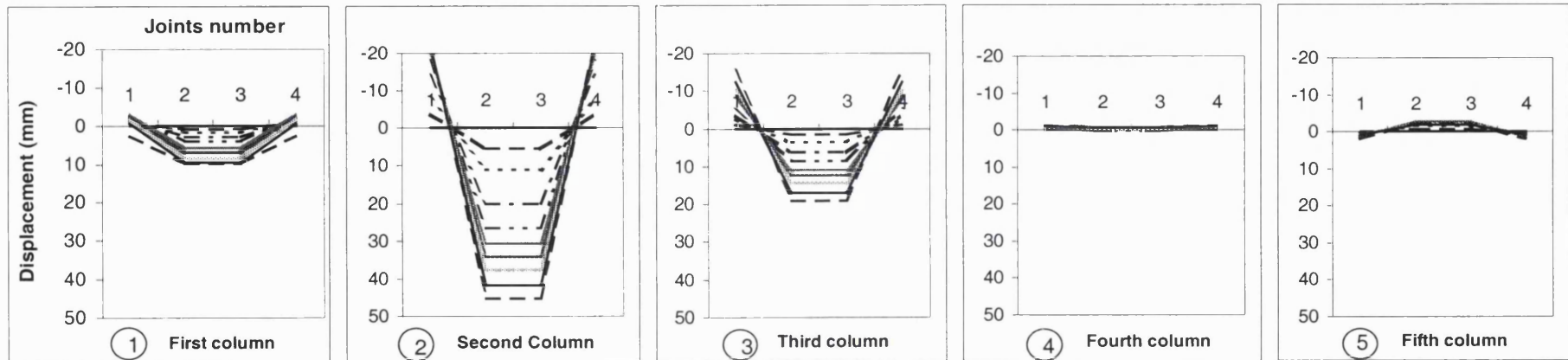


Figure 5.37 Displacement of different columns when load (2 - 18kg) applied on pontoon 7 (hinged connection)

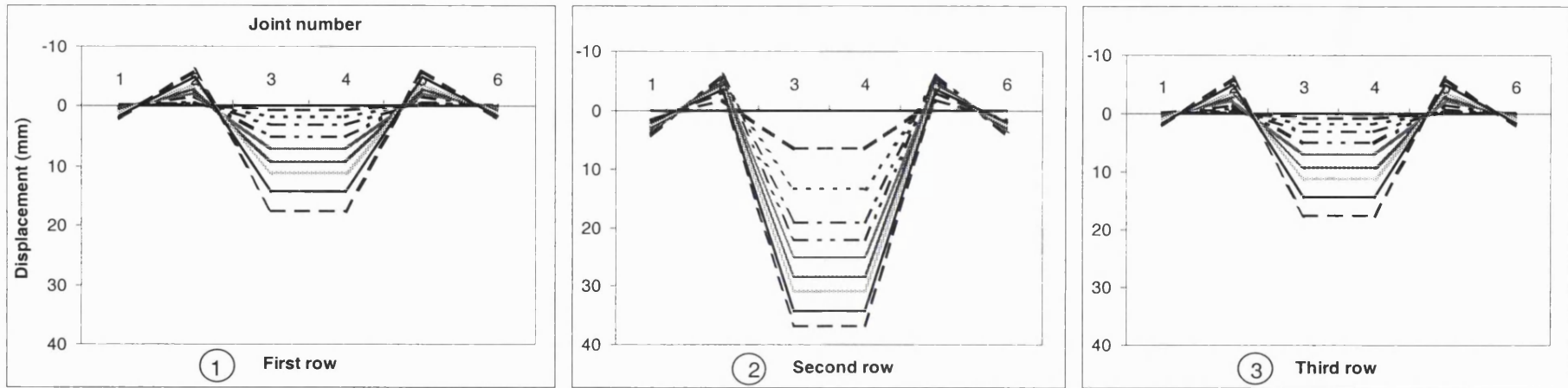


Figure 5.38 Displacement of different rows when load (2 - 18kg) applied on pontoon 8 (hinged connection)

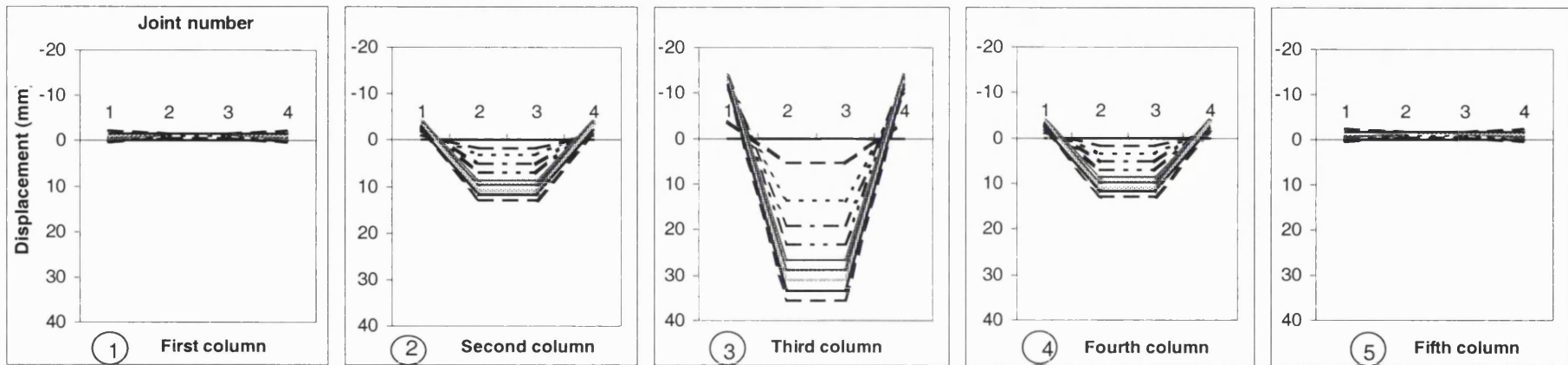


Figure 5.39 Displacement of different columns when load (2 - 18kg) applied on pontoon 8 (hinged connection)

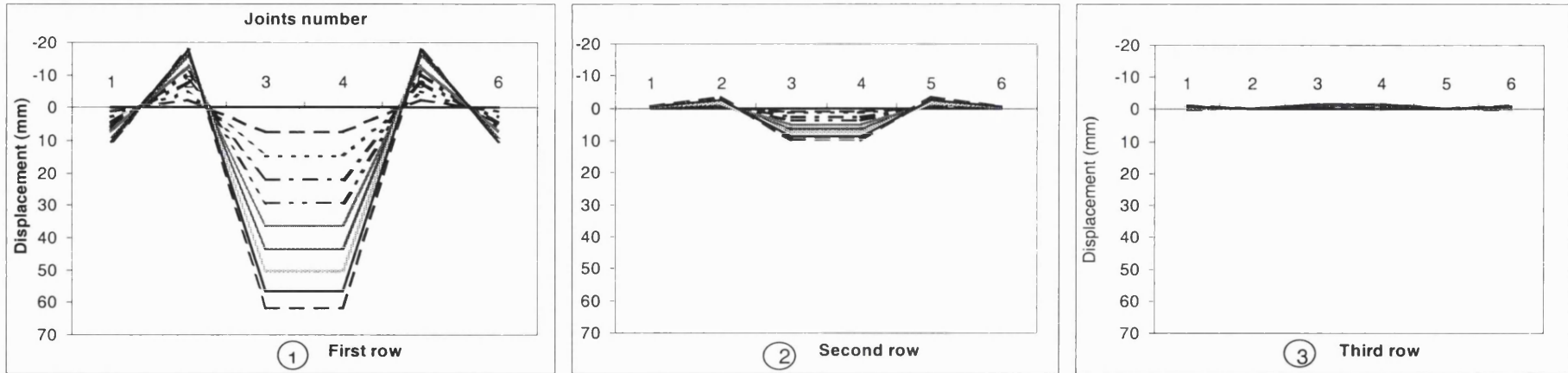


Figure 5.40 Displacement of different rows when load (2 - 18kg) applied on pontoon 3 (hinged connection)

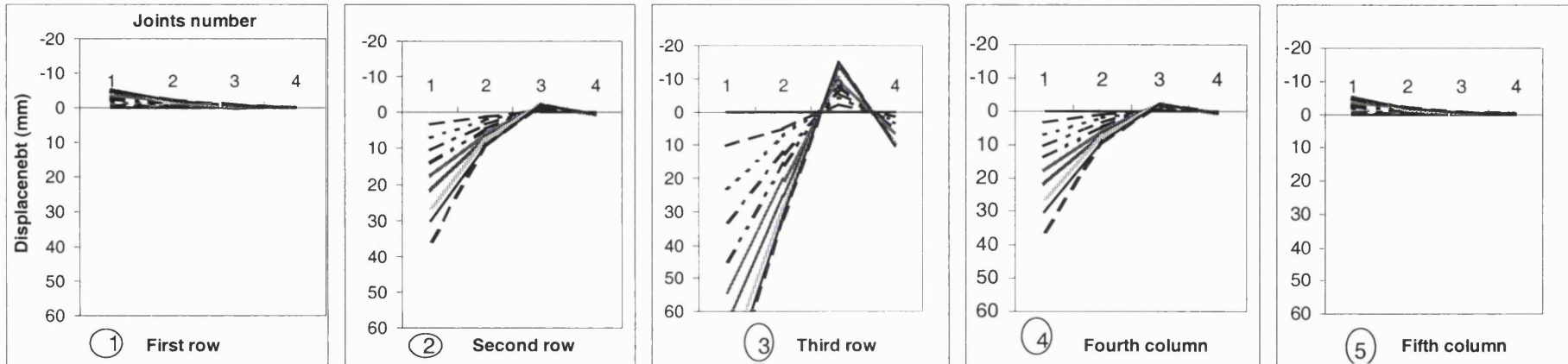


Figure 5.41 Displacement of different columns when load (2 - 18kg) applied on pontoon 3 (hinged connection)

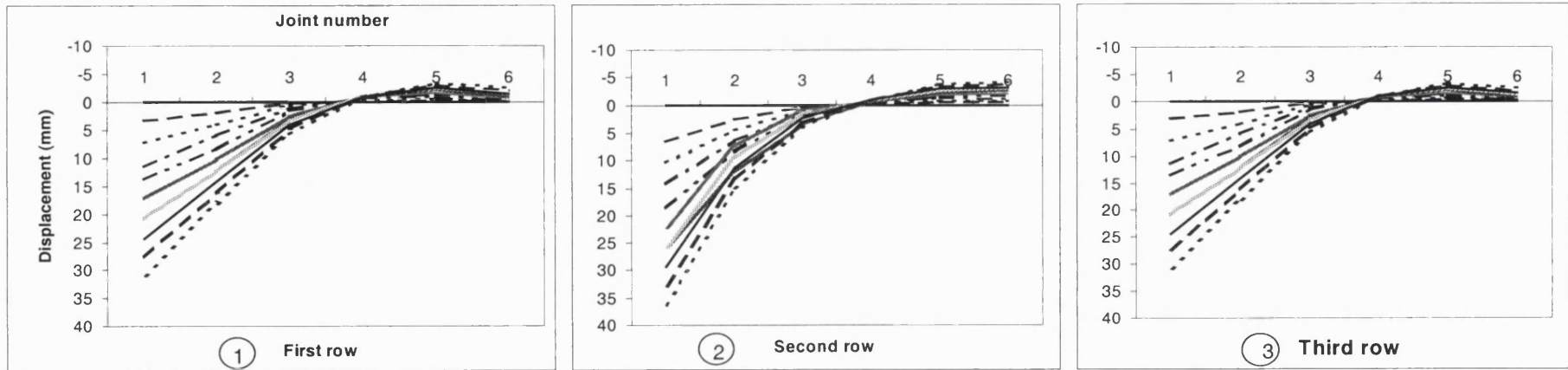


Figure 5.42 Displacement of different rows when load (2 - 20kg) applied on pontoon 6 (hinged-rigid connection)

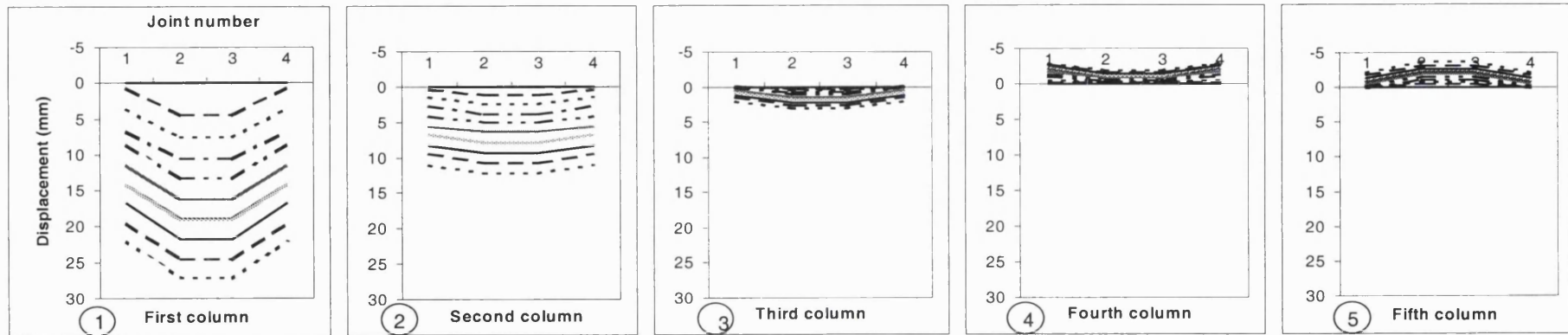


Figure 5.43 Displacement of different columns when load (2 - 20kg) applied on pontoon 6 (hinged-rigid connection)

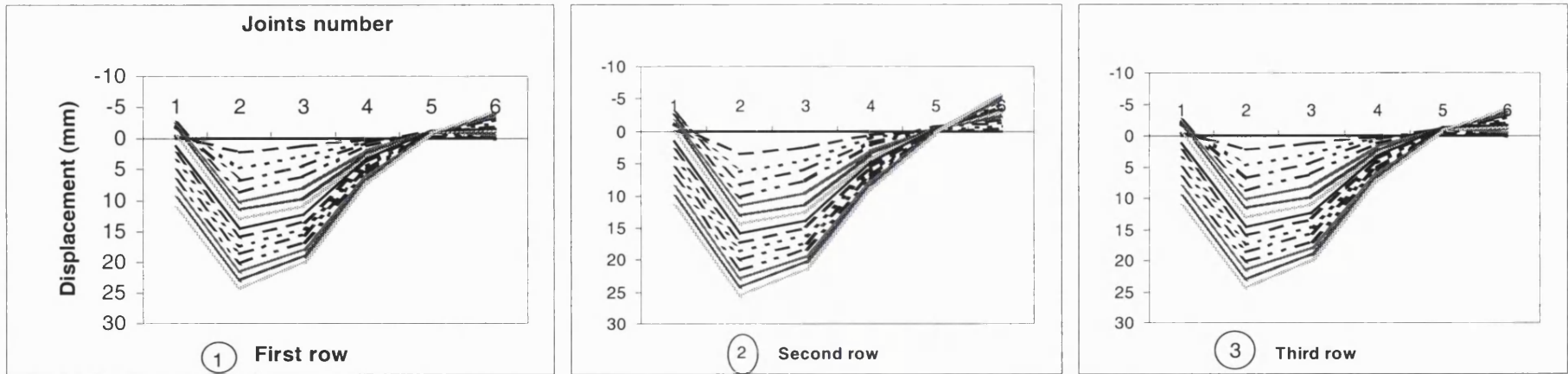


Figure 5.44 Displacement of different rows when load (2 - 30kg) applied on pontoon 7 (hinged-rigid connection)

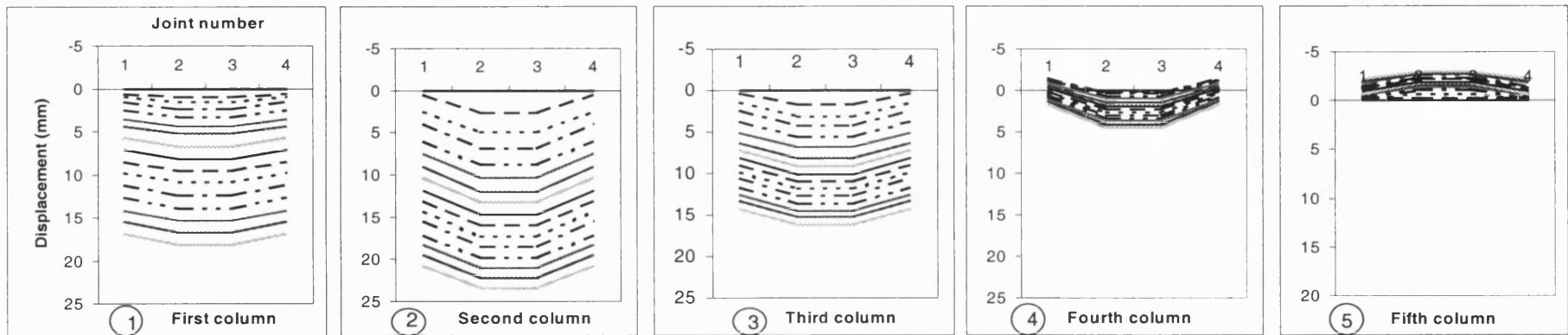


Figure 5.45 Displacement of different columns when load (2 - 30kg) applied on pontoon 7 (hinged-rigid connection)

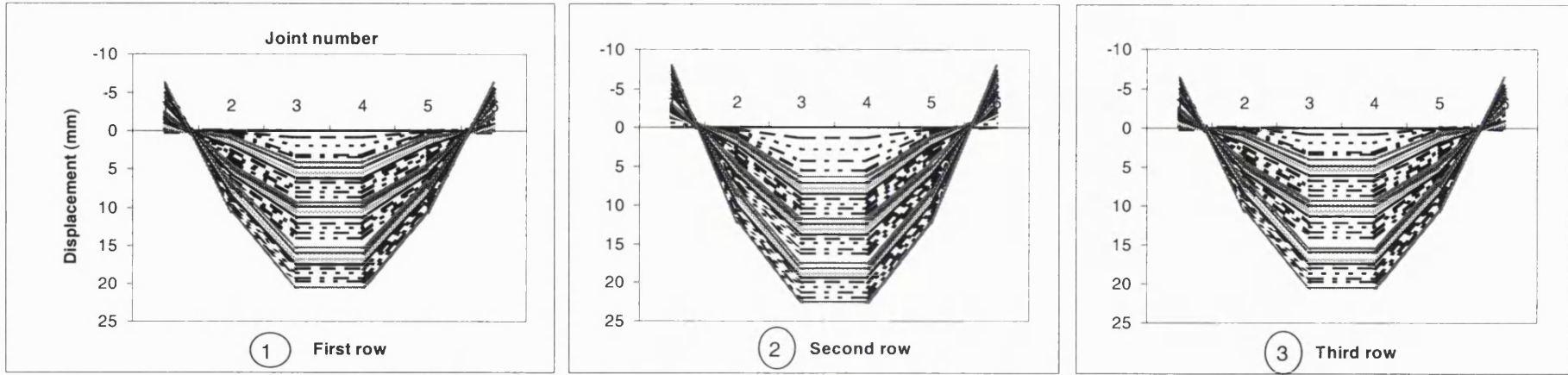


Figure 5.46 Displacement of different rows when load (1 -30kg) applied on pontoon 8 (hinged-rigid connection)

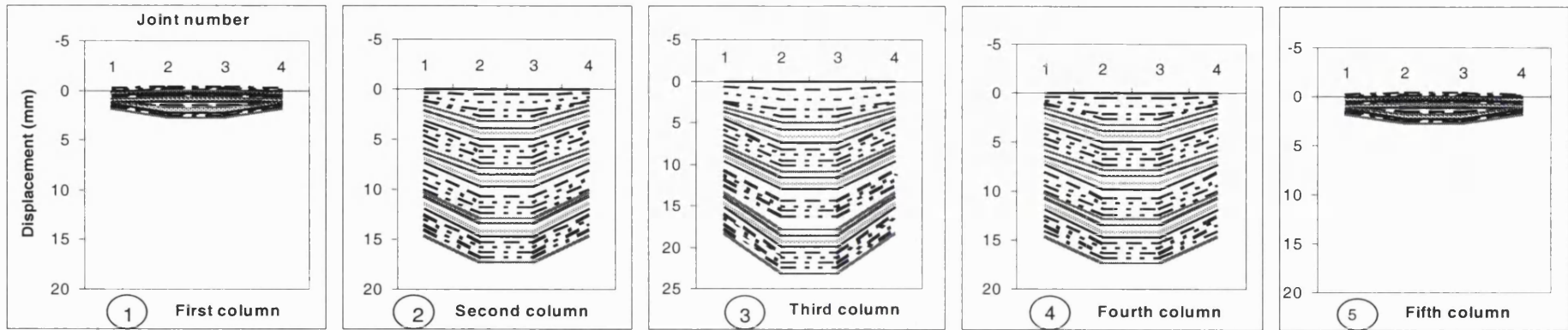


Figure 5.47 Displacement of different columns when load (1 - 30kg) applied on pontoon 8 (hinged-rigid connection)

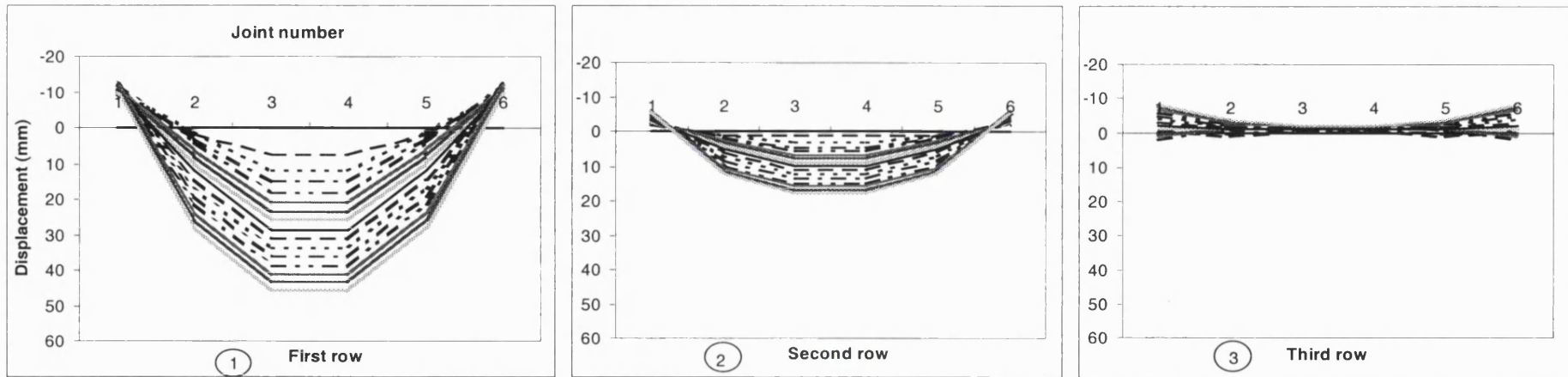


Figure 5.48 Displacement of different rows when load (2 - 30kg) applied on pontoon 3 (hinged-rigid connection)

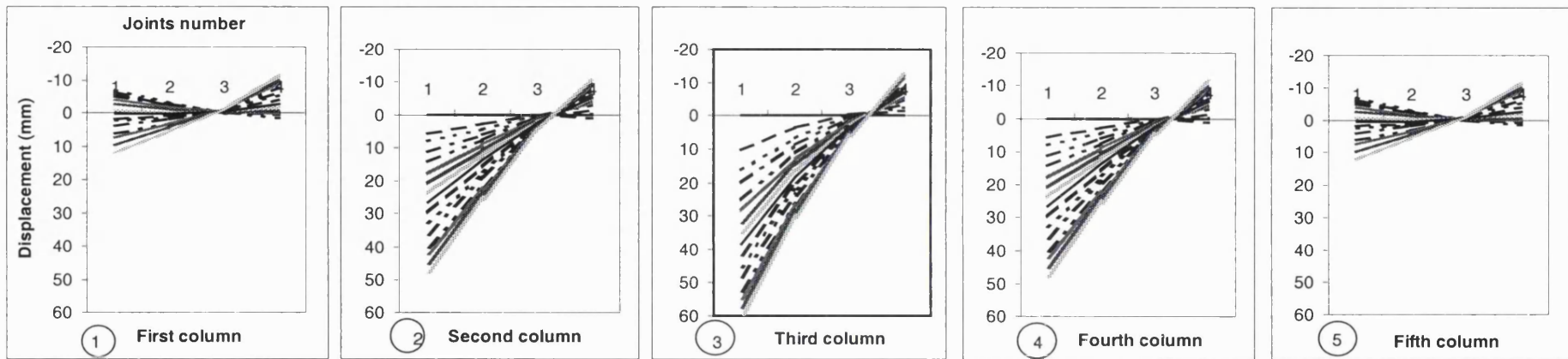


Figure 5.49 Displacement of different columns when load (2 - 30kg) applied on pontoon 3 (hinged-rigid connection)

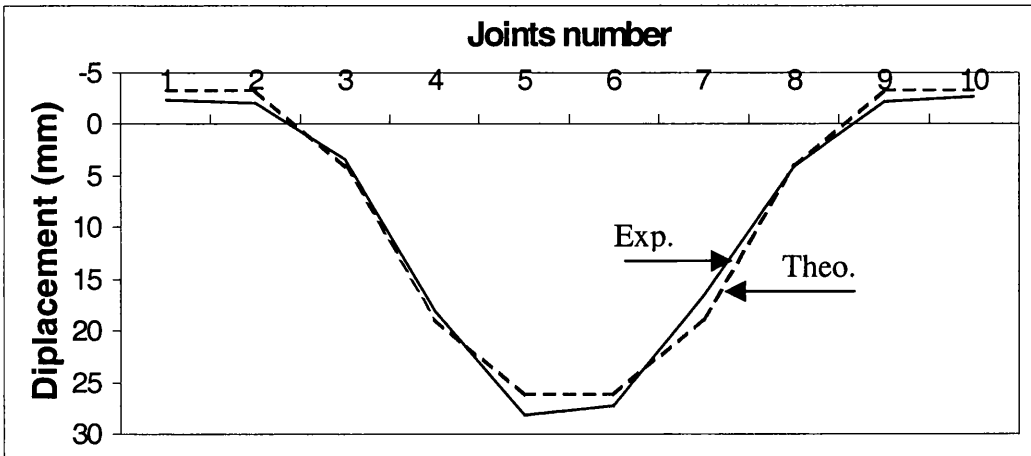


Figure 6.1 Theoretical (1) and experimental result when 15kg load applied on pontoon 5

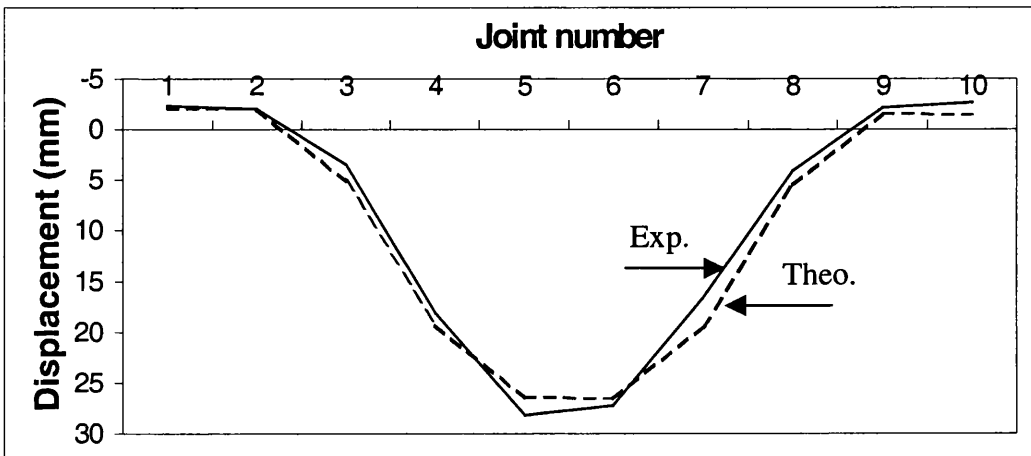


Figure 6.2 Theoretical (2) and experimental result when 15kg load applied on pontoon 5

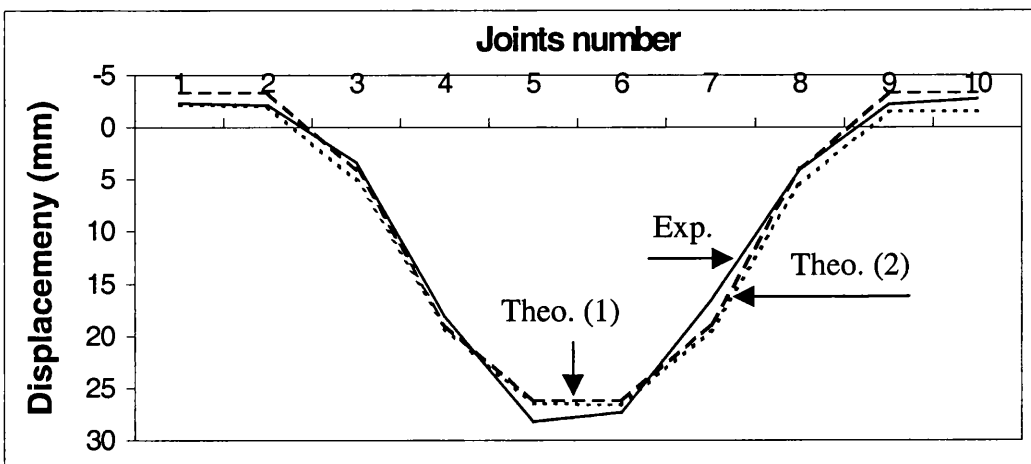


Figure 6.3 Theoretical (1,2) and experimental result when 15kg load applied on pontoon 5

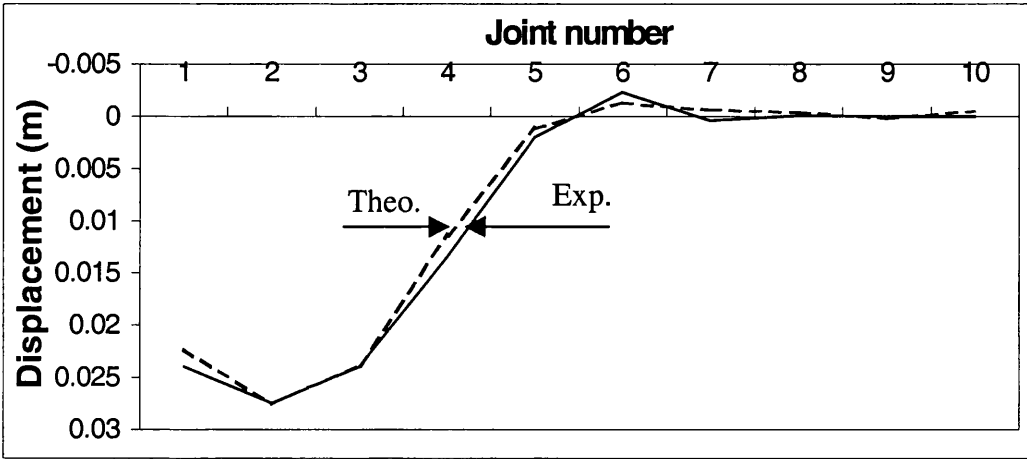


Figure 6.4 Theoretical (2) and experimental result when 12kg load applied on pontoon 2

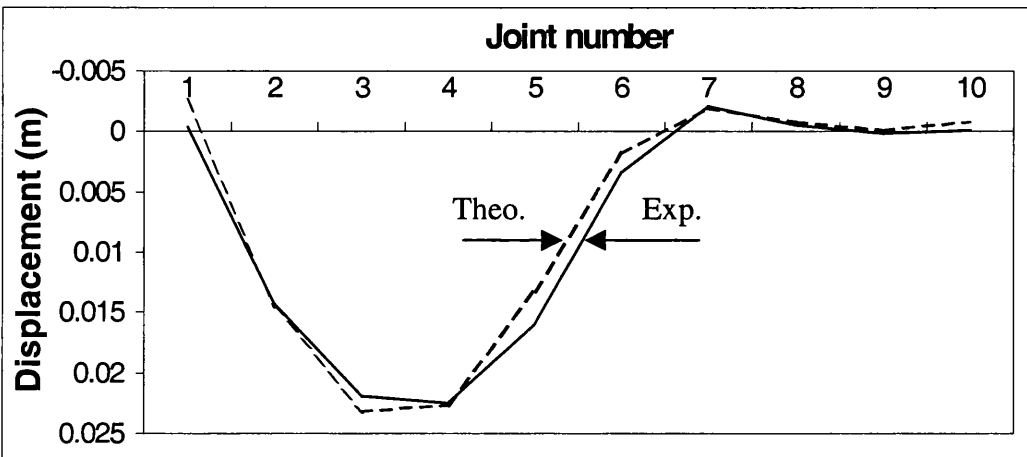


Figure 6.5 Theoretical (2) and experimental result when 12kg load applied on pontoon 3

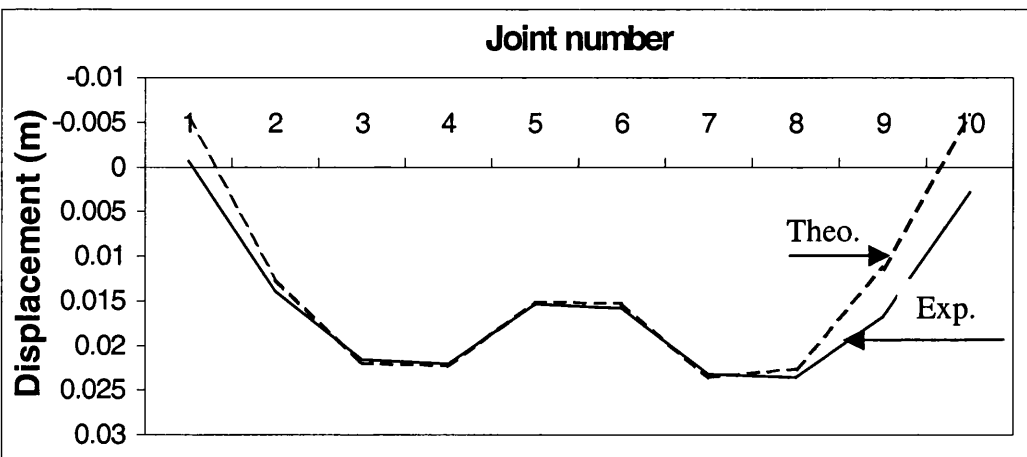


Figure 6.6 Theoretical (2) and experimental result when 12kg applied on pontoons 3 and 7

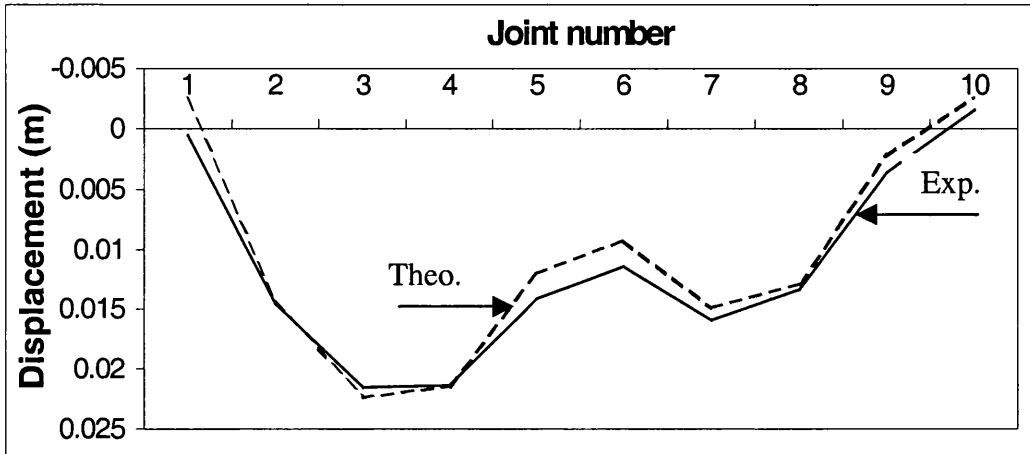


Figure 6.7 Theoretical (2) and experimental result when 12-6kg applied on pontoons 3-7

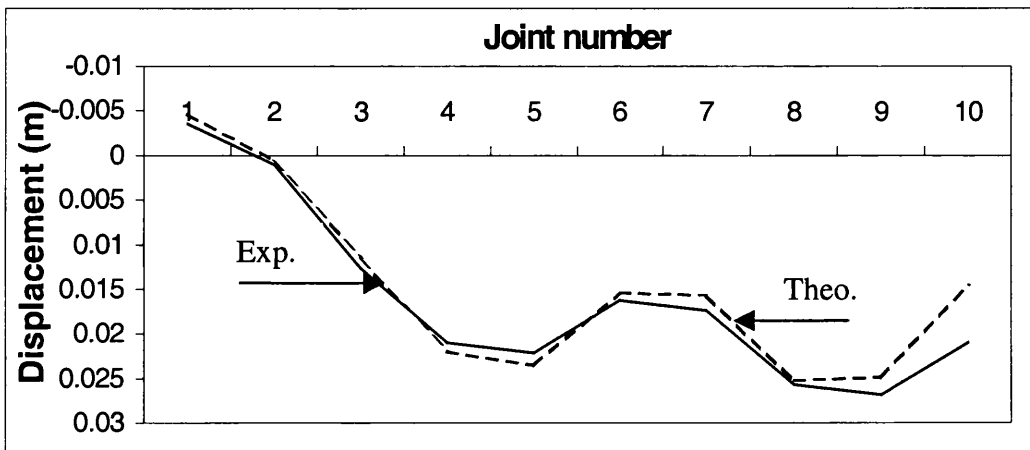


Figure 6.8 Theoretical (2) and experimental result when 12kg applied on pontoons 4 and 8

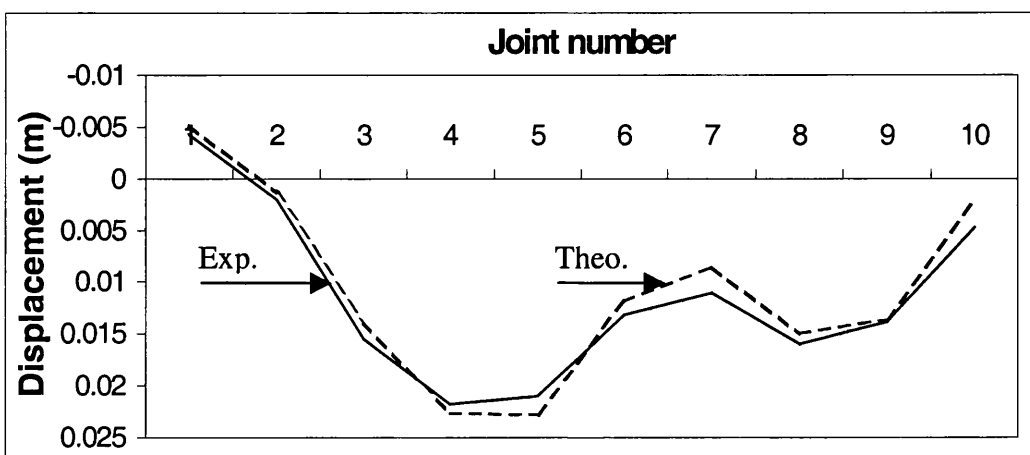


Figure 6.9 Theoretical (2) and experimental result when 12-6kg applied on pontoons 4-8

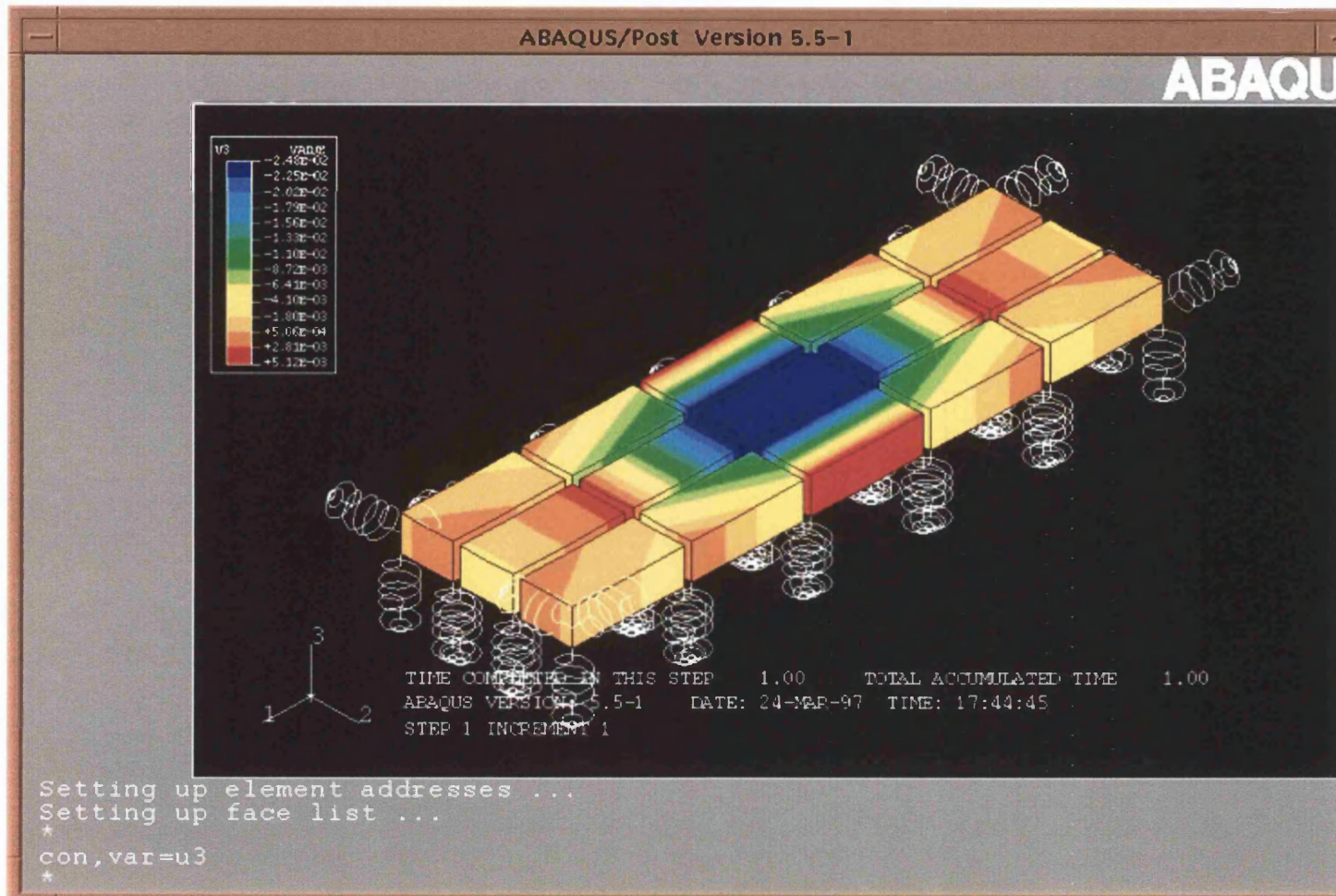


Figure 6.10 ABAQUS result when 15 kg load apply on central pontoon

## APPENDICES

### APPENDIX A

#### PROGRAM HINGE

```

C  DATE: 6.6.1995 (HINGE)
C
C  THIS PROGRAM IS FOR CALCULATION OF DISPLACEMENT AND ROTATION
C  OF N PONTOONS IN HINGE-CONNECTION
      INTEGER I,J,N,P,NP,R,II,Q(50)
      REAL A(50,50),F(50),X(50),DIS(50),TE(50),DTE(50),RIG(50,50),
& L,B,D,L1,T,D1,D2,H,EP,G,RO,M,ALPHA,BETA,GAMA,PSI,F1(50),
& ALPHA1,BETA1,GAMA1,PSI1,DIS1(25),DIS2(25),DTE1(25)
      CHARACTER*8 FILNAM
      PRINT*, 'INPUT FILE NAME'
      READ(*,8) FILNAM
8 FORMAT(A8)
      OPEN(UNIT=10,FILE=FILNAM,STATUS='OLD')
      READ(10,*) L
      READ(10,*) B
      READ(10,*) D
      READ(10,*) T
      READ(10,*) D1
      READ(10,*) D2
      READ(10,*) L1
      READ(10,*) H
      READ(10,*) G
      READ(10,*) RO
      PRINT*, 'ENTER NO. OF PON. NP='
      READ(*,*) NP
      EP=2*2*(D1-D2)/H
      AA=RO*G*L*B
      BB=RO*G*L*B*T*((T/2)+(L**2)/(12*T)-(D/2))
      ALPHA=0
      BETA=-(L+L1)/2

```

```

      GAMA=1
PSI=-(L+L1)/2
      ALPHA1=EP
      BETA1=0
      GAMA1=1
      PSI1=0
N=2*NP
      PRINT*,INPUT FILE NAME FOR F(I)'
      READ(*,8) FILNAM
      OPEN(UNIT=11,FILE=FILNAM,STATUS='OLD')
      DO 70 I=1,N
READ(11,*)F(I)
70 CONTINUE
C      DO 75 I=1,N
C      PRINT*,ENTER VALUE F(I)'
C 75  READ*,F(I)
      DO 76 I=1,N
76 F(I)=F(I)*G
      DO 80 I=1,N
      DO 80 J=1,N
80 A(I,J)=0
      DO 90 I=1,N-1,2
      A(I,I)=AA
      A(I+1,I+1)=BB
90 CONTINUE
      I=1
25 CALL COND(A,F,ALPHA,BETA,GAMA,PSI,I,N)
      I=I+2
      IF(I.LE.N-3)THEN
      GO TO 25
      ELSE
      END IF
      CALL GAUSS(A,F,X,N,RIG,F1)
      DO 100 I=1,N
      DO 100 J=1,N
100 A(I,J)=RIG(I,J)
      DO 105 I=1,N

```

```

105 F(I)=F1(I)
      CALLWR1(EP,AA,BB,ALPHA,BETA,GAMA,PSI,ALPHA1,BETA1,GAMA1,PSI1,
      N)
35   CALL DEF(X,L,L1,N,DIS,TE,DIS1,DIS2,DTE)
      CLOSE (UNIT=10)
CLOSE (UNIT=11)
      CALL WR2(A,F,X,DIS,TE,DIS1,DIS2,DTE,N)
      WRITE(1,*)'*****END*****'
      END
      *****
      SUBROUTINE COND(A,F,ALPHA,BETA,GAMA,PSI,I,N)
      DIMENSION A(50,50),F(50)
      A(I+1,I+1)=BETA*A(I,I+1)+BETA*A(I+1,I)+A(I+1,I+1)
      A(I+1,I+2)=BETA*A(I,I+2)+GAMA*A(I+1,I)+A(I+1,I+2)
      A(I+1,I+3)=BETA*A(I,I+3)+PSI*A(I+1,I)+A(I+1,I+3)
      A(I+2,I+1)=GAMA*A(I,I+1)+BETA*A(I+2,I)+A(I+2,I+1)
      A(I+2,I+2)=GAMA*A(I,I+2)+GAMA*A(I+2,I)+A(I+2,I+2)
      A(I+2,I+3)=GAMA*A(I,I+3)+PSI*A(I+2,I)+A(I+2,I+3)
      A(I+3,I+1)=PSI*A(I,I+1)+BETA*A(I+3,I)+A(I+3,I+1)
      A(I+3,I+2)=PSI*A(I,I+2)+GAMA*A(I+3,I)+A(I+3,I+2)
      A(I+3,I+3)=PSI*A(I,I+3)+PSI*A(I+3,I)+A(I+3,I+3)
      DO 40 S=1,I-1,1
      A(I+1,S)=BETA*A(I,S)+A(I+1,S)
      A(I+2,S)=GAMA*A(I,S)+A(I+2,S)
      A(I+3,S)=PSI*A(I,S)+A(I+3,S)
      A(I,S)=0
      A(S,I+1)=A(I+1,S)
      A(S,I+2)=A(I+2,S)
      A(S,I+3)=A(I+3,S)
      A(S,I)=A(I,S)
40 CONTINUE
      DO 41 S=I+4,N,1
      A(I+1,S)=BETA*A(I,S)+A(I+1,S)
      A(I+2,S)=GAMA*A(I,S)+A(I+2,S)
      A(I+3,S)=PSI*A(I,S)+A(I+3,S)
      A(I,S)=0
      A(S,I+1)=A(I+1,S)

```

```

A(S,I+2)=A(I+2,S)
A(S,I+3)=A(I+3,S)
A(S,I)=A(I,S)
41 CONTINUE
A(I,I+1)=BETA*A(I,I)
A(I,I+2)=GAMA*A(I,I)
A(I,I+3)=PSI*A(I,I)
A(I+1,I)=BETA*A(I,I)
A(I+2,I)=GAMA*A(I,I)
A(I+3,I)=PSI*A(I,I)
DO 42 J=I+1,I+3
42 F(I)=F(I)-ALPHA*A(J,I)
F(I+1)=BETA*F(I)+F(I+1)+ALPHA*BETA*A(I,I)
F(I+2)=GAMA*F(I)+F(I+2)+ALPHA*GAMA*A(I,I)
F(I+3)=PSI*F(I)+F(I+3)+ALPHA*PSI*A(I,I)
F(I)=-ALPHA*A(I,I)
A(I,I)=-A(I,I)
RETURN
END
*****
SUBROUTINE GAUSS(A,Y,X,N,RIG,F1)
DIMENSION A(50,50),Y(50),X(50),RIG(50,50),F1(50)
DO 50 I=1,N
DO 50 J=1,N
50 RIG(I,J)=A(I,J)
DO 51 I=1,N
51 F1(I)=Y(I)
DO 52 K=1,N-1
DO 53 I=K+1,N
Z=A(I,K)/A(K,K)
DO 54 J=K,N
54 A(I,J)=A(I,J)-A(K,J)*Z
53 Y(I)=Y(I)-Y(K)*Z
52 CONTINUE
X(N)=Y(N)/A(N,N)
DO 55 K=N-1,1,-1
SUM=Y(K)

```

```

      DO 56 J=K+1,N
56 SUM=SUM-X(J)*A(K,J)
55 X(K)=SUM/A(K,K)
      RETURN
      END
      *****

      SUBROUTINE DEF(X,Y,Z,N,DIS,TE,DIS1,DIS2,DTE)
      DIMENSION X(50),DIS(25),TE(25),DIS1(25),DIS2(25),DTE(25)
      DO 140 I=1,N/2
          DIS(I)=X(2*I-1)
          TE(I)=X(2*I)
140 CONTINUE
          DO 150 I=1,N/2
              DIS1(I)=DIS(I)-((Y+Z)/2)*TE(I)
              DIS2(I)=DIS(I)+((Y+Z)/2)*TE(I)
150 CONTINUE
          DO 155 I=1,N/2-1
              DTE(I)=TE(I+1)-TE(I)
155 CONTINUE
          RETURN
          END
          *****

      SUBROUTINEWR1(EP,AA,BB,ALPHA,BETA,GAMA,PSI,ALPHA1,BETA1,
& GAMA1,PSI1,N)
          WRITE(1,*)'*****EP,AA,BB*****'
          WRITE(1,*)EP,AA,BB
          WRITE(1,*)'*****ALPHA,BETA,GAMA,PSI*****'
          WRITE(1,*)ALPHA,BETA,GAMA,PSI
          WRITE(1,*)'*****ALPHA1,BETA1,GAMA1,PSI1*****'
          WRITE(1,*)ALPHA1,BETA1,GAMA1,PSI1
          RETURN
          END
          *****

      SUBROUTINE WR2(A,F,X,DIS,TE,DIS1,DIS2,DTE,N)
      DIMENSION A(50,50),F(50),X(50),DIS(25),TE(25),DIS1(25),
& DIS2(25),DTE(25)
          WRITE(1,*)'*****A(I,J)*****'

```

```
WRITE(1,*)((A(I,J),J=1,N),I=1,N)
  WRITE(1,*)'*****F(I)*****'
  WRITE(1,6)(F(I),I=1,N)
  WRITE(1,*)'*****X(I)*****'
  WRITE(1,6)(X(I),I=1,N)
  WRITE(1,*)'*****DIS(I),TE(I)*****'
  WRITE(1,7)(DIS(I),TE(I),I=1,N/2,1)
  WRITE(1,*)'*****DIS1(I),DIS2(I)*****'
  WRITE(1,7)(DIS1(I),DIS2(I),I=1,N/2,1)
  WRITE(1,*)'*****DTE(I)*****'
  WRITE(1,6)(DTE(I),I=1,N/2-1,1)
5 FORMAT(5(X,E12.5))
6 FORMAT(X,E12.5)
7 FORMAT(2(X,E12.5))
  RETURN
```

## APPENDIX B

### PROGRAM ELASTIC

```

C   DATE: 24.11.1995
C   THIS PROGRAM CALCULATE THE DISPLACEMENT AND ROTATIONS OF N
C   PONTOONS IN ELACTIC-CONNCTION.
      INTEGER I,J,N,P,NP,S,R,Q(25),II,III,D3,D4,H1,Q1(25)
      REAL A(50,50),F(50),X(50),DIS(25),TE(25),DTE(25),RIG(50,50),
! L,B,D,L1,T,D1,D2,H,EP,G,RO,M,ALPHA,BETA,GAMA,PSI,F1(50),
! U2(50),ALPHA1,BETA1,GAMA1,DIS1(25),DIS2(25),V(50),C,U(50),
! W(50),F2(50),C1,C2,C3,C4,W1(50),C5,C6,U3(50),F3(50),W2(50),
! O(50),O1(50),K(50,50),K1(50,50),DTE1(25),DTEF(25),DF(50),
! FT(50),AH(50,50),AG(50,50),CG(50),A1,A2,A3,A4,E1,E2,E3,E4,
! IX1,IX2,IX3,IX4,X1(50),AS(50,50),CH,ASH(50,50),AT(50,50),CE,
! KE,DTHE(25),DTHE1(25)
      CHARACTER*8 FILNAM
      PRINT*, 'INPUT FILE NAME'
      READ(*,8) FILNAM
8 FORMAT(A8)
      OPEN(UNIT=10,FILE=FILNAM,STATUS='OLD')
      READ(10,*) L
      READ(10,*) B
      READ(10,*) D
      READ(10,*) T
      READ(10,*) D1
      READ(10,*) D2
      READ(10,*) L1
      READ(10,*) H
      READ(10,*) G
      READ(10,*) RO
      PRINT*, 'ENTER NO. OF PON. NP='
      READ(*,*) NP
      EP=2*(D1-D2)/H
      AA=RO*G*L*B
      BB=RO*G*L*B*T*((T/2)+(L**2)/(12*T)-(D/2))
      ALPHA=0

```

```

      BETA=- (L+L1)/2
      GAMA=1
      PSI=- (L+L1)/2
      N=2*NP
      PRINT*, 'INPUT FILE NAME FOR F(I)'
      READ(*,8) FILNAM
      OPEN(UNIT=11,FILE=FILNAM,STATUS='OLD')
      DO 70 I=1,N
70    READ(11,*)F(I)
C     DO 75 I=1,N
C     PRINT*, 'ENTER VALUE F(I)'
C 75    READ*,F(I)
      DO 76 I=1,N
76    F(I)=G*F(I)
      CE=1
      PRINT*, 'ENTER K FOR ELASTIC-CONNECTION KE='
      READ(*,*) KE
      DO 80 I=1,N
      DO 80 J=1,N
80    AH(I,J)=0
      DO 82 I=1,N
      DO 82 J=1,N
82    AG(I,J)=0
      DO 84 I=1,N-1,2
      AH(I,I)=AA
      AH(I+1,I+1)=BB
84    CONTINUE
      DO 85 I=1,N/2-1
      AG(2*I,2*I)=CE*KE
      AG(2*I,2*I+2)=-CE*KE
      AG(2*I+2,2*I)=-CE*KE
      AG(2*I+2,2*I+2)=CE*KE
85    CONTINUE
      DO 87 I=1,N
      DO 87 J=1,N
87    AT(I,J)=AH(I,J)+AG(I,J)
      II=1

```

```

15  CALL COND (AT,F,ALPHA,BETA,GAMA,PSI,II,N)
    II=II+2
    IF(II.LE.N-3)THEN
    GO TO 15
    ELSE
    END IF
    *****

CALL GAUSS (AT,F,X,N,RIG,F1)
DO 102 I=1,N
DO 102 J=1,N
102 AT(I,J)=RIG(I,J)
    DO 107 I=1,N
107 F(I)=F1(I)
    *****
WRITE(1,*)'*****'
WRITE(1,*)((AH(I,J),J=1,N),I=1,N)
WRITE(1,*)'*****'
WRITE(1,*)((AG(I,J),J=1,N),I=1,N)
WRITE(1,*)'*****'
WRITE(1,*)((AT(I,J),J=1,N),I=1,N)
CALL WR1(EP,AA,BB,ALPHA,BETA,GAMA,PSI,ALPHA1,BETA1,GAMA1,PSI1)
CALL DEF(X,L,L1,N,DIS,TE,DIS1,DIS2,DTE)
CALL WR2(AT,F,X,DIS,TE,DIS1,DIS2,DTE,N)
CLOSE (UNIT=10)
CLOSE (UNIT=11)
WRITE(1,*)'*****END*****'
END
    *****

SUBROUTINE COND(A,F,ALPHA,BETA,GAMA,PSI,I,N)
DIMENSION A(50,50),F(50)
A(I+1,I+1)=BETA*A(I,I+1)+BETA*A(I+1,I)+A(I+1,I+1)
A(I+1,I+2)=BETA*A(I,I+2)+GAMA*A(I+1,I)+A(I+1,I+2)
A(I+1,I+3)=BETA*A(I,I+3)+PSI*A(I+1,I)+A(I+1,I+3)
A(I+2,I+1)=GAMA*A(I,I+1)+BETA*A(I+2,I)+A(I+2,I+1)
A(I+2,I+2)=GAMA*A(I,I+2)+GAMA*A(I+2,I)+A(I+2,I+2)
A(I+2,I+3)=GAMA*A(I,I+3)+PSI*A(I+2,I)+A(I+2,I+3)
A(I+3,I+1)=PSI*A(I,I+1)+BETA*A(I+3,I)+A(I+3,I+1)

```

```

A(I+3,I+2)=PSI*A(I,I+2)+GAMA*A(I+3,I)+A(I+3,I+2)
A(I+3,I+3)=PSI*A(I,I+3)+PSI*A(I+3,I)+A(I+3,I+3)
DO 40 S=1,I-1,1
A(I+1,S)=BETA*A(I,S)+A(I+1,S)
A(I+2,S)=GAMA*A(I,S)+A(I+2,S)
A(I+3,S)=PSI*A(I,S)+A(I+3,S)
A(I,S)=0
A(S,I+1)=A(I+1,S)
A(S,I+2)=A(I+2,S)
A(S,I+3)=A(I+3,S)
A(S,I)=A(I,S)
40 CONTINUE
DO 41 S=I+4,N,1
A(I+1,S)=BETA*A(I,S)+A(I+1,S)
A(I+2,S)=GAMA*A(I,S)+A(I+2,S)
A(I+3,S)=PSI*A(I,S)+A(I+3,S)
A(I,S)=0
A(S,I+1)=A(I+1,S)
A(S,I+2)=A(I+2,S)
A(S,I+3)=A(I+3,S)
A(S,I)=A(I,S)
41 CONTINUE
A(I,I+1)=BETA*A(I,I)
A(I,I+2)=GAMA*A(I,I)
A(I,I+3)=PSI*A(I,I)
A(I+1,I)=BETA*A(I,I)
A(I+2,I)=GAMA*A(I,I)
A(I+3,I)=PSI*A(I,I)
DO 42 J=I+1,I+3
42 F(I)=F(I)-ALPHA*A(J,I)
F(I+1)=BETA*F(I)+F(I+1)+ALPHA*BETA*A(I,I)
F(I+2)=GAMA*F(I)+F(I+2)+ALPHA*GAMA*A(I,I)
F(I+3)=PSI*F(I)+F(I+3)+ALPHA*PSI*A(I,I)
F(I)=-ALPHA*A(I,I)
A(I,I)=-A(I,I)
RETURN
END

```

\*\*\*\*\*

SUBROUTINE GAUSS(A,Y,X,N,RIG,F1)

DIMENSION A(50,50),Y(50),X(50),RIG(50,50),F1(50)

DO 50 I=1,N

DO 50 J=1,N

50 RIG(I,J)=A(I,J)

DO 51 I=1,N

51 F1(I)=Y(I)

DO 52 K=1,N-1

DO 53 I=K+1,N

Z=A(I,K)/A(K,K)

DO 54 J=K,N

54 A(I,J)=A(I,J)-A(K,J)\*Z

53 Y(I)=Y(I)-Y(K)\*Z

52 CONTINUE

X(N)=Y(N)/A(N,N)

DO 55 K=N-1,1,-1

SUM=Y(K)

DO 56 J=K+1,N

56 SUM=SUM-X(J)\*A(K,J)

55 X(K)=SUM/A(K,K)

RETURN

END

\*\*\*\*\*

SUBROUTINE DEF(X,Y,Z,N,DIS,TE,DIS1,DIS2,DTE)

DIMENSION X(50),DIS(25),TE(25),DIS1(25),DIS2(25),DTE(25)

DO 140 I=1,N/2

DIS(I)=X(2\*I-1)

TE(I)=X(2\*I)

140 CONTINUE

DO 150 I=1,N/2

DIS1(I)=DIS(I)-((Y+Z)/2)\*TE(I)

DIS2(I)=DIS(I)+((Y+Z)/2)\*TE(I)

150 CONTINUE

DO 155 I=1,N/2-1

DTE(I)=TE(I+1)-TE(I)

155 CONTINUE

```

RETURN
END
*****
SUBROUTINE
WR1(EP,AA,BB,ALPHA,BETA,GAMA,PSI,ALPHA1,BETA1,GAMA1,PSI1)
WRITE(1,*)*****EP,AA,BB*****'
WRITE(1,*)EP,AA,BB
WRITE(1,*)*****ALPHA,BETA,GAMA,PSI*****'
WRITE(1,*)ALPHA,BETA,GAMA,PSI
WRITE(1,*)*****ALPHA1,BETA1,GAMA1,PSI1*****'
WRITE(1,*)ALPHA1,BETA1,GAMA1,PSI1
RETURN
END
SUBROUTINE WR2(A,F,X,DIS,TE,DIS1,DIS2,DTE,N)
DIMENSION A(50,50),F(50),X(50),DIS(25),TE(25),DIS1(25),DIS2(25),DTE(25)
WRITE(1,*)*****A(I,J)*****'
WRITE(1,*)((A(I,J),J=1,N),I=1,N)
WRITE(1,*)*****F(I)*****'
WRITE(1,6)(F(I),I=1,N)
WRITE(1,*)*****X(I)*****'
WRITE(1,6)(X(I),I=1,N)
WRITE(1,*)*****DIS(I),TE(I)*****'
WRITE(1,7)(DIS(I),TE(I),I=1,N/2,1)
WRITE(1,*)*****DIS1(I),DIS2(I)*****'
WRITE(1,7)(DIS1(I),DIS2(I),I=1,N/2,1)
WRITE(1,*)*****DIS(I)*****'
WRITE(1,6)DIS1(1)
WRITE(1,6)(DIS2(I),I=1,N/2,1)
WRITE(1,*)*****DTE(I)*****'
WRITE(1,6)(DTE(I),I=1,N/2-1,1)
5 FORMAT(5(X,E12.5))
6 FORMAT(1(X,E12.5))
7 FORMAT(2(X,E12.5))
RETURN
END

```

## APPENDIX C

## PROGRAM RIGID

```

C  DATE: 6.6.1995 (RIGID)
C  THIS PROGRAM CALCULATE THE DISPLACEMENT AND ROTATIONS OF N
C  PONTTIONS IN RIGID- CONNECTION.
      INTEGER I,J,N,P,NP,R,II,Q(50)
      REAL A(50,50),F(50),X(50),DIS(50),TE(50),DTE(50),RIG(50,50),
! L,B,D,L1,T,D1,D2,H,EP,G,RO,M,ALPHA,BETA,GAMA,PSI,F1(50),
! ALPHA1,BETA1,GAMA1,DIS1(25),DIS2(25),DTE1(25)
      CHARACTER*8 FILNAM
      PRINT*, 'INPUT FILE NAME'
      READ(*,8) FILNAM
8 FORMAT(A8)
      OPEN(UNIT=10,FILE=FILNAM,STATUS='OLD')
      READ(10,*) L
      READ(10,*) B
      READ(10,*) D
      READ(10,*) T
      READ(10,*) D1
      READ(10,*) D2
      READ(10,*) L1
      READ(10,*) H
      READ(10,*) G
      READ(10,*) RO
      PRINT*, 'ENTER NO. OF PON. NP='
      READ(*,*) NP
      EP=2*2*(D1-D2)/H
      AA=RO*G*L*B
      BB=RO*G*L*B*T*((T/2)+(L**2)/(12*T)-(D/2))
      ALPHA=0
      BETA=-(L+L1)/2
      GAMA=1
      PSI=-(L+L1)/2
      ALPHA1=0
      BETA1=0

```

```

      GAMA1=1
      PSI1=0
      N=2*NP
      PRINT*, 'INPUT FILE NAME FOR F(I)'
      READ(*,8) FILNAM
      OPEN(UNIT=11,FILE=FILNAM,STATUS='OLD')
      DO 70 I=1,N
70 READ(11,*)F(I)
C      DO 75 I=1,N
C      PRINT*, 'ENTER VALUE F(I)'
C 75  READ*,F(I)
      DO 76 I=1,N
76 F(I)=F(I)*G
      DO 80 I=1,N
      DO 80 J=1,N
80 A(I,J)=0
      DO 90 I=1,N-1,2
      A(I,I)=AA
      A(I+1,I+1)=BB
90 CONTINUE
      I=1
25  CALL COND(A,F,ALPHA,BETA,GAMA,PSI,I,N)
      I=I+2
      IF(I.LE.N-3)THEN
      GO TO 25
      ELSE
      END IF
      I=2
26  CALL COND(A,F,ALPHA1,BETA1,GAMA1,PSI1,I,N)
      I=I+2
      IF(I.LE.N-2)THEN
      GO TO 26
      ELSE
      END IF
      CALL GAUSS(A,F,X,N,RIG,F1)
      DO 100 I=1,N
      DO 100 J=1,N

```

```

100 A(I,J)=RIG(I,J)
      DO 105 I=1,N
105 F(I)=F1(I)
      CALL WR1(EP,AA,BB,ALPHA,BETA,GAMA,PSI,ALPHA1,BETA1,GAMA1,PSI1,N)
35   CALL DEF(X,L,L1,N,DIS,TE,DIS1,DIS2,DTE)
      CLOSE (UNIT=10)
CLOSE (UNIT=11)
      CALL WR2(A,F,X,DIS,TE,DIS1,DIS2,DTE,N)
      WRITE(1,*)'*****END*****'
      END
      SUBROUTINE COND(A,F,ALPHA,BETA,GAMA,PSI,I,N)
      DIMENSION A(50,50),F(50)
      A(I+1,I+1)=BETA*A(I,I+1)+BETA*A(I+1,I)+A(I+1,I+1)
      A(I+1,I+2)=BETA*A(I,I+2)+GAMA*A(I+1,I)+A(I+1,I+2)
      A(I+1,I+3)=BETA*A(I,I+3)+PSI*A(I+1,I)+A(I+1,I+3)
      A(I+2,I+1)=GAMA*A(I,I+1)+BETA*A(I+2,I)+A(I+2,I+1)
      A(I+2,I+2)=GAMA*A(I,I+2)+GAMA*A(I+2,I)+A(I+2,I+2)
      A(I+2,I+3)=GAMA*A(I,I+3)+PSI*A(I+2,I)+A(I+2,I+3)
      A(I+3,I+1)=PSI*A(I,I+1)+BETA*A(I+3,I)+A(I+3,I+1)
      A(I+3,I+2)=PSI*A(I,I+2)+GAMA*A(I+3,I)+A(I+3,I+2)
      A(I+3,I+3)=PSI*A(I,I+3)+PSI*A(I+3,I)+A(I+3,I+3)
      DO 40 S=1,I-1,1
      A(I+1,S)=BETA*A(I,S)+A(I+1,S)
      A(I+2,S)=GAMA*A(I,S)+A(I+2,S)
      A(I+3,S)=PSI*A(I,S)+A(I+3,S)
      A(I,S)=0
      A(S,I+1)=A(I+1,S)
      A(S,I+2)=A(I+2,S)
      A(S,I+3)=A(I+3,S)
      A(S,I)=A(I,S)
40 CONTINUE
      DO 41 S=I+4,N,1
      A(I+1,S)=BETA*A(I,S)+A(I+1,S)
      A(I+2,S)=GAMA*A(I,S)+A(I+2,S)
      A(I+3,S)=PSI*A(I,S)+A(I+3,S)
      A(I,S)=0
      A(S,I+1)=A(I+1,S)

```

```

A(S,I+2)=A(I+2,S)
A(S,I+3)=A(I+3,S)
A(S,I)=A(I,S)
41 CONTINUE
A(I,I+1)=BETA*A(I,I)
A(I,I+2)=GAMA*A(I,I)
A(I,I+3)=PSI*A(I,I)
A(I+1,I)=BETA*A(I,I)
A(I+2,I)=GAMA*A(I,I)
A(I+3,I)=PSI*A(I,I)
DO 42 J=I+1,I+3
42 F(I)=F(I)-ALPHA*A(J,I)
F(I+1)=BETA*F(I)+F(I+1)+ALPHA*BETA*A(I,I)
F(I+2)=GAMA*F(I)+F(I+2)+ALPHA*GAMA*A(I,I)
F(I+3)=PSI*F(I)+F(I+3)+ALPHA*PSI*A(I,I)
F(I)=-ALPHA*A(I,I)
A(I,I)=-A(I,I)
RETURN
END
*****
SUBROUTINE GAUSS(A,Y,X,N,RIG,F1)
DIMENSION A(50,50),Y(50),X(50),RIG(50,50),F1(50)
DO 50 I=1,N
DO 50 J=1,N
50 RIG(I,J)=A(I,J)
DO 51 I=1,N
51 F1(I)=Y(I)
DO 52 K=1,N-1
DO 53 I=K+1,N
Z=A(I,K)/A(K,K)
DO 54 J=K,N
54 A(I,J)=A(I,J)-A(K,J)*Z
53 Y(I)=Y(I)-Y(K)*Z
52 CONTINUE
X(N)=Y(N)/A(N,N)
DO 55 K=N-1,1,-1
SUM=Y(K)

```

```

      DO 56 J=K+1,N
56 SUM=SUM-X(J)*A(K,J)
55 X(K)=SUM/A(K,K)
      RETURN
      END
      *****

      SUBROUTINE DEF(X,Y,Z,N,DIS,TE,DIS1,DIS2,DTE)
      DIMENSION X(50),DIS(25),TE(25),DIS1(25),DIS2(25),DTE(25)
      DO 140 I=1,N/2
          DIS(I)=X(2*I-1)
          TE(I)=X(2*I)
140 CONTINUE
          DO 150 I=1,N/2
              DIS1(I)=DIS(I)-((Y+Z)/2)*TE(I)
              DIS2(I)=DIS(I)+((Y+Z)/2)*TE(I)
150 CONTINUE
          DO 155 I=1,N/2-1
              DTE(I)=TE(I+1)-TE(I)
155 CONTINUE
          RETURN
          END
          *****

      SUBROUTINE MAX(X,N,M,P,Q)
      DIMENSION X(50),DTE1(25),Q(50)
      INTEGER P,Q
      REAL M
      M=-100
      DO 160 I=1,N/2-1
7      DTE1(I)=ABS(X(I))
          IF (DTE1(I).GT.M) THEN
              M=DTE1(I)
          ELSE
              END IF
160 CONTINUE
          II=0
          DO 161 I=1,N/2-1
              IF (INT(100000*ABS(X(I))).EQ.INT(100000*M)) THEN

```

```

II=II+1
Q(II)=I
END IF
161 CONTINUE
P=II
WRITE(1,*)P
WRITE(1,*)(Q(I),I=1,P)
RETURN
END
SUBROUTINE WR1(EP,AA,BB,ALPHA,BETA,GAMA,PSI,ALPHA1,BETA1,GAMA1,PSI1,N)
WRITE(1,*)'*****EP,AA,BB*****'
WRITE(1,*)EP,AA,BB
WRITE(1,*)'*****ALPHA,BETA,GAMA,PSI*****'
WRITE(1,*)ALPHA,BETA,GAMA,PSI
WRITE(1,*)'*****ALPHA1,BETA1,GAMA1,PSI1*****'
WRITE(1,*)ALPHA1,BETA1,GAMA1,PSI1
RETURN
END
SUBROUTINE WR2(A,F,X,DIS,TE,DIS1,DIS2,DTE,N)
DIMENSION A(50,50),F(50),X(50),DIS(25),TE(25),DIS1(25),DIS2(25),DTE(25)
WRITE(1,*)'*****A(I,J)*****'
WRITE(1,*)((A(I,J),J=1,N),I=1,N)
WRITE(1,*)'*****F(I)*****'
WRITE(1,6)(F(I),I=1,N)
WRITE(1,*)'*****X(I)*****'
WRITE(1,6)(X(I),I=1,N)
WRITE(1,*)'*****DIS(I),TE(I)*****'
WRITE(1,7)(DIS(I),TE(I),I=1,N/2,1)
WRITE(1,*)'*****DIS1(I),DIS2(I)*****'
WRITE(1,7)(DIS1(I),DIS2(I),I=1,N/2,1)
WRITE(1,*)'*****DTE(I)*****'
WRITE(1,6)(DTE(I),I=1,N/2-1,1)
5 FORMAT(5(X,E12.5))
6 FORMAT(X,E12.5)
7 FORMAT(2(X,E12.5))
RETURN
END

```

**APPENDIX D****PROGRAM RIGID1**

```

C  DATE: 17.8.1995
C
C  THIS PROGRAM IS FOR HINGE-RIGID CONNECTION IN ONE DIRECTION.
C
      INTEGER I,J,N,P,NP,S,R,Q(25),III,II,D3,D4,H1,Q1(25)
      REAL A(50,50),F(50),X(50),DIS(25),TE(25),DTE(25),RIG(50,50),
! L,B,D,L1,T,D1,D2,H,EP,G,RO,M,ALPHA,BETA,GAMA,PSI,F1(50),
! U2(50),ALPHA1,BETA1,GAMA1,DIS1(25),DIS2(25),V(50),C,U(50),
! W(50),F2(50),C1,C2,C3,C4,W1(50),A1(50,50),U1(50),E(50,50),
! E1(50,50),C5,C6,U3(50),F3(50),A2(50,50),E2(50,50),A3(50,50),
! W2(50),O(50),O1(50),K(50,50),K1(50,50),DTE1(25),DTEF(25),
! DF(50),FT(50)
      CHARACTER*8 FILNAM
      PRINT*, 'INPUT FILE NAME'
      READ(*,8) FILNAM
8 FORMAT(A8)
      OPEN(UNIT=10,FILE=FILNAM,STATUS='OLD')
      READ(10,*) L
      READ(10,*) B
      READ(10,*) D
      READ(10,*) T
      READ(10,*) D1
      READ(10,*) D2
      READ(10,*) L1
      READ(10,*) H
      READ(10,*) G
      READ(10,*) RO
      PRINT*, 'ENTER NO. OF PON. NP='
      READ(*,*) NP
      EP=2*(D1-D2)/H
      AA=RO*L*B
      BB=RO*L*B*T*((T/2)+(L**2)/(12*T)-(D/2))
      ALPHA=0

```

```

      BETA=-(L+L1)/2
      GAMA=1
      PSI=-(L+L1)/2
      ALPHA1=EP
      BETA1=0
      GAMA1=1
      PSI1=0
N=2*NP
      PRINT*,INPUT FILE NAME FOR V(I)'
      READ(*,8) FILNAM
      OPEN(UNIT=11,FILE=FILNAM,STATUS='OLD')
      DO 70 I=1,N
70    READ(11,*)V(I)
C     DO 75 I=1,N
C     PRINT*,ENTER VALUE V(I)'
C 75  READ*,V(I)
C     DO 76 I=1,N
C 76  V(I)=V(I)*G
      DO 80 I=1,N
      DO 80 J=1,N
80  A(I,J)=0
      DO 90 I=1,N-1,2
      A(I,I)=AA
      A(I+1,I+1)=BB
90  CONTINUE
      *****
      DO 192 I=1,N
      DO 192 J=1,N
192  E(I,J)=A(I,J)
      DO 193 I=1,N
      DO 193 J=1,N
193  K(I,J)=A(I,J)
C     DO 91 III=1,N
      III=9
      IF (V(III).NE.0)THEN
          U(III)=(V(III)/ABS(V(III)))*1
          F(III)=U(III)

```

```

        END IF
        U1(III)=U(III)
        DF(III)=F(III)*1
        F2(III)=F(III)
        F3(III)=F(III)
        WRITE(1,*)U1(III)
        *****
II=1
15  CALL COND(E,U1,ALPHA,BETA,GAMA,PSI,II,N)
    II=II+2
    IF(II.LE.N-3)THEN
    GO TO 15
    ELSE
    END IF
    CALL GAUSS(E,U1,X,N,RIG,U2)
    DO 102 I=1,N
    DO 102 J=1,N
102  E1(I,J)=RIG(I,J)
    DO 107 I=1,N
107  U1(I)=U2(I)
    CALL DEF(X,L,L1,N,DIS,TE,DIS1,DIS2,DTE)
C   CALL WR2(E,U1,X,DIS,TE,DIS1,DIS2,DTE,N)
    *****

        C3=MOD(III,2)
        WRITE(1,*)C3
        WRITE(1,*)EP
            IF (C3.EQ.1)THEN
                D3=(III-1)/2
                D4=(III+1)/2
            ELSE
                D3=(III-2)/2
                D4=(III)/2
        END IF
        C1=EP/DTE(D3)
        C2=EP/DTE(D4)
            IF (ABS(C1).GT.ABS(C2))THEN
                C=C1

```

```

                ELSE
                C=C2
            END IF
        WRITE(1,*)C1,C2,C
        *****
        S=0
44 II=1
25  CALL COND(K,F,ALPHA,BETA,GAMA,PSI,II,N)
    II=II+2
    IF(II.LE.N-3)THEN
        GO TO 25
    ELSE
        END IF
    CALL GAUSS(K,F,X,N,RIG,F1)
    DO 101 I=1,N
    DO 101 J=1,N
101 K(I,J)=RIG(I,J)
    DO 106 I=1,N
106 F(I)=F1(I)
    CALL DEF(X,L,L1,N,DIS,TE,DIS1,DIS2,DTE)
C    CALL WR2(K,F,X,DIS,TE,DIS1,DIS2,DTE,N)
    *****
88  IF (C.GT.0)THEN
    ALPHA1=-EP
        CALL MAXS(DTE,N,M,P,Q,EP)
    ELSE
        ALPHA1=EP
    CALL MINM(DTE,N,M,P,Q,EP)
    END IF
    IF (M.GE.EP)THEN
WRITE(1,*)F3(III)
        GO TO 77
    ELSE
        GO TO 67
    END IF
77  DO 693 I=1,N
    DO 693 J=1,N

```

```

693  K1(I,J)=K(I,J)
      DO 113 I=1,N
113  FT(I)=F(I)
      DO 97 I=1,P
      R=2*Q(I)
      CALL COND(K1,FT,ALPHA1,BETA1,GAMA1,PSI1,R,N)
97   CONTINUE
      CALL GAUSS(K1,FT,X,N,RIG,F1)
      DO 401 I=1,N
      DO 401 J=1,N
401  K1(I,J)=RIG(I,J)
      DO 406 I=1,N
406  FT(I)=F1(I)
      CALL DEF(X,L,L1,N,DIS,TE,DIS1,DIS2,DTE)
C    CALL WR2(K1,FT,X,DIS,TE,DIS1,DIS2,DTE,N)
      GO TO 88
67   IF (ABS(F3(III)).GE.ABS(V(III)))THEN
      WRITE(1,*)F3(III)
      GO TO 66
      ELSE
      END IF
      GO TO 87
*****
87   DO 593 I=1,N
      DO 593 J=1,N
593  K(I,J)=A(I,J)
      DO 13 I=1,N
13  F(I)=0
      F(III)=F2(III)+S*DF(III)
      F3(III)=F(III)
      S=S+1
      WRITE(1,*)F(III)
      GO TO 44
*****
66   CLOSE (UNIT=10)
      CLOSE (UNIT=11)
      CALL WR1(EP,AA,BB,ALPHA,BETA,GAMA,PSI,ALPHA1,BETA1,GAMA1,PSI1)

```

```

CALL WR2(K,F,X,DIS,TE,DIS1,DIS2,DTE,N)
WRITE(1,*)'*****END*****'
END
*****
SUBROUTINE COND(A,F,ALPHA,BETA,GAMA,PSI,I,N)
DIMENSION A(50,50),F(50)
A(I+1,I+1)=BETA*A(I,I+1)+BETA*A(I+1,I)+A(I+1,I+1)
A(I+1,I+2)=BETA*A(I,I+2)+GAMA*A(I+1,I)+A(I+1,I+2)
A(I+1,I+3)=BETA*A(I,I+3)+PSI*A(I+1,I)+A(I+1,I+3)
A(I+2,I+1)=GAMA*A(I,I+1)+BETA*A(I+2,I)+A(I+2,I+1)
A(I+2,I+2)=GAMA*A(I,I+2)+GAMA*A(I+2,I)+A(I+2,I+2)
A(I+2,I+3)=GAMA*A(I,I+3)+PSI*A(I+2,I)+A(I+2,I+3)
A(I+3,I+1)=PSI*A(I,I+1)+BETA*A(I+3,I)+A(I+3,I+1)
A(I+3,I+2)=PSI*A(I,I+2)+GAMA*A(I+3,I)+A(I+3,I+2)
A(I+3,I+3)=PSI*A(I,I+3)+PSI*A(I+3,I)+A(I+3,I+3)
DO 40 S=1,I-1,1
A(I+1,S)=BETA*A(I,S)+A(I+1,S)
A(I+2,S)=GAMA*A(I,S)+A(I+2,S)
A(I+3,S)=PSI*A(I,S)+A(I+3,S)
A(I,S)=0
40 CONTINUE
DO 41 S=I+4,N,1
A(I+1,S)=BETA*A(I,S)+A(I+1,S)
A(I+2,S)=GAMA*A(I,S)+A(I+2,S)
A(I+3,S)=PSI*A(I,S)+A(I+3,S)
A(I,S)=0
41 CONTINUE
A(I,I+1)=BETA*A(I,I)
A(I,I+2)=GAMA*A(I,I)
A(I,I+3)=PSI*A(I,I)
A(I+1,I)=BETA*A(I,I)
A(I+2,I)=GAMA*A(I,I)
A(I+3,I)=PSI*A(I,I)
DO 42 J=I+1,I+3
42 F(I)=F(I)-ALPHA*A(J,I)
F(I+1)=BETA*F(I)+F(I+1)+ALPHA*BETA*A(I,I)
F(I+2)=GAMA*F(I)+F(I+2)+ALPHA*GAMA*A(I,I)

```

```
F(I+3)=PSI*F(I)+F(I+3)+ALPHA*PSI*A(I,I)
```

```
F(I)=-ALPHA*A(I,I)
```

```
A(I,I)=-A(I,I)
```

```
RETURN
```

```
END
```

```
*****
```

```
SUBROUTINE GAUSS(A,Y,X,N,RIG,F1)
```

```
DIMENSION A(50,50),Y(50),X(50),RIG(50,50),F1(50)
```

```
DO 50 I=1,N
```

```
DO 50 J=1,N
```

```
50 RIG(I,J)=A(I,J)
```

```
DO 51 I=1,N
```

```
51 F1(I)=Y(I)
```

```
DO 52 K=1,N-1
```

```
DO 53 I=K+1,N
```

```
Z=A(I,K)/A(K,K)
```

```
DO 54 J=K,N
```

```
54 A(I,J)=A(I,J)-A(K,J)*Z
```

```
53 Y(I)=Y(I)-Y(K)*Z
```

```
52 CONTINUE
```

```
X(N)=Y(N)/A(N,N)
```

```
DO 55 K=N-1,1,-1
```

```
SUM=Y(K)
```

```
DO 56 J=K+1,N
```

```
56 SUM=SUM-X(J)*A(K,J)
```

```
55 X(K)=SUM/A(K,K)
```

```
RETURN
```

```
END
```

```
*****
```

```
SUBROUTINE DEF(X,Y,Z,N,DIS,TE,DIS1,DIS2,DTE)
```

```
DIMENSION X(50),DIS(25),TE(25),DIS1(25),DIS2(25),DTE(25)
```

```
DO 140 I=1,N/2
```

```
DIS(I)=X(2*I-1)
```

```
TE(I)=X(2*I)
```

```
140 CONTINUE
```

```
DO 150 I=1,N/2
```

```
DIS1(I)=DIS(I)-((Y+Z)/2)*TE(I)
```

```

DIS2(I)=DIS(I)+((Y+Z)/2)*TE(I)
150 CONTINUE
DO 155 I=1,N/2-1
DTE(I)=TE(I+1)-TE(I)
155 CONTINUE
RETURN
END
*****

SUBROUTINE MAXS(X,N,M,P,Q,EP)
DIMENSION X(50),Q(50)
INTEGER P,Q
REAL M,EP
M=-100
DO 160 I=1,N/2-1
IF (X(I).GT.M.AND.INT(1E6*X(I)).NE.INT(1E6*EP))THEN
M=X(I)
ELSE
END IF
160 CONTINUE
II=0
DO 161 I=1,N/2-1
IF (INT(1E6*X(I)).EQ.INT(1E6*M)
!.OR.INT(1E6*X(I)).EQ.ABS(INT(1E6*EP)))THEN
II=II+1
Q(II)=I
END IF
161 CONTINUE
P=II
WRITE(1,*)P
WRITE(1,*)(Q(I),I=1,P)
RETURN
END
*****

SUBROUTINE MINM(X,N,M,P,Q,EP)
DIMENSION X(50),Q(50)
INTEGER P,Q
REAL M,EP

```

```

M=100
DO 160 I=1,N/2-1
IF (X(I).LT.M.AND.INT(1E6*X(I)).NE.INT(1E6*EP))THEN
M=X(I)
ELSE
END IF
160 CONTINUE
II=0
DO 161 I=1,N/2-1
IF (INT(1E6*X(I)).EQ.INT(1E6*M)
!.OR.INT(1E6*X(I)).EQ.INT(1E6*EP)
!.OR.INT(1E6*X(I)).EQ.INT(-1E6*EP))THEN
II=II+1
Q(II)=I
END IF
161 CONTINUE
P=II
WRITE(1,*)P
WRITE(1,*)(Q(I),I=1,P)
RETURN
END
*****
SUBROUTINE
WR1(EP,AA,BB,ALPHA,BETA,GAMA,PSI,ALPHA1,BETA1,GAMA1,PSI1)
WRITE(1,*)'*****EP,AA,BB*****'
WRITE(1,*)EP,AA,BB
WRITE(1,*)'*****ALPHA,BETA,GAMA,PSI*****'
WRITE(1,*)ALPHA,BETA,GAMA,PSI
WRITE(1,*)'*****ALPHA1,BETA1,GAMA1,PSI1*****'
WRITE(1,*)ALPHA1,BETA1,GAMA1,PSI1
RETURN
END
*****
SUBROUTINE WR2(A,F,X,DIS,TE,DIS1,DIS2,DTE,N)
DIMENSION A(50,50),F(50),X(50),DIS(25),TE(25),DIS1(25),DIS2(25),DTE(25)
WRITE(1,*)'*****A(I,J)*****'
C WRITE(1,*)((A(I,J),J=1,N),I=1,N)

```

```

WRITE(1,*)'*****F(I)*****'
WRITE(1,6)(F(I),I=1,N)
WRITE(1,*)'*****X(I)*****'
WRITE(1,6)(X(I),I=1,N)
WRITE(1,*)'*****DIS(I),TE(I)*****'
WRITE(1,7)(DIS(I),TE(I),I=1,N/2,1)
WRITE(1,*)'*****DIS1(I),DIS2(I)*****'
WRITE(1,7)(DIS1(I),DIS2(I),I=1,N/2,1)
WRITE(1,*)'*****DIS(I)*****'
WRITE(1,6)DIS1(1)
WRITE(1,6)(DIS2(I),I=1,N/2,1)
WRITE(1,*)'*****DTE(I)*****'
WRITE(1,6)(DTE(I),I=1,N/2-1,1)
5 FORMAT(5(X,E12.5))
6 FORMAT(1(X,E12.5))
7 FORMAT(2(X,E12.5))
RETURN
END

```

## APPENDIX E

## PROGRAM RIGID2

```

C   DATE: 17.8.1995
C
C   THIS PROGRAM IS FOR HINGE-RIGID CONNECTION IN TWO DIRECTION.
C
      INTEGER I,J,N,P,NP,S,R,Q(25),III,II,D3,D4,H1,Q1(25)
      REAL A(50,50),F(50),X(50),DIS(25),TE(25),DTE(25),RIG(50,50),
! L,B,D,L1,T,D1,D2,H,EP,G,RO,M,ALPHA,BETA,GAMA,PSI,F1(50),
! U2(50),ALPHA1,BETA1,GAMA1,DIS1(25),DIS2(25),V(50),C,U(50),
! W(50),F2(50),C1,C2,C3,C4,W1(50),A1(50,50),U1(50),E(50,50),
! E1(50,50),C5,C6,U3(50),F3(50),A2(50,50),E2(50,50),A3(50,50),
! W2(50),O(50),O1(50),K(50,50),K1(50,50),DTE1(25),DTEF(25),
! DF(50),FT(50)
      CHARACTER*8 FILNAM
      PRINT*, 'INPUT FILE NAME'
      READ(*,8) FILNAM
8 FORMAT(A8)
      OPEN(UNIT=10,FILE=FILNAM,STATUS='OLD')
      READ(10,*) L
      READ(10,*) B
      READ(10,*) D
      READ(10,*) T
      READ(10,*) D1
      READ(10,*) D2
      READ(10,*) L1
      READ(10,*) H
      READ(10,*) G
      READ(10,*) RO
      PRINT*, 'ENTER NO. OF PON. NP='
      READ(*,*) NP
      EP=2*(D1-D2)/H
      AA=RO*L*B
      BB=RO*L*B*T*((T/2)+(L**2)/(12*T)-(D/2))

```

```

ALPHA=0
BETA=-((L+L1)/2)
GAMA=1
PSI=-((L+L1)/2)
ALPHA1=EP
BETA1=0
GAMA1=1
PSI1=0
N=2*NP
PRINT*, 'INPUT FILE NAME FOR V(I)'
READ(*,8) FILNAM
OPEN(UNIT=11,FILE=FILNAM,STATUS='OLD')
DO 70 I=1,N
70 READ(11,*)V(I)
C DO 75 I=1,N
C PRINT*, 'ENTER VALUE V(I)'
C 75 READ*,V(I)
C DO 76 I=1,N
C 76 V(I)=V(I)*G
DO 80 I=1,N
DO 80 J=1,N
80 A(I,J)=0
DO 90 I=1,N-1,2
A(I,I)=AA
A(I+1,I+1)=BB
90 CONTINUE
*****
DO 192 I=1,N
DO 192 J=1,N
192 E(I,J)=A(I,J)
DO 193 I=1,N
DO 193 J=1,N
193 K(I,J)=A(I,J)
C DO 91 III=1,N
III=9
IF (V(III).NE.0)THEN
U(III)=(V(III)/ABS(V(III)))*1

```

```

        F(III)=U(III)
        END IF
    U1(III)=U(III)
    DF(III)=F(III)*1
    F2(III)=F(III)
    F3(III)=F(III)
    WRITE(1,*)U1(III)
    *****

    II=1
15  CALL COND(E,U1,ALPHA,BETA,GAMA,PSI,II,N)
    II=II+2
    IF(II.LE.N-3)THEN
    GO TO 15
    ELSE
    END IF
    CALL GAUSS(E,U1,X,N,RIG,U2)
    DO 102 I=1,N
    DO 102 J=1,N
102 E1(I,J)=RIG(I,J)
    DO 107 I=1,N
107 U1(I)=U2(I)
    CALL DEF(X,L,L1,N,DIS,TE,DIS1,DIS2,DTE)
C   CALL WR2(E,U1,X,DIS,TE,DIS1,DIS2,DTE,N)
    *****

        C3=MOD(III,2)
        WRITE(1,*)C3
        WRITE(1,*)EP
            IF (C3.EQ.1)THEN
                D3=(III-1)/2
                D4=(III+1)/2
            ELSE
                D3=(III-2)/2
                D4=(III)/2
        END IF
        C1=EP/DTE(D3)
        C2=EP/DTE(D4)
            IF (ABS(C1).GT.ABS(C2))THEN

```

```

        C=C1
        ELSE
        C=C2
    END IF
WRITE(1,*)C1,C2,C
*****
S=0
44 II=1
25  CALL COND(K,F,ALPHA,BETA,GAMA,PSI,II,N)
    II=II+2
    IF(II.LE.N-3)THEN
    GO TO 25
    ELSE
    END IF
    CALL GAUSS(K,F,X,N,RIG,F1)
DO 101 I=1,N
DO 101 J=1,N
101 K(I,J)=RIG(I,J)
    DO 106 I=1,N
106 F(I)=F1(I)
    CALL DEF(X,L,L1,N,DIS,TE,DIS1,DIS2,DTE)
C    CALL WR2(K,F,X,DIS,TE,DIS1,DIS2,DTE,N)
*****
88  IF (C.GT.0)THEN
    ALPHA1=-EP
        CALL MAXS(DTE,N,M,P,Q,EP)
        ELSE
        ALPHA1=EP
    CALL MINM(DTE,N,M,P,Q,EP)
    END IF
    IF (M.GE.EP)THEN
WRITE(1,*)F3(III)
        GO TO 77
        ELSE
        GO TO 67
        END IF
77  DO 693 I=1,N

```

```

        DO 693 J=1,N
693   K1(I,J)=K(I,J)
        DO 113 I=1,N
113  FT(I)=F(I)
            DO 97 I=1,P
            R=2*Q(I)
            CALL COND(K1,FT,ALPHA1,BETA1,GAMA1,PSI1,R,N)
97   CONTINUE
        CALL GAUSS(K1,FT,X,N,RIG,F1)
        DO 401 I=1,N
        DO 401 J=1,N
401  K1(I,J)=RIG(I,J)
        DO 406 I=1,N
406  FT(I)=F1(I)
        CALL DEF(X,L,L1,N,DIS,TE,DIS1,DIS2,DTE)
C    CALL WR2(K1,FT,X,DIS,TE,DIS1,DIS2,DTE,N)
        GO TO 88
67   IF (ABS(F3(III)).GE.ABS(V(III)))THEN
        WRITE(1,*)F3(III)
        GO TO 66
        ELSE
        END IF
        GO TO 87
        *****
87   DO 593 I=1,N
        DO 593 J=1,N
593  K(I,J)=A(I,J)
        DO 13 I=1,N
13  F(I)=0
        F(III)=F2(III)+S*DF(III)
        F3(III)=F(III)
        S=S+1
        WRITE(1,*)F(III)
        GO TO 44
        *****
66   CLOSE (UNIT=10)
        CLOSE (UNIT=11)

```

```
CALL WR1(EP,AA,BB,ALPHA,BETA,GAMA,PSI,ALPHA1,BETA1,GAMA1,PSI1)
```

```
CALL WR2(K,F,X,DIS,TE,DIS1,DIS2,DTE,N)
```

```
WRITE(1,*)'*****END*****'
```

```
END
```

```
*****
```

```
SUBROUTINE COND(A,F,ALPHA,BETA,GAMA,PSI,I,N)
```

```
DIMENSION A(50,50),F(50)
```

```
A(I+1,I+1)=BETA*A(I,I+1)+BETA*A(I+1,I)+A(I+1,I+1)
```

```
A(I+1,I+2)=BETA*A(I,I+2)+GAMA*A(I+1,I)+A(I+1,I+2)
```

```
A(I+1,I+3)=BETA*A(I,I+3)+PSI*A(I+1,I)+A(I+1,I+3)
```

```
A(I+2,I+1)=GAMA*A(I,I+1)+BETA*A(I+2,I)+A(I+2,I+1)
```

```
A(I+2,I+2)=GAMA*A(I,I+2)+GAMA*A(I+2,I)+A(I+2,I+2)
```

```
A(I+2,I+3)=GAMA*A(I,I+3)+PSI*A(I+2,I)+A(I+2,I+3)
```

```
A(I+3,I+1)=PSI*A(I,I+1)+BETA*A(I+3,I)+A(I+3,I+1)
```

```
A(I+3,I+2)=PSI*A(I,I+2)+GAMA*A(I+3,I)+A(I+3,I+2)
```

```
A(I+3,I+3)=PSI*A(I,I+3)+PSI*A(I+3,I)+A(I+3,I+3)
```

```
DO 40 S=1,I-1,1
```

```
A(I+1,S)=BETA*A(I,S)+A(I+1,S)
```

```
A(I+2,S)=GAMA*A(I,S)+A(I+2,S)
```

```
A(I+3,S)=PSI*A(I,S)+A(I+3,S)
```

```
A(I,S)=0
```

```
40 CONTINUE
```

```
DO 41 S=I+4,N,1
```

```
A(I+1,S)=BETA*A(I,S)+A(I+1,S)
```

```
A(I+2,S)=GAMA*A(I,S)+A(I+2,S)
```

```
A(I+3,S)=PSI*A(I,S)+A(I+3,S)
```

```
A(I,S)=0
```

```
41 CONTINUE
```

```
A(I,I+1)=BETA*A(I,I)
```

```
A(I,I+2)=GAMA*A(I,I)
```

```
A(I,I+3)=PSI*A(I,I)
```

```
A(I+1,I)=BETA*A(I,I)
```

```
A(I+2,I)=GAMA*A(I,I)
```

```
A(I+3,I)=PSI*A(I,I)
```

```
DO 42 J=I+1,I+3
```

```
42 F(I)=F(I)-ALPHA*A(J,I)
```

```
F(I+1)=BETA*F(I)+F(I+1)+ALPHA*BETA*A(I,I)
```

```
F(I+2)=GAMA*F(I)+F(I+2)+ALPHA*GAMA*A(I,I)
```

```
F(I+3)=PSI*F(I)+F(I+3)+ALPHA*PSI*A(I,I)
```

```
F(I)=-ALPHA*A(I,I)
```

```
A(I,I)=-A(I,I)
```

```
RETURN
```

```
END
```

```
*****
```

```
SUBROUTINE GAUSS(A,Y,X,N,RIG,F1)
```

```
DIMENSION A(50,50),Y(50),X(50),RIG(50,50),F1(50)
```

```
DO 50 I=1,N
```

```
DO 50 J=1,N
```

```
50 RIG(I,J)=A(I,J)
```

```
DO 51 I=1,N
```

```
51 F1(I)=Y(I)
```

```
DO 52 K=1,N-1
```

```
DO 53 I=K+1,N
```

```
Z=A(I,K)/A(K,K)
```

```
DO 54 J=K,N
```

```
54 A(I,J)=A(I,J)-A(K,J)*Z
```

```
53 Y(I)=Y(I)-Y(K)*Z
```

```
52 CONTINUE
```

```
X(N)=Y(N)/A(N,N)
```

```
DO 55 K=N-1,1,-1
```

```
SUM=Y(K)
```

```
DO 56 J=K+1,N
```

```
56 SUM=SUM-X(J)*A(K,J)
```

```
55 X(K)=SUM/A(K,K)
```

```
RETURN
```

```
END
```

```
*****
```

```
SUBROUTINE DEF(X,Y,Z,N,DIS,TE,DIS1,DIS2,DTE)
```

```
DIMENSION X(50),DIS(25),TE(25),DIS1(25),DIS2(25),DTE(25)
```

```
DO 140 I=1,N/2
```

```
DIS(I)=X(2*I-1)
```

```
TE(I)=X(2*I)
```

```
140 CONTINUE
```

```
DO 150 I=1,N/2
```

```

DIS1(I)=DIS(I)-((Y+Z)/2)*TE(I)
DIS2(I)=DIS(I)+((Y+Z)/2)*TE(I)
150 CONTINUE
DO 155 I=1,N/2-1
DTE(I)=TE(I+1)-TE(I)
155 CONTINUE
RETURN
END
*****
SUBROUTINE MAXS(X,N,M,P,Q,EP)
DIMENSION X(50),Q(50)
INTEGER P,Q
REAL M,EP
M=-100
DO 160 I=1,N/2-1
IF (X(I).GT.M.AND.INT(1E6*X(I)).NE.INT(1E6*EP))THEN
M=X(I)
ELSE
END IF
160 CONTINUE
II=0
DO 161 I=1,N/2-1
IF (INT(1E6*X(I)).EQ.INT(1E6*M)
! .OR.INT(1E6*X(I)).EQ.ABS(INT(1E6*EP)))THEN
II=II+1
Q(II)=I
END IF
161 CONTINUE
P=II
WRITE(1,*)P
WRITE(1,*)(Q(I),I=1,P)
RETURN
END
*****
SUBROUTINE MINM(X,N,M,P,Q,EP)
DIMENSION X(50),Q(50)
INTEGER P,Q

```

```

REAL M,EP
M=100
DO 160 I=1,N/2-1
IF (X(I).LT.M.AND.INT(1E6*X(I)).NE.INT(1E6*EP))THEN
M=X(I)
ELSE
END IF
160 CONTINUE
II=0
DO 161 I=1,N/2-1
IF (INT(1E6*X(I)).EQ.INT(1E6*M)
! .OR.INT(1E6*X(I)).EQ.INT(1E6*EP)
! .OR.INT(1E6*X(I)).EQ.INT(-1E6*EP))THEN
II=II+1
Q(II)=I
END IF
161 CONTINUE
P=II
WRITE(1,*)P
WRITE(1,*)(Q(I),I=1,P)
RETURN
END
*****
SUBROUTINE
WR1(EP,AA,BB,ALPHA,BETA,GAMA,PSI,ALPHA1,BETA1,GAMA1,PSI1)
WRITE(1,*)'*****EP,AA,BB*****'
WRITE(1,*)EP,AA,BB
WRITE(1,*)'*****ALPHA,BETA,GAMA,PSI*****'
WRITE(1,*)ALPHA,BETA,GAMA,PSI
WRITE(1,*)'*****ALPHA1,BETA1,GAMA1,PSI1*****'
WRITE(1,*)ALPHA1,BETA1,GAMA1,PSI1
RETURN
END
*****
SUBROUTINE WR2(A,F,X,DIS,TE,DIS1,DIS2,DTE,N)
DIMENSION A(50,50),F(50),X(50),DIS(25),TE(25),DIS1(25),DIS2(25),DTE(25)
WRITE(1,*)'*****A(I,J)*****'

```

```

C  WRITE(1,*)((A(I,J),J=1,N),I=1,N)
    WRITE(1,*)'*****F(I)*****'
    WRITE(1,6)(F(I),I=1,N)
    WRITE(1,*)'*****X(I)*****'
    WRITE(1,6)(X(I),I=1,N)
    WRITE(1,*)'*****DIS(I),TE(I)*****'
    WRITE(1,7)(DIS(I),TE(I),I=1,N/2,1)
    WRITE(1,*)'*****DIS1(I),DIS2(I)*****'
    WRITE(1,7)(DIS1(I),DIS2(I),I=1,N/2,1)
    WRITE(1,*)'*****DIS(I)*****'
    WRITE(1,6)DIS1(1)
    WRITE(1,6)(DIS2(I),I=1,N/2,1)
    WRITE(1,*)'*****DTE(I)*****'
    WRITE(1,6)(DTE(I),I=1,N/2-1,1)
5  FORMAT(5(X,E12.5))
6  FORMAT(1(X,E12.5))
7  FORMAT(2(X,E12.5))
    RETURN
    END

```

**APPENDIX F****PROGRAM PONTINPUT1**

```

DEFDBL A-Z: DEFINT I-J: CLS : NM = 0: LOCATE , , 0
2 DIM AI(299), KK(299), P(299), AF(300), M(300), EI(299)
3 LOCATE 7, 27: PRINT " IN THE NAME OF GOD"
4 LOCATE 10, 23: PRINT "ANALYSIS OF FLOATING STRUCTURE": PRINT : PRINT
5 PRINT TAB(8); "THIS PROGRAM IS FOR ANALYSIS OF FLOATING STRUCTURE FOR"
6 PRINT TAB(8); "LIVE LOAD AND DEAD LOAD DUE TO WEIGHT OF THE STRUCTURE"
7 PRINT TAB(8); "THIS PROGRAM IS FOR  CALCULATION OF MOMENT, SHEAR AND"
8 PRINT TAB(8); "DISPLACEMENT"
9 IF INKEY$ = "" THEN 9
10 CLS : SEL$ = "CHOSE ONE OF THE NUMBERS"
11 CLS : LOCATE 8, 20: PRINT "SHAP OF STRUCTURE AND LOAD CASES"
12 LOCATE 12, 20: PRINT "1-SYMETRIC STRUCTURE"
13 LOCATE 14, 20: PRINT "2-ANSYMETRIC STRUCTURE"
14 LOCATE 16, 20: PRINT "3-CONTINUE STRUCTURE"
15 LOCATE 20, 20: PRINT SEL$; : INPUT M0: IF 0 < M0 AND M0 < 4 GOTO 18 ELSE 11
16 '
17 CLS : IF NM < 8 THEN NM = NM + 1: M1 = NM: GOTO 30
18 CLS : IF M0 = 1 THEN PRINT : PRINT : PRINT TAB(8); "IN THIS CASE THE AXES OF
SYMETRY IS IN THE MIDEL OF MID PONTOON": PRINT TAB(19); "THE LAST JOINT IS IN
THIS AXES": GOTO 19
19 LOCATE 6, 20: PRINT "1-NUMBER OF JOINT"
20 LOCATE 8, 20: PRINT "2-MODUL OF ELASTICITY"
21 LOCATE 10, 20: PRINT "3-MOMENT OF INERTIA OF PONTOON"
22 LOCATE 12, 20: PRINT "4-K FOR ELASTIC FUNDATION"
23 LOCATE 14, 20: PRINT "5-FREE-RIGID ROTAITION"
24 LOCATE 16, 20: PRINT "6-LENGTH OF PONTOONS"
25 LOCATE 18, 20: PRINT "7-LOAD ACTING ON STRUCTURE"
26 IF NM > 0 THEN GOTO 29
27 PRINT : PRINT TAB(10); "ALL INFORMATION WILL BE ASKED IN NUMERICAL
ORTHER": PRINT TAB(11); "CORECTION OF INPUT IS POSIBLE AFTER LOADING": PRINT
TAB(20); "PRESS <CR> FOR CONTINUE"
28 IF INKEY$ = CHR$(13) THEN 17 ELSE 28

```

```

29 LOCATE 22, 20: PRINT SEL$; : INPUT M1
30 ON M1 GOTO 32, 33, 35, 45, 55, 62, 65
31 GOTO 87
32 CLS : LOCATE 12, 20: PRINT "NUMBER OF JOINTS": PRINT : PRINT TAB(32); "N="; :
INPUT N: N = ABS(INT(N)): IF N <> 0 GOTO 16 ELSE 32
33 CLS : LOCATE 12, 20: PRINT "MODULUS OF ELASTICITY": PRINT : PRINT TAB(32); "E=";
: INPUT EE
34 GOTO 16
35 CLS : LOCATE 8, 20: PRINT "MOMENT OF INERTIA OF PONTOON"
36 LOCATE 12, 20: PRINT "1-MOMENT OF INERTIA IS CONSTANT"
37 LOCATE 14, 20: PRINT "2-MOMENT OF INERTIA IS NOT CONSTANT"
38 LOCATE 18, 20: PRINT SEL$; : INPUT M2
39 IF M2 = 1 THEN 42
40 FOR J = 1 TO N - 1: CLS : LOCATE 13, 20: PRINT "I("; J; ")="; : INPUT AI(J): NEXT J
41 GOTO 16
42 CLS : LOCATE 13, 20: PRINT "Ix="; : INPUT AI
43 FOR J = 1 TO N - 1: AI(J) = AI: NEXT J
44 GOTO 16
45 CLS : LOCATE 8, 21: PRINT "ELASTICITY FOR ELASTIC FOUNDATION"
46 LOCATE 12, 20: PRINT "1-ELASTICITY IS EQUAL FOR ALL PONTOON"
47 LOCATE 14, 20: PRINT "2-ELASTICITY IS NOT EQUAL FOR ALL PONTOON"
48 LOCATE 18, 20: PRINT SEL$; : INPUT M3
49 IF M3 = 1 THEN 52
50 FOR J = 1 TO N - 1: CLS : LOCATE 13, 20: PRINT "K("; J; ")="; : INPUT KK(J): NEXT J
51 GOTO 16
52 CLS : LOCATE 13, 20: PRINT "K="; : INPUT KK
53 FOR J = 1 TO N - 1: KK(J) = KK: NEXT J
54 GOTO 16
55 CLS : LOCATE 8, 20: PRINT "RIGID ROTATION"
56 LOCATE 10, 20: PRINT : PRINT " IN POSETIVE ROTATION THE TOP WILL BE UNTHER
COMPRSION"
57 LOCATE 12, 20: PRINT : PRINT " IN NEGATIVE ROTATION THE BOTTON WILL BE
UNTHER COMPRSION"
58 LOCATE 14, 20: PRINT "ABSLUT OF ROTATION MUST BE INPUT"
59 LOCATE 16, 20: PRINT "1- MAXIMUM POSETIVE ROTATION"; : LOCATE 20, 20: INPUT
T1: T1 = ABS(T1)

```

```

60 LOCATE 18, 20: PRINT "1- MAXIMUM NEGATIVE ROTATION"; : LOCATE 22, 20: INPUT
T2: T2 = ABS(T2)
61 GOTO 16
62 CLS : LOCATE 12, 20: PRINT " LENGTH OF EACH PONTOON": PRINT : PRINT TAB(32);
"L="; : INPUT L: GOTO 16
63 LOCATE 15, 20: PRINT "L= "; : INPUT L
64 GOTO 16
65 CLS : LOCATE 8, 20: PRINT "LOADING"
66 LOCATE 11, 20: PRINT "1-DISTRIBUTED LOAD ON PONTOON"
67 LOCATE 13, 20: PRINT "2-POINT LOAD ON JOINTS"
68 LOCATE 15, 20: PRINT "3-MOMENT ON JOINTS"
69 LOCATE 19, 20: PRINT SEL$; : INPUT M4
70 ON M4 GOTO 72, 83, 85
71 GOTO 16
72 M6 = 1: CLS : LOCATE 8, 20: PRINT "DISTRIBUTED LOAD ON PONTOONS"
73 LOCATE 12, 20: PRINT "1-DISTRIBUTED LOAD IS CONSTANT ON ALL PONTOONS"
74 LOCATE 14, 20: PRINT "2-DISTRIBUTED LOAD IS CONSTANT ON SOME PONTOONS"
75 LOCATE 18, 20: PRINT SEL$; : INPUT M5
76 ON M5 GOTO 80, 78
77 GOTO 65
78 M10 = 1: FOR J = 1 TO N - 1: CLS : LOCATE 13, 20: PRINT "P("; J; ")="; : INPUT P(J): NEXT J
79 GOTO 65
80 M9 = 1: CLS : LOCATE 13, 20: PRINT "P="; : INPUT P
81 FOR J = 1 TO N - 1: P(J) = P: NEXT J
82 GOTO 65
83 M7 = 1: FOR J = 1 TO N: CLS : LOCATE 13, 20: PRINT "F("; J; ")="; : INPUT AF(J): NEXT J
84 GOTO 65
85 M8 = 1: FOR J = 1 TO N: CLS : LOCATE 13, 20: PRINT "M("; J; ")="; : INPUT M(J): NEXT J
86 GOTO 65
87 CLS : LOCATE 11, 1
88 PRINT : PRINT TAB(8); "IF CORECTION IS NESESERY PRES <Y>": PRINT : PRINT
TAB(20); "IF NOT PRESS <CR>"
89 PRINT : PRINT : PRINT TAB(24); "<Y> OR <CR>"; : INPUT M$
90 IF M$ = "Y" OR M$ = "y" THEN 16 ELSE IF M$ = "" GOTO 91 ELSE 87
91 BEEP
92 OPEN "O", 1, "PONT.DAT": PRINT "      <writing data in pont.dat >"
93 PRINT #1, M0, "; Structure type"

```

```
94 PRINT #1, N, "; Number of Nodes"
95 PRINT #1, EE, "; Modulus of Elasticity"
96 PRINT #1, M2, "; IF=1 Constant I ELSE variable I"
97 IF M2 = 1 THEN PRINT #1, AI ELSE FOR I = 1 TO N - 1: PRINT #1, AI (I): NEXT I
98 PRINT #1, M3, "; IF=1 Constant K ELSE variable I"
99 IF M3 = 1 THEN PRINT #1, KK ELSE FOR I = 1 TO N - 1: PRINT #1, KK (I): NEXT I
100 PRINT #1, T1, "; Positive Rigid Rotation"
101 PRINT #1, T2, "; Negative Rigid Rotation"
102 PRINT #1, L, "; Member Lengths"
103 PRINT #1, M6, M7, M8, M9, M10
104 PRINT #1, "; Load-Codes: Distributed; joint-Moment-& Forces"
105 IF M6 = 1 THEN IF M5 = 1 THEN PRINT #1, P ELSE FOR I = 1 TO N - 1: PRINT #1, P(I):
NEXT I
106 IF M7 = 1 THEN FOR I = 1 TO N: PRINT #1, AF (I): NEXT I
107 IF M8 = 1 THEN FOR I = 1 TO N: PRINT #1, M (I): NEXT I
108 END
```

## APPENDIX G

### PROGRAM PONTOON

```

1 CLOSE
2 DEFDBL A-Z: DEFINT I-J
3 DIM AI(200), K(200, 4), F(200), KK(200), P(200), AF(200), M(200), EI(200), T1(200), T2(200),
M1(200), M2(200), TL(200), TR(200), ML(200), MR(200), T(200), J(200), Y(200), RT(200), kA(200,
4), KB(4, 4), R(100), FA(200), TT(200)
4 COLOR 7, 1: CLS : J$(0) = "fixed (-)": J$(1) = "pin": J$(2) = "fixed (+)": S$(1) = "SYMMETRIC
STRUCTURE": S$(2) = "ANTISYMMETRIC STRUCTURE": S$(3) = "BEAM ON ELASTIC
FOUNDATION"

5 PRINT " **BEGINNING THE PROGRAM **"
6 OPEN "I", 1, "C:\BASIC\PONT.DAT": PRINT
7 LINE INPUT #1, D$: M0 = VAL(D$)
8 LINE INPUT #1, D$: N = VAL(D$)
9 LINE INPUT #1, D$: EE = VAL(D$)
10 LINE INPUT #1, D$: M2 = VAL(D$)
11 IF M2 = 1 THEN INPUT #1, AI: FOR I = 1 TO N - 1: AI(I) = AI: NEXT ELSE FOR I = 1 TO N -
1: INPUT #1, AI(I): NEXT I
12 LINE INPUT #1, D$: M3 = VAL(D$)
13 IF M3 = 1 THEN INPUT #1, KK: FOR I = 1 TO N - 1: KK(I) = KK: NEXT ELSE FOR I = 1 TO N
- 1: INPUT #1, KK(I): NEXT
14 LINE INPUT #1, D$: T1 = ABS(VAL(D$))
15 LINE INPUT #1, D$: T2 = -ABS(VAL(D$))
16 LINE INPUT #1, D$: L = ABS(VAL(D$))
17 INPUT #1, M6, M7, M8, M9, M10
18 LINE INPUT #1, D$
19 IF M9 = 1 THEN INPUT #1, P: FOR I = 1 TO N - 1: P(I) = P: NEXT
20 IF M10 = 1 THEN FOR I = 1 TO N - 1: INPUT #1, P(I): NEXT I
21 IF M7 = 1 THEN FOR I = 1 TO N: INPUT #1, AF(I): NEXT I
22 IF M8 = 1 THEN FOR I = 1 TO N: INPUT #1, M(I): NEXT I
23 CLOSE: OPEN "O", #1, " pont.out "

```

```
24 PRINT #1, "IN THE NAME OF GOD"
25 PRINT #1, "ANALYSIS OF THE FLOATING STRUCTUR"
26 PRINT #1, $$ (M0)
27 PRINT #1, "NUMBER OF JOINTS:"; N
28 PRINT #1, "NUMBER OF MEMBERS:"; N - 1
29 PRINT #1, "CONSTANT E"; EE; "ALL"
30 PRINT #1, "MEMBER PROPERTIES:"
31 IF M2 = 1 THEN 33
32 FOR J = 1 TO N - 1: PRINT #1, "I("; J; ")="; AI(J): NEXT J: GOTO 34
33 PRINT #1, "CONSTANT I"; AI(1); "ALL"
34 PRINT #1, "SPRING COEFICENT:"
35 IF M3 = 1 THEN 37
36 FOR J = 1 TO N - 1: PRINT #1, "K("; J; ")="; KK(J): NEXT J: GOTO 38
37 PRINT #1, "CONSTANT K"; KK(1); "ALL"
38 PRINT #1, "RIGID ROTATIONS:"
39 PRINT #1, "POSETIVE ROTATION:"; T1: PRINT #1, "NEGATIVE ROTATION:"; T2
40 PRINT #1, "CONSTANT MEMBERS LENGTH:"; L; "ALL"
41 PRINT #1, "LOADING CASES:"
42 IF M6 = 1 THEN PRINT #1, "MEMBERS LOADS:"
43 IF M9 = 1 THEN PRINT #1, "CONSTANT DISTRIBUTED P="; P(1); "ALL"
44 IF M10 <> 1 THEN 47
45 FOR J = 1 TO N - 1: IF P(J) <> 0 THEN PRINT #1, "P("; J; ")="; P(J)
46 NEXT J
47 IF M7 <> 1 THEN 50
48 PRINT #1, "JOINT LOADS:": FOR J = 1 TO N: IF AF(J) <> 0 THEN PRINT #1, "F("; J; ")=";
AF(J)
49 NEXT J
50 IF M8 <> 1 THEN 53
51 PRINT #1, "JOINT MOMENTS:": FOR J = 1 TO N: IF M(J) <> 0 THEN PRINT #1, "M("; J; ")=";
M(J)
52 NEXT J
53 REM

54 REM BEGINNING THE PROGRAM
55 IF M0 = 3 THEN GOSUB 453: R = 1: S = 1: R(S) = 1: GOTO 86
56 LL = L: LP = L: IF M0 = 1 THEN LL = L / 2
57 F(1) = AF(1): F(2) = M(1): O = 0
```

```

58 FOR I = 1 TO N - 1: J1 = 2 * I - 1: EI(I) = EE * AI(I): J(I) = 0
59 GOSUB 223
60 NEXT I: IF M0 = 1 THEN J(N) = 1: SS = N: L = LL: GOSUB 319: L = LP
61 S = 0: R = 0

62 S = S + 1: PRINT : PRINT : PRINT "BEGINNING THE CYCLE("; S; ")"

63 GOSUB 109
64 FOR I = 1 TO N - 1: IF I = N - 1 THEN L = LL
65 IF J(I) <> 0 THEN 69
66 IF J(I + 1) = 0 THEN GOSUB 234
67 IF J(I + 1) <> 0 THEN GOSUB 248
68 GOTO 71
69 IF J(I + 1) = 0 THEN GOSUB 265
70 IF J(I + 1) <> 0 THEN GOSUB 281
71 T1(I) = 0: M1(I) = 0: T2(I) = 0: M2(I) = 0
72 FOR J = 1 TO 4: IXJ = 2 * I - 2 + J
73 T1(I) = T1(I) + KB(1, J) * FA(IXJ)
74 M1(I) = M1(I) + KB(2, J) * FA(IXJ)
75 T2(I) = T2(I) - KB(3, J) * FA(IXJ)
76 M2(I) = M2(I) - KB(4, J) * FA(IXJ)
77 NEXT J
78 IF J(I) <> 0 THEN 82
79 IF J(I + 1) = 0 THEN GOSUB 295
80 IF J(I + 1) <> 0 THEN GOSUB 300
81 GOTO 84
82 IF J(I + 1) = 0 THEN GOSUB 306
83 IF J(I + 1) <> 0 THEN GOSUB 312
84 NEXT I: L = LP
85 GOSUB 171: FOR I = 1 TO N: PRINT I, J$(J(I) + 1): NEXT I

86 PRINT "R="; R: FOR I = 1 TO N - 1: Y(I) = Y(I) + FA(2 * I - 1) * R(S)
87 RT(I) = RT(I) + FA(2 * I) * R(S)
88 TL(I) = TL(I) + T1(I) * R(S)
89 ML(I) = ML(I) + M1(I) * R(S)
90 TR(I) = TR(I) + T2(I) * R(S)
91 MR(I) = MR(I) + M2(I) * R(S)

```

```

92 NEXT I
93 Y(N) = Y(N) + FA(2 * N - 1) * R(S)
94 RT(N) = RT(N) + FA(2 * N) * R(S)
95 GOSUB 96: IF R >= 1 THEN : END ELSE GOTO 62

96 REM SUBROUTINE NO.1
97 PRINT #1, "CYCLE LOADS;": R(S) = R(S) + R(S - 1)
98 PRINT #1, "R("; S; ")="; R(S)
99 PRINT #1, " ": PRINT #1, "  DISPLACEMENTS OF ALL JOINTS:"
100 PRINT #1, "  JNT  DEFL.Y    ROTN.Z    COND."
101 FOR I = 1 TO N: PRINT #1, USING "#####"; I; : PRINT #1, USING "#####.#####";
Y(I); RT(I); : PRINT #1, "    "; J$(J(I) + 1): NEXT I
102 PRINT #1, " ": PRINT #1, " FORCES AT END OF MEMBERS"
103 PRINT #1, " MBR JNT  SHEAR.Y    MOMENT.Z"
104 FOR I = 1 TO N - 1
105 PRINT #1, USING "#####"; I; : PRINT #1, USING "#####.#####"; TL(I); : PRINT #1,
USING "#####.#####"; ML(I)
106 PRINT #1, USING "#####"; I + 1; : PRINT #1, USING "#####.#####"; TR(I); : PRINT #1,
USING "#####.#####"; MR(I)
107 NEXT: PRINT #1, "*****"
108 RETURN

109 REM SUBROUTINE NO.2
110 FOR I = 1 TO 2 * N - 1 STEP 2: FOR J = 1 TO 4: KA(I, J) = K(I, J)
111 IF J(I / 2 + .5) = 0 THEN KA(I + 1, J) = 0 ELSE KA(I + 1, J) = K(I + 1, J)
112 NEXT J: FA(I) = F(I): IF J(I / 2 + .5) = 0 THEN FA(I + 1) = 0 ELSE FA(I + 1) = F(I + 1)
113 NEXT I
114 A = KA(1, 4): PRINT "Reducing joint 1"
115 IF A <= 0 THEN 146
116 KA(1, 4) = SQR(A)
117 FOR I = 2 TO 4: Z = 5 - I
118 KA(I, Z) = KA(I, Z) / KA(1, 4)
119 NEXT I
120 FOR J = 2 TO 2 * N - 1: IF J - INT(J / 2) * 2 = 1 THEN PRINT "Reducing joint"; INT(J / 2 + .5)
121 IF KA(J, 4) = 0 THEN 144
122 X = 0: IF J > 4 THEN 127
123 FOR IXJ = 1 TO J - 1: Z = 4 - J + IXJ

```

```

124 X = X + KA(J, Z) * KA(J, Z)
125 NEXT IXJ
126 GOTO 130
127 FOR IXJ = J - 3 TO J - 1: Z = 4 - J + IXJ
128 X = X + KA(J, Z) * KA(J, Z)
129 NEXT IXJ
130 A = KA(J, 4) - X
131 IF A <= 0 THEN 146
132 KA(J, 4) = SQR(A)
133 IF J = 2 * N THEN 144
134 FOR I1 = J + 1 TO 2 * N: X = 0: IF I1 > 4 THEN 138
135 FOR IXJ = 1 TO J - 1: X = X + KA(I1, 4 - I1 + IXJ) * KA(J, 4 - J + IXJ)
136 NEXT IXJ
137 GOTO 141
138 IF I1 - 2 - J > 0 THEN 141
139 FOR IXJ = I1 - 3 TO J - 1: X = X + KA(I1, 4 - I1 + IXJ) * KA(J, 4 - J + IXJ)
140 NEXT IXJ
141 IF J + 4 - I1 <= 0 THEN 143
142 KA(I1, 4 - I1 + J) = (KA(I1, 4 - I1 + J) - X) / KA(J, 4)
143 NEXT I1
144 NEXT J
145 GOTO 148
146 PRINT "MATRIX OF COFFICIENTS IS NOT POSITIVE DEFINITE"
147 PRINT "END": END
148 N = 2 * N
149 FA(1) = FA(1) / KA(1, 4): PRINT
150 FOR I1 = 2 TO N: X = 0: IF KA(I1, 4) = 0 THEN 158 ELSE : IF I1 - 2 * INT(I1 / 2) = 1 THEN :
PRINT "Forward sweep joint"; INT(I1 / 2 + .5)
151 IF I1 > 4 THEN 155
152 FOR IXJ = 1 TO I1 - 1: X = X + KA(I1, 4 - I1 + IXJ) * FA(IXJ)
153 NEXT IXJ
154 GOTO 157
155 FOR IXJ = I1 - 3 TO I1 - 1: X = X + KA(I1, 4 - I1 + IXJ) * FA(IXJ)
156 NEXT IXJ
157 FA(I1) = (FA(I1) - X) / KA(I1, 4)
158 NEXT I1: PRINT
159 IF KA(N, 4) <> 0 THEN FA(N) = FA(N) / KA(N, 4)

```

```

160 FOR I1 = 1 TO N - 1: X = 0: IF KA(N - I1, 4) = 0 THEN 168 ELSE IF I1 - 2 * INT(I1 / 2)=1
THEN PRINT "Backward sweep joint";INT(I1/2+.5)
161 IF 3 - I1 <= 0 THEN 165
162 FOR IXJ= N + 1 - I1 TO N: X = X + KA(IXJ, N - IXJ - I1+4)*FA(IXJ)
163 NEXT IXJ
164 GOTO 167
165 FOR IXJ=N -I1 + 1 TO N - I1 + 3: X=X + KA(IXJ,N-IXJ-I1+4)*FA(IXJ)
166 NEXT IXJ
167 FA(N - I1) = (FA(N - I1) - X) / KA(N - I1, 4)
168 NEXT I1
169 N = N / 2
170 RETURN

171 REM SUBROUTINE NO.3
172 REM FINDING THE MINIMUM FORCEFOR CYCLE(S)
173 IF M0 = 1 AND N = 3 THEN L2 = L / 2 ELSE L2 = L
174 XJ = 10 ^ 6: YJ = 10 ^ 6
175 FOR I = 2 TO N - 1: IF I = N - 1 THEN L2 = LL
176 TT(I)=(FA(2 *I - 1)- FA(2 * I + 1))/L2-(FA(2 * I - 3)-FA(2*I1))/ L
177 P1 = (T1 - T(I)) / TT(I)
178 IF P1 <= .000001 OR P1 > XJ THEN 180
179 XJ = P1: S1 = I
180 P2 = (T2 - T(I)) / TT(I)
181 IF P2 > YJ OR P2 <= .000001 THEN 183
182 YJ = P2: S2 = I
183 NEXT I: CLS
184 IF YJ < XJ THEN 191
185 R(S) = XJ: SS = S1
186 IF J(SS) = 0 THEN 189
187 J(SS) = 0: O = 0: PRINT "JOINT"; SS; "IS POSITIVE OPENED"
188 GOTO 196
189 J(SS) = 1: O = 1: PRINT "JOINT"; SS; "IS LOCKED IN POSITIVE ROTATION"
190 GOTO 196
191 IF J(S2) = 0 THEN 194
192 J(S2) = 0: O = 0: PRINT "JOINT"; S2; "IS NEGATIVE OPENED"
193 GOTO 195
194 J(S2) = -1: O = 1: PRINT "JOINT"; S2; "IS LOCKED IN NEGATIVE ROTATION"

```

```

195 R(S) = YJ: SS = S2
196 SSX = SS: GOSUB 211: R= R + R(S): IF R > 1 THEN R(S)= R(S)-(R - 1)
197 FOR I= 2 TO N - 1: T(I)= T(I) + R(S) * TT(I): IF SSX = I THEN 207
198 RR = .000001: IF J(I) = 0 THEN RR = .00001
199 IF ABS(T(I) / T2 - 1) >= RR THEN 203
200 T(I) = T2
201 SS = I: IF J(I) = 0 THEN J(I) = -1: O = 1: PRINT "JOINT"; SS; "IS LOCKED IN NEGATIVE
ROTATION" ELSE J(I) = 0: O = 0: PRINT "JOINT"; SS; " IS NEGATIVE OPENED"
202 GOSUB 211
203 IF ABS(T(I) / T1 - 1) >= RR THEN 207
204 T(I) = T1
205 SS = I: IF J(I) = 0 THEN J(I) = 1: O = 1: PRINT "JOINT"; SS; "IS LOCKED IN POSITIVE
ROTATION" ELSE J(I) = 0: O = 0: PRINT "JOINT"; SS; " IS POSITIVE OPENED"
206 GOSUB 211
207 NEXT I
208 PRINT "R("; S; ")="; R(S)
209 IF R = 1 THEN RETURN 56
210 RETURN

211 REM SUBROUTINE NO.4
212 IF O = 0 THEN 218
213 IF J(SS - 1) = 0 THEN GOSUB 319
214 IF J(SS - 1) <> 0 THEN GOSUB 333
215 IF J(SS + 1) = 0 THEN GOSUB 352
216 IF J(SS + 1) <> 0 THEN GOSUB 366
217 RETURN
218 IF J(SS - 1) = 0 THEN GOSUB 425
219 IF J(SS - 1) <> 0 THEN GOSUB 386
220 IF J(SS + 1) = 0 THEN GOSUB 439
221 IF J(SS + 1) <> 0 THEN GOSUB 405
222 RETURN

223 REM SUBROUTINE NO.5
224 REM ASSEMBLY FORCES & STIFFNESS MATRIX FOR TWO PINED SUPPORT BEAM
225 IF I = N - 1 THEN L = LL
226 F(J1) = F(J1) + P(I) * L / 2
227 F(J1 + 2) = F(J1 + 2) + P(I) * L / 2 + AF(I + 1)

```

```

228 F(J1 + 3) = F(J1 + 3) + M(I + 1)
229 K(J1, 4) = K(J1, 4) + KK(I) * L / 3
230 K(J1 + 2, 2) = K(J1 + 2, 2) + KK(I) * L / 6
231 K(J1 + 2, 4) = K(J1 + 2, 4) + KK(I) * L / 3
232 IF I = N - 1 THEN L = LP
233 RETURN

234 REM SUBROUTINE NO.6
235 REM STIFFNESS MATRIX FOR TWO PINNED SUPPORT BEAM ELEMENT
236 '      0-----0
237 KB(1, 1) = KK(I) * L / 3
238 KB(1, 2) = 0
239 KB(1, 3) = KK(I) * L / 6
240 KB(1, 4) = 0
241 KB(2, 1) = KB(1, 2)
242 KB(2, 2) = 0
243 KB(2, 3) = 0
244 KB(2, 4) = 0
245 KB(3, 1) = KB(1, 3): KB(3, 2) = KB(2, 3): KB(3, 3) = KB(1, 1): KB(3, 4) = KB(1, 2)
246 KB(4, 1) = KB(1, 4): KB(4, 2) = KB(2, 4): KB(4, 3) = KB(3, 4): KB(4, 4) = KB(2, 2)
247 RETURN

248 REM SUBROUTINE NO.7
249 REM STIFFNESS MATRIX FOR PINNED-FIXED SUPPORT BEAM ELEMENT
250 '      0-----1
251 KB(1, 1) = 3 * EI(I) / L ^ 3 + 33 * KK(I) * L / 140
252 KB(1, 2) = 0
253 KB(1, 3) = -3 * EI(I) / L ^ 3 + 39 * KK(I) * L / 280
254 KB(1, 4) = 3 * EI(I) / L ^ 2 - 11 * KK(I) * L ^ 2 / 280
255 KB(2, 1) = KB(1, 2)
256 KB(2, 2) = 0
257 KB(2, 3) = 0
258 KB(2, 4) = 0
259 KB(3, 1) = KB(1, 3): KB(3, 2) = KB(2, 3)
260 KB(3, 3) = 3 * EI(I) / L ^ 3 + 17 * KK(I) * L / 35
261 KB(3, 4) = -3 * EI(I) / L ^ 2 - 3 * KK(I) * L ^ 2 / 35
262 KB(4, 1) = KB(1, 4): KB(4, 2) = KB(2, 4): KB(4, 3) = KB(3, 4)

```

263  $KB(4, 4) = 3 * EI(I) / L + 2 * KK(I) * L^3 / 105$

264 RETURN

265 REM SUBROUTINE NO.8

266 REM STIFFNESS MATRIX FOR FIXED-PINNED SUPPORT BEAM ELEMENT

267 ' 1-----0

268  $KB(1, 1) = 3 * EI(I) / L^3 + 17 * KK(I) * L / 35$

269  $KB(1, 2) = 3 * EI(I) / L^2 + 3 * KK(I) * L^2 / 35$

270  $KB(1, 3) = -3 * EI(I) / L^3 + 39 * KK(I) * L / 280$

271  $KB(1, 4) = 0$

272  $KB(2, 1) = KB(1, 2)$

273  $KB(2, 2) = 3 * EI(I) / L + 2 * KK(I) * L^3 / 105$

274  $KB(2, 3) = -3 * EI(I) / L^2 + 11 * KK(I) * L^2 / 280$

275  $KB(2, 4) = 0$

276  $KB(3, 1) = KB(1, 3): KB(3, 2) = KB(2, 3)$

277  $KB(3, 3) = 3 * EI(I) / L^3 + 33 * KK(I) * L / 140$

278  $KB(3, 4) = 0$

279  $KB(4, 1)=KB(1, 4): KB(4, 2)=KB(2, 4): KB(4, 3)=KB(3, 4):KB(4,4)=0$

280 RETURN

281 REM SUBROUTINE NO.9

282 REM STIFFNESS MATRIX FOR TWO FIXED SUPPORT BEAM ELEMENT

283 ' 1-----1

284  $KB(1, 1) = 12 * EI(I) / L^3 + 13 * KK(I) * L / 35$

285  $KB(1, 2) = 6 * EI(I) / L^2 + 11 * KK(I) * L^2 / 210$

286  $KB(1, 3) = -12 * EI(I) / L^3 + 9 * KK(I) * L / 70$

287  $KB(1, 4) = 6 * EI(I) / L^2 - 13 * KK(I) * L^2 / 420$

288  $KB(2, 1) = KB(1, 2)$

289  $KB(2, 2) = 4 * EI(I) / L + KK(I) * L^3 / 105$

290  $KB(2, 3) = -KB(1, 4)$

291  $KB(2, 4) = 2 * EI(I) / L - KK(I) * L^3 / 140$

292  $KB(3, 1) = KB(1, 3): KB(3, 2) = KB(2, 3): KB(3, 3) = KB(1, 1): KB(3, 4) = -KB(1, 2)$

293  $KB(4, 1) = KB(1, 4): KB(4, 2) = KB(2, 4): KB(4, 3) = KB(3, 4): KB(4, 4) = KB(2, 2)$

294 RETURN

295 REM SUBROUTINE NO.10

296 REM SHEARS FOR TWO PINNED SUPPORT BEAM ELEMENT

$$297 \quad T1(I) = T1(I) - P(I) * L / 2$$

$$298 \quad T2(I) = T2(I) + P(I) * L / 2$$

299 RETURN

300 REM SUBROUTINE NO.11

301 REM SHEARS & MONENT FOR PINNED-FIXED SUPPORT BEAM ELEMENT

$$302 \quad T1(I) = T1(I) - 3 * P(I) * L / 8$$

$$303 \quad T2(I) = T2(I) + 5 * P(I) * L / 8$$

$$304 \quad M2(I) = M2(I) - P(I) * L ^ 2 / 8$$

305 RETURN

306 REM SUBROUTINE NO.12

307 REM SHEARS & MONENT FOR FIXED-PINNED SUPPORT BEAM ELEMENT

$$308 \quad T1(I) = T1(I) - 5 * P(I) * L / 8$$

$$309 \quad T2(I) = T2(I) + 3 * P(I) * L / 8$$

$$310 \quad M1(I) = M1(I) - P(I) * L ^ 2 / 8$$

311 RETURN

312 REM SUBROUTINE NO.13

313 REM SHEARS & MONENT FOR FIXED-FIXED SUPPORT BEAM ELEMENT

$$314 \quad T1(I) = T1(I) - P(I) * L / 2$$

$$315 \quad T2(I) = T2(I) + P(I) * L / 2$$

$$316 \quad M1(I) = M1(I) - P(I) * L ^ 2 / 12$$

$$317 \quad M2(I) = M2(I) - P(I) * L ^ 2 / 12$$

318 RETURN

319 REM SUBROUTINE NO.14

320 REM ADDING STIFNESS & FORCE MATRIX OF PINNED-FIXED ELEMENT TO TWO

PINNED ELEMENT

$$321 \quad ' \quad 0 \text{-----} 0 \text{----} > 0 \text{-----} 1$$

$$322 \quad J1 = 2 * SS - 3: I = SS - 1$$

$$323 \quad F(J1) = F(J1) - P(I) * L / (8)$$

$$324 \quad F(J1 + 2) = F(J1 + 2) + P(I) * L / (8)$$

$$325 \quad F(J1 + 3) = F(J1 + 3) - P(I) * L ^ 2 / (8)$$

$$326 \quad K(J1, 4) = K(J1, 4) + 3 * EI(I) / L ^ 3 - .0976 * KK(I) * L$$

$$327 \quad K(J1 + 2, 2) = K(J1 + 2, 2) - 3 * EI(I) / L ^ 3 - .0274 * KK(I) * L$$

$$328 \quad K(J1 + 3, 1) = K(J1 + 3, 1) + 3 * EI(I) / L ^ 2 - 11 * KK(I) * L ^ 2 / 280$$

```

329 K(J1 + 2, 4) = K(J1 + 2, 4) + 3 * EI(I) / L ^ 3 + .01524 * KK(I) * L
330 K(J1 + 3, 3) = K(J1 + 3, 3) - 3 * EI(I) / L ^ 2 - 3 * KK(I) * L^2/35
331 K(J1 + 3, 4) = K(J1 + 3, 4) + 3 * EI(I) / L + 2 * KK(I) * L^3/105
332 RETURN

```

```

333 REM SUBROUTINE NO.15

```

```

334 REM ADDING STIFNESS & FORCE MATRIX OF TWO FIXED ELEMENT TO TWO FIXED-
PINNED ELEMENT

```

```

335 '      1-----0 ----> 1-----1
336 J1 = 2 * SS - 3: I = SS - 1
337 F(J1) = F(J1) - P(I) * L / 8
338 F(J1 + 1) = F(J1 + 1) - P(I) * L ^ 2 / 24
339 F(J1 + 2) = F(J1 + 2) + P(I) * L / 8
340 F(J1 + 3) = F(J1 + 3) - P(I) * L ^ 2 / 12
341 K(J1, 4) = K(J1, 4) + 9 * EI(I) / L ^ 3 - .1143 * KK(I) * L
342 K(J1 + 1, 3) = K(J1 + 1, 3) + 3 * EI(I) / L ^ 2 - .0333 * KK(I) * L^2
343 K(J1 + 2, 2) = K(J1 + 2, 2) - 9 * EI(I) / L ^ 3 - .0107 * KK(I) * L
344 K(J1 + 3, 1) = K(J1 + 3, 1) + 6 * EI(I) / L ^ 2 - 13 * KK(I) * L^2/420
345 K(J1 + 1, 4) = K(J1 + 1, 4) + EI(I) / L - KK(I) * L ^ 3 / 105
346 K(J1 + 2, 3) = K(J1 + 2, 3) - 3 * EI(I) / L ^ 2 - .0083 * KK(I) * L^2
347 K(J1 + 3, 2) = K(J1 + 3, 2) + 2 * EI(I) / L - KK(I) * L ^ 3 / 140
348 K(J1 + 2, 4) = K(J1 + 2, 4) + 9 * EI(I) / L ^ 3 + .1357 * KK(I) * L
349 K(J1 + 3, 3) = K(J1 + 3, 3) - 6 * EI(I) / L ^ 2 - 11 * KK(I) * L^2/210
350 K(J1 + 3, 4) = K(J1 + 3, 4) + 4 * EI(I) / L + KK(I) * L ^ 3 / 105
351 RETURN

```

```

352 REM SUBROUTINE NO.16

```

```

353 REM ADDING STIFNESS & FORCE MATRIX OF FIXED-PINNED ELEMENT TO TWO
PINNED ELEMENT

```

```

354 '      0-----0 ----> 1-----0
355 J1 = 2 * SS - 1: I = SS
356 F(J1) = F(J1) + P(I) * L / 8
357 F(J1 + 1) = F(J1 + 1) + P(I) * L ^ 2 / 8
358 F(J1 + 2) = F(J1 + 2) - P(I) * L / 8
359 K(J1, 4) = K(J1, 4) + 3 * EI(I) / L ^ 3 + .1524 * KK(I) * L
360 K(J1 + 1, 3) = K(J1 + 1, 3) + 3 * EI(I) / L ^ 2 + 3 * KK(I) * L ^ 2/35
361 K(J1 + 2, 2) = K(J1 + 2, 2) - 3 * EI(I) / L ^ 3 - .0274 * KK(I) * L

```

```

362 K(J1 + 1, 4) = K(J1 + 1, 4) + 3 * EI(I) / L + 2 * KK(I) * L ^ 3 / 105
363 K(J1 + 2, 3) = K(J1 + 2, 3) - 3 * EI(I) / L ^ 2 + 11 * KK(I) * L ^ 2 / 280
364 K(J1 + 2, 4) = K(J1 + 2, 4) + 3 * EI(I) / L ^ 3 - .0976 * KK(I) * L
365 RETURN
366 REM SUBROUTINE NO.17
367 REM ADDING STIFNESS & FORCE MATRIX OF TWO FIXED ELEMENT TO TWO
PINNED-FIXED ELEMENT
368 '      0-----1 ----> 1-----1
369 J1 = 2 * SS - 1: I = SS: IF I = N - 1 THEN L = LL
370 F(J1) = F(J1) + P(I) * L / 8
371 F(J1 + 1) = F(J1 + 1) + P(I) * L ^ 2 / 12
372 F(J1 + 2) = F(J1 + 2) - P(I) * L / 8
373 F(J1 + 3) = F(J1 + 3) + P(I) * L ^ 2 / 24
374 K(J1, 4) = K(J1, 4) + 9 * EI(I) / L ^ 3 + .1357 * KK(I) * L
375 K(J1 + 1, 3) = K(J1 + 1, 3) + 6 * EI(I) / L ^ 2 + 11 * KK(I) * L ^ 2 / 210
376 K(J1 + 2, 2) = K(J1 + 2, 2) - 9 * EI(I) / L ^ 3 - .0107 * KK(I) * L
377 K(J1 + 3, 1) = K(J1 + 3, 1) + 3 * EI(I) / L ^ 2 - .081 * KK(I) * L ^ 2
378 K(J1 + 1, 4) = K(J1 + 1, 4) + 4 * EI(I) / L + KK(I) * L ^ 3 / 105
379 K(J1 + 2, 3) = K(J1 + 2, 3) - 6 * EI(I) / L ^ 2 + 13 * KK(I) * L ^ 2 / 420
380 K(J1 + 3, 2) = K(J1 + 3, 2) + 2 * EI(I) / L - KK(I) * L ^ 3 / 140
381 K(J1 + 2, 4) = K(J1 + 2, 4) + 9 * EI(I) / L ^ 3 - .1143 * KK(I) * L
382 K(J1 + 3, 3) = K(J1 + 3, 3) - 3 * EI(I) / L ^ 2 - .03333 * KK(I) * L ^ 2
383 K(J1 + 3, 4) = K(J1 + 3, 4) + EI(I) / L - KK(I) * L ^ 3 / 105
384 IF I = N - 1 THEN L = LP
385 RETURN

386 REM SUBROUTINE NO.18
387 REM MINUS STIFNESS & FORCE MATRIX OF FIXED-PINNED ELEMENT ON TWO
FIXED ELEMENT
388 '      1-----1 ----> 1-----0
389 J1 = 2 * SS - 3: I = SS - 1
390 F(J1) = F(J1) + P(I) * L / 8
391 F(J1 + 1) = F(J1 + 1) + P(I) * L ^ 2 / 24
392 F(J1 + 2) = F(J1 + 2) - P(I) * L / 8
393 F(J1 + 3) = F(J1 + 3) + P(I) * L ^ 2 / 12
394 K(J1, 4) = K(J1, 4) - 9 * EI(I) / L ^ 3 + .1143 * KK(I) * L
395 K(J1 + 1, 3) = K(J1 + 1, 3) - 3 * EI(I) / L ^ 2 + .0333 * KK(I) * L ^ 2

```

```

396 K(J1 + 2, 2) = K(J1 + 2, 2) + 9 * EI(I) / L ^ 3 + .0107 * KK(I)*L
397 K(J1 + 3, 1) = K(J1 + 3, 1) - 6 * EI(I) / L ^ 2 + 13*KK(I)*L^2/420
398 K(J1 + 1, 4) = K(J1 + 1, 4) - EI(I) / L + KK(I) * L ^ 3 / 105
399 K(J1 + 2, 3) = K(J1 + 2, 3) + 3 * EI(I) / L ^ 2 + .0083*KK(I)*L^2
400 K(J1 + 3, 2) = K(J1 + 3, 2) - 2 * EI(I) / L + KK(I) * L ^ 3 / 140
401 K(J1 + 2, 4) = K(J1 + 2, 4) - 9 * EI(I) / L ^ 3 - .1357 * KK(I)*L
402 K(J1 + 3, 3) = K(J1 + 3, 3) + 6 * EI(I) / L ^ 2 + 11*KK(I)*L^2/210
403 K(J1 + 3, 4) = K(J1 + 3, 4) - 4 * EI(I) / L - KK(I) * L ^ 3 / 105
404 RETURN

405 REM SUBROUTINE NO.19
406 REM MINUS STIFNESS & FORCE MATRIX OF PINNED-FIXED ELEMENT ON TWO
FIXED ELEMENT
407 '      1-----1 -----> 0-----1
408 J1 = 2 * SS - 1: I = SS: IF I = N - 1 THEN L = LL
409 F(J1) = F(J1) - P(I) * L / 8
410 F(J1 + 1) = F(J1 + 1) - P(I) * L ^ 2 / 12
411 F(J1 + 2) = F(J1 + 2) + P(I) * L / 8
412 F(J1 + 3) = F(J1 + 3) - P(I) * L ^ 2 / 24
413 K(J1, 4) = K(J1, 4) - 9 * EI(I) / L ^ 3 - .1357 * KK(I) * L
414 K(J1 + 1, 3) = K(J1 + 1, 3) - 6 * EI(I) / L ^ 2 - 11*KK(I)*L^2/210
415 K(J1 + 2, 2) = K(J1 + 2, 2) + 9 * EI(I) / L ^ 3 + .0107 * KK(I)*L
416 K(J1 + 3, 1) = K(J1 + 3, 1) - 3 * EI(I) / L ^ 2 + .081 *KK(I)*L^2
417 K(J1 + 1, 4) = K(J1 + 1, 4) - 4 * EI(I) / L - KK(I) * L ^ 3 / 105
418 K(J1 + 2, 3) = K(J1 + 2, 3) + 6 * EI(I) / L ^ 2 - 13*KK(I)*L^2/420
419 K(J1 + 3, 2) = K(J1 + 3, 2) - 2 * EI(I) / L + KK(I) * L ^ 3 / 140
420 K(J1 + 2, 4) = K(J1 + 2, 4) - 9 * EI(I) / L ^ 3 + .1143 * KK(I)*L
421 K(J1 + 3, 3) = K(J1 + 3, 3) + 3 * EI(I) / L ^ 2 + .03333*KK(I)*L^2
422 K(J1 + 3, 4) = K(J1 + 3, 4) - EI(I) / L + KK(I) * L ^ 3 / 105
423 IF I = N - 1 THEN L = LP
424 RETURN

425 REM SUBROUTINE NO.20
426 REM MINUS STIFNESS & FORCE MATRIX OF TWO PINNED ELEMENT ON PINNED-
FIXED ELEMENT
427 '      0-----1 -----> 0-----0
428 J1 = 2 * SS - 3: I = SS - 1

```

```

429 F(J1) = F(J1) + P(I) * L / 8
430 F(J1 + 2) = F(J1 + 2) - P(I) * L / 8
431 F(J1 + 3) = F(J1 + 3) + P(I) * L ^ 2 / 8
432 K(J1, 4) = K(J1, 4) - 3 * EI(I) / L ^ 3 + .0976 * KK(I) * L
433 K(J1 + 2, 2) = K(J1 + 2, 2) + 3 * EI(I) / L ^ 3 + .0274 * KK(I)*L
434 K(J1 + 3, 1) = K(J1 + 3, 1) - 3 * EI(I) / L ^ 2 + 11*KK(I)*L^2/280
435 K(J1 + 2, 4) = K(J1 + 2, 4) - 3 * EI(I) / L ^ 3 - .01524 *KK(I)*L
436 K(J1 + 3, 3) = K(J1 + 3, 3) + 3 * EI(I) / L ^ 2 + 3 *KK(I)*L^2/35
437 K(J1 + 3, 4) = K(J1 + 3, 4) - 3 * EI(I) / L - 2 * KK(I) * L^3/105
438 RETURN

439 REM SUBROUTINE NO.21
440 REM MINUS STIFNESS & FORCE MATRIX OF TWO PINNED ELEMENT ON:FIXED-
PINNED ELEMENT
441 '      1-----0 ----> 0-----0
442 J1 = 2 * SS - 1: I = SS
443 F(J1) = F(J1) - P(I) * L / 8
444 F(J1 + 1) = F(J1 + 1) - P(I) * L ^ 2 / 8
445 F(J1 + 2) = F(J1 + 2) + P(I) * L / 8
446 K(J1, 4) = K(J1, 4) - 3 * EI(I) / L ^ 3 - .1524 * KK(I) * L
447 K(J1 + 1, 3) = K(J1 + 1, 3) - 3 * EI(I) / L ^ 2 - 3 *KK(I)*L^2/35
448 K(J1 + 2, 2) = K(J1 + 2, 2) + 3 * EI(I) / L ^ 3 + .0274 * KK(I)*L
449 K(J1 + 1, 4) = K(J1 + 1, 4) - 3 * EI(I) / L - 2 * KK(I) * L^3/105
450 K(J1 + 2, 3) = K(J1 + 2, 3) + 3 * EI(I) / L ^ 2 - 11*KK(I)*L^2/280
451 K(J1 + 2, 4) = K(J1 + 2, 4) - 3 * EI(I) / L ^ 3 + .0976 * KK(I)*L
452 RETURN

453 REM SUBROUTIN NO.22
454 REM BEAB ON ELASTIC FOUNDATION
455 '      1-----1
456 F(1) = AF(1): F(2) = M(1)
457 FOR I = 1 TO N - 1: J1 = 2 * I - 1: EI(I) = EE * AI(I): J(I) = 1
458 F(J1) = F(J1) + P(I) * L / 2
459 F(J1 + 1) = F(J1 + 1) + P(I) * L ^ 2 / 12
460 F(J1 + 2) = F(J1 + 2) + P(I) * L / 2 + AF(I + 1)
461 F(J1 + 3) = F(J1 + 3) - P(I) * L ^ 2 / 12 + M(I + 1)
462 K(J1, 4) = K(J1, 4) + 12 * EI(I) / L ^ 3 + 13 * KK(I) * L / 35

```

```
463 K(J1 + 1, 3) = K(J1 + 1, 3) + 6 * EI(I) / L ^ 2 + 11 * KK(I) * L ^ 2 / 210
464 K(J1 + 2, 2) = K(J1 + 2, 2) - 12 * EI(I) / L ^ 3 + 9 * KK(I) * L / 70
465 K(J1 + 3, 1) = K(J1 + 3, 1) + 6 * EI(I) / L ^ 2 - 13 * KK(I) * L ^ 2 / 420
466 K(J1 + 1, 4) = K(J1 + 1, 4) + 4 * EI(I) / L + KK(I) * L ^ 3 / 105
467 K(J1 + 2, 3) = K(J1 + 2, 3) - 6 * EI(I) / L ^ 2 + 13 * KK(I) * L ^ 2 / 420
468 K(J1 + 3, 2) = K(J1 + 3, 2) + 2 * EI(I) / L - KK(I) * L ^ 3 / 140
469 K(J1 + 2, 4) = K(J1 + 2, 4) + 12 * EI(I) / L ^ 3 + 13 * KK(I) * L / 35
470 K(J1 + 3, 3) = K(J1 + 3, 3) - 6 * EI(I) / L ^ 2 - 11 * KK(I) * L ^ 2 / 210
471 K(J1 + 3, 4) = K(J1 + 3, 4) + 4 * EI(I) / L + KK(I) * L ^ 3 / 105
472 IF I = 1 THEN GOSUB 409
473 IF I = N - 1 THEN GOSUB 390
474 NEXT I: J$(2) = "fix": J(1) = 0: J(N) = 0
475 GOSUB 109
476 FOR I = 1 TO N - 1: GOSUB 281
477 IF I = 1 THEN GOSUB 248
478 IF I = N - 1 THEN GOSUB 265
479 T1(I) = 0: M1(I) = 0: T2(I) = 0: M2(I) = 0
480 FOR J = 1 TO 4: IXJ = 2 * I - 2 + J
481 T1(I) = T1(I) + KB(1, J) * FA(IXJ)
482 M1(I) = M1(I) + KB(2, J) * FA(IXJ)
483 T2(I) = T2(I) - KB(3, J) * FA(IXJ)
484 M2(I) = M2(I) - KB(4, J) * FA(IXJ)
485 NEXT J
486 GOSUB 312
487 NEXT I
488 RETURN
```

**APPENDIX H****RESULT OF EXAMPLE WITH REAL DIMENTIONS**

IN THE NAME OF GOD

ANALYSIS OF THE FLOATING STRUCTUR

SYMMETRIC STRUCTURE

NUMBER OF JOINTS: 9

NUMBER OF MEMBERS: 8

CONSTANT E 21000000000 ALL

MEMBER PROPERTIES:

CONSTANT I 3.2 ALL

SPRING COEFICENT:

CONSTANT K 12000 ALL

RIGID ROTATIONS:

POSITIVE ROTATION: +0.01

NEGATIVE ROTATION: -0.01

CONSTANT MEMBERS LENGTH: 12 ALL

LOADING CASES:

MEMBERS LOADS:

P (8)= 12000

CYCLE LOADS;

R (1)= .1074984088234942

DISPLACEMENTS OF ALL JOINTS:

JNT	DEFL.Y	ROTN.Z	COND.
1	-0.000015	0.000000	pin
2	0.000030	0.000000	pin
3	-0.000104	0.000000	pin
4	0.000385	0.000000	pin
5	-0.001436	0.000000	pin
6	0.005359	0.000000	pin

7	-0.020000	0.000000	fixed (-)
8	0.074641	0.000000	pin
9	0.074643	0.000000	fixed (+)

## FORCES AT END OF MEMBERS

MBR	JNT	SHEAR.Y	MOMENT.Z
1	1	0.0000	0.0000
	2	-1.0659	0.0000
2	2	-1.0659	0.0000
	3	4.2635	0.0000
3	3	4.2635	0.0000
	4	-15.9882	0.0000
4	4	-15.9882	0.0000
	5	59.6891	0.0000
5	5	59.6891	0.0000
	6	-222.7683	0.0000
6	6	-222.7683	0.0000
	7	831.3842	0.0000
7	7	831.3842	0.0000
	8	-3102.7683	0.0000
8	8	-3102.7683	0.0000
	9	-737.1422	11519.6418

## CYCLE LOADS;

R (2)= .1815271425532142

## DISPLACEMENTS OF ALL JOINTS:

JNT	DEFL.Y	ROTN.Z	COND.
1	0.000020	0.000000	pin
2	-0.000039	0.000000	pin
3	0.000137	0.000000	pin
4	-0.000508	0.000000	pin
5	0.001894	0.000000	pin
6	-0.007068	0.000000	pin

7	-0.007076	0.002113	fixed (-)
8	0.112933	0.000000	fixed (+)
9	0.112937	0.000000	fixed (+)

## FORCES AT END OF MEMBERS

MBR	JNT	SHEAR.Y	MOMENT.Z
1	1	-0.0000	0.0000
	2	1.4057	0.0000
2	2	1.4057	0.0000
	3	-5.6229	0.0000
3	3	-5.6229	0.0000
	4	21.0857	0.0000
4	4	21.0857	0.0000
	5	-78.7200	0.0000
5	5	-78.7200	0.0000
	6	293.7943	0.0000
6	6	293.8638	0.0000
	7	1312.3579	-9636.0196
7	7	1567.6131	-9636.0196
	8	-6053.8453	0.0000
8	8	-6053.9149	0.0000
	9	-1115.3129	21507.5135

## CYCLE LOADS;

R(3) = .2109428733973617

## DISPLACEMENTS OF ALL JOINTS:

JNT	DEFL.Y	ROTN.Z	COND.
1	0.000004	0.000000	pin
2	-0.000008	0.000000	pin
3	0.000028	0.000000	pin
4	-0.000103	0.000000	pin
5	0.000386	0.000000	pin
6	-0.001439	0.000000	pin

7	-0.001381	0.002118	pin
8	0.118676	0.000002	fixed (+)
9	0.118688	0.000000	fixed (+)

## FORCES AT END OF MEMBERS

MBR	JNT	SHEAR.Y	MOMENT.Z
1	1	-0.0000	0.0000
	2	0.2862	0.0000
2	2	0.2862	0.0000
	3	-1.1446	0.0000
3	3	-1.1446	0.0000
	4	4.2923	0.0000
4	4	4.2923	0.0000
	5	-16.0247	0.0000
5	5	-16.0247	0.0000
	6	59.8065	0.0000
6	6	59.8762	0.0000
	7	262.9692	-1945.3101
7	7	630.7055	-1945.9689
	8	-7814.6921	23869.5353
8	8	-7814.7620	23869.5353
	9	-1172.1059	50829.6938

## CYCLE LOADS;

R (4)= .4606965268454378

## DISPLACEMENTS OF ALL JOINTS:

JNT	DEFL.Y	ROTN.Z	COND.
1	0.000058	0.000000	pin
2	-0.000117	0.000000	pin
3	0.000408	0.000000	pin
4	-0.001517	0.000000	pin
5	0.005661	0.000000	pin
6	-0.021125	0.000000	fixed (-)

7	0.072089	0.002118	pin
8	0.192322	0.000012	fixed (+)
9	0.192365	0.000000	fixed (+)

## FORCES AT END OF MEMBERS

MBR JNT	SHEAR.Y	MOMENT.Z
1 1	-0.0000	0.0000
2	4.2017	0.0000
2 2	4.2017	0.0000
3	-16.8067	0.0000
3 3	-16.8067	0.0000
4	63.0253	0.0000
4 4	63.0253	0.0000
5	-235.2943	0.0000
5 5	-235.2943	0.0000
6	878.1519	0.0000
6 6	878.2216	0.0000
7	-2791.1427	-1945.3101
7 7	-2424.8934	-1945.9689
8	-21463.7929	124071.9784
8 8	-21220.6304	104246.8398
9	-1899.7064	173606.2824

## CYCLE LOADS;

R (5)= .9999999999999999

## DISPLACEMENTS OF ALL JOINTS:

JNT	DEFL.Y	ROTN.Z	COND.
1	-0.000405	0.000000	pin
2	0.000810	0.000000	pin
3	-0.002835	0.000000	pin
4	0.010529	0.000000	pin
5	-0.039282	0.000000	fixed (-)
6	0.025614	0.007642	fixed (-)

7	0.210575	0.002118	pin
8	0.331256	0.000036	fixed (+)
9	0.331376	0.000000	fixed (+)

## FORCES AT END OF MEMBERS

MBR JNT	SHEAR.Y	MOMENT.Z
1 1	-0.0000	0.0000
2	-29.1581	0.0000
2 2	-29.1581	0.0000
3	116.6323	0.0000
3 3	116.6323	0.0000
4	-437.3712	0.0000
4 4	-437.3712	0.0000
5	1632.8525	0.0000
5 5	1633.1040	0.0000
6	2617.6625	-34849.5518
6 6	3540.8861	-34849.5518
7	-13464.0337	-1945.3101
7 7	-13101.7879	-1945.9689
8	-52117.7210	371991.3633
8 8	-51416.4083	314784.0261
9	-3272.5105	478846.4062